BERICHTE
aus dem Fachbereich Geowissenschaften
der Universität Bremen

No. 184

Volbers, A.

PLANKTIC FORAMINIFERA AS PALEOCEANOGRAPHIC INDICATORS: PRODUCTION, PRESERVATION, AND RECONSTRUCTION OF UWELLING INTENSITY. IMPLICATIONS FROM LATE QUATERNARY SOUTH ATLANTIC SEDIMENTS.

Berichte, Fachbereich Geowissenschaften, Universität Bremen, No. 184,
122 pages, Bremen 2001

ISSN 0931-0800

The "Berichte aus dem Fachbereich Geowissenschaften" are produced at irregular intervals by the Department of Geosciences, Bremen University.

They serve for the publication of experimental works, Ph.D.-theses and scientific contributions made by members of the department.

Reports can be ordered from:

Gisela Boelen

Sonderforschungsbereich 261

Universität Bremen

Postfach 330 440

D 28334 BREMEN

Phone: (49) 421 218-4124

Fax: (49) 421 218-3116

e-mail: boelen@uni-bremen.de

Citation:

Volbers, A.

Planktic foraminifera as paleoceanographic indicators: production, preservation, and reconstruction of upwelling intensity. Implications from late Quaternary South Atlantic sediments.

Berichte, Fachbereich Geowissenschaften, Universität Bremen, No. 184, 122 pages, Bremen, 2001.

ISSN 0931-0800

Vor der Erkenntnis sind Berge Berge
und Bäume Bäume.

Während der Erkenntnis sind Berge die Thronsitze von Geistern und
Bäume die Träger der Weisheit.

Nach der Erkenntnis sind Berge Berge
und Bäume Bäume.

altes asiatisches Sprichwort

Preface *„The farther backward you can look, the farther forward you are likely to see" Winston Churchill*

Since it was realized that human CO_2 emission during the last 250 years increased the atmospheric CO_2 content by almost 30% of the pre-industrial level, reliable predictions about the Earth`s climate became urgently requested. Nowadays, the results of future global climate scenarios are spread by newspapers, reflecting the urgent demand of the general public to be well-informed about possible climate change triggered by natural and anthropogenic factors (e.g. Lossau, 1999; Rahmstorf, 1999; Wille, 1999). Unfortunately, the climate system does not exclusively consist of the atmosphere but also includes influences from the cryophere, the biosphere, the lithosphere, and in particular, the oceans (Macdonald and Wunsch, 1996). The ocean carbon reservoir is about 60 times larger than the atmosphere and about 20 times larger than the terrestrial biosphere (Stocker, 1999) and has been driving the atmosphere during the late Quaternary (Broecker, 1982).

From the geologist`s point of view we live in an ice age period which periodically switches from cold periods associated with low CO_2 values (around 200 ppm) to warm periods with high CO_2 values (285 ppm; Petit et al., 1999). Transitions from glacial to interglacial are externally forced and involve changes in the distribution of solar radiation (wobbles in the orbit of the Earth, the so-called Milankovich cycles) and involve changes in oceanic circulation (e.g. Ganopolski et al., 1998). Deep-sea sediments, which contain the tests of marine organisms, preserve information about ocean currents and water mass properties of the past. They reveal sudden spikes in oceanic conditions that correspond to climate shifts on land as recorded in the Greenland ice cap (Bond et al. 1993; Marchitto et al., 1998; Severinghaus et al., 1998). Even millennial to century time scales seem to be associated with well-organized and coherent changes in large-scale circulation pattern (e.g. Dansgaard et al., 1993; Charles et al., 1996; Dickson, 1997; Sutton and Allen, 1997). However, the climate system itself seems to be a highly non-linear system. It has a self-regulating tendency and suddenly switches from one condition to another when a critical point has passed (Rahmstorf, 1999). To predict future climate changes, the effect of additional anthropogenic CO_2 on our climate depends on our knowledge of the time scales and pattern associated with the natural level of variability on the decadal to century time scale and the long-term climatic cycles (Stocker, 1999).

No single mechanism is adequate to explain the 80 ppm glacial to interglacial change, and contributions from temperature, sea ice, biologic pumping, nutrient deepening, and $CaCO_3$ cycling must be called upon (Broecker and Peng, 1989; Broecker, 1992). This PhD thesis focuses on the calcareous sediments of the South Atlantic which contain useful information on the paleo-ocean. It was carried out as part of the Collaborative Research Centre (Sonderforschungsbereich) No. 261: „The South Atlantic in the late Quaternary: Reconstruction of material budget and current systems" in the subproject B3: „Calcareous plankton and carbonate budget". It consists of four parts: Part I provides the scientific background to the main problems and the methods used in this study whereas Part II concentrates on the publications that have been submitted to international journals. Part III summarizes the main conclusions and part IV contains a list of presentations at national and international conferences.

Table of contents

Abstract

To explain the lowered atmospheric CO_2 content of glacial times, lysocline reconstructions play an important role as they are useful tools to determine variations in the depth gradient of understaturation in the deep ocean (Berger 1977; Broecker and Clark, 1999). When investigating calcium carbonate dissolution thoughout the different hydrologic and ecologic settings of the South Atlantic, a reliable proxy is needed. As shown in manuscript 2 and 3, conventional calcium carbonate dissolution proxies are biased by increased surface productivity and could mimic calcium carbonate dissolution in high productive upwelling regions. So far, only a time-consuming multi-proxy approach consisting of several conventional dissolution proxies indicates the alteration of a sediment sample with certainty. However, in high-productivity regions even a multi-proxy approach could hardly determine whether the sediment reflects its original (unaltered) composition or not (manuscript 1). To overcome this problem, all further investigations were carried out with the *Globigerina bulloides* dissolution index (BDX'), an independent calcium carbonate dissolution proxy, that concentrates on the ultrastructure of the planktic foraminifera *Globigerina bulloides*. The degree of dissolution is reflected by five dissolution stages determined from test morphology.

In this thesis the position of the modern calcite lysocline was determined via the BDX'. In the eastern South Atlantic basin, the calcite lysocline is located between 4400 m (Walvis Ridge-Angola Basin) and 3600 m in the equatorial region. Detailed investigations of three continental margin transects reveal an on average shallower lysocline at the continental margins located between 3400 and 3600 m. In the western South Atlantic and the Cape Basin, the calcite lysocline is located at around 4000 m and seems to be closely related to the North Atlantic Deep Water (NADW) and Antarctic Bottom Water (AABW) transition, where a sharp change in carbonate ion concentration occurs (Berger, 1968; manuscript 2). In order to reconstruct deep water mass distribution pattern in the Atlantic Ocean and to evaluate changes in deep-sea calcium carbonate preservation, the position of the calcite lysocline during the Last Glacial Maxium (LGM) was determined. It was located several hundred meters shallower compared to its modern position in the western and eastern South Atlantic basin. This observation suggests that the modern west-east asymmetrie was not present during the LGM due to a rise of southern deep waters in the water column compensating for the decrease in NADW formation (manuscript 3).

The investigations of this thesis not only focus on both the spacial and temporal dissolution of planktic foraminiferal carbonate in South Atlantic deep-sea sediments but also on planktic foraminiferal production and detailed species investigation. The production of planktic foraminifera in the Benguela upwelling region (determined via the planktic foraminiferal number per g sediment) seems to be generally lower during periods of increased coastal upwelling. This is in accordance with our findings from surface sediment studies, with a minimum of 25% contribution of planktic foraminiferal carbonate to total $CaCO_3$ in this region, in contrast to an on average 40% in the overall South Atlantic. Besides variations in the $CaCO_3$ cycle, the strength of the biologic pump is expected

to influence the CO_2 content of our atmosphere. Specific species, such as *Neogloboquadrina pachyderma* sin. and *Neogloboquadrina pachyderma* dex. were successfully used to determine the areal extent and the strength of northern Benguela upwelling cells. Planktic foraminiferal species distribution patterns show that during the late Quaternary northern Benguela upwelling cells were variable in size, from smaller to up to three times larger than today. In terms of the CO_2 budget, coastal upwelling regions are of great importance due to the upwelling of CO_2-rich subsurface water and the massive production of organic material in the surface waters (e.g. Schrader, 1992). CO_2 is fixed in organic matter by marine phytoplankton and is partly transported to the sea floor (biological pump; Broecker, 1982). According to Broecker (1992), changes in the efficiency of the biological pump could strongly influcence the atmospheric CO_2 content: If all the nutrients were to be efficiently extracted from surface waters, the atmospheric CO_2 content would drop to about 150 ppm whereas a sterile ocean would make it rise to about 470 ppm. However, altough the strength of the biological pump is expected to be one of the major factors influencing the atmopheric CO_2 content, the complex relationship of long-term climatic cycles and atmospheric CO_2 content is not yet fully understood (Stouffer et al., 1994).

Literature:

Berger, W.H., 1968. Planktonic foraminifera: selective solution and paleoclimatic interpretation, Deep-Sea Res. 15, 31-43.

Berger, W.H., 1977. Deep-sea carbonate and the deglaciation preservation spike in pteropods and foraminifera. Nature 269, 301-304.

Bond, G., Broecker, W., Johnsen, S., McManus, J., Labeyrie, L., Jouzel, J. and Bonani, G., 1993. Correlations between climate records from North Atlantic sediments and Greenland ice. Nature 365, 143-147.

Broecker, W.S., 1982. Ocean chemistry during glacial time. Geochimica et Cosmochimica Acta 46, 1689-1705.

Brocker, W.S., 1992. The glacial world according to wally, a „proto" book. Draft, copyright applied for. Available at the Lamont-Doherty Geological Observatory of Columbia University Palisades, N.Y. 10964, U.S.A.

Broecker, W.S. and Peng, T.-H., 1989. The cause of the glacial to interglacial atmosheric CO_2 change: a polar alkalinity hypothesis, Global Biogeochemical cycles 3(3), 215-239.

Broecker, W.S. and Clark, E., 1999. $CaCO_3$ size distribution: A paleocarbonate ion proxy? Paleoceanography 14 (3), 596-604.

Charles, C.D., Lynch-Stieglitz, J., Ninnemann, U.S., and Fairbanks, R.G., 1996. Climate connections between the hemisphere revealed by deep sea sediment core/ice core correlations. Earth Planet. Sci. Lett. 142, 19-27.

Dansgaard, W., Johnsen, S.J., Clausen, H.B., Dahl-Jensen, D., Gundestrup, N.S., Hammer, C.U., Hvidberg, C.S., Steffensen, J.P., Sveinbjörnsdottir, A.E., Jouzel, J., Bond, G., 1993. Evidence for general instability of past climate from a 250-kyr ice-core record. Nature 364, 218-220.

Dickson, B., 1997. Form the Labroador Sea to global change. Nature, 386, 649-650.

Ganopolski, A., Rahmstorf, S., Petoukhow, V. and Claussen, M., 1998. Simulation of modern and glacial climates with a coupled global model of intermediate complexity. Nature 391, 351-356.

Lossau, N., 1999. Der Golfstrom könnte plötzlich ausbleiben. Die Welt, 28.01.1999.

Macdonald, A.M. and Wunsch, C., 1996. An estimate of global ocean circulation and heat fluxes. Nature 382, 436-439.

Marchitto, T.M, Curry, W.B., and Oppo, D.W., 1998. Millennial-scale changes in North Atlantic circulation since the last glaciation. Nature 393, 557-561.

Petit, J.R., Jouzel, J., Raynaud, D., Barkov, N.I., Barnola, J.-M., Basile, I., Bender, M., Chappellaz, J., Davis, M., Delaygue, G., Delmotte, M., Kotlyakov, V.M., Legrand, M. Kipenkov, V. Lorius, C., Pépin, L., Ritz, C., Saltzman, E., and Stievenard, M., 1999. Climate and atmospheric history of the past 420,000 years from the Vostok ice core, Antarctica. Nature 399, 429-436.

Rahmstorf, S., 1999. Die Welt fährt Achterbahn. Süddeutsche Zeitung, 3./4.7. 1999 (http://www.pik-potsdam.de/~stefan/).
Schrader, H., 1992. Costal upwelling and atmospheric CO_2 changes over the last 400,000 years: Peru. Marine Geology 107, 239-248.
Severinghaus, J.P., Sowers, T., Brook, E.J., Alles, R.B. and Bender, M.L., 1998. Timing of abrupt climate change at the end of the Younger Dryas interval from thermally fractionated gases in polar ice. Nature 391, 141-146.
Stocker, T., 1999. The Ocean in the climate system. Lecture Notes to Swiss Climate Summer School, 1999 (http://www.climate.unibe.ch/~stocker).
Stouffer, R.J, Manabe, S. and Vinnikow, K.Y., 1994. Model assessment of the role of natural variability in recent global warming, Nature 367, 634-636.
Sutton, R.T. and Allen, M.R, 1997. Decadal predictability of Narth Atlantic Sea surface temperature and climate. Nature 388, 563-565.
Wille, J. 1999. Wenn der Golfstrom kippt. Interview with Stefan Rahmstorf. Frankfurter Rundschau, 16.2.99 (http://www.pik-potsdam.de/~stefan/).

Part I *Introduction*

1. Modern global ocean circulation

The world´s oceans circulation was firstly described by Broecker as the „Global Ocean Conveyor Belt" (Broecker et al., 1985; Gordon, 1986; Broecker, 1991). This concept illustrates the idea that all oceans are connected through one coherent circulation system, which transportes heat and salt between them (thermohaline circulation). That is, in general, mainly wind-driven warm water transport along the surface and cold water transport back through the depth. However, it was finally realized that the circulation loops in the Atlantic and Pacific are only weakly connected, and that the oceans do not respond as one system (Rahmstorf, 1991; Macdonald and Wunsch, 1996; Schlitzer, 1996). Nevertheless, in particular the North Atlantic is regarded to play a key role in the global circulation. Warm surface waters (Fig. 1, in red) are supplied to the Arctic region where they release heat to the surrounding air and sink in the Greenland, Iceland, and Labrador Seas to form North Atlantic Deep Water (NADW, in lightblue, Fig. 1). As long as salty water from the south is supplied and vertical mixing continually removes water from the surface, the system is stable regarding the formation of NADW (Rahmstorf, 1997a,b) and deep water moves across the deep ocean basins to the Indian Ocean and the Pacific Ocean, where it is reheated and finally turns back northward.

1.1 Modern oceanography of the South Atlantic

1.1.1 Modern South Atlantic surface circulation

The South Atlantic plays a key role in redistributing heat from the southern hemisphere towards the northern hemisphere. It contributes to the mild climate of northern Europe today, which is around 10°C warmer compared to the Pacific region at similar latitudes (Roemmich and Wunsch, 1985; Manabe and Stouffer, 1988). In order to do this, water from the South Atlantic moves north at shallow depths: Where the South Equatorial Current (SEC) splits into two currents, its upper branch, the Northern Brazil Current (NBC), transfers warm water and heat across the equator (Fig. 1). Parts of this water is then turned eastward by the North Equatorial Counter Current (NECC) towards the African coast, where it joints the Guinea Current (GC). Along the coast of Brazil, the other branch of warm SEC water, the Brazil Current (BRC), turns to the south and forms the western limb of the subtropical gyre.

The South Atlantic subtropical gyre dominates the South Atlantic surface circulation. Its southern part consists of the South Atlantic Current (SAC) which moves to the east (Stramma and Peterson, 1991). At the southern tip of Africa the SAC encounters the Aghulas Current (AC) which imports warm surface water from the Indian and Pacific Ocean („warm water route"). In contrast, cold water enters the South Atlantic via the Drake Passage (Gordon, 1986; Rintoul, 1991) and moves

northward as surface or intermediate water („cold water route"; Georgi, 1979; Piola and Georgi, 1982).

The eastern part of the South Atlantic subtropical gyre is the Benguela Current (BC) which flows northward along the coast of Namibia until it splits into the Benguela Oceanic Current (BOC) and the Benguela Coastal Current (BCC; Currie, 1953). The BCC follows the coast until it encounters the Angola Current (AC) which carries warm water southwards (Angola-Benguela front, ABF; Hart and Currie, 1960). At around 30°S, the BOC turns to the northwest and feeds the SEC (Stramma and Peterson, 1989). The SEC varies seasonally according to the strength of the trade winds, which reach maximum during austal winter (Jun-Sep). This coincids with lowest temperatures in the Benguela region according to the enhanced coastal upwelling of cold and nutrient rich waters. The BC does not seem to be strong enough at present to cause extreme cooling in the central equatorial Atlantic (Mix and Morey, 1996) but seems to have enhanced equatorial seasonality during distinct time periods of the late Quaternary (Little et al. 1997a, manuscript 4, Part II). The Benguela region should therefore be regarded as a crucial system influencing not only the equatorial region but also cross-equatorial teleconnections between the South and North Atlantic (Little et al., 1997b).

1.1.2 South Atlantic intermediate and deep water circulation

Besides the supply of South Atlantic surface waters to high northern latitudes, intermediate and deep water masses from the south move across the equator towards the north (Fig. 1 and 2). According to Gordon et al. (1992), most of the net meridional flow within the South Atlantic heading towards the north occurs in the Antarctic Intermediate Water (AAIW) layer rather than in the thermocline layer (above 9°C). The South Atlantic AAIW is characterized by a salinity minimum lying at around 800 m to 1000 m and local oxygen and silica extrema (Talley, 1996). Its high oxygen content reflects its recent contact with the atmosphere since its sources are the surface waters in northern Drake Passage and the Falkland Current loop (Talley, 1996). AAIW and the Upper Circumpolar Water (UCDW) have low calcium carbonate ion concentration ($[Co_3^{2-}]$) compared to the surrounding water mass bodies and can be traced by their low aragonite preservation potential. The saturation state of aragonite in these waters is close to the aragonite saturation and these intermediate water masses are highly corrosive to aragonite as shown by Gerhardt and Henrich (2001). UCDW originates near Antarctica where NADW is returned from the Pacific via the ACC (Reid, 1989).

Besides the formation of deep water near the Antarctic continent, the North Atlantic is the only place, where deep water is formed. Accordingly, the Atlantic deep water circulation is marked by various interactions of NADW and AABW (Fig. 1 and 2, in light and dark blue), water masses which differ significantly in their physical properties, nutrient concentration, and carbonate ion concentration ($[CO_3^{2-}]$). NADW is a relatively warm and well-ventilated water mass and occurs

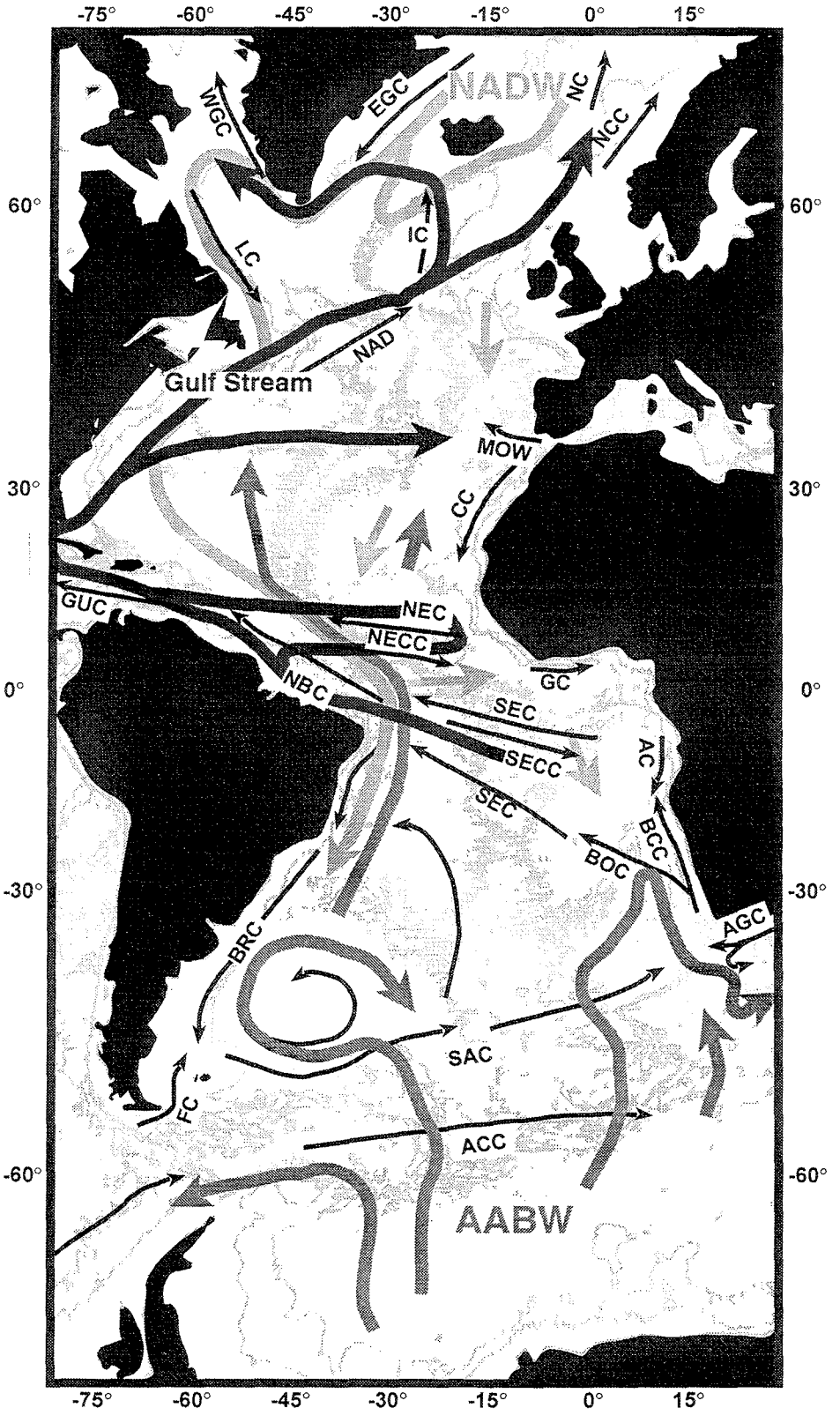

Fig. 1: Schematic South Atlantic circulation pattern (modified after Peterson and Strammer, 1991; Faugères et al., 1993; Sarnthein et al., 1994; Reid, 1996; Sarnthein, et al. 2001). **Surface currents in black** (small arrows): AC, Angola Current; ACC, Antarctic Circumpolar Current; AGC, Agulhas Current; BCC, Benguela Coastal Current; BOC, Benguela Oceanic Current; BRC, Brazil Current; CC: Canary Current; EGC, East Greenland Current; FC, Falkland Current; GC, Guinea Current; GUC, Guayana Current; IC, Irminger Current; LC, Labrador Current; MOW, Mediterranean Outflow Water; NAD, North Atlantic Drift; NC, Norwegian Current; NCC, Norwegian Coastal Current; NEC, North Equatorial Current; NECC, North Equatorial Counter Current; SAC, South Atlantic Current; SEC, South Equatorial Current; SECC, South Equatorial Counter Current; WGC, West Greenland Current. **In black (large arrows): Warm water transport** of south Atlantic surface and intermediate waters to high northern lattitudes. **In grey:** South Atlantic **deep-sea water masses,** NADW, North Atlantic Deep Water (lightgrey); AABW, Antarctic Bottom Water (darkgrey).

roughly the depth interval between 2000 and 4000 m in the western South Atlantic and in the Cape Basin (Dickson and Brown, 1994). It can be distinguished from other deep water masses by its low nutrient concentration and relatively high $\delta^{13}C$ values of dissolved inorganic carbon. After being drawn into the Antarctic Circumpolar Current (ACC) it is swept into the Indian and Pacific Oceans.

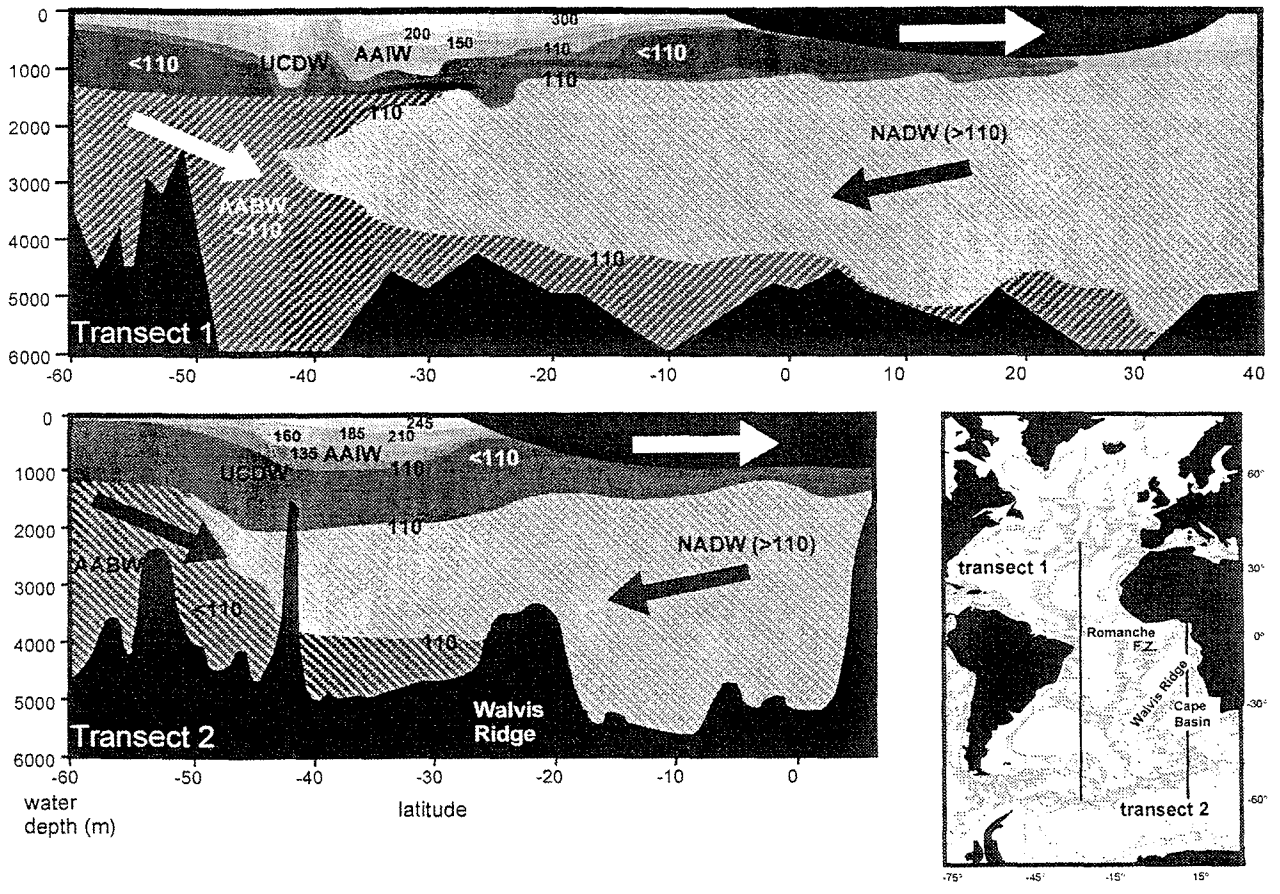

Fig. 2: Distribution pattern of North Atlantic Deep Water (NADW, lightgrey) and Antarctic Bottom Water (AABW, darkgrey) based on $[CO_3^{2-}]$ which was calculated from GEOSECS data (µmol/l, Bainbridge, 1981) and interpolated between individual GEOSECS stations (western Atlantic section after Gerhardt and Henrich, 2001). In the eastern South Atlantic the northward flow of AABW is hindered by the Walvis Ridge, whereas it reaches the North Atlantic through the western South Atlantic basin. In red: warm South Atlantic surface and intermediate water moves northward across the equator.

In the Atlantic Ocean, the relatively warm and saline NADW subdivides the Circumpolar Deep Waters (CDW) at mid depth (Fig. 2). In general, the circumpolar waters are much lower in oxygen and much higher in nutrients than those from the North Atlantic (e.g. Reid, 1996). The upper branch, the Upper Circumpolar Deep Water (UCDW), can be traced through the Atlantic Ocean due to its silica maximum (Talley, 1996). The Lower Circumpolar Deep Water (LCDW) from the Drake Passage overrides the denser waters from the Weddell Sea and fills the deep western basin and the Cape Basin. The LCDW and the Weddell Sea Deep Water (WSDW) are commonly referred to as AABW, a cold water mass of low salinity (Siedler et al., 1996; Fig. 1 and 2, dark blue). The inflow of AABW into the eastern South Atlantic basin is controlled by the submarine barriers of the Mid-Atlantic Ridge in the west, and by the Walvis Ridge in the south. Since only small quantities of AABW can enter

in the west, and by the Walvis Ridge in the south. Since only small quantities of AABW can enter the Guinea and Angola Basin via the Romanche Fracture Zone (sill depth 4350 m) and the Walvis Passage (sill depth around 4200 m), they are predominately filled by NADW (Van Bennekom and Berger, 1984; Shannon and Chapman, 1991; Warren and Speer, 1991; Mercier et al., 1994).

In the South Atlantic, calcium carbonate dissolution patterns are expected to be connected predominantly to the different deep water mass properties, in particular to their saturation state with respect to calcium carbonate. Since NADW is slightly supersaturated with respect to calcite, calcareous sediments should be well-preserved until the NADW/AABW boundary is encountered (Berger, 1968). In view of the minor contribution of AABW to the deep bottom waters of the Guinea and Angola Basin, their preservation potential should be much better compared to all other deep South Atlantic basins. However, this is not necessarily the case as discussed in detail in manuscript 2 (Part II). In the western South Atlantic and Cape Basin the calcium carbonate preservation level (calcite lysocline) is predominantly tied to the NADW/AABW interface (manuscript 2 and 3, Part II). The determination of the calcite lysocline can therefore give strong indications of the deep water mass distribution pattern in the South Atlantic of the past (manuscript 4, Part II).

1.2 Future and past oceanography of the South Atlantic

The pathways of large amounts of heat, freshwater and nutrients, their transport mechanisms and their stability are critical issues in understanding the present state of climate and the possibilities of future changes (e.g. Ganachaud and Wunsch, 2000). Regarding the heat transport to high northern latitudes, model studies suggest that the circulation is sensitive to increases in the atmospheric greenhouse-gas concentration (Rahmstorf, 1997a,b; Marotzke & Stone, 1995; Wood et al. 1999). A CO_2-induced warming of the atmosphere would increase the poleward transport of water vapour. If precipitation and meltwater runoff into the North Atlanic are strongly enhanced, some studies indicate a complete shutdown of the conveyor-belt within the twenty-second century (e.g. Rahmstorf and Ganopolski, 1997). Once switched off, the transport of warm water could be stopped for centuries because the climate system might have moved on to a new stable condition. More recent models, like the one presented by Wood et al. (1999), do not reach the point of NADW collapse, but suggests a decrease in the overall volume of water transported by the Atlantic conveyor belt of around 25%.

The deep water formation in high northern latitudes does not only seem to be the key to predicting future climate, but also to reconstruct past climate changes. Simulating the climate of the LGM is important because estimates of future changes must be consistent with the sensitivity of the climate system to altered forcing parameters. In addition, climate models must be able to simulate the full range of dynamical behaviour of the climate system, and extreme climatic periods, such as the LGM, may be the most critical tests (Stocker, 1998). During the LGM 50 million km^3 of water were locked in huge ice sheets, lowering sea level by more than 120 meters (see excellent summary in Stocker,

1998). Ocean model studies (e.g. Fichefet et al., 1994) and sediment core data (e.g. Curry et al., 1988; Sarnthein et al., 1994; Sarnthein et al., 2001) suggest that ocean circulation during the LGM was different from the one today. As shown by Broecker (1997), benthic foraminiferal $\delta^{13}C$ data from sites throughout the North Atlantic indicate that NADW formation was reduced during the LGM. According to the computer model of Ganopolski et al. (1998) simulating the atmospheric and oceanic circulations of the LGM, ocean circulation changes might have amplified Northern Hemisphere cooling during the LGM by about 50%. In response to sea-ice advance from around 75°N to 55°N, a southward shift of NADW formation occured (Ganopolski et al., 1998; Stocker, 1998). As the density of the sinking waters was reduced, they penetrated less deeply, resulting in the formation of Glacial North Atlantic Intermediate Water (GNAIW; Boyle and Keigwin, 1987; Zahn, 1992; Weaver et al., 1994, Broecker, 1997). Accordingly, AABW would have penetrated into the northern North Atlantic, as indeed is indicated by paleoceanographic data (e.g. Duplessy et al., 1988; Sarnthein et al. 1994). Periodic switches between GNAIW and NADW were assumed to have occured during the early and late Pleistocene with great impact on the water mass circulation in the South Atlantic (McIntyre et al., 1999; Venz et al., 1999; Austin and Evans, 2000). The modern asymmetry between the western and eastern South Atlantic regarding its deep water mass distribution may have not existed during times of decreased NADW production. From $\delta^{13}C$ data it was inferred that AABW may have crossed the Walvis Ridge and entered the Angola Basin during glacial and semiglacial periods (such as OIS 3; Bickert, 1992).

These late Pleistocene shifts in the NADW/AABW transition as determined by proxies such as $\delta^{13}C$ or Ca/Cd are also reflected by changes in the calcium carbonate preservation pattern (manuscript 3, Part II) as they are linked with a redistribution of the carbonate system, including a reduction in the atmopsheric CO_2 content and a shallowing of the calcite lysocline in the South Atlantic deep basins.

2. Calcareous deep-sea sediments in the South Atlantic

Around 55% of the ocean`s surface is covered by carbonate-rich sediments (Milliman, 1993). In particular, within the South Atlantic, most biogenic sediments are calcareous and originate from various micro- and nannofossil groups. Recent investigations confirm that planktic foraminifera, coccolithoporids, and pteropods are the main contributors to South Atlantic deep-sea sediments (Baumann et al., in prep.). High relative proportions of pteropodal calcium carbonate (>30%) seem to be restricted to the South American continental margin because aragonite preservation potential depends on shallow water depth (Gerhardt and Henrich, 2001). Calcareous dinoflagellates (personal communication, A. Vink) and benthic foraminifera contribute to on average <5% of the total marine calcium carbonate on the sea-floor. In particular planktic foraminifera and coccolithophorids dominate the sea-floor below 2500 m water depth (Baumann et al., in prep.).

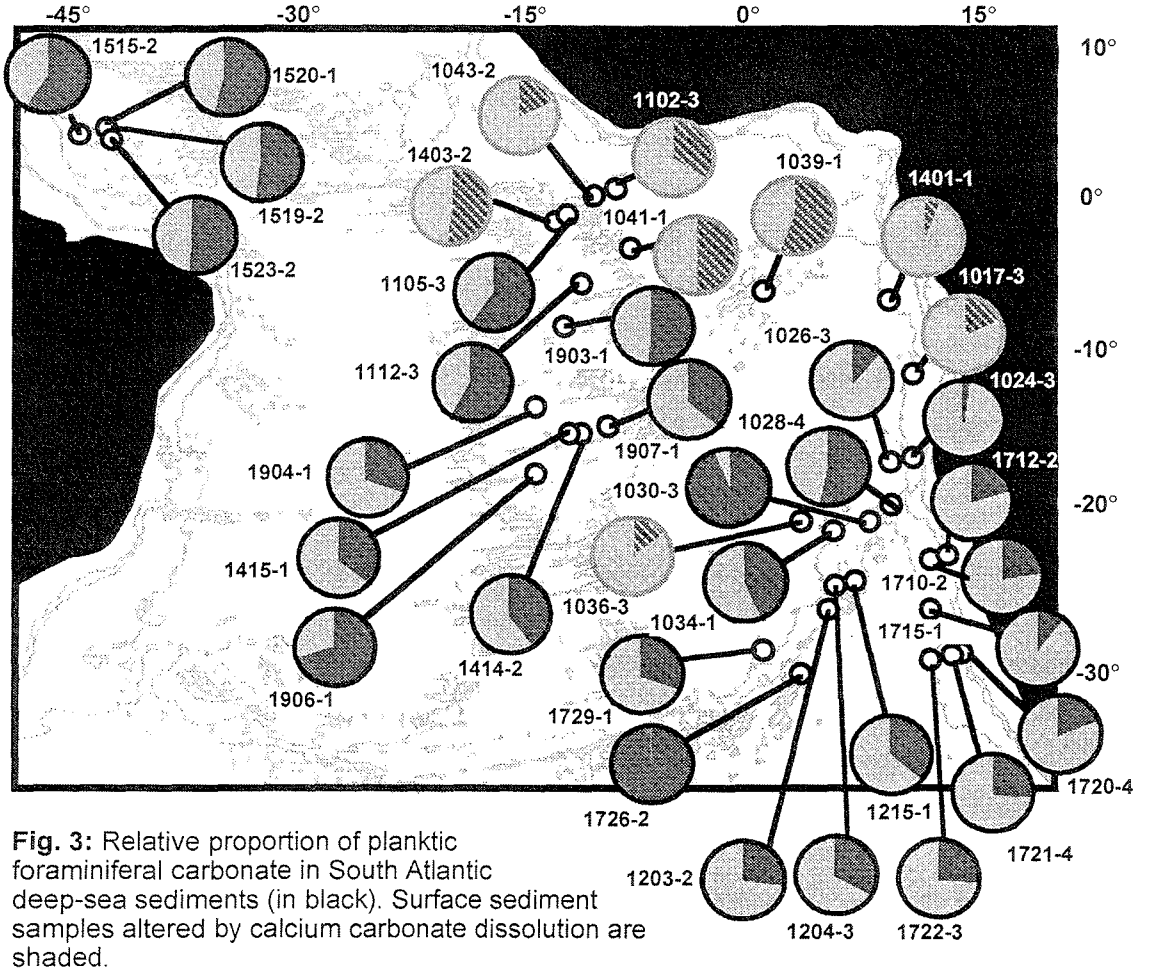

Fig. 3: Relative proportion of planktic foraminiferal carbonate in South Atlantic deep-sea sediments (in black). Surface sediment samples altered by calcium carbonate dissolution are shaded.

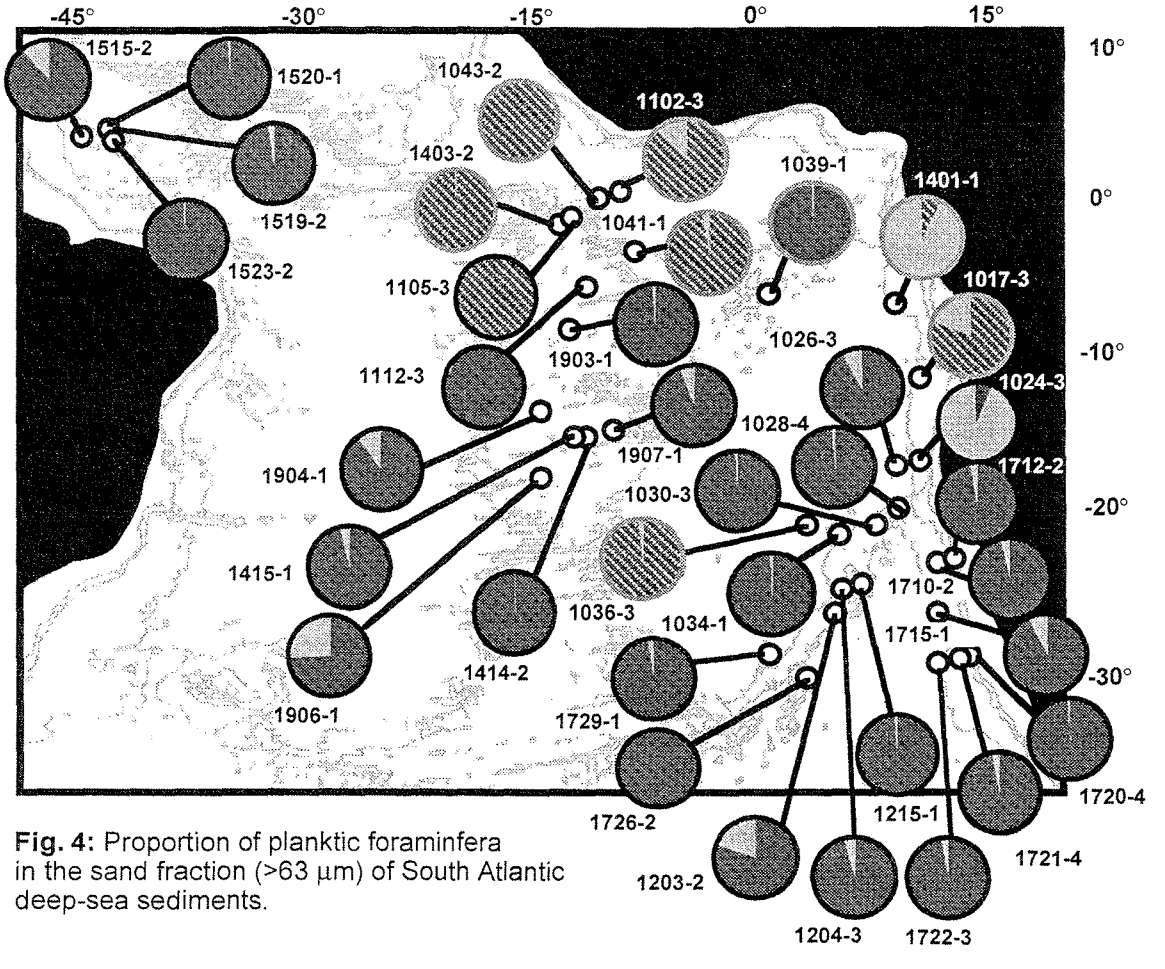

Fig. 4: Proportion of planktic foraminfera in the sand fraction (>63 µm) of South Atlantic deep-sea sediments.

The contribution of planktic foraminiferal carbonate to the total calcium carbonate accumulation on the sea-floor was determined from South Atlantic surface sediments by A. Volbers (contribution to the manuscript Baumann et al., in prep.). Fig. 3 shows the minimum contribution of planktic foraminiferal carbonate to calcareous deep-sea sediments. To calculate the minimum contribution of this microfossil group, investigations were restricted to the sand fraction (>63 µm) because of the small size and weight of juvenile planktic foraminifera in the silt fraction (2-63 µm). Although the proportion of planktic foraminiferal carbonate (in relation to 100% $CaCO_3$) is rather underestimated, it is the main constituent in the western equatorial Atlantic, of Mid-Atlantic Ridge sediments, and on parts of the Walvis Ridge. Its average contribution to South Atlantic total calcium carbonate is >40%, whereas it is at minimum on the eastern African continental margin where cold and nutrient-rich water upwell (<25%).

To get reliable estimations of planktic foraminiferal calcium carbonate production, dissolution in the water column and at the water-sediment interface should be minimal. For this reason, surface sediment samples that were significantly altered by calcium carbonate dissolution were marked by blue circles. As expected, these samples generally contain smaller percentages of planktic foraminiferal carbonate than samples from shallower water depth nearby. However, a massive decrease in planktic foraminferal carbonate is first observed >4500 m in the equatorial South Atlantic region.

2.1 Planktic foraminifera as paleo-environmental proxies

As shown in Fig. 3, planktic foraminifera are not only among the main contributors to total $CaCO_3$ in deep-sea sediments, they almost exclusively comprise the sand fraction (>63 µm) of surface sediment samples, even if they are significantly altered by calcium carbonate dissolution (Fig. 4). Their high relative abundance and good preservation potential make them ideal proxies. They are unicellular organisms which secrete low-Mg calcite tests in a varity of shapes up to 1 mm in size. Most species live in the upper 50 m of the ocean but some species, such as *Globorotalia scitula*, *Globorotalia crassaformis,* and *Hastigerina pelagica*, prefer water depth between 100 m and 300 m (e.g. Kemle-von Mücke and Oberhänsli, 1999). As environmental conditions in the surface water currents are reliably traced by the abundance of individual species (e.g. Thiede, 1975; Oberhänsli et al., 1992; Pflaumann et al., 1996; Niebler & Gersonde, 1998; Mix et al., 1999), they provide a useful tool for the reconstruction of past oceanic conditions.

Already 100 years ago it was recognized that the species distribution of planktic foraminifera is closely linked to surrounding water temperature (Murray and Renard, 1891; Murray, 1897) and that the oceans could be divided into five planktic foraminiferal provinces: tropical, subtropical, transition, subpolar, and polar (Bé and Tolderlund, 1971). When it became obvious, that recent and fossil planktic foraminiferal assemblages varied significantly over time, Imbrie and Kipp (1971) correlated

recent planktic foraminiferal assemblages with sea-surface temperatures (SSTs) to determine paleo SSTs. Within the CLIMAP project (1976, 1981, 1984) paleo SSTs of the world ocean were calculated for distinct time periods, such as the LGM.

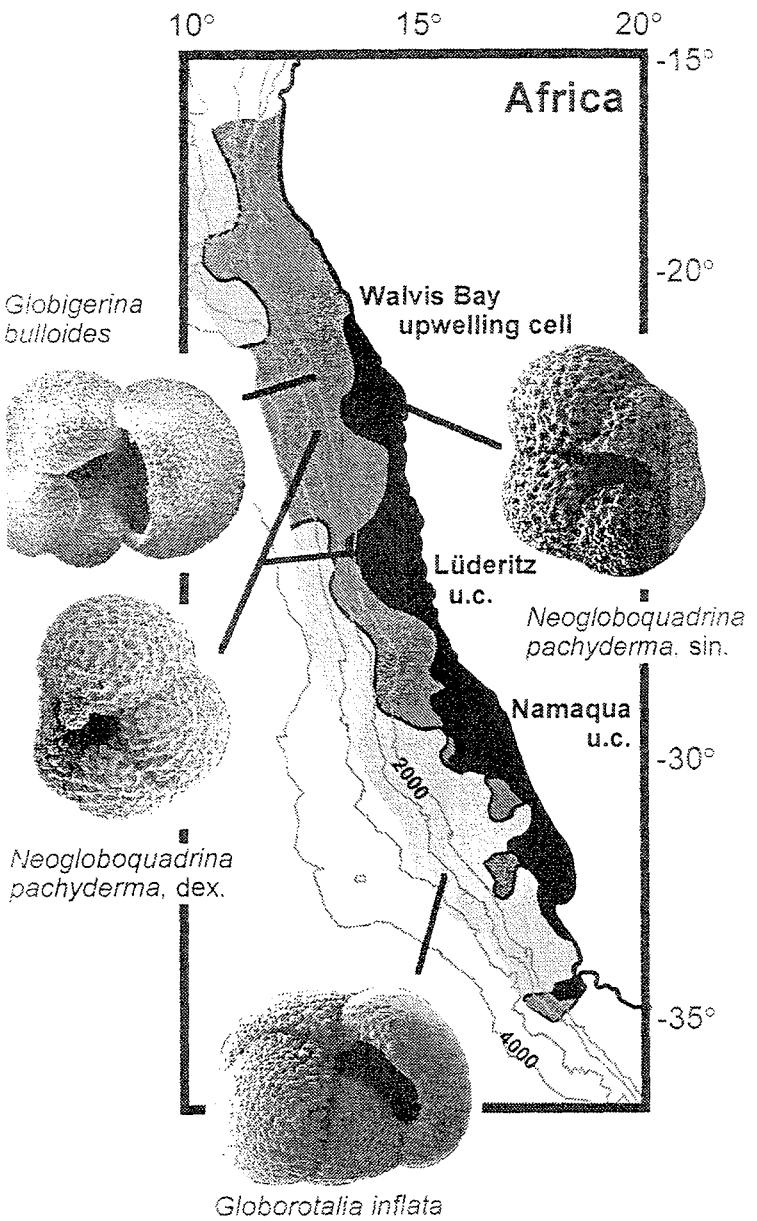

These micropaleontologic studies were mostly restricted to the tropics and subtropics. The factor model by Niebler and Gersonde (1998) covered the tropics and the high latitudes of the South Altantic with exception of the coastal upwelling regions (reconstructed paleo SSTs for the Benugela region would be <5°C during OIS 3; Volbers et al., 1999). This is because the upwelling fauna consits of *Neogloboquadrina pachyderma* sin. (Giraudeau, 1993; Ufkes and Zachariasse, 1993), which was previously regared as a typical polar species (e.g. Bé and Tolderlund, 1971). However, minor abundances of *N. pachyderma* sin. were also reported from the Oman and Somalia upwelling regions where its growth and reproduction seems to be tied to the upwelling period (Ivanova et al., 1999). Its massive occurrence in the Benguela coastal waters (Ufkes & Zachariasse, 1993) with maximum abundances of >80% in late Quaternary sediments, called PS events by Little et al. (1997a), was attributed to intensified upwelling, increased productivity, and lower sea surface temperatures in the Benguela region (Oberhänsli, 1991; Schmidt, 1992; Little et al., 1997a,b; Ufkes et al., 2000).

Fig. 5: Characteristic planktic foraminiferal species dominate the different hydrographic regimes of the Benguela upwelling region and were successfully used to reconstruct the extent of northern Benguela upwelling cells during the late Quaternary.

Recently, the Benguela upwelling system was covered by local factor models. The Benguela model builds upon the findings of Giraudeau and Rogers (1994) and was applied to seven gravity cores in the Benguela region (manuscript 4). *Neogloboquadrina pachyderma* (sinistral coiling) is found

almost exclusively in surface sediments beneath the modern Benguela coastal upwelling cells together with *N. pachyderma* (dextral coiling). In contrast, the more open-oceanic species *Globorotalia inflata* reflects the outer limits of the Benguela upwelling system. The eutrophic to mesotrophic regime in between is dominated by *Globigerina bulloides* and *N. pachyderma* dex. (Fig. 4). Investigations of gravity core material from this region (GeoB 1710-3) show that the same species dominate the planktic foraminiferal assemblages of the last 245.000 years (manuscript 4).

However, preferential dissolution of the more susceptible species is a potential problem when working with factor models (e.g. Niebler, 1995). Delicate species might be dissolved and increase the relative percentage of the more resistant ones (e.g. Ruddiman and Heezen, 1967; Berger et al., 1982). Secondary altered samples must be identified and excluded to obtain reliable results. Besides various conventional calcium carbonate dissolution proxies, such as the ratio of benthic to planktic foraminifera or the fragmentation index (see summary in manuscript 2, Part II), characteristic planktic foraminfera have been widely used as dissolution proxies (e.g. Henrich, 1986; Dittert and Henrich, 2000). Planktic foraminifera have relatively low species diversities but extraordinary high individual numbers compared to benthic foraminifera. In particular *Globigerina bulloides* lives in almost all different hydrographic regimes of the South Atlantic, making it the ideal proxy to determine the degree of calcium carbonate dissolution within a sample (Fig. 5).

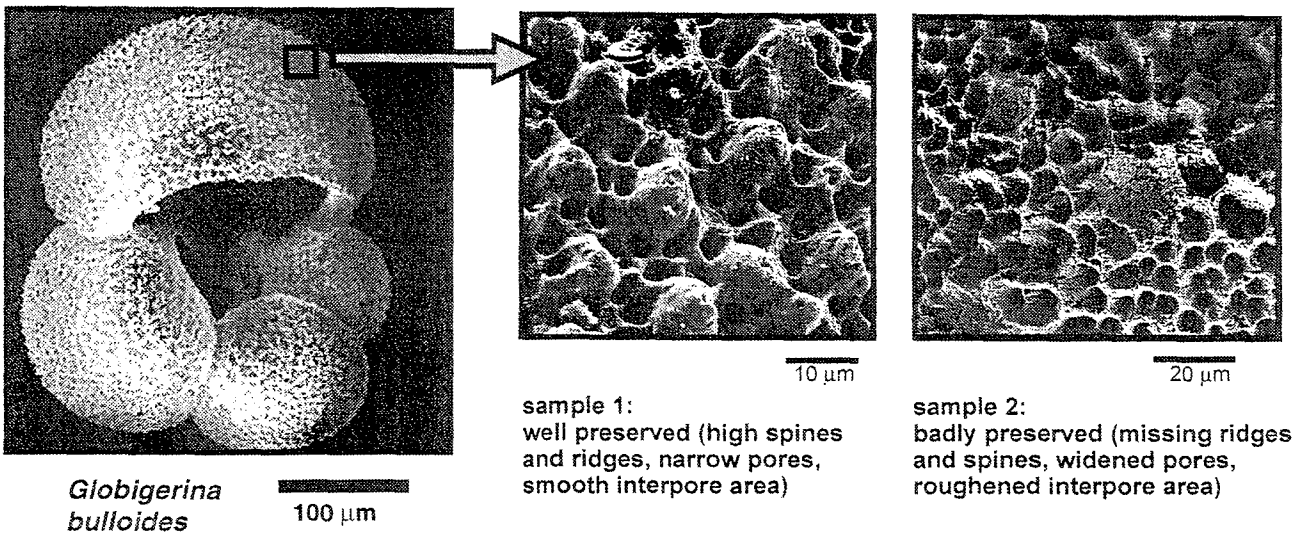

Fig. 6: a) SEM photo of *Globigerina bulloides* (overview). b) *G. bulloides* of sample 1 was recovered from shallow water depth whereas c) *G. bulloides* of sample 2 was taken from below the sedimentary calcite lysocline. Both specimen were investigated regarding their ultrastructural preservation features.

The calcareous tests of planktic foraminifera accumulate on the sea-floor and provide important paleoceanographic tools because of their calcium carbonate preservation potential (e.g. Berger,1979; Dittert and Henrich, 2000). Besides proxy data determined from benthic foraminifera, such as $\delta^{13}C$ and Ca/Cd (e.g. Curry and Lohmann, 1982; Boyle and Keigwin, 1987; Bickert and Wefer, 1996, 1999; Oppo and Horrowitz, 2000), dissolution indices which describe the ultrastructural preservation state of planktic foraminiferal tests (*N. pachyderma* index, Henrich,

1986; BDX', manuscript 1,2, Part II), serve as independent tools to reconstruct paleo water mass distributions (manuscript 3, Part II).

2.2 The marine calcium carbonate system

As emphasized by Schneider et al. (2000), the description of marine carbonates has always delt with the production of calcium carbonate and the biologically, physically and chemically mediated processes governing their distribution on the sea-floor. In this PhD thesis, calcium carbonate dissolution in South Atlantic sediments was investigated via several „classic" („conventional") dissolution proxies, such as the fragmentation index and the benthic to planktic foraminiferal ratio (manuscript 1 and 2, Part II), and an independent SEM index, the BDX' (manuscript 1-3, Part II). This study therefore concentrates on this complex topic from the sedimentological point of view and uses the concepts of the „sedimentary" lysocline („foram lysocline", „Peterson's level"; excellent summary is provided by Seibold and Berger, 1993) which is discussed in more detail in Part II.

Small changes in the chemistry of the ocean can attribute to a marked change in the atmospheric CO_2 reservoir. The exchange of CO_2 between the ocean and the atmosphere depends on the difference in partial pressure at the air/sea water interface. When the partial pressure of the atmosphere exceeds the partial pressure of the surface waters, CO_2 is taken up by the ocean. Besides the temperature dependent solubility of CO_2 in sea water, the capacity of the surface ocean to take up CO_2 is enhanced by the production and downward transport of organic carbon generated in the surface waters.

(1) Formation of organic carbon: $CO_2 + H_2O \Rightarrow CH_2O + O_2$

In contrast, the formation of calcium carbonate (particulate inorganic carbon, PIC) increases the partial pressure of the surface water CO_2 (PCO_2).

(2) Formation of carbonate: $Ca^{2+} + 2HCO_3^- \Rightarrow CaCO_3 + H_2O + CO_2$

A steady-state balance between the supply rate of calcium carbonate to the oceans and the alteration and removal of carbonate by burial in sediments determine the atmospheric CO_2 concentration on a timescale of thousands of years. The present-day production of $CaCO_3$ in the world ocean was estimated to be 5.3 billion tons per year (Milliman, 1993). 3.2 billion tons are supposed to accumulate in bottom sediments (Milliman, 1993) whereas the rest is dissolved in the water column or at the sea-floor.

(3) Dissolution of carbonate: $CaCO_3 + H^+ \Leftrightarrow Ca^{2+} + HCO_3^-$

$CaCO_3 + H_2CO_3 \Leftrightarrow Ca^{2+} + 2\,HCO_3^-$

According to Milliman (1993), the Atlantic accounts for more than 40% of the global deep-sea total carbonate accumulation because it is supposed to have an on average deep lysocline (Berger, 1968). Since calcareous sediments are dominated by calcite, the term „lysocline" commonly refers to the calcite lysocline. Nevertheless, around 10% of the total carbonate production consists of aragonite, a metastable polymorph of $CaCO_3$, mainly secreted by pteropods (Fabry, 1990; Berner and Honjo, 1981). The aragonite lysocline is therefore encountered at much shallower depth in the South Atlantic than the calcite lysocline (e.g. Gerhardt and Henrich, 2001).

Calcite solubility increases with water depth (pressure effect). One of the primary controls on the depth of the lysocline is the calcite saturation depth, the depth at which the carbonate ion concentration $[CO_3^{2-}]$ of the bottom water equals the $[CO_3^{2-}]$ at calcite saturation. Below this level, the water is undersaturated with respect to calcite and calcareous sediments dissolve. The preservation potential of calcareous sediments should be reduced when bathed by water masses with lower $[CO_3^{2-}]$ compared to NADW, such as AAIW and AABW.

However, investigations of surface sediment material reveal that significant calcite dissolution seems to occur in shallower depth (sedimentary lysocline) than predicted from hydrographic data (Emerson and Bender, 1981). Benthic flux chamber experiments and microelectrode measurements of pore waters suggest that calcium carbonate dissolves even in supersaturated waters (Archer et al., 1989; Hales et al., 1994; Jahnke et al., 1994). This „respiratory dissolution" („supralysoclinal dissolution") seems to be the result of biological mediation (Milliman, 1999). Much of the carbon that escapes the ongoing recycling process of the upper water column as organic matter is respired or reminieralized by benthic organisms in the sediment. The decay of organic material is expected to produce CO_2, to lower the $[CO_3^{2-}]$ in the pore waters, and to create a microenvironment that drives $CaCO_3$ dissolution even above the lysocline (Emerson and Bender, 1981; Archer, 1991; Jahnke et al., 1994).

(4) Dissolution of calcium carbonate due to CO_2 release from organic matter oxidation (taken from Schneider et al., 2000):

$$(CH_2O)_{106}(NH_3)_{16}(H_3PO_4) + 138\ O_2 + 124\ CaCO_3 \Rightarrow 230\ HCO_3^- + 16\ NO_3^- + HPO_4^{2-} + 124\ Ca^{2+} + 16\ H_2O$$

The onset of $CaCO_3$ dissolution in the sediments may occur 0.5 to 1 km above the chemical saturation horizon in the ocean water (Emerson and Bender, 1981; Milliman, 1993) or even shallower (manuscript 2, Part II). A decoupling of the sedimentary lysocline from the calcium carbonate saturation horizon is expected to occur in high-productivity regions because of the increased supply of organic material to surface sediments. However, studies in the South Atlantic reveal that it is not limited to the Benguela region but also seems to occur in regions with low sedimentation rates (manuscript 2, Part II).

As critizied by Emerson and Bender (1981) models used to explain the relationship between calcite saturation in the oceans and the preservation of calcareous sediments have not considered the effect of metabolic CO_2 generated at the sediment water interface. A change in the relative rates at which organic carbon and $CaCO_3$ are deposited on the sea floor should drive a compensating change in ocean pH. When the organic-carbon-driven dissolution is taken into account, a 40% decrease in the calcite deposition rate would be enough to decrease the atmposheric CO_2 concentration to the glacial value (Archer and Maier-Reimer, 1994).

To correctly interprete the accumulation of calcium carbonate in sediments over time, e.g. Catubig et al. (1998) tried to determine the global deep-sea burial rate of calcium carbonate during the LGM, we need to understand what drives calcium carbonate dissolution. As emphasized by Martin and Sayles (1996), calcite dissolution driven by organic matter oxidation may mask the effects of variations in surface water $CaCO_3$ productivity and bottom water chemistry on the accumulation rate of $CaCO_3$ in deep-sea sediments. The observation, that the level of equal preservation (the position of the modern sedimentary calcite lysocline) does not necessarily follow the level of equal calcite saturation in the water column, is of great importance when reconstructing the calcite lysocline during the LGM (manuscript 3, part II).

But how to quantify the local impact of respiratory dissolution on calcareous deep-sea sediments? The development of in situ benthic flux chambers and in situ microelectrode profilers (Archer et al., 1989; Berelson et al, 1990; Jahnke et al., 1994; Hales et al., 1994) has increased our knowledge about local $CaCO_3$ dissolution rates. In situ measurements from the Ceara Rise indicate that 36% to 66% of the calcium carbonate deposited at sites at and above the saturation horizon is lost (Martin and Sayles; 1996). These estimates exceed $CaCO_3$ dissolution rates in the order of 20% to 40% as postulated by Emerson and Archer (1990) and Jahnke et al. (1994). Even higher rates were reported from the continental slope off Gabon: The work of Pfeifer et al. (in prep.) based on in situ microsensor measurements of O_2, pH, pCO_2 and Ca^{2+}, suggests around 90% redissolution of the calcite flux to the sediment at intermediate water depth.

3. Material and methods

All sediment samples investigated in this study were collected during various R/V Meteor and Polarstern cruises throughout the Atlantic Ocean. The study area stretches from 30°N to 40°S with a detailed focus on the South Atlantic Ocean. The investigated sediments contain high abundances of planktic foraminifera from all different hydrographic regimes of the South Atlantic, such as eutrophic coastal and equatorial upwelling regimes and mesotrophic and oligotrophic regions with additional input of terrestrial material.

3.1 Sediment surface samples

Surface sediments were obtained using a multiple corer (MUC) or a giant box corer (GKG). They were sectioned into 1 cm samples and stored at either 4°C or -18°C.

3.1.1 Planktic foraminiferal carbonate determination in South Atlantic surface sediments

Surface sediment material was weighed and wet-sieved to separate the fine (<63µm) from the coarse fraction (>63µm) which was then dried and weighed. To determine the weight of the calcareous fraction of a surface sample, $CaCO_3$ data were obtained from the PANGAEA-database (www.pangaea.de) and from T. Wagner and P. Müller (unpubl. data) and multiplied with the sample weight (bulk sediment material). The main assumption made when calculating the percentage of planktic foraminiferal carbonate on the total $CaCO_3$ content ($CaCO_3$=100%) of a deep-sea sediment samples fraction is that the majority of planktic foraminifera is concentrated in the sand fraction.

To determine the percentage of planktic foraminifera within the sand fraction, the sand fraction was split into subsamples and all planktic foraminifera and their fragments were counted. The weight of the sand fraction was multiplied with the percentage of planktic foraminifera in the sand fraction to determine the weight of the planktic foraminferal carbonate of the sample. Finally, the weight of the planktic foraminiferal carbonate was divided by the weight of the calcareous fraction of the sample and yielded the percentage of planktic foraminiferal carbonate in the total $CaCO_3$ content of a sediment surface sample. The calculated planktic foraminiferal carbonate must be treated as a minimum value because juvenile planktic foraminifera and small fragments are primarily found in the silt fraction. They were excluded from this calculation because extraordinarily high species numbers would have been needed to determine the weight of planktic foraminifera in this fraction.

3.1.2 Calcium carbonate preservation of Atlantic surface samples

The main focus of this study is the spatial and temporal distribution of calcareous deep-sea sediments within the South Atlantic Ocean. 193 surface samples from the Atlantic Ocean were examined for their calcium carbonate preservation potential. For the determination of dissolution stages based on planktic foraminiferal ultrastructural breakdown, 30 *G. bulloides* specimen per sample were hand-picked from the >125µm fraction, glued to a SEM stub, and gold coated. The chambers were investigated at 3,000x magnification to study *G. bulloides* ultrastructure (spines, ridges, interpore areas, and pores) in detail with a ZEISS DSM 940 A (10 mm working distance, 10 kN accellerating voltage). The BDX' is characterized by six stages of preservation (worsening from 0 to 5), which are described and illustrated in more detail in manuscript 2, part II. Via the BDX' preservation curve pattern, the positions of the modern sedimentary calcite lysoclines of all South Atlantic deep-sea basin and continental margins were determined.

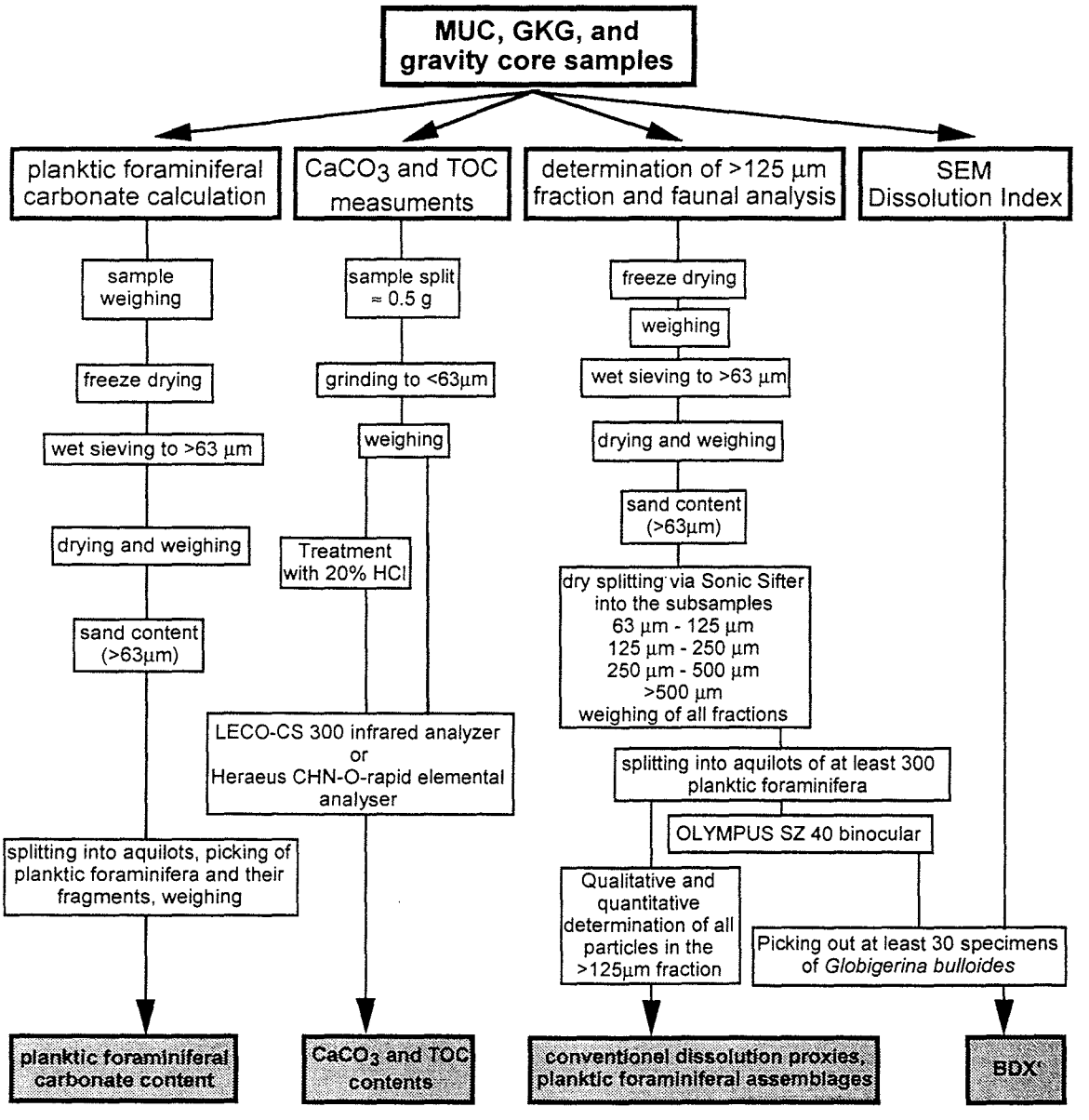

Fig. 7: Flow-chart of all methods used. Investigations of the sand fraction were carried out under a OLYMPUS 40 binocular whereas the ultrastructural preservation states of *G. bulloides* tests were completed by SEM investigations. To determine the bulk carbonate content (%-$CaCO_3$) and total organic carbon content (TOC) sediment samples were analyzed using a LECO infrared analyser and a Heraeus elemental analyser.

3.2 LGM samples

3.2.1. Calcium carbonate preservation of selected South Atlantic LGM samples

The LGM was defined as the 23 to 19 ka calendar age period (or 19.5-16.1 ka corrected ^{14}C age) at the first EPILOG workshop in May 1999 in Delmenhorst. To gain further information on the South Atlantic during the LGM, 48 core locations were chosen for detailed investigation at Bremen University. The stratigraphic control in all investigated cores is based on either oxygen isotope stratigraphy or ^{14}C measurements. Further details on stratigraphy are given in Niebler et al. (subm.). LGM material was wet-sieved to separate the fine from the coarse fraction which was then dried and weighed. Whenever available, 30 *G. bulloides* from the LGM coarse fraction were investigated

to determine the position of the sedimentary calcite lysocline in the South Atlantic deep sea basin and coastal regions. They were hand-picked, glued to a SEM stub, and gold coated for SEM investigation as described in section 3.1, further details are provided in manuscript 3 (Part II).

3.3 Gravity cores

Gravity core GeoB 1710-3 was recovered from the continental slope off Namibia during R/V Meteor cruise M20/2 (23.43°S, 11.7°E). 1045 cm core material were taken from 2987 m water depth (Schulz et al., 1992). Oxygen isotope analyses from the benthic foraminifera *Cibicidoides wuellerstorfi* provide the basic stratigrapic framework for the core (Bickert and Wefer, 1999). For micropaleontological investigations, all samples were freeze-dried, weighed, and washed through a 63 µm sieve. The samples were then dry-sieved and splitted into the fractions 63-125 µm, 125-250 µm, 250-500 µm, and >500 µm.

3.3.1. Determination of the >125 µm fraction of GeoB 1710-3 samples

The fraction >125 µm was investigated under a OLYMPUS SZ 40 microscope. All particles of an aquilot of at least 300 particles were counted to determine the relative percentages of each particle group. These data were used to calculate several conventional dissolution indices, such as the fragmentation index, the benthic to planktic foraminiferal ratio, the radiolaria to planktic foraminifera ratio, and the planktic foraminiferal number. Additionally, the relative percentage of resistant planktic foraminifera, sponge spiculae, and pellets were tested as dissolution proxies. All proxies used in this study were introduced and discussed in detail in manuscript 1.

3.3.2 Determination of planktic foraminifera species of GeoB 1710-3 samples

To monitor the Benguela upwelling intensity over the last 245 kyrs, census counts of planktic foraminifera were carried out. All samples were split into subsamples using a microsplitter. A minimum of at least 300 non-fragmented planktic foraminiferal specimen were identified using an OLYMPUS SZ 40 microscope. All planktic foraminiferal species were identified using the taxonomic concepts of Hemleben et al. (1989). For the purpose of this paper, right-coiling *N. pachyderma* and *N. pachyderma-N. dutertrei* intergrates (PDI) were grouped as *N. pachyderma* dex. whereas species with a wider opening and at least five chambers were counted as *N. dutertrei*.

Since an ideal reference data set consisting of 135 surface samples from the southwest African coastal upwelling area off SW Africa was made available by Giraudeau and Rogers (1994) and Niebler (1995), a factor model for the Benguela region could be created. The transfer function was calculated with the program package CABFAC of Klovan & Imbrie (1971) and Imbrie & Kipp (1971) (for details see manuscript 4, Part II). Q-mode factor analysis was completed in order to define a transfer function for the estimations of past SSTs according to the statistical method developed by Imbrie & Kipp (1971). The Benguela factor model consists of three planktic foraminiferal assemblages, called „factors", which explain 95,3% of the total variance. The equation „F135-15-3" (135 surface samples, 15 taxa, 3 factors) was developed for paleotemperature reconstruction.

Foraminiferal assemblages of GeoB 1710-3, RC13-229 (25.30°S/11.18°E), and five cores from Walvis Ridge (GeoB 1220-1, 24.03°S/5.31°E; GeoB 1032-3, 22.92°S/6.04°E; GeoB 1031-4, 21.88°S/7.10°E; GeoB 1028-5, 20.11°S/9.19°E; DSDP 532, 19.44°S/10.31°E) were then compared with the Benguela factor model and spatial and temporal extent of northern Benguela upwelling cells were reconstructed (manuscript 4, part II).

3.3.3 Calcium carbonate preservation of GeoB 1710-3 samples

To validate the results of the conventional proxies introduced in manuscript 1 (part II), the BDX' proxy was carried out on each sample. In order to do this, at least 30 *G. bulloides* were investigated as described in 3.1 and manuscript 2 (part II).

4. References

Archer, D, 1991. Modeling the calcite lysocline, J. Geophys. Res. 96 (17), 17037-17050.

Archer, D., Emerson, S. and Reimer, C., 1989. Dissolution of calcite in deep-sea sediments: pH and O_2 microelectrode results. Geochimica et Cosmochimica Acta 53, 2831-2845.

Archer, D.E. and Maier-Reimer, E., 1994. Effect of deep-sea sedimentary calcite preservation on atmospheric CO_2 concentration. Nature 367, 260-264.

Austin, W.E.N. and Evans, J.R., 2000. Benthic foraminifera and sediment grain size variability at intermediate water depths in the Northeast Atlantic during the late Pliocene-early Pleistocene. Marine Geology 170, 423-441.

Bainbridge, A.E., 1981. GEOSECS Atlantic Expedition, Hydrographic Data, 1972-1973. National Science Foundation, Superintendent of Documents, US Government Printing Office, Washington DC, pp. 1-121.

Baumann, K.-H., Böckel, D., Dittert, N., Donner, B., Esper, O., Gerhardt, S., Henrich, R., Kinkel, H., Vink, A., Volbers, A. Willems, H., Zonneveld, K. (in prep.). Contribution of calcareous plankton groups to the carbonate budget of South Atlantic surface sediments.

Bé, A. W.H. and Tolderlund, D.S., 1971. Distribution and ecology of living planktonic foraminifera in surface waters of the Atlantic and Indian Oceans, in The micropaleontology of oceans, edited by Funnell, D.M. and Riedel, W.R., pp. 105-149, Cambridge University Press, Cambridge.

Berelson, W.M, Hammond, D.E., O'Neill, D. Chu, X.-M., Chin, C., and Zuckin, J., 1990. Benthic fluxes and pore water studies from sediments of the central equatorial Pacific: nutrient diagenesis. Geochimica et Cosmochimica Acta 54, 3001-3012.

Berger, W.H., 1968. Planktonic foraminifera: selective solution and paleoclimatic interpretation, Deep-Sea Res. 15, 31-43.

Berger, W.H.,1979. Preservation of foraminifera. In Foraminiferal ecology and palecology., edited by Lipps, J.H., Berger, W.H., Buzas, M.A., Douglas, R.G., Ross, C.A., pp. 105-155, Society of Economic Paleontologists and Mineralogists, Houston.

Berger, W.H., Bonneau, M.-C., and Parker, F.-L., 1982. Foraminifera on the deep-sea floor: lysocline and dissolution rate. Oceanol. Acta 5 (2), 249-258.

Berner, R.A. and Honjo, S., 1981. Pelagic sedimentation of aragonite: its geochemical significance. Science 211, 940-942.

Bickert, T., 1992. Rekonstruktion der spätquartären Bodenwasserzirkulation im östlichen Südatlantik über stabile Isotope benthischer Foraminiferen. Berichte aus dem Fachbereich Geowissenschaften der Universität Bremen, vol. 27, 205 pp.

Bickert, T. and Wefer, G., 1996. Late Quaternary deep water circulation in the South Atlantic: Reconstruction from carbonate dissolution and benthic stable isotopes, in The South Atlantic: Present and past circulation, edited by Wefer, G., Berger, W.H., Siedler, G., and Webb, D.J., pp. 599-620, Springer, Berlin, Heidelberg.

Bickert, T. and Wefer, G., 1999. South Atlantic and benthic foraminifer $\delta^{13}C$-deviations: Implications for reconstructing the Late Quaternary deep-water circulation, Deep-Sea Res., 46, 437-452.

Boyle, E. and Keigwin, L.D., 1987. North Atlantic thermohaline circulation during the past 20,000 years linked to high-latitude surface temperature. Nature 30, 35-40.

Broecker, W.S., 1991. The great ocean conveyor. Oceanogr. 4, 79-89.

Broecker, W.S., 1997. Thermohaline circulation, the Achilles heel of our climate system: Will man made CO_2 upset the current balance? Science 278. 1582-1588.

Broecker, W.S., Peteet, D.M., and Rind, D., 1985. Does the ocean-atmosphere system have more than one stable mode of operation? Nature 315, 21-26.
Catubig, N.R., Archer, D.E., Francois, R., deMenocal, P, Howard, W., and Yu, E.-F., 1998. Global deep-sea burial rate of calcium carbonate during the last glacial maximum. Paleoceanography 13 (3), 298-310.
CLIMAP Project Member, 1976. The surface of the ice-age Earth. Science 191, 1131-1137.
CLIMAP Project Member, 1981. Seasonal reconstructions of the Earth's surface at the last glacial maximum. Geol. Soc. Am, GSA Map and Chart Ser. MC-36, Boulder, Colorado, 18 pp.
CLIMAP Project Member, 1984. The last interglacial Ocean. Quat. Res 21, 123-224.
Currie, R., 1953. Upwelling in the Benguela Current. Nature 171, 497-500.
Curry, W.B., Duplessy, J.C., Labeyrie, L.D., and Shackleton, N.J., 1988. Changes in the distribution of $\delta^{13}C$ of deep water ΣCO_2 between the last glaciation and the Holocene. Paleoceanography 3, 317-341.
Curry, W.B. and Lohmann, G.P., 1982. Carbon isotopic changes in benthic foraminifera from the western South Atlantic: reconstruction of glacial abysal circulation patterns. Quaternary Research 18, 218-235.
Dickson, R.R. and Brown, J., 1994. The production of North Atlantic Deep Waters: Sources, rates and pathways. J. Geophys. Res. 99 (C6), 12319-12341.
Dittert, N. and Henrich, R., 2000. Carbonate dissolution in the South Atlantic Ocean: evidence from ultrastructure breakdown in *Globigerina bulloides*. Deep-Sea Res. I 47, 603-620.
Duplessy, J.C., Shackleton, N.J., Fairbanks, R.G., Labeyrie, L., Oppo, D., and Kallel, N., 1988. Deepwater source variation during the last climateic cycle and their impact on global deepwater circulation. Paleoceanography 3, 343-360, 1988.
Emerson, S. and Archer, E., 1990. Calcium carbonate preservation in the ocean. Phil Trans R Soc Lond A 331, 29-40.
Emerson, S. and Bender, M., 1981. Carbon fluxes at the sediment-water interface of the deep-sea: calcium carbonate preservation. J. Mar. Res. 39, 139-162.
Fabry, V.J., 1990. Shell growth rates of pteropod and heteropod molluscs and aragonite production in the open ocean: implications for the marine carbonate system. Journal of Marine Research 48, 209-213.
Faugères, J.C., Mézerais, M.L., Stow, D.A.V., 1993. Contourite drift types and their distribution in the North and South Atlantic Ocean basins. Sedimentary Geology 82, 189-203.
Fichefet, T., Hovine, S., and Duplessy, J. C.A., 1994. A model study of the Atlantic thermohaline circulation during the last glacial maximum. Nature 372, 252-255.
Ganachaud, A. and Wunsch, C., 2000. Improved estimates of global ocean circulation, heat transport and mixing from hydrographic data. Nature 408, 453- 457.
Ganopolski, A., Rahmstorf, S., Petoukhow, V., and Claussen, M., 1998. Simulation of modern and glacial climates with a coupled global model of intermediate complexity. Nature 391, 351-356.
Gerhardt, S. and Henrich, R. (2001). Shell preservation of Limacina inflata (Pteropoda) in surface sediments from the Central and South Atlantic Ocean: a new proxy to determine the aragonite saturation state of water masses. Deep-Sea Res. I 48 (9), 2051-2071.
Georgi, D.T., 1979. Modal properties of Antarctic Intermediate Water in the southeast Pacific and the South Atlantic. J. Phys. Oceanogr. 9, 456-468.
Giraudeau, J., 1993. Planktonic foraminiferal assemblages in surface sediments from the southwest African continental margin. Mar. Geol., 110, 47-62.
Giraudeau, J. and Rogers, J., 1994. Phytoplankton biomass and sea-surface temperature estimates from sea-bed distribution of nannofossils and planktonic foraminifera in the Benguela upwelling system. Micropaleontology 40(3), 275-285.
Gordon, A.L., 1986. Interocean exchange of thermocline water. J. Geophys. Res. 91, 5037-5046.
Gordon, A.L., Weiss, R.F., Smethie, W.M. Jr., and Warner, M.J., 1992. Thermocline and intermediate water communication between the South Atlatnic and Indian Oceans. J. Geophys. Res. 97 (C5), 7223-7240.
Hales, B., Emerson, S., and Archer, D., 1994. Respiration and dissolution in the sediments of the western North Atlantic: estimates from models of in situ microelectrode measurements of pore water oxygen and pH. Deep-Sea Res. 41(4), 695-719.
Hart, T.J. and Currie, R.I., 1960. The Benguela Current. Discovery Report 31, 123-298.
Hemleben, C., Spindler, M., and Anderson, O.R., 1989. Modern planktonic foraminifera, pp. 363. Springer, New York.
Henrich, R., 1986. A calcite dissolution pulse in the Norwegian-Greeland Sea during the last deglaciation. Geol. Rundsch. 75, 805-827.
Imbrie, J. and Kipp, N.G., 1971. A new micropaleontological method for quantitative paleoclimatology: Application to a late Pleistocene Caribbean core. In The late Cenozoic glacial ages, edited by Turekian, K.K., pp. 71-181, Yale Univ. Press, New Haven.
Ivanova, E.M., Conan, S.M.-H., Peeters, F.J.C., and Troelstra, S.R., 1999. Living *Neogloboquadrina*

pachyderma sin and its distribution in the sediments from Oman and Somalia upwelling areas. Marine Micropaleontolgy 36, 91-107.

Jahnke, R.A., Craven, D.B., and Gaillard, J.-F., 1994. The influence of organic matter diagenesis on $CaCO_3$ dissolution at the deep-sea floor. Geochimica et Cosmochimica Acta 58 (11), 2799-2809.

Kemle-von Mücke, S. and Oberhänsli, H., 1999. The distribution of living planktic foraminifera in relation to Southeast Atlantic Oceanography, in Use of proxies in paleoceanography: examples from the South Atlantic, edited by Fischer, G. and Wefer, G., pp. 91-115. Springer-Verlag, Berlin, Heidelberg.

Klovan, J.E. and Imbrie, J., 1971. An algorithm and FORTRAN IV Program for large scale Q-mode factor analysis and calculation of factor scores. Mathematical Geology 3, 61-77.

Little, M.G., Schneider, R.R., Kroon, D., Price, B., Bickert, T., and Wefer, G., 1997a. Rapid palaeoceanographic changes in the Benguela Upwelling System for the last 160,000 years as indicated by abundances of planktonic foraminifera. Palaeogeogr., Palaeoclimat., Palaeoecol.130, 135-161.

Little, M.G., Schneider, R.R., Kroon, D., Price, B., Summerhayes, C.P., and Segl, M., 1997b. Trade wind forcing of upwelling, seasonality, and Heinrich events as a response to sub-Milankovitch climate variability. Paleoceanography 12(4), 568-576.

Macdonald, A.M. and Wunsch, C., 1996. An estimate of global ocean circulation and heat fluxes. Nature 382, 436-439.

Manabe, S. and Stouffer, R.J., 1988. Two stable equilibra of a coupled ocean-atmophere mode. J. Clim. I, 841-866.

Marotzke, I. and Stone, R.H., 1995. Atmospheric transports, the thermohaline cirulation, and flux adjustments in a simple coupled model. J. Phys. Oceanogr. 25, 1350-1364.

Martin, W.R. and Sayles, F.L., 1996. $CaCO_3$ dissolution in sediments of the Ceara Rise, western equatorial Atlantic. Geochimica et Cosmochimica Acta 60 (2), 243-263.

Mc Intyre, Ravelo, A.C., and Delaney, M.L., 1999. North Atlantic Intermediate Waters in the late Pliocene to early Pleistocene. Paleoceanography 14(3), 324-335.

Mercier, H., Speer, K.G., and Honnorez, J., 1994. Flow pathways of bottom water through the Romanche and Chain Fracture Zones. Deep-Sea Res. 41(10), 1457-1477.

Miliman, J.D., 1993. Production and accumulation of calcium carbonate in the ocean: budget of a nonsteady state. Global Biogeochemical cycles 7(4), 927-957.

Milliman, J.D., Troy, P.J., Balch, W.M., Adams, A.K., Li, Y.-H., and Mackenzie, F.T., 1999. Biologically mediated dissolution of calcium carbonate above the chemical lysocline? Deep-Sea Res. I 46, 1653-1669.

Mix, A.C. and Morey, A.E., 1996. Climate feedback and Pleistocene variations in the Atlantic South Equatorial Current. In The South Atlantic: present and past circulation, edited by Wefer, G., Berger, W.H., Siedler, G., and Webb, D.J., pp. 503-525, Springer, Berlin, Heidelberg.

Mix, A. C., Morey, A. E., Pisias, N. G., and Hostetler, S. W., 1999. Foraminiferal faunal estimates of paleotemperature: Circumventing the no-analog problem yields cool ice age tropics. Paleoceanography 14(3), 350-359.

Murray, J., 1897. On the distribution of the pelagic foraminifera at the surface and on the floor of the ocean. Nat. Sci 11, 17-27.

Murray, J. and Renard, A.F., 1891. Deep-sea deposits based on the speciments collected during the voyage of H.M.S. Challenger in the years 1872-1876. Reports Voyage Challenger, London, 525 pp.

Niebler, H.-S., 1995. Rekonstruktion von Paläo-Umweltparametern anhand von stabilen Isotopen und Faunen-Vergesellschaftungen planktischer Foraminiferen im Südatlantik. Berichte zur Polarforschung, vol. 167, pp. 198.

Niebler, H.-S. and Gersonde, R., 1998. A planktic foraminiferal transfer function for the southern South Atlantic Ocean, Marine Micropaleontology 34, 213-234.

Niebler, H.-S., Mulitza, S., Donner, B., Arz, H., Pätzlold, J., and Wefer, G., subm. Sea-surface temperatures in the equatorial and south Atlantic Ocean during the Last Glacial Maximum (23-19 ka). Submitted to Paleoceanography.

Oberhänsli, H., 1991. Upwelling signals at the Northeastern Walvis Ridge during the past 500,000 years. Paleoceanography, 6(1), 53-71.

Oberhänsli, H., Bénier, C., Meinecke, G., Schmidt, H., Schneider, R., and Wefer, G., 1992. Planktonic foraminifers as tracers of ocean currents in the eastern South Atlantic. Paleoceanography 7(5), 607-632.

Oppo, D.W. and Horowitz, M., 2000. Glacial deep water geometry: South Atlantic benthic forminiferal Cd/Ca and $\delta^{13}C$ evidence. Paleoceanography 15 (2), 147-160.

Peterson, R.G. and Stramma, L., 1991. Upper-level circulation in the South Atlantic Ocean. Prog. Oceanog. 26, 1-173.

Pflaumann, U., Dupra, J., Pujol, C., and L. Labeyrie, 1996. SIMMAX: A modern analog technique to deduce Atlantic sea surface temperatures from planktonic foraminifera in deep-sea sediments. Paleoceanography 11, 15-35.

Pfeifer, K., Hensen, C., Adler, M., Wenzhöfer, F., Weber, B., and Schulz, H.D., in prep. Modeling of subsurface calcite dissolution regarding respiration and reoxidation processes of marine sediments in the equatorial upwelling off Gabon.

Piola, A. and Georgi, D., 1982. Circumpolar properties of Antarctic Intermediate Water and Subantarctic Mode Water. Deep Sea Res. 29, 687-711.

Rahmstorf, S., 1991. A zonal-averaged model of the ocean's response to climatic change. J. Geophys. Res. 96, 6951-6963.

Rahmstorf, S., 1997a. Risk of sea-change in the Atlantic. Nature 388, 825-826.

Rahmstorf, S., 1997b. Climate Impact Research: Why, How and When? Talk at the Symposion Berlin-Brandenburg Academy of Sciences and German Academy Leopoldina Berlin, 28.10.1997 (http://www.pik-potsdam.de/~stefan/Lectures/list.html).

Rahmstorf, S. and Ganoposky, A., 1997. Simple theoretical model may explain apparent climate instability. J. Clim. 12, 1349-1352.

Reid, J.L, 1989. On the total geostrophic circulation of the South Atlantic Ocean: flow pattern, tracers, and transports. Prog. of Oceanography 23 (3), 149-244.

Reid, J.R., 1996. On the circulation of the South Atlantic Ocean. In The South Atlantic: Present and past circulation, edited by Wefer, G., Berger, W.H., Siedler, G., and Webb, D.J., pp. 13-44, Springer, Berlin, Heidelberg.

Rintoul, S.R., 1991. South Atlantic interbasin exchange. J. Geophys. Res. 96, 2675-2692.

Roemmich, D. and Wunsch, C, 1985. Two transatlantic sections: meridional circulation and heat flux in the subtropical North Atlanic Ocean. Deep Sea Res. 32, 619-664.

Ruddiman, W.F. and Heezen, B.C., 1967. Differential solution of planktonic foraminifera. Deep-Sea Res. 14, 801-808.

Sarnthein,M., Winn, K., Jung, S.J.A., Duplessy, J.C., Labeyrie, L.D., Erlenkeuser, H., and Ganssen, G., 1994. Changes in East Atlantic deepwater circulation over the last 30,000 years: eight time slice reconstructions. Paleoceanography 9, 209-267.

Sarnthein, M, Stattegger, K., Dreger, D., Erlenkeuser, H., Grootes, P., Haupt, B.J., Jung, S., Kiefer, T., Kuhnt, W., Pflaumann, U., Schäfer-Neth, C., Schulz, H., Schulz, M. Seidov, D., Simstich, J., van Kreveld, S., Vogelsang, E., Völker, A., and Weinelt, M., 2001. Fundamental modes and abrupt changes in North Atlantic circulation and climate over the last 60 ky- concepts, reconstruction and numerical modeling, in The northern North Atlantic, edited by Schäfer, P., Ritzrau, W., Schlüter, M., and Thiede, J., pp. 365-410. Springer, Berlin, Heidelberg, New York.

Schmidt, H., 1992. Der Benguela-Strom im Bereich des Walfisch-Rückens im Spätquartär, Berichte aus dem Fachbereich Geowissenschaften der Universität Bremen, vol. 28, pp. 172.

Schlitzer, R., 1996. Mass and heat transport in the South Atlantic derived from historical hydrographic data, in The South Atlantic: Present and Past Circulation, edited by Wefer, G., Berger, W.H., Siedler, G., and Webb, D.J., pp. 305-323, Springer, Berlin, Heidelberg.

Schneider, R.R., Schulz, H.D., and Hensen, C., 2000. Marine carbonates: their formation and destruction, in Marine geochemistry, edited by Schulz, H.D. and Zabel, M., pp. 283-307, Springer, Berlin, Heidelberg, New York.

Schulz, H.D., Beese, D., Breitzke, L., Brück, B., Brügger, B., Dahmke, A., Dehning, D., Diekampf, V., Donner, B., Ehrhardt, I., Gerlach, H., Giese, M., Glud, R., Gumprecht, R., Gundersen, J., Henning, R., Hinrichs, S., Petermann, H., Richter, M., Sagemann, J., Schmidt, W., Schneider, R., Scholz, M., Segl, M., Werner, U., and Zabel M., 1992. Bericht und erste Ergebnisse über die Meteor-Fahrt M20/2. Abidjan - Dakar, 27.12.1991-3.2.1992. Berichte aus dem Fachbereich Geowissenschaften der Universität Bremen, Vol. 25, pp. 173.

Seibold, E. and Berger, W.H.,1993. The sea floor. Springer, 356 pp.

Shannon, L.V. and Chapman, P., 1991. Evidence of Antarctic Bottom Water in the Angola Basin at 32°S. Deep-Sea Res. 38 (10), 1299-1304.

Siedler, G., Müller, T.J., Onken, R., Arhan, M., Mercier, H., King, B.A., and Saunders, P.M.,, 1996. The Zonal WOCE Sections in the South Atlantic, in The South Atlantic: Present and past circulation, edited by Wefer, G., Berger, W.H., Siedler, and Webb, D.J., pp. 83-104, Springer, Berlin, Heidelberg.

Smethie, W.M., Jr. and Fine, R.A., 2001. Rates of North Atlantic Deep Water formation calculated from chlorofluorocarbon inventories. Deep-Sea Res.I 48, 189-215.

Stocker, T.F., 1998. A glimpse of the glacial. Nature 391, 338-339.

Strammer, L. and Peterson, R.G., 1989. Geostrophic transport in the Benguela Current region. Journal of Physical Oceanography 19, 1440-1448.

Talley, L.D., 1996. Antarctic Intermediate Water in the South Atlantic, in The South Atlantic: Present and past circulation, edited by Wefer, G., Berger, W.H., Siedler, G., and Webb, D.J., pp. 219-238, Springer, Berlin Heidelberg.

Thiede, J., 1975. Distribution of foraminifera in surface waters of a coastal upwelling area, Nature 253, 712-714.

Ufkes, E. and Zachariasse, W.-J., 1993. Origin of coiling differences in living neogloboquadrinids in the Walvis Bay region, off Namibia, southwest Africa. Micropaleont. 39 (3), 283-287.

Ufkes, E., Jansen, J.H.F., and Schneider, R.R., 2000. Anomalous occurrences of Neogloboquadrina pachyderma (left) in a 420-ky upwelling record from Walvis Ridge (SE Atlantic). Marine Micropaleontology 40, 23-42.

Van Bennekom, A.J. and Berger, G.W., 1984. Hydrography and silica budget of the Angola Basin. Netherlands Journal of Sea Research 17, 149-200.

Venz, K.A., Hodell, D.A., Stanton, C., and Warnke, D.A., 1999. A 1.0 Myr record of Glacial North Atlantic Intermediate Water variability from ODP site 982 in the northeast Atlantic. Paleoceanography 14 (1), 42-52.

Volbers, A., Henrich, R., and Niebler, H.-S., 1999. Examination of late Quaternary planktic foraminiferal assemblages and investigations of carbonate preservation in the sediment core GeoB 1710-3 from the eastern South Atlantic. Poster, Workshop on Paleoceanography, Bern, Schwitzerland.

Warren, B. and Speer, K.G., 1991. Deep circulation in the eastern South Atlantic ocean, Deep-Sea Res. 38 (1), 281-322.

Weaver, A.J., Aura, S.M., and Myers, P.G., 1994. Interdecadal variability in an idealised model of the North Atlantic. J Geophys. Res. 99, 12423-12442.

Wood, R.A., Keen, A.B, Michell, J.F.B., and Gregory, J.M., 1999. Changing spatial structure of the thermohaline cirulation in response to atmospheric CO_2 forcing in a climate model. Nature 399, 572-575.

Zahn, R. 1992. Deep ocean circulation puzzle, Nature 356, 744-746.

Part II *Publications*

1. *Late Quaternary variations in calcium carbonate preservation of deep-sea sediments in the northern Cape Basin: results from a multiproxy approach* by Volbers, A.N.A. and Henrich, R. Submitted to Marine Geology (Special Issue „Neogene and Quaternary evolution of the Benguela System").

In this paper, sediment core material from station GeoB 1710-3 in the northern Cape Basin was investigated regarding its calcium carbonate preservation potential. Various parameters in deep-sea sediments are used as indicators of calcium carbonate dissolution, such as the $CaCO_3$ content, the rain ratio, the sand fraction, the fragmentation index, the planktic foraminiferal concentration, the radiolarian to planktic foraminiferal ratio, the benthic to planktic foraminiferal ratio, and resistant planktic foraminifera. However, very few studies address the question of whether ecological boundary conditions or dissolution processes have caused the observed downcore fluctuations of these proxy parameters. As verified by the *Globigerina bulloides* dissolution index (BDX') (Volbers and Henrich, subm.), results of the most commonly used proxies do not only monitor dissolution within these calcareous sediments but also reflect changes in carbonate accumulation during variable upwelling intensity. Several times during the past 245 kyrs, northern Benguela upwelling cells were displaced westward (Volbers et al., subm) and GeoB 1710-3 sediments reflect these changes in upwelling productivity. Accordingly, most conventional proxy parameters misrepresent the extent of calcium carbonate dissolution. *Globigerina bulloides* ultrastructural investigations reveal persistent good carbonate preservation thoughout the past 245 kyrs with the exception of one pronounced dissolution event at early Oxygen Isotopic Stage (OIS) 6.

2. *Present water mass calcium carbonate corrosiveness in the eastern South Atlantic inferred from ultrastructural breakdown of Globigerina bulloides in surface sediments.* Volbers, A.N.A. and Henrich, R. Submitted to Earth and Planetary Science Letters.

In this manuscript, the BDX' is applied to 118 surface sediments from the eastern South Atlantic to determine the calcite lysocline from the Guinea, Angola and Cape Basin and continental margins regimes. The Atlantic is regarded as a huge carbonate depocenter because the critical undersaturation depth of calcite (hydrographic lysocline) is at around 4400 m in the Cape Basin and 5000 m in the Angola Basin. However, ultrastructural investigations of *Globigerina bulloides* show that calcium carbonate dissolution starts several 100 m shallower depending on the investigated region. In the Cape Basin, the sedimentary calcite lysocline coincids with the NADW/AABW transition. The situation is different for the Guinea and Angola Basin: AABW is virtually absent and the carbonate saturation changes little with depth. In the vicinity of the Walvis Ridge, the sedimentary calcite lysocline is located at 4400 m whereas it was found at around 4000 m water depth at the Mid-Atlantic Ridge. In the equatorial South Atlantic and along the coastal transects it was determined between 3400 and 3600 m. Indeed, the decoupling of the hydrographic and sedimentary calcite lysocline is predicted locally and a calcium carbonate flux out of the sediments was measured in several studies. The respiration of organic matter, which produces metabolic CO_2,

seems to create microenvironments favorable for dissolution of calcite even if the overlying bottom waters are supersaturated with respect to $CaCO_3$. In this regard, this study may help to evaluate the effects of metabolic CO_2 production on calcareous sediments.

3. *Calcium carbonate corrosiveness in the South Atlantic basin during the LGM as inferred from changes in the preservation of Globigerina bulloides: A proxy to determine deep water circulation pattern?* Volbers, A.N.A. and Henrich, R. To be submitted to Paleoceanography.

In order to determine the position of the sedimentary calcite lysocline in the South Atlantic during the LGM, LGM (23-19 cal-ky-BP) samples from 48 core locations were investigated regarding the ultrastructural preservation state of *G. bulloides*. In addition, 75 surface samples from the western South Atlantic were analysed to determine the modern position of the sedimentary calcite lysocline in this region. Today, the modern lysocline seems to be linked to the NADW/AABW transition as observed in the Cape Basin. When compared to the core-top data set, BDX' data determined from LGM sediment material point to a rather less stratified ocean than compared to the modern South Atlantic Ocean. In addition, the position of the calcite lysocline was similar in the western and eastern basin, indicating that the access of Southern Component Water (SCW) to the eastern South Atlantic basins was not limited as it is today.

4. *Paleoceanographic changes in the northern Benguela upwelling system over the last 245.000 years as derived from planktic foraminifera assemblages.* Volbers, A.N.A, Niebler, H.-S., Giraudeau, J., Schmidt, H., Henrich, R. Submitted to Deep-Sea Res.

Here, the spatial and temporal variability in the degree of upwelling during the late Quaternary was reconstructed from planktic foraminiferal assemblages. In order to do this, a factor model and a temperature transfer function were calculated exclusively for the Benguela region. Three hydrographic regimes (open-oceanic, intermediate, upwelling) were distinguished by factor analysis and applied to seven sediment cores from the Walvis Ridge and the northern Cape Basin. Distinct upwelling events were recognized during oygen isotopic event (OIE) 7.4, 6.5/6.4, 6.2, 5.53, 5.4, 5.2, 4.2 and during OIS 3 and 2. During periods of intensified upwelling, northern Benguela upwelling cells were displaced westward and increased in size, covering areas at least three times as large as at the present day. During OIE 7.4 and 5.4 the maximum upwelling extent was recorded and during OIE 5.1 upwelling was at its minimum. Paleo sea surface temperature (SST) reconstructions, derived from planktic foraminifera using the classical transfer function approach, document lower SSTs during periods of intensified upwelling whereas SSTs derived from alkenones in contrast show glacial to interglacial temperature shifts. A good correlation between upwelling events in the northern Benguela region and increases in equatorial seasonality implies that both regions respond to the same mechanism, probably changes in the trade wind intensity.

Contribution to the synthesis publications of the SFB 261, subprojects A2 and B3, edited by Wefer, G., Mulitza, S., and Ratmeyer, V. (to be published), Springer:

5. *Contribution of calcareous plankton groups to the carbonate budget of South Atlantic surface sediments.* Baumann, K.-H., Böckel, D., Donner, B., Gerhardt, S., Henrich, R., Vink, A., Volbers, A. Willems, H., Zonneveld, K. (in prep.).

6. *Carbonate preservation in deep and intermediate water masses: evolution and geologic record.* Henrich, R., Baumann, K.-H., Dittert, N., Gerhardt,S., Kinkel, H., Volbers, A. (in prep.).

7. *Palaeoenvironmental information gained from coccolith, dinoflagellate cyst and planktic foraminifer distributions in South Atlantic surface sediments.* Vink, A., Willems, H., Baumann, K.-H., Böckel, B., Zonneveld, K.A.F., Kinkel, H., Volbers, A., Esper, O. (in prep.).

8. *Late Quaternary paleoceanographic synthesis derived from calcareous planktion groups and dinoflagellate cysts.* Zonneveld, K., Baumann, K.-H., Böckel, B., Dittert, N., Esper, O., Gerhardt, S., Henrich, R., Höll, C., Kinkel, H., Volbers, A., Willems, H. (in prep.).

9. *Diagenetic processes at the benthic boundary layer (in the South Atlantic).* Hensen, C., Pfeifer, K., Wenzhöfer, F., Volbers, A., Schulz, S. (in prep.).

1. Late Quaternary variations in calcium carbonate preservation of deep-sea sediments in the northern Cape Basin: results from a multiproxy approach

Andrea N.A. Volbers and Rüdiger Henrich

University of Bremen, Faculty of Geosciences, Department of Paleoceanography and Sedimentology, P.O. Box 33 04 40, D-28334 Bremen, Germany,
phone: +49(0)421 218 7135 fax: ++49 (421) 218 7431 email: avolbers@uni-bremen.de

Abstract

In this study, we test various parameters in deep-sea sediments (bulk sediment parameters and changes in microfossil abundances and preservation character) which are generally accepted as indicators of calcium carbonate dissolution. We investigate sediment material from station GeoB 1710-3 in the northern Cape Basin (eastern South Atlantic), 280 km away from the Namibian coast, well outside today's coastal upwelling. As northern Benguela upwelling cells were displaced westward and periodically proceeded the core location during the past 245 kyrs (Volbers et al., subm.), GeoB 1710-3 sediments reflect these changes in upwelling productivity. Results of the most commonly used calcium carbonate dissolution proxies do not only monitor dissolution within these calcareous sediments but also reflect changes in upwelling intensity. Accordingly, these conventional proxy parameters misrepresent, to some extent, the extent of calcium carbonate dissolution. These results were verified by an independent dissolution proxy, the *Globigerina bulloides* dissolution index (BDX') (Volbers and Henrich, subm.). The BDX' is based on SEM ultrastructural investigation of planktic foraminiferal tests and indicates persistent good carbonate preservation throughout the past 245 kyrs, with the exception of one pronounced dissolution event at early Oxygen Isotopic Stage (OIS) 6.

The early OIS 6 is characterised by calcium carbonate contents, sand contents, and planktic foraminiferal concentrations all at their lowest levels for the last 245 kyrs. At the same time, the ratio of radiolarian to planktic foraminiferal abundances, and the ratio of benthic to planktic foraminiferal tests are strongly increased, as is the rain ratio, the fragmentation index, and the BDX'. The sedimentary calcite lysocline rose above the core position and GeoB 1710-3 sediments were heavily altered, as attested to by the unusual accumulation of pellets, aggregates, sponge spicules, radiolaria, benthic foraminifera, and planktic foraminiferal assemblages.

Solely the early OIS 6 dissolution event altered the coarse fraction intensely, and is therefore reflected by all conventional calcium carbonate preservation proxies and the BDX'. We attribute the more than 1000 m rise of the sedimentary calcite lysocline to the combination of two processes: a)

a prominent change in the deep-water mass distribution within the South Atlantic and b) intense degradation of organic material within the sediment (preserved as maximum total organic carbon content) creating microenvironments favorable for calcium carbonate dissolution.

1. Introduction

Deep sea carbonates cover almost half the total area of the ocean floor, (e.g. Berger et al., 1976) but on a global scale, only a fraction of the calcite, produced in the water column mainly by planktic foraminifera and coccolithophorids, is buried (Archer and Maier-Reimer, 1994; Hales et al., 1994; Archer, 1996; Hales and Emerson, 1997). The preservation potential of calcium carbonate depends on many variables, and attempts to assess calcium carbonate dissolution in deep-sea sediments are commonly based on various lithologic and microfossil parameters (e.g. Thunell, 1976; Peterson and Prell, 1985; Boltovskoy and Totah, 1992; Broecker and Clark, 1999; Broecker et al., 1999; Dittert et al., 1999; Li et al., 2000). The most popular dissolution proxies are the $CaCO_3$ content, the rain ratio, the sand fraction, the fragmentation index, the planktic foraminiferal concentration, the radiolarian to planktic foraminiferal ratio, the benthic to planktic foraminiferal ratio, and resistant planktic foraminifera. Nevertheless, it is well known that these proxies are not exclusively controlled by calcium carbonate dissolution but that they also respond to dynamic and ecological factors such as terrigenous dilution, lateral transport, winnowing of sediment, and regional and temporal changes in productivity (e.g. Diester-Haass, 1976, 1977, 1978, 1985; Wu and Berger, 1991; Matthewson et al., 1995; Huang et al., 2000; Wagner, 2000). Very few studies address the question of whether ecological boundary conditions or dissolution processes have caused the observed downcore fluctuations of these proxy parameters. Here we present data from a late Quaternary sediment core obtained in the vicinity of the Benguela Upwelling System, which is one of the five great continental margin upwelling systems, and belongs amongst the high productivity regions of the oceans (Berger, 1989). From various studies it was indicated that many marine nanno- and microfossil organism groups respond to productivity and water temperature changes in this region (e.g. Giraudeau, 1993; Giraudeau

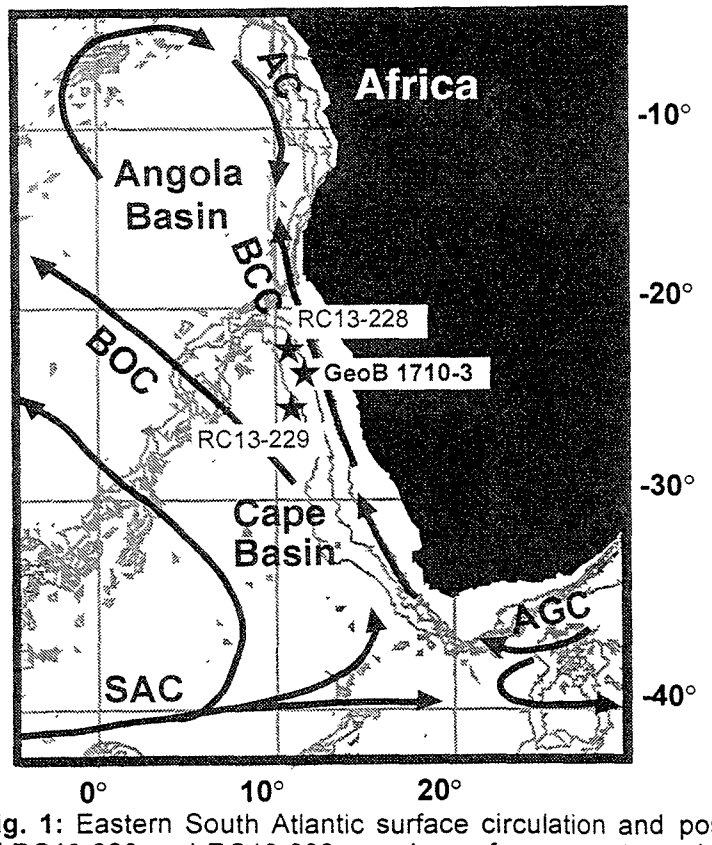

Fig. 1: Eastern South Atlantic surface circulation and position of gravity core GeoB 1710-3. Positions of RC13-228 and RC13-229 are shown for comparison. AC... Angola Current, BCC... Benguela Coastal Current, BOC... Benguela Oceanic Current, SAC... South Atlantic Current, AGC... Agulhas Current

and Rogers, 1994; Schmiedl and Mackensen, 1997; Abrantes et al., 2000; Volbers and Henrich, subm.). It may therefore be expected that some of the conventional calcium carbonate dissolution proxies, e.g. the ratio of radiolaria to planktic foraminifera index, may respond primarily to these ecological changes. In order to overcome this problem, multiproxy approaches were applied to determine calcium carbonate dissolution in high productive oceanic settings. Here we present data from a late Quaternary sediment core obtained in the vicinity of the Benguela Upwelling System, which is one of the five great continental margin upwelling systems, and belongs amongst the high productivity regions of the oceans (Berger, 1989). From various studies it was indicated that many marine nanno- and microfossil organism groups respond to productivity and water temperature changes in this region (e.g. Giraudeau 1993, Giraudeau and Rogers, 1994, Schmiedl and Mackensen, 1997; Abrantes et al., 2000; Volbers and Henrich, subm.). It may therefore be expected that some of the conventional calcium carbonate dissolution proxies, e.g. the ratio of radiolaria to planktic foraminifera index, may respond primarily to these ecological changes. In order to overcome this problem, multiproxy approaches were applied to determine calcium carbonate dissolution in high productive oceanic settings.

In this study, we apply a little known dissolution proxy, the *Globigerina bulloides* dissolution index (BDX'), to validate the preservation potential of calcareous sediments from the northern Cape Basin throughout the last 245 kyrs by comparing results from BDX' profiles with associated conventional dissolution proxies. The fundamentals of the recently introduced BDX' (Volbers and Henrich, subm.) were established by van Kreveld-Alfane (1996) and Dittert and Henrich (2000) and are based on scanning electronic microscope (SEM) ultrastructural investigation of planktic foraminiferal test features. The BDX' is a reliable indicator that detects the onset of significant calcium carbonate dissolution within South Atlantic sediments and was successfully employed to determine the depth of the sedimentary calcite lysocline using surface sediments from the South Atlantic deep basins (Guinea, Angola and Cape Basin) and from the high-productivity coastal regions (Congo region, Namibian coast) (Volbers and Henrich, subm.).

2. Outline of investigated carbonate preservation proxies

Many different carbonate preservation proxies have been established for various geographical and oceanic settings, some of them based on bulk sediment parameters (calcium carbonate content, sand content, organic carbon/inorganic carbonate ratio), others on changes in microfossil abundances and preservation character (planktic and benthic foraminifera, radiolaria).

2.1 Bulk sediment parameters

The calcium carbonate content of a sediment ($CaCO_3$, wt-%) most easily depicts possible dissolution if the production rate of calcium carbonate is constant through time. The deep-sea calcium carbonate content is controlled by the production of various calcareous micro- and nannofossil groups and dilution effects such as high input of dust material, riverine supply of terrigenous sediments and resuspension from the continental shelves. To correct for dilution

effects, the calcium carbonate mass accumulation rate (MAR) was calculated by multiplying the carbonate weight percentage by the dry bulk density and the linear sedimentation rate.

Calcium carbonate dissolution has been reported to occur even well above the (hydrographic) lysocline (Berger, 1977; Emerson and Bender, 1981; Milliman et al., 1999; Volbers and Henrich, subm.; this paper). Indeed, the oxidation of organic matter produces CO_2 that triggers calcium carbonate dissolution at the sediment surface and in the sediment (Archer et al., 1989; Jahnke et al., 1994), a process which is enhanced in high productivity areas. The amount of total organic carbon (TOC, wt-%) and the ratio of organic carbon (TOC) to inorganic carbon ($CaCO_3$), expressed as the rain ratio, are used to detect possible dissolution of calcareous sediments. The source of the organic matter is important as different marine and terrigenous compounds range from highly reactive to highly refractory (Eppley and Peterson, 1979; Lee et al., 1983; Wakeham et al., 1984; Wakeham and Canuel, 1988; Wakeham and Lee, 1989; Hung et al., 2000).

The sand content (fraction >63 µm, in wt-%) of deep-sea carbonates decreases during the dissolution process because foraminiferal tests weaken due to carbonate loss and finally break up into smaller fragments (Berger et al., 1982; Wu and Berger, 1991). The coarse fraction is a reliable proxy to determine calcium carbonate dissolution if the ratio between nannofossils (e.g. coccolithophores) and microfossils (e.g. planktic foraminifera) is constant through time. The concentration of planktic foraminifera per gram sediment also referred to as foraminiferal number (e.g. Howard and Prell, 1994; Dittert et al., 1999), depends on the interplay of fragmentation and productivity.

2.2 Microfossil indices

From all tested proxies in this study, the fragmentation index is one of the most widely used indicators of calcium carbonate dissolution (e.g. Keigwin, 1976; Peterson and Prell, 1985; Le and Shackleton, 1992; Howard and Prell, 1994) although fragmentation increases before significant overall carbonate loss begins (Howard and Prell, 1994). Nevertheless, the fragmentation index does not exclusively respond to calcium carbonate dissolution as considerable numbers of fragments exist even in sediments from shallow depths (Berger et al., 1982). The fragmentation index is biased by the fragment preservation and dissolution as the ratio of conserved to lost fragments is not expressed by this index. In addition, the fragmentation index is sensitive to artefacts introduced during samples preparation, as mechanical forces during preparation can lead to increased fragmentation.

Benthic foraminifera are about three times more resistant to dissolution than planktic foraminifera (Berger, 1975). According to Parker and Berger (1971), unaltered foraminiferal sediments have a ratio of planktic to benthic foraminifera around 99:1, a notable decrease in this ratio could reflect the effect of calcium carbonate dissolution. In the past, the contents of benthic foraminifers were used to determine assemblage alterations (Diester-Haass, 1985; Oberhänsli, 1991). Like benthic

foraminifera, radiolarians tend to increase in relative abundance during the progression of the calcium carbonate dissolution process and were used as proxy to determine the calcite lysocline (e.g. Wu and Berger, 1991).

As planktic foraminifera secrete calcareous tests, they experience characteristic ultrastructural alteration with proceeding dissolution (e.g. Berger et al., 1975; Henrich et al., 1989; Henrich, 1989). *Globigerina bulloides* was chosen for ultrastructural investigation as it is susceptible to carbonate dissolution. According to Thunell and Honjo (1981) it has a high susceptibilty ranking, although it was considered more intermediate by Parker and Berger (1971). *Globigerina bulloides* is among the most abundant planktic foraminifera in the eastern South Atlantic, at present, (Kemle-von Mücke and Oberhänsli, 1999) and over the past 245 kyrs (Oberhänsli, 1991; Volbers et al., subm.). In this study, the methods of van Kreveld (1996) and Dittert and Henrich (2000) were refined and yielded the *Globigerina bulloides* dissolution index (BDX'). It is a reliable indicator of foraminiferal carbonate preservation with 5 dissolution stages described by distinct dissolution features.

In the past, dissolution experiments involving the ranking of most planktic foraminifera with respect to calcium carbonate corrosiveness were run (e.g. Parker and Berger, 1971; Thunell, 1976; Thunell and Honjo, 1981; Sautter and Sancetta, 1992). During the ongoing dissolution process, tests of the thick-walled planktic and benthic foraminifera were preferentially accumulated (Ruddiman and Heezen, 1967; Berger, 1973; Berger et al., 1982). Calcium carbonate dissolution is a selective process which increases the proportion of resistant to non-resistant planktic foraminiferal species (Ruddiman and Heezen, 1967; Berger et al., 1982). Increases in the relative percentage of single species, such as *Globorotalia tumida, Spaerodinella dehiscens*, *Pulleniatina obliqulobulata*, *Globorotalia menardii* (Ruddiman and Heezen, 1967; Wu and Berger, 1991), *Globorotalia inflata* (Niebler, 1995), and *Neogloboquadrina pachyderma* (Diester-Haass, 1985; Oberhänsli, 1991), were used to check whether or not calcareous sediments were altered by dissolution.

3. Material and methods

Gravity core GeoB 1710-3 (23.43°S, 11.7°E, 2987 m water depth, 1045 cm core length) was recovered from the continental slope off Namibia (Fig. 1) during R.V. Meteor cruise M20/2 (Schulz et al., 1992). Oxygen isotope analyses from the benthic foraminifera Cibicidoides wuellerstorfi provide the basic stratigraphic framework for the core (Fig. 2a, Bickert and Wefer, 1999). The total carbon (TC) and total organic carbon (TOC) contents of bulk sediments were measured with a Heraeus CHN-O-Rapid elemental analyser by P.J. Müller (unpubl. data). Further details on sampling and elemental analysis are given in Müller et al. (1994).

For micropaleontological investigations, all samples were freeze-dried, weighed, and washed through a 63 µm sieve. The samples were then dry-sieved into the fractions 63-125 µm, 125-250 µm, 250-500 µm, and >500 µm. The sand content (>63 µm, in wt-%) was determined by T. Bickert

(unpubl. data). Census counts of planktic foraminifera were conducted on the >125 µm fraction (Volbers et al., subm.) using an OLYMPUS SZ 40 binucular microscope. All samples were split into subsamples using a microsplitter with an aquilot of at least 300 non-fragmented planktic foraminiferal specimens.

For the determination of dissolution stages based on planktic foraminiferal ultrastructural breakdown, 30 *G. bulloides* specimen per sample were glued to a SEM stub and gold coated. The chambers were investigated at 3,000x magnification to study in detail their preservation in terms of four ultrastructural features (spines, ridges, interpore areas, and pores) with a ZEISS DSM 940 A (10 mm working distance, 10 kN accellarating voltage). The BDX' is characterized by six stages of preservation (worsening from 0 to 5), which are briefly described in the following:

stage 0-1 (excellent preservation): only observed on G. bulloides tests taken from mooring samples, recognized by round pores, smooth interpore area, intact ridges, and high spines.
stage 1-2 (very good to good preservation): identified by slightly widened pores, partly etched interpore areas, slightly denuded ridges and spines, hardly observed in surface sediment samples.
stage 2-3 (good to moderate preservation): recognized by funnel-like pores, etched and roughened interpore areas, denuded ridges and spines.
stage 3-4 (bad preservation): revealed by partly interconnected pores, partial removal of the surface layer, strongly reduced ridges and spines.
stage 4-5 (very bad preservation): indicated by interconnected pores, removal of surface layer, missing ridges and spines.
stage 5: indicated by the absence of intact tests due to severe dissolution.

The BDX' value was calculated according to the following equations:

$$P=(P_{(pores)}+P_{(interpore\ area)}+P_{(spines)}+P_{(ridges)})/4 \qquad (1)$$

The preservation state (P, between 0.5 and 4.5) of each single *G. bulloides* is calculated from the preservation of each investigated criterion (pores, interpore area, spines, and ridges) divided by the number of criteria, which is four. This method assures that every criterion is judged equally when calculating the BDX':

$$BDX'= \sum P/ nT \qquad (2)$$

With $\sum P$ as the sum of all individual preservation states of G. bulloides divided by the number of investigated tests (nT).

Since the term „calcite lysocline" is subject to different scientific use, we apply the definition of Milliman et al. (1999) with the top of the (sedimentary) calcite lysocline marked by the first observation of significant carbonate dissolution in calcareous sediments, a situation, which is reflected by the BDX' preservation stage 3 (Volbers and Henrich, subm.).

3. Results

3.1 Bulk sediment parameters as dissolution proxies

Calcium carbonate content

The sediments of GeoB 1710-3 show generally higher $CaCO_3$ (wt-%) contents in interglacial and interstadial periods than in glacials (Fig. 2b).

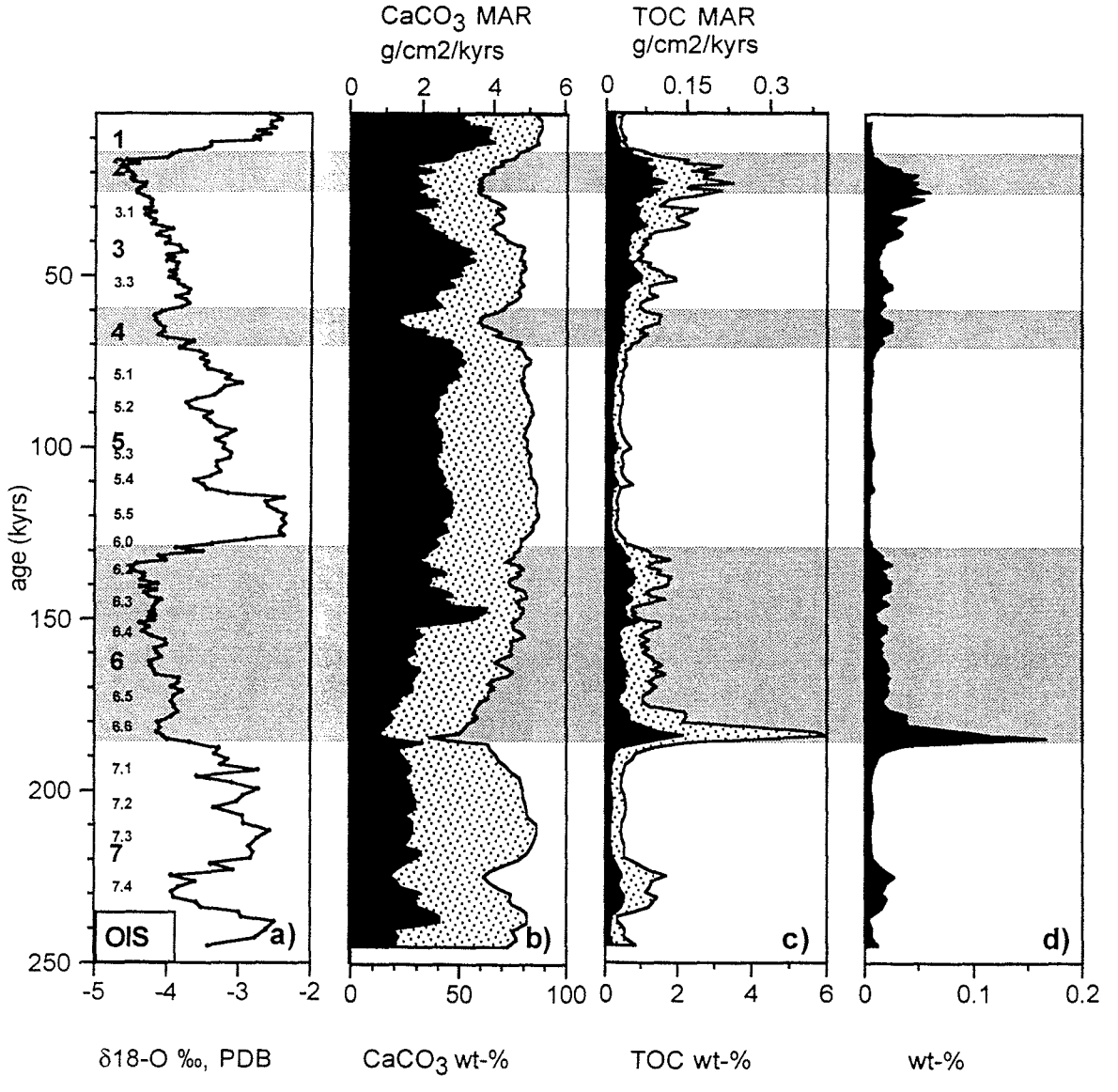

Fig. 2: Bulk parameter as calcium carbonate dissolution proxies. a) The oxygen isotope record of *Cibicidoides wuellerstorfi* in GeoB 1710-3 provides the stratigraphic framework for this core (Bickert and Wefer, 1999), shaded areas indicate glacial periods. b) Calcium carbonate content in wt-% (shaded, unpubl. data P.J. Müller) and carbonate mass accumulation rate in g/cm^2/kyrs. c) Total organic carbon content in wt-% (shaded) taken from Kirst et al. (1999) and TOC mass accumulation rate in g/cm^2/kyrs. d) Carbon rain ratio in wt-%.

Maximum $CaCO_3$ values occur during OIS 7 and 1, minimum $CaCO_3$ values (around 30 wt-%) were obtained at early OIS 6. Low values (down to 60 wt-%) are recorded during lower OIS 2 and upper OIS 4. During the cool oxygen isotopic event (OIE) 7.4 values of 60 wt-%$CaCO_3$ are observed. Interestingly, no correspondent decrease in carbonate content is observed during the cool OIE 5.4 and 5.2. The $CaCO_3$ pattern and the carbonate MAR are similar with higher carbonate during

interglacials compared to glacial periods. Carbonate MAR values range from a minimum of 0.86 g/cm^2/kyrs at early OIS 6 to a maxima of 4.01 g/cm^2/kyrs in the Holocene.

Total organic carbon content (TOC) and the organic/inorganic carbon ratio (rain ratio)

From the overall trend, TOC increases during glacial periods by about 1-2 wt-% on average (for comparison with the $CaCO_3$ MAR, the TOC MAR is also plotted in Fig. 2c; Kirst et al., 1999).

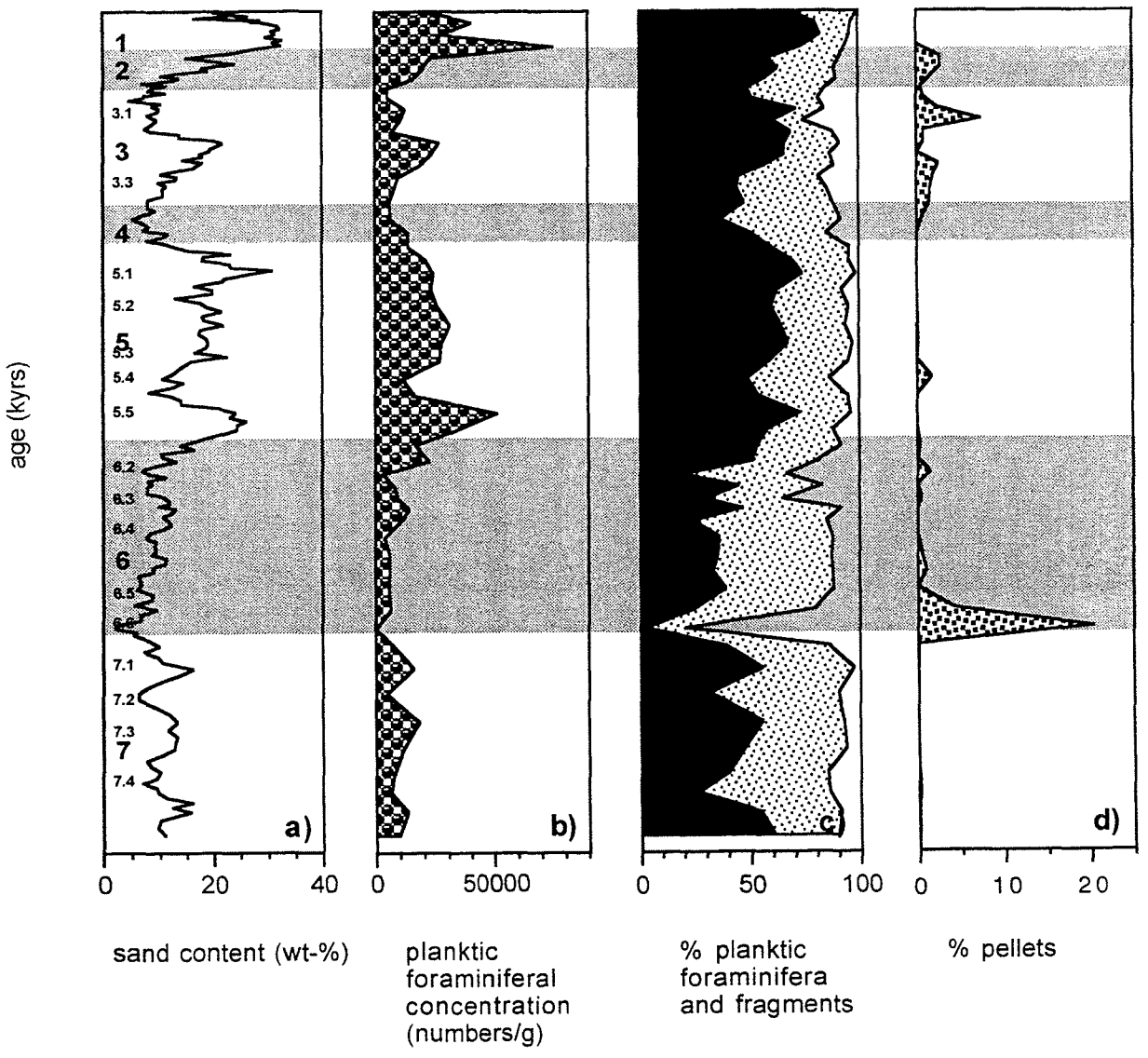

Fig. 3: Microfossils as calcium carbonate dissolution proxies. a) Sand content (% fraction >63 µm in wt-%) as determined by T. Bickert (unpubl. data). b) Planktic foraminiferal concentration (Σplanktic foraminifera/g dry bulk sediment). c) Whole foraminifera and fragment contributions to the >125 µm fraction. d) Constribution of pellets of the >125 µm fraction. Shaded areas indicate glacial periods.

In addition, the TOC record shows pronounced maxima at the beginning of OIS 6 (6 wt-%) and fluctuations at a high level (3 wt-%TOC) in OIS 2. The rain ratio displays a pattern similar to the TOC record and is significantly increased at early OIS 6 and during the OIS 3-2 transition (Fig. 2d).

Sand (coarse) fraction content and planktic foraminiferal concentration

The coarse fraction (Fig. 3b) has three pronounced maxima (25-30%) during OIE 5.5, 5.1, and at the beginning of the Holocene. From the overall trend, increased mean values close to or above 20% are observed during middle OIS 3 and OIE 5.3-5.2 whereas much lower values are recorded during OIS 7 (Fig 3b). Low values (around and below 10%) are indicated for glacial OIS 6, 4, and lower stage 2, as well as at the beginning and at the end of OIS 3.

The planktic foraminiferal concentration is related to the sand content, since planktic foraminifera make up the majority of the particles within the fraction >125 µm of GeoB 1710-3 sediments. The record of planktic foraminiferal tests per gram sediment shows a first-order pattern with a tendency towards higher values in interglacials with maxima during OIE 5.5 and just before the Holocene (Fig. 3c). The total numbers of planktic foraminifera per gram sediment vary from 3.000 to 75.000. At the beginning of OIS 6 the lowest values during the past 245 kyrs are recorded.

3.2 Abundance and character of microfossils as dissolution proxies

Fragmentation index (FI)

The fragmentation index reflects a trend towards better preservation (low values) from OIS 6 to the Holocene (Fig. 4b). OIS 6 is characterized by the largest FI values (>0.5), while OIS 4 and 2 are less pronounced in this way. During several distinct cold periods of interglacials, such as OIE 7.4 and 7.2, the FI is greater than 0.5. At early stage 6 the FI is at maximum with an FI of 0.9.

Ratio of radiolarian to planktic foraminiferal abundance (R/PF), ratio of benthic to planktic foraminiferal abundance (BF/PF)

The ratio of radiolarian to planktic foraminiferal abundance is <0.2 throughout the last 245 kyrs, with the exception of OIS 7 and 6. At OIE 7.4 and 7.2 the R/PF index is slightly increased (up to 0.25, Fig. 4c), as it is even more significantly during OIS 6 with peak values close to 0.5 in the upper part of OIS 6. At early OIS 6 the maximum ratio of 0.9 is displayed. In general, the proportion of benthic/planktic foraminifera shows low variablility (<0.2), with the exception of OIS 6. At the beginning of OIS 6, the ratio is at a maximum (0.8, Fig. 4d). Interestingly, the shifts in the general curve of the benthic/planktic foraminiferal record and in the radiolarian/planktic foraminiferal record covary strikingly over the past 245 kyrs.

Globigerina bulloides dissolution index (BDX')

Generally, the BDX' values are low (BDX' between 2-3) over the past 245 kyrs. They show an increasing trend from OIS 7 towards the beginning of OIS 6 and a decreasing trend from early stage 6 towards OIS 2 (Fig. 4e). At the beginning of OIS 6 the BDX' maximum of 4 is displayed.

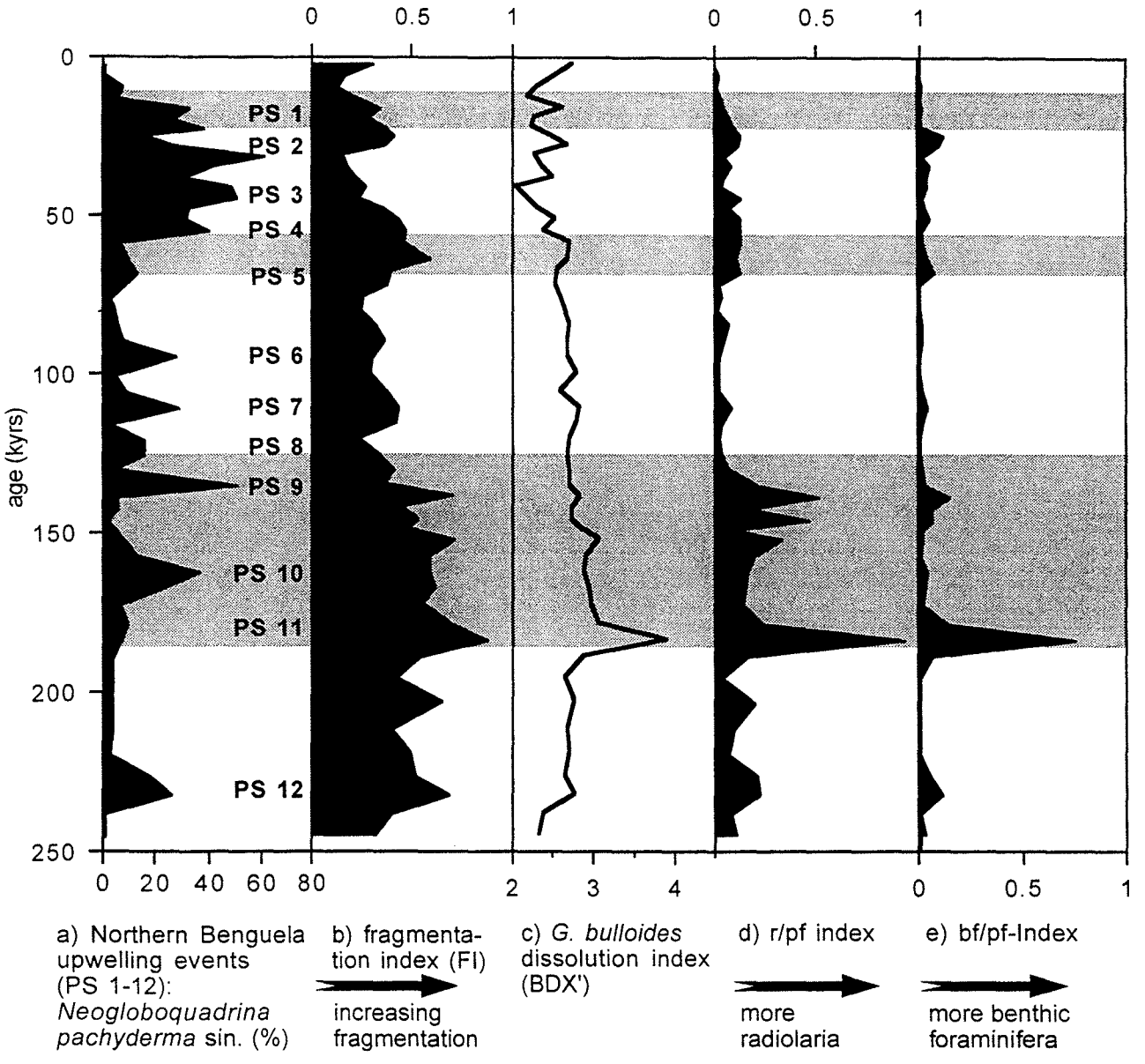

Fig. 4: Microfossils and microfossil ratios as calcium carbonate dissolution proxies. Shaded areas indicate glacial periods. a) Relative percentages of the planktic foraminifer *Neogloboquadrina pachyderma* (sinistral) relate to enhanced upwelling intensity. Peak abundances of *N. pachyderma* sin. (PS events, Little et al. 1997a, Volbers et al. subm.) show increased upwelling intensity. b) The ratio of whole planktic foraminferal tests and their fragments is expressed as fragmentation index. c) R/PF: ratio of radiolaria vs. planktic foraminifera in the 125 µm fraction. d) BF/PF: ratio of benthic vs. planktic foraminfera in the 125 µm fraction. e) BDX': *Globigerina bulloides* dissolution index.

Resistant planktic foraminifera

Relative abundances of the conventional resistant planktic foraminifera species are plotted in Fig. 5. Total *Neogloboquadrina pachyderma* species (sinistral and dextral coiling) dominate over total *Globorotalia inflata* (sin. and dex.), total *Globorotalia truncatulinoides* (sin and dex), and *Globorotalia minuta* in relative abundance. *Globorotalia menardii*, *Globorotalia crassaformis*, and *Globorotalia theyeri* are on average less than 1% and were therefore not plotted. *Neogloboquadrina pachyderma* (sin and dex, Fig. 5a) has maxima of up to 80% during OIS 3, with varying abundances of up to 60% during OIS 6 and OIE 7.4. *Globorotalia inflata* (sin. and dex., Fig. 5b) shows peak abundances during OIE 5.5 and 5.1 of >20%.

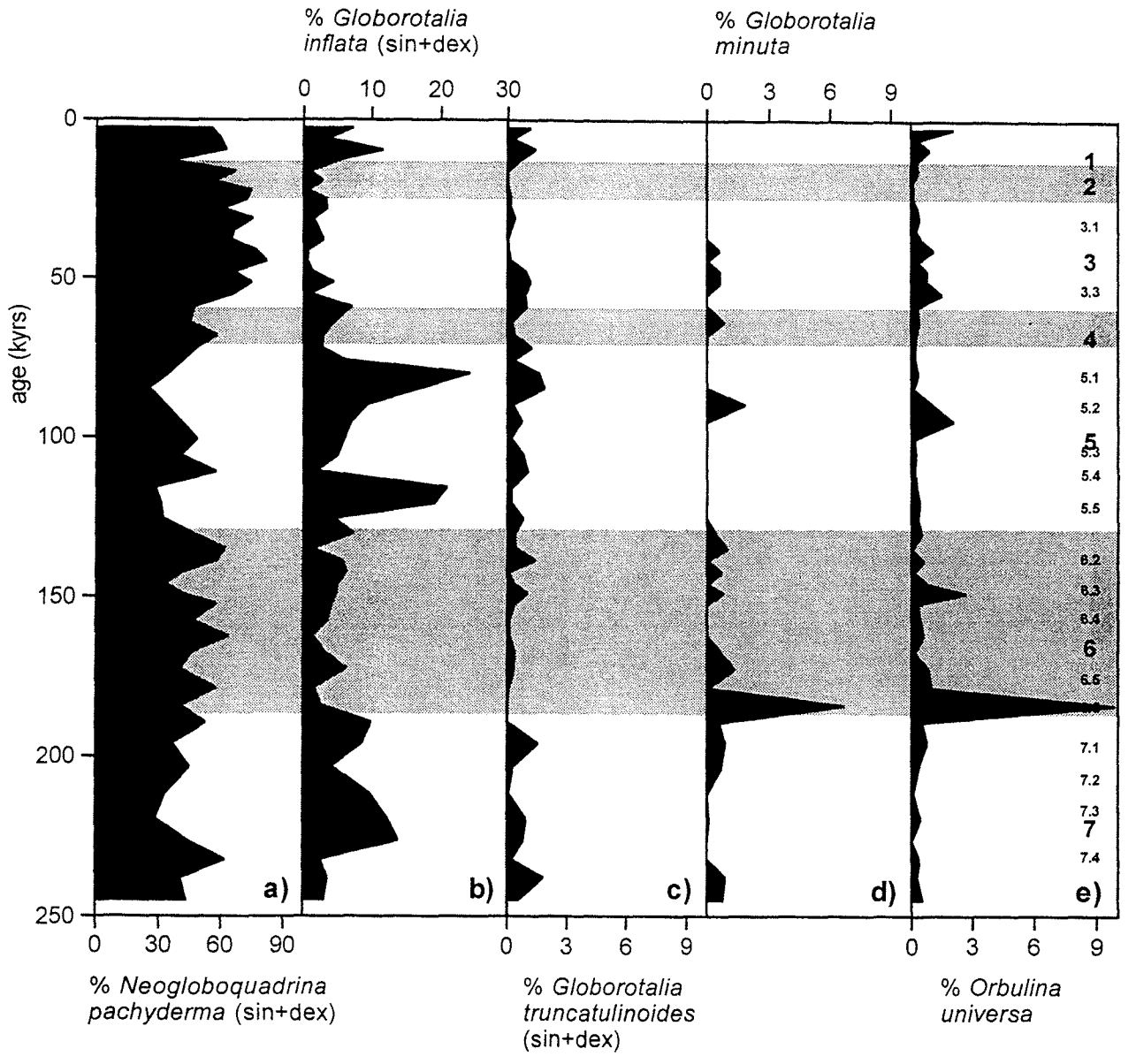

Fig. 5: Vertical distribution (%) of dissolution resistant planktic foraminiferal species. Shaded areas indicate glacial periods.

Relative abundances of *Globorotalia truncatulinoides* (sin and dex, Fig. 5c) are below 3% and show no characteristic distribution pattern. In contrast, *Globorotalia minuta* (Fig. 5d) has relative abundances of <2%, with the exception of a peak abundance of 6% at early stage 6. As the same pattern was observed for *Orbulina universa*, a more susceptible species (Parker and Berger, 1971; Thunell and Honjo, 1982), we plotted its relative abundances in Fig. 5e for comparison.

4. Discussion

Various conventional dissolution proxies have been investigated to evaluate their reliability to detect calcium dissolution in deep-sea sediments from the Benguela high productivity regime. In this study, the BDX' serves as an independent dissolution proxy since it sensitively detects calcium carbonate dissolution in eastern South Atlantic surface sediments. According to an earlier study, conventional

proxies, such as $CaCO_3$ content, TOC content, and rain ratio, fail to determine the sedimentary calcite lysocline in coastal high productive regions (Volbers and Henrich, subm.).

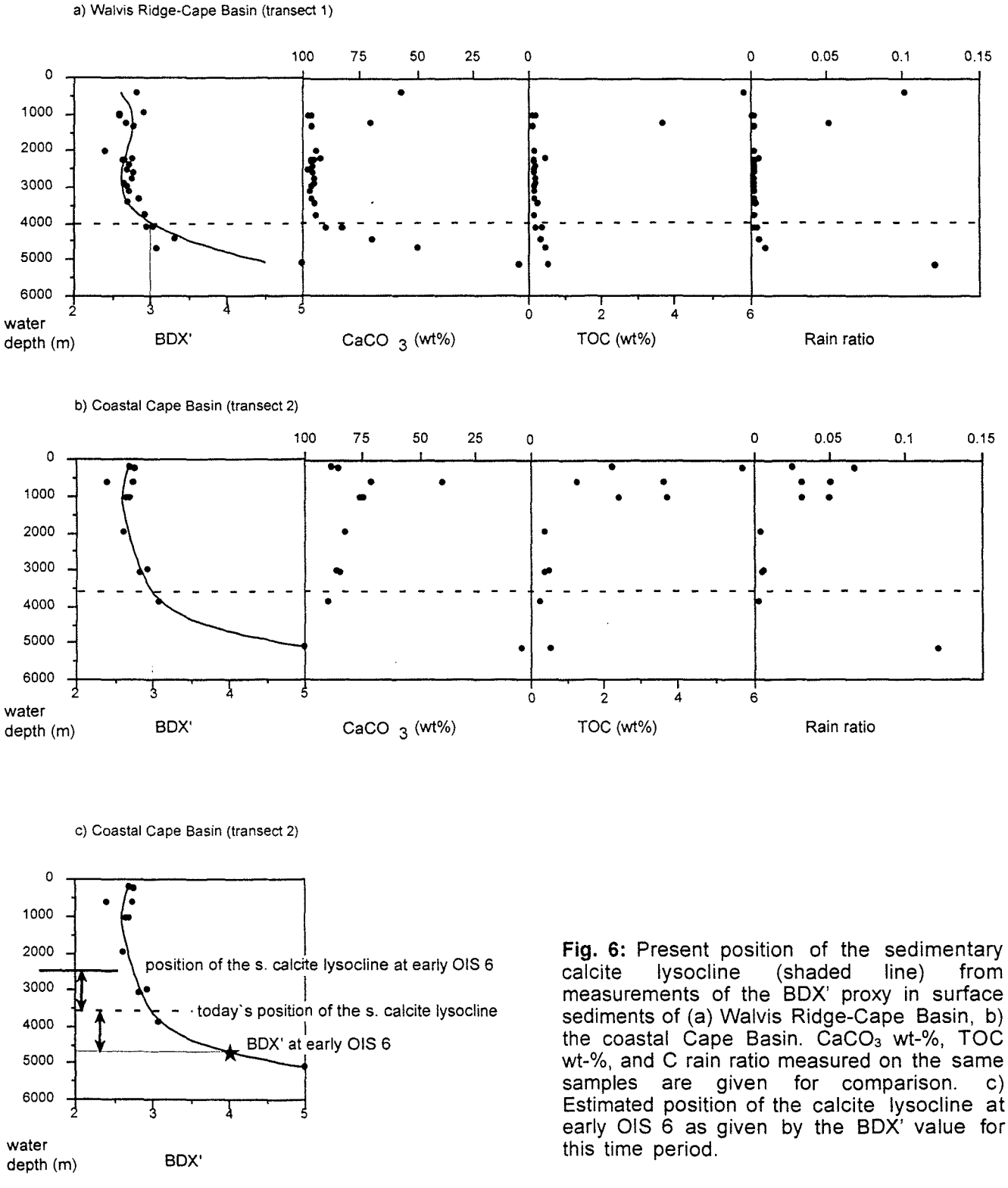

Fig. 6: Present position of the sedimentary calcite lysocline (shaded line) from measurements of the BDX' proxy in surface sediments of (a) Walvis Ridge-Cape Basin, b) the coastal Cape Basin. $CaCO_3$ wt-%, TOC wt-%, and C rain ratio measured on the same samples are given for comparison. c) Estimated position of the calcite lysocline at early OIS 6 as given by the BDX' value for this time period.

In the Namibian coastal region, TOC contents are increased by a factor of three and sediment accumulation rates are increased by a factor of four compared to the more open-ocean regime of the northern Cape Basin, which is also reflected by an around 400 m shallower coastal calcite lysocline (Fig. 6a,b, Volbers and Henrich, subm.). Comparative studies of the Walvis Ridge and the coastal upwelling area off Namibia show an enhanced decay of organic matter in the sediments of

the coastal transect as reported by lower $\delta^{13}C$ values derived from benthic foraminifera (Bickert and Wefer, 1999). As the organic matter is mostly degraded within the oxygenic layer, the degradation process is limited by the distribution of oxygen within the sediment (Emerson and Hedges, 1988). In-situ microelectrode and shipboard measurements showed that oxygen penetrates only 13 mm into the sediments in the eastern Atlantic upwelling sites (Rühlemann et al., 1999).

GeoB 1710-3 (2987 m water depth) is part of the high productive coastal region for which the modern sedimentary calcite lysocline was determined to lie at around 3600 m. As the upwelling intensity of the northern Benguela upwelling cells has changed over the last 245 kyrs (Volbers et al., subm.) the interplay of increased supply and decay of marine organic matter and rapid burial rates in this region may have displaced the sedimentary calcite lysocline to shallower depth compared to its present position. Based on *G. bulloides* ultrastructural investigations, a significant rise of the sedimentary calcite lysocline is only indicated to have occurred during OIS 6 (Fig. 6c).

Based on the $CaCO_3$ profile of GeoB 1710-3 (Fig. 2), the minimum is reflected at early OIS 6 when BDX' values are at a maximum, indicating a severe dissolution event. In addition, $CaCO_3$ values are lower during OIE 7.4 and OIS 4, and 2. If the production rate of calcium carbonate was constant through time, calcium carbonate dissolution would be indicated by reduced $CaCO_3$ contents. However, in the modern ocean, the relative abundance of $CaCO_3$ varies and is controlled by productivity (e.g. high numbers of planktic foraminifera, coccolithophorids, pteropods) and dilution (input of dust material, riverine supply of terrigenous sediments, resuspension from the shelves). For the investigated region, terrestrial input via rivers or wind is apparently very low considering that sedimentary organic material is primarily of marine origin as indicated by low C/N ratios and $\delta^{13}C_{org}$ values of about -20 ‰ (pers. communication, P.J. Müller). Therefore changes that relate to the upwelling process, such as nutrient concentration, sea surface temperature (SST), and salinity, seem to regulate $CaCO_3$ concentrations, as these parameters stimulate the growth of phyto- and zooplankton communities. The $CaCO_3$ content alone can turn out to be the least reliable variable to detect dissolution processes (Thunell, 1976) and if during OIE 7.4, early OIS 6, and OIS 4 a significant $CaCO_3$ loss had occurred as suggested from carbonate MAR, it should be monitored by other dissolution proxies.

The sand content of GeoB 1710-3 sediments range from 3 to 30 % and consists mainly of planktic foraminifera, with minor radiolaria and benthic foraminifera. The sand content is lowest at early OIS 6 (around 3 wt-%) when significant dissolution is indicated by maximum BDX' values. However, as low values (<10 wt-%) were achieved not only during OIS 7.4 and OIS 4, but also during OIE 7.2, during OIS 6, and OIE 5.4, the sand content may not solely respond to calcium carbonate dissolution but rather vary with upwelling intensity. Accordingly, the planktic foraminferal concentration decreases with increasing upwelling intensity and since the sand fraction consists mainly of planktic foraminifera, changes in upwelling intensity are monitored by the sand content.

Upwelling productivity in particular can induce distinct assemblages of benthic foraminifera and a large population size (Altenbach and Sarnthein, 1989). Paleoproductivity changes as well as selective calcium carbonate dissolution are therefore reflected by changing microfossil ratios (e.g. Li et al., 2000). Planktic foraminiferal records from several sediment cores recovered from the Walvis Ridge and the northern Cape Basin indicate changes in the spatial and temporal variability of upwelling during the past 245 kyrs. During periods of intensified upwelling (OIE 7.4, 6.5/6.4, 6.2, 5.53, 5.4, 5.2, 4.2, OIS 3 and 2, Fig. 4a) northern Benguela upwelling cells were displaced westward and increased in size, covering areas at least three times as large as at the present day (Volbers et al., subm.). High fertility conditions during northern Benguela upwelling events were reported from high-productivity fauna of benthic foraminifera (OIE 7.4, 5.4, 5.2, OIS 3-2) and an increase in the benthic foraminiferal accumulation rate (BFAR) by a factor of 3 during early stage 6, OIE 6.2, 5.4, 5.2, and OIS 4-2 in GeoB 1710-3 sediments (Schmiedl and Mackensen, 1997). As a consequence, the ratio of benthic to planktic foraminifera responds to the varying intensity of upwelling during the past 245 kyrs and reflects changes in living conditions in the first place. To discriminate between changes in upwelling intensity and calcium carbonate dissolution events in the Benguela region, other proxies are indispensable.

As previously introduced by Diester-Haass (1976, 1977, 1978) the radiolaria to planktic foraminifera index from sediments in upwelling regions serves as a fertility indicator rather than as a reliable dissolution proxy. This seems to be true for the fraction >125 µm, as the radiolaria to planktic foraminifera index and the benthic to planktic foraminifera index of GeoB 1710-3 show similar curve patterns. In contrast, radiolarian accumulation rates presented by Abrantes (2000) from GeoB 1710-3 show only minimal fluctuations over the past 245 kyrs, if we exclude maximum abundance during OIS 2. If we compare radiolarian data from two sediment cores close to GeoB 1710-3 (RC13-228 and RC13-229, Fig. 1), peak accumulation rates over the last 180 kyrs are limited to the respective core position (Charles and Morley, 1988). The opal content in sediments from coastal upwelling seems to be a local phenomenon which is linked to higher fertility in surface water (Diester-Haass 1977). Therefore the radiolaria to planktic foraminfera index cannot serve as a reliable calcium carbonate dissolution proxy in this high-productivity region.

Not only benthic foraminifera and radiolaria respond to changes in upwelling productivity, but also characteristic planktic foraminiferal assemblages are linked to the upwelling process (Little et al., 1997a,b; Volbers et al., subm.). Census counts of the >125 µm fraction have shown changes in the planktic foraminiferal species composition over the past 245 kyrs. Periods of increased upwelling, reflected by high relative percentages of N. pachyderma (sinistral coiling), coincide with a low foraminiferal concentration and low sand contents (Fig. 3b,c). Therefore periods of relatively low foraminiferal concentration and low sand content during OIE 7.5, OIS 4, and 2 appear to show periods of lower planktic foraminiferal carbonate production.

Even the planktic foraminiferal fragmentation seems to be related to ecological processes, as fragments of planktic foraminifera are produced by the macrozooplankton that prey on them (Hopkins, 1985). This would explain why considerable numbers of fragments exist even in sediments from shallow depth (Berger et al., 1982). In addition, we observe a trend of decreasing amplitude of fragmentation towards younger ages in GeoB 1710-3 sediments, probably indicating additional breakdown of microfossils due to pressure increase during the sediment accumulation process. Nevertheless, the dissolution event at early OIS 6 indicated by the BDX' and all conventional proxies is reflected by a maximum in the fragmentation index.

Regarding the low BDX' data, GeoB 1710-3 sediments are well-preserved and indicate, with the exception of OIS 6, a deep sedimentary calcite lysocline (below 3000 m) during the last 245 kyrs.

Calcium carbonate preservation during OIS 6

During early OIS 6, a maximum in BDX' documents significant dissolution and indicates a rise of the sedimentary calcite lysocline towards more intermediate depth. The sedimentary calcite lysocline in the northern coastal Cape Basin was close to the depth at which the core was taken between the past 180 and 150 kyrs. Moreover, the sedimentary calcite lysocline was at its shallowest position during early OIS 6. We estimate its position via the BDX' preservation curve pattern from surface sediments of this region. BDX' of around 4 would occur at a water depth of 4700 m, 1100 m beneath the modern sedimentary calcite lysocline. If a similar preservation pattern existed during early OIS 6, the sedimentary calcite lysocline at that time would have been positioned 1100 m shallower at around 2500 m (Fig. 6c).

The massive carbonate dissolution event at early OIS 6 was probably not triggered by a single mechanism alone. According to Howard and Prell (1994) the calcite lysocline in the northern Cape Basin was at least 900 m shallower compared to today as determined from RC13-228 and RC13-229 sediments. RC13-228 contains a higher $CaCO_3$ content (around 53 wt-%) at early OIS 6 than GeoB 1710-3 sediments (around 35 w%) although RC13-228 was recovered from greater water depth. Dissolution should effect GeoB 1710-3 sediments to a much lesser extent compared to RC13-228 sediments if carbonate chemistry is exclusively linked to changes in the relative flux of North Atlantic Deep Water (NADW). Previous studies suggest that reduced admixing of NADW into the Southern Ocean occurs during glacial periods (e.g. Oppo et al., 1990; Raymo et al., 1990) and therefore controls Southern Ocean deepwater carbonate chemistry (Howard and Prell, 1994). If a change in deep-water distribution was exclusively responsible for calcium carbonate dissolution at early OIS 6, it should affect RC13-229 the most (as it does, $CaCO_3$ <15 wt-%) and RC13-228 more heavily than GeoB 1710-3 (which is not the case). All cores are located close to one another and we would expect equal changes in productivity for all three cores so that the $CaCO_3$ content can be used to determine calcium carbonate dissolution. As GeoB 1710-3 sediments are more heavily effected by the early OIS 6 dissolution event than the RC 13-228 sediments, we suggest an additional reduction in the carbonate ion content ($[CO_3^{2-}]$) at GeoB 1710-3 core position.

The maximum TOC of 6 wt-% correlates well with the observed dissolution event at early OIS 6 and indicates further [CO_3^{2-}] reduction via the decomposition of organic material. However, the doubling of the TOC content compared to OIS 2 at the GeoB 1710-3 location is not seen in other sediment cores from this region (Oberhänsli, 1991; Schmidt 1992; Oppo and Rosenthal, 1994) and therefore appears to be a local phenomenon. Amongst the mechanisms for producing this TOC peak are firstly, temporarily enhanced supply of organic material by fecal pellets, and/or secondly, the lateral contribution of reworked organic matter from shallow water areas.

At early OIS 6, when TOC is at maximum (Fig. 2b), dark pellets comprise up to 20% of the coarse fraction, suggesting a rather fresh character of the incorporated organic matter. A second maximum of grey-coloured pellets (3 to 8%) during OIS 3 and 2 coincides with moderately elevated TOC contents exceeding 2 wt-%. As pellets are primarily biogenic, they contain fine, suspended particulate matter which was biologically packed by marine heterotrophs and escaped the continous recycling process in the upper photic layer (Fowler and Knauer, 1986). About 20 to 30% of the organic carbon from the phytoplankton ingested by herbivorous zooplankton, which are typically copepods in upwelling areas, are encapsulated in durable, fast-sinking packets (Eppley and Peterson, 1979). Although pellets are grazed in the water column, they frequently reach the seafloor intact, particularly in areas which are exposed to anoxic conditions (Porter, 1984). Based on the observed difference in colour between OIS 6 and 2 pellets, we propose, that either more organic matter must have been supplied or oxic respiration was less effective during early OIS 6 relative to OIS 2. The organic matter in these well-preserved pellets may then have been partially oxidized by secondary oxidants, such as NO_3^-, MnO_2, Fe_2O_3, and SO_4^{2-} (Bender and Heggie, 1984; Canfield, 1989). These secondary early diagenetic processes likely produced sufficient metabolic CO_2 to further lower the [CO_3^{2-}] at the core location. This scenario would create microenvironments favorable to calcium carbonate dissolution as recorded by peak values in all conventional and new dissolution proxies.

In the Benguela region, high TOC values are thought to reflect primarily input from marine export production, and in particular high TOC during OIS 4 to 2 should be indicative of intense upwelling (Kirst et al., 1999). As for OIS 4 to 2, intensified upwelling can be reconstructed from various micro- and nannofossil groups, it is documented neither by characteristic planktic or benthic foraminiferal assemblages nor by increased abundances of diatoms or radiolaria during early OIS 6 (Schmiedl and Mackensen, 1997; Abrantes, 2000; Volbers et al., subm., Fig. 7). It was suggested by Abrantes (2000) that this may indicate a change in phytoplankton productivity at early OIS 6 either due to a change in the nutrient ratio, or similar nutrient conditions during weak upwelling conditions.

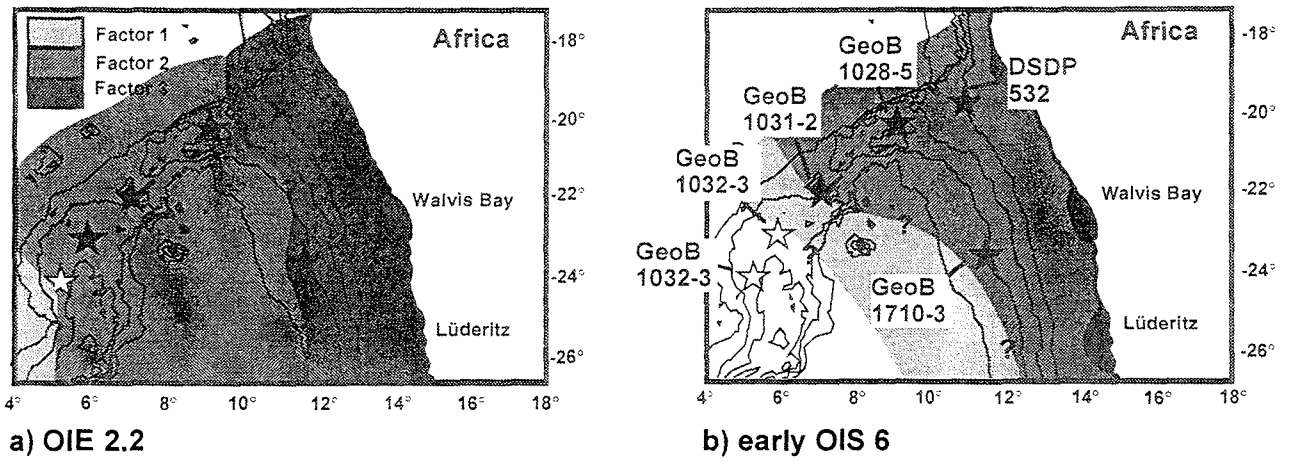

Fig. 7: Reconstruction of northern Benguela upwelling for the OIE 2.2 and early OIS 6 time slices (Volbers et al., subm.) from planktic foraminiferal factor assemblages. Factor 1: open ocean assemblage, Factor 2: intermediate assemblage, Factor 3: coastal upwelling assemblage. The inferred distribution of factor assemblage during early OIS 6 is similar to present.

According to Abrantes (2000), this event may indicate warm-water intrusions of saline Angola Current waters in the Benguela region, comparable to the modern „Benguela Ninos", as far south as 25°S (Shannon et al., 1986; Kirst et al., 1999). Increased warm water protrusions at early stage 6 could be reflected by peak abundance of *O. universa* (Fig. 5) which shows a well-developed latitudinal distribution today. High abundances of this species are related to a combination of warm and nutrient-rich conditions which characterize the surface waters of the northern Benguela region (Giraudeau, 1993).

Another possibility for the local increase in TOC is the contribution of marine organic material by lateral transport. Increased transfer of organic matter from the shelf to the deeper areas is suggested to have occurred during glacial periods, when sea level was lowered and circulation intensified (Diester-Haass, 1985). As reported by Summerhayes et al. (1995), the high amount of TOC during OIS 4 and 2 from northern Cape Basin cores consists primarily of reworked organic carbon of predominantly marine origin that was eroded from the continental shelves. When sea level was lowest during OIS 2 (130 m below its present position), organic matter previously deposited on the continental shelf was eroded and dumped on the continental slope. The same mechanism could have provided additional organic carbon from the shelves to the deeper parts of the northern Cape Basin at early OIS 6. This would explain why the doubling in TOC at early stage 6 is not reflected in RC13-229 sediments.

Nevertheless, the severe dissolution event at early OIS 6 is reflected in all proxies tested in this study. The $CaCO_3$ and sand content are lowest, whereas TOC and rain ratio are highest as is the fragmentation index. The coarse fraction has undergone severe alterations which led to an accumulation of pellets, aggregates, sponge spicules, radiolaria, and benthic foraminifera. As the planktic foraminiferal concentration is at a minimum, the ratio of radiolaria to planktic foraminifera,

and benthic foraminifera to planktic foraminifera increased significantly. The BDX' reflects maximum alteration of the ultrastructure of *G. bulloides* throughout the past 245 kyrs. The few planktic foraminiferal species preserved are not only the classic resistant species, such as *N. pachyderma*, *G. inflata*, and *G. minuta* but also the more susceptible species *Orbulina universa*. During early OIS 6, warm water protrusions, comparable to the modern Benguela Nino events, might have taken place and this species would have had a much higher percentage in the original planktic foraminiferal assemblage. As the species distribution of planktic foraminifera relates both to the upwelling process and to warm-water protrusions from the Angola region (Giraudeau and Rogers, 1994; Little et al., 1997 a,b; Volbers et al., subm.), relative percentages of planktic foraminifera fail to reflect the effects of calcium carbonate dissolution in this region.

5. Conclusions

Several independent proxies have been investigated in order to test their sensitivity towards calcium carbonate dissolution. The following conclusions can be drawn:

1. As GeoB 1710-3 was recovered in the vicinity of the Benguela upwelling system, the most commonly used proxies do not quantifiy calcium carbonate dissolution within calcareous sediments but insteadt are primarily related to changes in upwelling intensity. The validity of these proxies, such as bulk sediment parameters and microfossil ratios, is therefore strongly biased and may lead to erroneous interpretations of sediment data. The use of these conventional proxies should therefore be limited to regions with more constant hydrographic conditions such as found in the open-ocean regime. This is best demonstrated by the comparison of core top samples from the Namibian upwelling transect and the Walvis Ridge: The $CaCO_3$ and TOC content are reliable indicators to determine the position of the sedimentary calcite lysocline in the vicinity of the Walvis Ridge whereas in coastal regions, they are primarily responding to changes in upwelling intensity. In these regions, an independent proxy is needed to evaluate the extent of calcium carbonate dissolution.

2. If dissolution is intense, productivity effects on carbonate content can be relatively obscure. If dissolution events alter the composition of calcareous sediments significantly, this is not only reflected by decreasing BDX' but also by maximum values of all commonly used calcium carbonate dissolution proxies. Intense dissolution events, like the early OIS 6 event, may therefore be characterized by a multiproxy approach conducted with the conventional calcium carbonate dissolution proxies. The BDX' constitutes a reliable alternative to this time-consuming multiproxy approach.

3. The intense dissolution event at early OIS 6 coincides with a local maximum in the TOC content that appears to have additionally lowered the $[CO_3^{2-}]$ of the pore waters, triggering calcium carbonate dissolution. Two mechanisms are considered to be important to produce the observed

TOC peak: The temporarily increased supply and good preservation of relatively fresh marine organic material stored in pellets, and/or the reworking of organic matter from the adjacent shelf areas.

Acknowledgements

We thank P.J. Müller and T. Bickert, who supplied unpublished data to us. C. Devey kindly corrected the English. We would like to thank S. Gerhardt and T. Wagner for discussions and comments on the manuscript. Helpful suggestions and reviews by G. Mortyn and an anonymous reviewer are gratefully acknowledged. This research was funded by the Deutsche Forschungsgemeinschaft (Sonderforschungsbereich 261 at Bremen University, Contribution No. 321). All data presented in this paper are archived in the PANGAEA database at the Alfred Wegener Institute for Polar and Marine Research (http://www.pangaea.de/home/avolbers).

References

Abrantes, F., 2000. 200 000 yr diatom records from Atlantic upwelling sites reveal maximum productivity during LGM and a shift in phytoplanktion community structure at 185 000 yr. Earth Planet Sci. Lett. 176, 7-16.

Altenbach, A.V., Sarnthein, M., 1989. Productivity record in benthic foraminifera. In: Berger, W.H., Smetacek, V.S., Wefer, G. (Eds.), Productivity of the ocean: present and past. Reports of the Dahlem Workshop on productivity of the ocean: present and past, John Wiley & Sons, 255-269.

Archer, D., Emerson, S, Reimer, C., 1989. Dissolution of calcite in deep-sea sediments: pH and O_2 microelectrode results. Geochimica et Cosmochimica Acta 53, 2831-2845.

Archer, D., 1996. A data-driven model of the global calcite lysocline. Global biogeochemical cycles 10 (3), 511-526.

Archer, D., Maier-Reimer, E., 1994. Effect of deep-sea sedimentary calcite preservation on atmospheric CO_2 concentration. Nature 367, 260-263.

Bender, M.L., Heggie, D.T., 1984. Fate of organic carbon reaching the deep sea floor: a status report. Geochimica et Cosmochimica Acta 48, 977-986.

Berger, W.H., 1975. Deep-sea carbonates: dissolution profiles from foraminiferal preservation. In: Sliter, W.V., Bé, A. W. H., Berger, W.H. (Eds.), Dissolution of deep-sea carbonate. Cushman Foundation, Spec. Publ. 13, 82-86.

Berger, W.H., Adelseck C.G., Mayer, L.A.. 1976. Distribution of carbonate in surface sediments of the Pacific Ocean. J. Geophys. Res. 81, 2617-2627.

Berger, W.H., 1977. Deep-sea carbonate and the deglaciation preservation spike in pteropods and foraminifera. Nature 269, 301-304.

Berger, W.H., Bonneau, M.-C., Parker, F.-L., 1982. Foraminifera on the deep-sea floor: lysocline and dissolution rate. Oceanol. Acta 5 (2), 249-258.

Berger, W.H., 1989. Global maps of ocean productivity. In: Berger, W.H., Smetacek, V.S., Wefer, G (Eds), Productivity of the ocean: present and past. John Wiley & Sons, 429-455.

Bickert, T, Wefer, G., 1999. South Atlantic and benthic foraminifer $d^{13}C$-deviations: Implications for reconstructing the Late Quaternary deep-water circulation, Deep-Sea Res. 46, 437-452.

Boltovskoy, E., Totah, V.I., 1992. Preservation index and preservation potential of some foraminiferal species. J. Foraminiferal Res. 22 (3), 267-273.

Broecker, W.S., Clark, E., 1999. $CaCO_3$ size distribution: A paleocarbonate ion proxy? Paleoceanography 14 (3), 596-604.

Broecker, W.S., Clark, E., McCorkle, D.C, Peng, T.-H., Hajdas, I., Bonani, G., 1999. Evidence for a reduction in the carbonate ion content of the deep sea during the course of the Holocene. Paleoceanography 14, 6, 744-752.

Canfield, D.E., 1989. Sulfate reduction and oxic respiration in marine sediments: implications for organic carbon preservation in euxinic environments. Deep-Sea Res. 36, 121-138.

Charles, C.D., Morley, J.J., 1988. The paleoceanographic significance of the radiolarian Didymocyrtis tetrathalamus in eastern Cape Basin sediments. Palaeogeogr., Palaeoclimatol., Palaeoecol. 66, 113-126.

Diester-Haass, L., 1976. Quaternary accumulation rates of biogenous and terrigenous components on the East Atlantic continental slope off NW Africa, Mar. Geol. 21, 1-14.
Diester-Haass, L., 1977. Radiolarian/planktonic foraminiferal ratios in a coastal upwelling region, J. of Foraminiferal Res. 7 (1), 26-33.
Diester-Haass, L., 1978. Sediments as an indicator of upwelling. In: Boje, R., Tomczak, M. (Eds.), Upwelling ecosystems, Springer, Berlin, 261-281.
Diester-Haass, L. 1985. Late Quaternary sedimentation on the eastern Walvis Ridge, SE Atlantic (HPC 532 and 4 poston cores). Mar. Geol. 65, 145-189.
Dittert, N., Baumann, K.-H., Bickert, T., Henrich, R., Huber, R., Kinkel, H., Meggers, H., 1999. Carbonate dissolution in the deep ocean: methods, quantification and paleoceanographic application. In: Fischer, G., Wefer, G., Proxies in paleoceanography - examples from the South Atlantic. Springer-Verlag Berlin, Heidelberg, pp. 255-284.
Dittert, N., Henrich, R., 2000. Carbonate dissolution in the South Atlantic Ocean: evidence from ultrastructure breakdown in *Globigerina bulloides*. Deep-Sea Res. I 47, 603-620.
Emerson, S., Bender, M., 1981. Carbon fluxes at the sediment-water interface of the deep-sea: calcium carbonate preservation. J. Mar. Res. 39, 139-162.
Emerson, S., Hedges, J.I., 1988. Processes controlling the organic carbon content of open ocean sediments. Paleoceanography 3 (5), 621-634.
Eppley, R.W., Peterson, B.J., 1979. Particulate organic matter flux and planktonic new production in the deep ocean. Nature 282, 677-680.
Fowler, S.W., Knauer, G.A., 1986. Role of large particles in the transport of elements and organic compunds through the oceanic water column. Prog. Oceanogr. 16, 147-186.
Giraudeau, J., 1993. Planktonic foraminiferal assemblages in surface sediments from the southwest African continental margin. Mar. Geol. 110, 47-62.
Giraudeau, J., Rogers, J., 1994. Phytoplankton biomass and sea-surface temperature estimates from sea-bed distribution of nannofossils and planktonic foraminifera in the Benguela upwelling system. Micropaleont. 40 (3), 275-285.
Hales, B., Emerson, S., Archer, D., 1994. Respiration and dissolution in the sediments of the western North Atlantic: estimates from models of in situ microelectrode measurements of porewater oxygen and pH. Deep-Sea Res. I 41, 695-719.
Hales, B., Emerson, S., 1997. Calcite dissolution in sediments of the Ceara Rise: In situ measurements of porewater O_2, pH, and $CO_{2(aq)}$. Geochimica et Cosmochimica Acta 61 (3), 501-514.
Henrich, R., Kassens, H., Vogelsang, E., Thiede, J., 1989. Sedimentary facies of glacial-interglacial cycles in the Norwegian Sea during the last 350 ka. Mar. Geol. 86, 283-319.
Henrich, R., 1989. Glacial/interglacial cycles in the Norwegian Sea: sedimentology, paleoceanography, and evolution of Late Pliocene to Quaternary northern hemisphere climate. Proc. ODP, Sci. Results 104, 189-232.
Hopkins, T.L., 1985. Food web of Antarctic midwater ecosystem. Mar. Biol. 89, 197-212.
Howard, W.R., Prell, W.L., 1994. Late Quaternary $CaCO_3$ production and preservation in the Southern Ocean: Implications for oceanic and atmosheric carbon cycling. Paleoceanography 9 (3), 453-482.
Huang, Y., Dupond, L., Sarnthein, M., Hayes, J.M., Eglinton, G., 2000. Mapping of C4 plant input from North West Africa into North East Atlantic sediments. Geochimica et Cosmochimica Acta 64 (2), 3505-3513.
Jahnke, R.A, Craven, D.B., Gaillard, J.-F., 1994. The influence of organic matter diagenesis on $CaCO_3$ dissolution at the deep-sea floor. Geochimica et Cosmochimica Acta 58 (11), 2799-2809.
Kirst, G.J., Schneider, R.R., Müller, P.J., von Storch, I., Wefer, G, 1999. Late Quaternary temperature variability in the Benguela Current system derived from alkenones. Quat. Res. 52, 92-103.
Keigwin, L.D., 1976. Late Cenozoic planktonic foraminiferal biostratigraphy and paleoceanography of the Panama Basin. Micropaleont. 22, 419-422.
Kemle-von Mücke, S., Oberhänsli, H. 1999. The distribution of living planktic foraminifera in relation to Southeast Atlantic Oceanography. In: Fischer, G., Wefer, G. (Eds.), Use of proxies in paleoceanography: examples from the South Atlantic. Springer-Verlag, Berlin, Heidelberg, 91-115.
Le, J., Shackleton, N.J., 1992. Carbonate dissolution flucutation in the western equatorial Pacific during the Late Quaternary. Paleoceanography 7, 21-42.
Lee, C., Wakeham, S.G., Farrington, J.W., 1983. Variations in the composition of particulate organic matter in a time-series sediment trap. Marine Chemistry 13, 181-194.
Li, B., Yoon, H.-I., Park, B.-K., 2000. Foraminiferal assemblages and $CaCO_3$ dissolution since the last deglaciation in the Maxwell Bay, King George Island, Antarctica. Mar. Geol. 169, 239-257.
Little, M.G., Schneider, R.R., Kroon, D., Price, B., Summerhayes, C.P., Segl, M., 1997a. Trade Wind forcing of upwelling, seasonality, and Heinrich events as a response to sub-Milankovitch climate variability. Paleoceanography 12(4), 568-576.
Little, M.G., Schneider, R.R., Kroon, D., Price, B., Bickert, T., Wefer, G., 1997b. Rapid palaeoceanographic changes in the Benguela Upwelling System for the last 160,000 years as

indicated by abundances of planktonic foraminifera. Palaeogeogr., Palaeoclimat., Palaeoecol. 130, 135-161.

Matthewson, A.P., Shimmield, G.B., Kroon, D., 1995. A 300 kyr high-resolution aridity record of the North African continent. Paleoceanography 10 (3), 677-692.

Milliman, J.D., Troy, P. J., Balch, W.M., Adams, A.K., Li, Y.-H., Mackenzie, F.T., 1999. Biologically mediated dissolution of calcium carbonate above the chemical lysocline? Deep-Sea Res. I, 46, 1653-1669.

Müller, P.J., Schneider, R., Ruhland, G., 1994. Late Quaternary PCO_2 variations in the Angola current: Evidence from organic carbon $d^{13}C$ and alkenone temperatures. In: Zahn, R., Kaminski, M.A., Labeyrie, L., Pederson, T.F. (Eds.), Carbon cycling in the glacial ocean: Constraints on the ocean`s role in global change. Springer, New York, pp. 343-366.

Niebler, H.-S., 1995. Rekonstruktion von Paläo-Umweltparametern anhand von stabilen Isotopen und Faunen-Vergesellschaftungen planktischer Foraminiferen im Südatlantik. Berichte zur Polarforschung 167, 1-198.

Oberhänsli, H., 1991. Upwelling signals at the Northeastern Walvis Ridge during the past 500,000 years. Paleoceanography 6 (1), 53-71.

Oppo, D.W., Fairbanks, R.G., Gordon, A.L., 1990. Late Pleistocene Southern Ocean $\delta^{13}C$ variability. Paleoceanography 5 (1), 43-54.

Oppo, D. W., Rosenthal, Y., 1994. Cd/Ca changes in a deep Cape Basin core over the past 730,000 years: Response of circumpolar deepwater variability to northern hemishpere ice sheet melting? Paleoceanography 9 (5), 661-675.

Parker, F.L., Berger, W.H., 1971. Faunal and solution pattern of planktonic foraminifera in surface sediments of the south Pacific. Deep-Sea Res. 18, 73-107.

Peterson, L.C., Prell, W.L., 1985. Carbonate dissolution in recent sediments of the eastern equatorial Indian Ocean: Preservation patterns and carboante loss above the lysocline. Mar. Geol. 64, 259-290.

Porter, K.G., 1984. Alternate fate of planktonic detritus: Organic deposition and the geological record. Bulletin of Marine Science 35, 587-600.

Raymo, M.E., Ruddiman, W.F., Shackleton, N.J, Oppo, D.W., 1990. Evolution of Atlantic-Pacific $\delta^{13}C$ gradients over the last 2.5 m.y. Earth Plan. Sci. Lett. 97, 353-368.

Ruddiman, W.F., Heezen, B.C., 1967. Differential solution of planktonic foraminifera. Deep-Sea Res. 14, 801-808.

Rühlemann, C., Müller, P.J., Schneider, R.R., 1999. Organic carbon and carbonate as paleoproductivity proxies: examples from high and low productivity areas of the tropical Atlantic. In: Fischer, G., Wefer, G. (Eds.), Use of proxies in paleoceanography: examples from the South Atlantic. Springer-Verlag, Berlin, Heidelberg, 315-344.

Sautter, L.R., Sancetta, C., 1992. Seasonal associations of phytoplankton and planktic foraminifera in an upwelling region and their contribution to the seafloor, Marine Micropaleontol. 18, 263-278.

Schmiedl, G., Mackensen, A., 1997. Late Quarternary paleoproductivity and deep water circulation in the eastern South Atlantic Ocean: Evidence from benthic foraminifera. Paleogeog. Paleoclimat., Paleoecol. 130, 43-80.

Schmidt, H., 1992. Der Benguela-Strom im Bereich des Walfisch-Rückens im Spätquartär. Berichte aus dem Fachbereich Geowissenschaften der Universität Bremen, Bremen, 28, 1-172.

Schulz, H.D., Beese, D., Breitzke, L., Brück, B., Brügger, B., Dahmke, A., Dehning, D., Diekampf, V., Donner, B., Ehrhardt, I., Gerlach, H., Giese, M., Glud, R., Gumprecht, R., Gundersen, J., Henning, R., Hinrichs, S., Petermann, H., Richter, M., Sagemann, J., Schmidt, W., Schneider, R., Scholz, M., Segl, M., Werner, U., Zabel, M., 1992. Bericht und erste Ergebnisse über die Meteor-Fahrt M20/2. Abidjan - Dakar, 27.12.1991-3.2.1992. Berichte aus dem Fachbereich Geowissenschaften der Universität Bremen 25, 1-173.

Shannon, L.V., Boyd, A.J., Brundrit, G.B., Taunton-Clark, J., 1986. On the existence of an El Nino-type phenomenon in the Benguela System. J. Mar. Res. 44, 495-520.

Summerhayes, C.P., Kroon, D., Rosell-Melé, R.W., Jordan, R.W., Schrader, H.-J., Hearn, R., Villanueva, J., Grimalt, J.O., Eglington, G., 1995. Variablity in the Benguela Current upwelling system over the past 70,000 years. Prog. Oceanog. 35, 207-251.

Thunell, R.C., 1976. Optimum indices of calcium carbonate dissolution in deep-sea sediments. Geology 4, 525-528.

Thunell, R.C., Honjo, S., 1981. Calcite dissolution and the modification of planktonic foraminiferal assemblages. Mar. Micropaleontol. 6, 169-182.

van Kreveld-Alfane, S. 1996. Late Quaternary sediment records of mid-latitude northeast Atlantic calcium carbonate production and dissolution. Ph.D. thesis, University of Amsterdam, FEBO B.V., Enschede, The Netherlands.

Volbers, A.N.A., and Henrich, R. (subm). Present water mass calcium carbonate corrosiveness in the eastern South Atlantic inferred from ultrastructural breakdown of *Globigerina bulloides* in surface sediments. Submitted to Earth and Planetary Science Letters.

Volbers, A.N.A., Niebler, H.-S., Giraudeau, J., Schmidt, H., Henrich, R. (subm.). Paleoceanographic changes in the northern Benguela upwelling system over the last 245.000 years as derived from planktic foraminifera assemblages. Submitted to Deep-Sea Res.

Wagner, T., 2000. Control of organic carbon accumulation in the late Quaternary equatorial Atlantic (Ocean Drilling Program sites 664 and 663): Productivity versus terrigenous supply. Paleoceanography 15 (2), 181-199.

Wakeham, S.G., Lee, C., Farrington, J.W., Gagosian, R.B., 1984. Biogeochemistry of particulate organic matter in the oceans: results from sediment trap experiments. Deep-Sea Res. 31 (5), 509-528.

Wakeham, S.G., Canuel, E.A., 1988. Organic geochemistry of particulate matter in the eastern tropical North Pacific Ocean: Implications for paticle dynamics. J. of Mar. Res. 46, 183-213.

Wakeham, S.G., Lee, C., 1989. Organic geochemistry of particulate matter in the ocean: The role of particles in oceanic sedimentary cycles. Org. Geochm. 14 (1), 83-96.

Wu, G., Berger, W.H., 1991. Pleistocene $\delta^{18}O$ records from Ontong-Java Plateau: Effects of winnowing and dissolution. Mar. Geol. 96, 193-209.

2. Present water mass calcium carbonate corrosiveness in the eastern South Atlantic inferred from ultrastructural breakdown of *Globigerina bulloides* in surface sediments

Andrea N.A. Volbers and Rüdiger Henrich

Faculty of Geosciences, Department of Paleoceanography and Sedimentology, P.O. Box 33 04 40, D-28334 Bremen, Germany

Abstract

The Atlantic is regarded as the largest present-day deep-sea carbonate sink [1] as, with an on average deep calcite lysocline, it serves as a huge carbonate depocenter. However, calculations and models that attribute the calcite lysocline to the critical undersaturation depth (hydrographic or chemical lysocline) and not to the depth at which significant calcium carbonate dissolution is observed (sedimentary calcite lysocline) strongly overestimate the preservation potential of calcareous deep-sea sediments. From hydrographic parameters alone, one would expect significant calcium carbonate dissolution to begin firstly below 5000 m in the deep Guinea and Angola Basin and below 4400 m in the Cape Basin. Our study clearly shows that it starts between 400 to 1600 m shallower depending on the different hydrographic settings.

In the Cape Basin the sedimentary calcite lysocline coincids with the interface of North Atlantic Deep Water (NADW) and Antarctic Bottom Water (AABW). The AABW/NADW transition is encountered at around 4000 m water depth and marked by distinct gradients in salinity, temperature, and carbonate ion concentration ($[CO_3^{2-}]$). It is also reflected in the preservation state of the planktic foraminifera *Globigerina bulloides* which we use as a proxy to determine the onset of significant calcite dissolution in surface sediments (*G. bulloides* dissolution index, BDX' [2]).

Within the northern Cape Basin, the sedimentary calcite lysocline lies at 4000 m water depth whereas it is around 400 m shallower in the vicinity of the Benguela upwelling system. The coastal areas are affected by increased supply of organic matter, most of which is degraded at or near the sediment-water interface. The resultant production of metabolic CO_2 seems to create microenvironments favorable for dissolution of calcite well above the hydrographic lysocline.

The calcium carbonate preservation potential of the Angola Basin, where virtually no AABW is present even at great depth, is generally expected to be much better. Our results indicate that this is not the case. We present four transects across the Guinea and Angola Basins with obviously different regional control parameters reflected by different levels of the sedimentary calcite

lysocline: 3400 m (coastal Angola Basin), 3600 m (equatorial region), 4000 m (Mid-Atlantic-Ridge) and 4400 m (Walvis Ridge-Angola Basin transect). Hence, the sedimentary calcite lysoclines were encountered between 600 to 1600 m shallower than the hydrographic lysocline. In these regions, the variable interplay of organic matter degradation and sediment accumulation seems to account for the different positions of the sedimentary calcite lysocline.

The exact positioning of the calcite lysocline is important because of its potential as a significant sink and buffer with relevance for the ongoing CO_2 debate. As the BDX' has proved its usefulness as reliable indicator of the sedimentary calcite lysocline in the modern eastern South Atlantic ocean, it may serve as an excellent tool to grasp the changes in the positions of the calcite lysocline during the late Quaternary.

1. Introduction

Since the ocean contains more than 60 times the CO_2 of the atmosphere [3] it plays a very important role in global CO_2 budgeting, in particular during the Quaternary climatic oscillations. The Southern Oceans have a great impact on atmospheric CO_2 relative to their surface area and seem to play a key role as a mixing zone in the deep-water circulation pattern [4]. In particular, the South Atlantic has been the subject of intense investigation because it drives the global thermohaline circulation [5]. The Atlantic deep water circulation is marked by various interactions of North Atlantic Deep Water (NADW) and Antarctic Bottom Water (AABW), water masses which differ significantly in their physical properties, nutrient concentration, and carbonate ion concentration ($[CO_3^{2-}]$). NADW is a relatively warm and well-ventilated water mass that forms from highly saline surface waters at high northern lattitudes [6]. In the western South Atlantic and in the Cape Basin, it is encountered roughly between 2000 and 4000 m water depth overriding the AABW, which is a cold water mass (potential temperature <1.6°C, [7]) of low salinity [8,9]. The movement of AABW northwards into the eastern South Atlantic basins is hindered by the Walvis Ridge, and only small quantities can enter the Angola Basin via the Walvis Passage (Fig. 1) [10]. Further inflow of AABW from the west is limited by the submarine barriers of the Mid-Atlantic Ridge permitting AABW to penetrate into the Guinea and Angola Basin via the Romanche Fracture Zone. The water that enters the eastern basins above the controlling sill depth of 4350 m is relatively old and depleted in oxygen with a potential temperature of 0.9°C [11-13]. In contrast to the western South Atlantic and the Cape Basin, which contain deep waters well below 0.5°C, the Guinea and Angola Basin deep waters are nowhere colder than slightly below 2°C, as they contain admixtures of only 28% and 19% AABW, respectively [12]. This limited supply of the more corrosive AABW to the eastern South Atlantic basins is expected to have a significant impact on the calcium carbonate preservation potential of these basins compared to the Cape Basin and the western South Atlantic.

In the western South Atlantic and Cape Basin, the calcium carbonate preservation level is predominantly tied to the NADW/AABW interface [14]. The preservation of calcitic tests of planktic

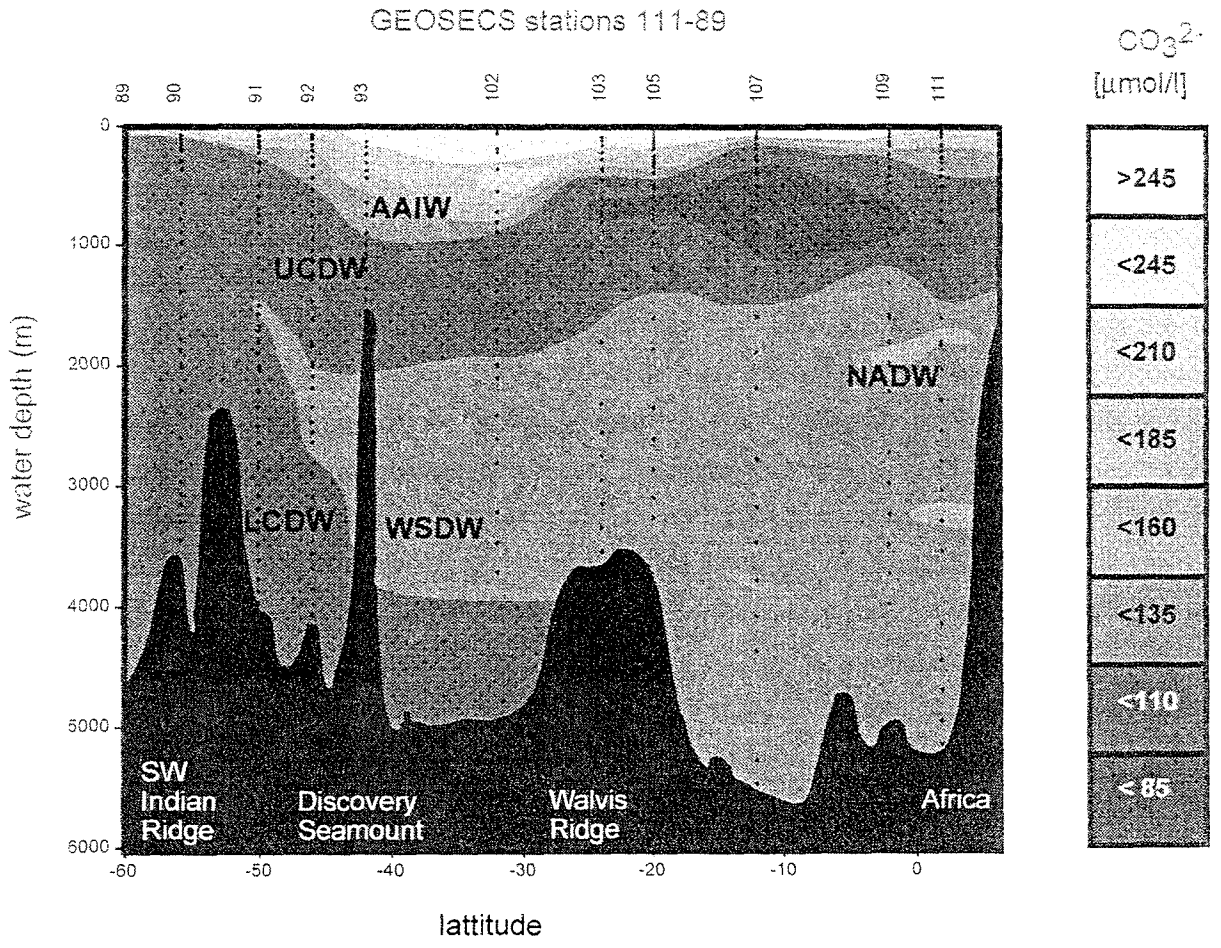

Fig. 1: Present water mass distribution of the east Atlantic shown as N-S transect. W.R.... Walvis Ridge, S.L.R... Sierra Leone Rise, AAIW... Antarctic Intermediate Water, NADW... North Atlantic Deep Water, UCDW... Upper Circumpolar Deep Water, LCDW... Lower Circumpolar Deep Water, WSDW... Weddell Sea Deep Water. Distribution of LCDW and WSDW (commonly refered to as AABW) to the south eastern basin is impeded by the Walvis Ridge. GEOSECS location (115-89) from which CO_3^{2-} [µmol/l] concentration were calculated are marked on top.

foraminifera strongly decreases below this boundary, which was therefore previously described as the „foraminiferal lysocline" [15]. Below this lysocline the $CaCO_3$ content of a deep-sea sediment drops rapidly from around 90% to 10% [3]. We make use of this phenomenon as we examine the breakdown of the planktic foraminifera *Globigerina bulloides* in great detail. In earlier studies [e.g. 2], the *Globigerina bulloides* dissolution index (BDX') has been shown to detect calcite dissolution within deep-sea sediments very precisely. We use this index here to check the relationship between the different preservation states of *G. bulloides* compared with the overall water mass distribution in the eastern South Atlantic Ocean.

In general, water masses that are undersaturated with respect to calcite, such as AABW, cause significant calcite dissolution in surface sediments as they strive to attain equilibrium. In contrast, NADW is slightly supersaturated with respect to calcite [3] and calcareous sediments should be

well-preserved until the NADW/AABW boundary is encountered. As the Guinea Basin and Angola Basin are filled mainly with NADW, a deep calcite lysocline is expected to be located around the water depth where the in situ [CO_3^{2-}] falls below the saturation concentration due to the increased solubility of $CaCO_3$ with increasing pressure and hence water depth.

In addition, the interplay of organic content and sedimentation rate is expected to contribute significantly to the calcium carbonate dissolution of deep-sea sediments. The respiration of organic matter stimulates calcite dissolution even if the overlying bottom waters are supersaturated with respect to $CaCO_3$. Sediment studies, benthic flux chamber experiments, and microelectrode measurements of pore waters point out that calcium carbonate may dissolve above the chemical lysocline in supersaturated waters [16,17]. This „respiratory dissolution" or „supralysoclinal dissolution" seems to be the result of biological mediation [18], particularly affecting high-productivity regions, e.g. upwelling systems, where nutrient enriched waters create a high productivity regime. An increase in the organic carbon export also increases the amount of bicarbonate in the deep oceans because most of the organic carbon is respired or remineralized by benthic organisms in the sediment. As this process produces CO_2 it creates a microenvironment that drives the dissolution of calcite particles even above the lysocline [17,19,20]. The amount of calcium carbonate that is lost by this mechanism was estimated to be around 20% [1] up to 40-50% [21] or even 40-80% [19, 22]. For this reason it has been concluded that the onset of $CaCO_3$ dissolution in the sediments may occur 0.5 to 1 km above the chemical saturation horizon in the ocean water [19, 22]. On the other hand, rapid sedimentation can protect calcitic tests from further dissolution by reducing the time span that they are exposed to seawater. As the organic matter is mostly degraded within the oxygenic milieu, the degradation process is limited to the distribution of oxygen within the sediment [23]. In-situ microelectrode and shipboard measurements show that oxygen penetrates only 13 mm into the sediments in the eastern Atlantic upwelling sites [24].

As we expected to encounter a decoupling of the calcium carbonate saturation horizon and the sedimentary lysocline depth in high-productivity regions, we studied six transects covering the different regional settings in the eastern South Atlantic. Nowadays, ocean-wide hydrographic section data from e.g. the Geochemical Ocean Sections Study (GEOSECS) or the World Ocean Circulation Experiment (WOCE) are widely used [25,26] to describe today`s large-scale water mass distribution (Fig. 2) and their physicochemical properties, but reliable paleoceanographic proxies of these physicochemical properties back into the fossil record are still in high demand within the scientific community. In this respect, lysocline reconstructions play an important role in models which seek to explain the 1/3 decrease of the atmospheric CO_2 during the last glacial maximum (LGM, 23-19 kyrs) [27]. As the BDX' is solely determined by carbonate corrosion it can provide an independent tool to determine the water mass configuration during the past, e.g. during the LGM and other time slices.

2. Material and Methods

2.1 Surface samples

We studied 118 samples from Guinea, Angola and Cape Basin and the eastern equatorial Atlantic which were collected with gravity corers during various RV METEOR cruises between 30 m and 5700 m water depth (Fig. 2). These are aligned along six transects through the major eastern south Atlantic basins between 5°S to 30°S and 2°W to 15°E.

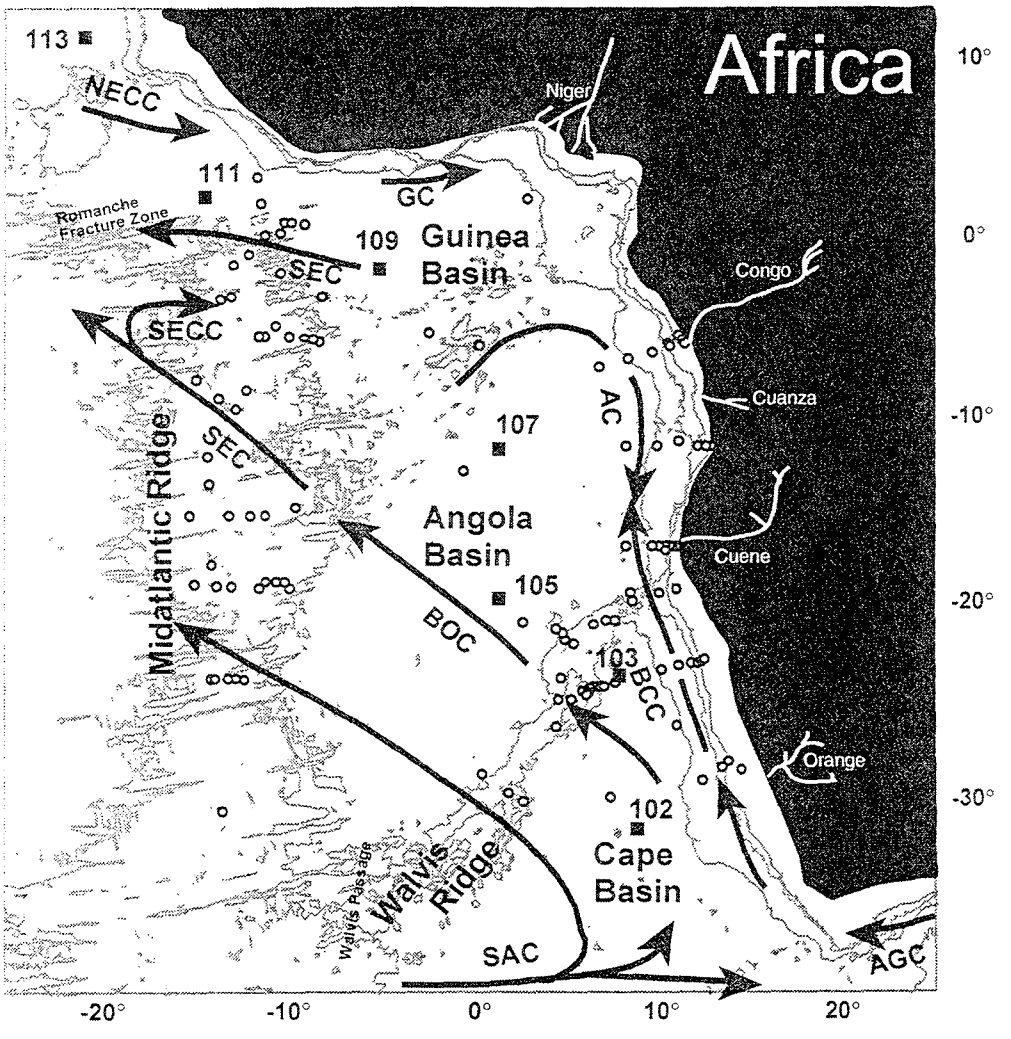

Fig. 2: Eastern South Atlantic hydrography. AC... Angola Current, AGC... Agulhas Current, BCC... Benguela Coastal Current, BOC... Benguela Oceanic Current, GC... Guinea Current, SAC... South Atlantic Current, SEC... South Equatorial Current. Open circles prepresent investigated sediment surface samples, rectangles represent GEOSECS stations.

2.2 *Globigerina bulloides* dissolution index (BDX')

In this study, we chose *G. bulloides*, a non-symbiotic spinose planktic foraminifera, because of its extensive spatial and environmental distribution. This species is among the most abundant planktic foraminifera in the eastern South Atlantic today [28] and constantly available through time [29]. As this species also has a high dissolution susceptibility ranking [30], it turns out to be the perfect indicator for the determination of the foraminiferal carbonate preservation state. With it, even minimal changes in the calcium carbonate preservation of the fraction >125 µm can be detected [2]. An

improvement of earlier methods [31,32] yielded the *Globigerina bulloides* dissolution index (BDX', [2]) applied in this study (Fig. 4). It is a reliable indicator of foraminiferal carbonate preservation via the identification of six dissolution stages based on at four distinct ultrastructural features (spines, pores, ridges, interpore area). The following is a brief characterization of the preservation features and preservation stages used in this study (Fig. 4):

stage 0-1 (excellent preservation): recognized by round pores, smooth interpore areas, intact ridges, and high spines. It is only observed on *G. bulloides* tests taken from mooring samples (after storage in mercury-saturated seawater which, of course, may have led to some additional dissolution features).

stage 1-2 (very good to good preservation): identified by slightly widened pores, partly etched interpore areas, slightly denuded ridges and spines. Only observed at *G. bulloides* tests taken from mooring samples, hardly observed in surface sediment samples.

stage 2-3 (good to moderate preservation): recognized by funnellike pores, etched and roughened interpore areas, denuded ridges and spines. This preservation stage is normally found in surface sediments under slightly corrosive conditions.

stage 3-4 (bad preservation): revealed by partly interconnected pores, partial removal of the surface layer, strongly reduced ridges and spines. It is an indicator of moderate corrosive conditions much as occur during the respiration of organic matter in the eastern South Atlantic surface sediments.

stage 4-5 (very bad preservation): indicated by interconnected pores, removal of the surface layer, missing ridges and spines. This preservation stage is found in surface sediments under highly corrosive conditions.

stage 5: indicated by the absence of intact tests due to severe dissolution.

Fig. 3: Progressive dissolution of *Globigerina bulloides* ultrastructure. The BDX' [2] consits of six dissolution stages that are determined by the decreasing preservation state of the four ultrastructural test features: pores, interpore space, spines, and ridges. As dissoluiton proceeds, pores get widened, the interpore areas is etched, ridges and spines become denuded until the specimen is finally brocken down (BDX'=5)

Whenever available, 30 specimen per sample were glued to a SEM stub, gold coated and investigated with a ZEISS DSM 940 A (10 mm working distance, 10 kN accelarating voltage). Ultrastructural investigations were carried out at a magnification of 4000x. When the sediment material was limited, at least 10 *G. bulloides* tests were examined to determine the BDX'. The BDX' value was calculated according to the follwing equations:

$$P=(P_{(pores)}+P_{(interpore\ area)}+P_{(spines)}+P_{(ridges)})/4 \quad (1)$$

The preservation state (P, between 0.5 and 4.5) of each single *G. bulloides* is calculated from the preservation of each criterion investigated (pores, interpore area, spines, and ridges) divided by the number of criteria, which is four. This method assures that every criterion is judged equally when calculating the BDX':

$$BDX'= \sum P/ nT \quad (2)$$

With $\sum P$ as the sum of all individual preservation states of *G. bulloides* divided by the number of investigated tests (nT).

Since the term „calcite lysocline" is subject to different scientific use, we apply the definition of Milliman [22] with the top of the (sedimentary) calcite lysocline marked by the first observation of significant carbonate dissolution in calcareous sediments which is reflected by the BDX' preservation stage of 3 [2].

3. Hydrographic setting of studied transects

Two out of the six investigated transects cover the northern Cape Basin and four cover the Angola Basin (Fig. 4) according to their different deep-water mass distribution patterns. Within either basin different hydrographic regimes were covered to compare their impacts on calcium carbonate preservation.

3.1 Cape Basin

The hydrography of the northern Cape Basin is dominated by the Benguela Current (BC) which extends from 35°S to 17°S and interacts with the warm Angola Current in the north and the Angulhas Current in the south (Fig. 1). At about 30°S, the BC splits into the Benguela Oceanic Current (BOC) which flows to the west across the Walvis Ridge (Walvis Ridge-Cape Basin transect) and the colder Benguela Coastal Current (BCC) moving northward. The Coastal Cape Basin transect is influenced by the wind-driven upwelling of cold, nutrient-rich subsurface waters including the broad mixing area, which extends more than 600 km seaward [33]. The Southwest-African shelf and continental slope are influenced by the coastal upwelling with primary production rates >100 gC/m^2/year and organic material flux rates>5gC/m^2/year, which is reflected in total organic carbon (TOC) values >>2wt% [34]. Carbonate production is estimated to be 30-40 g/m^2/year in the eastern high productivity areas [22], and large areas exhibit very low oxygen concentrations

[35]. Relative to the Walvis Ridge (transect 2), accumulation rates along the Southwest-African coast (transect 1) are higher by more than a factor of 4. As the main wind direction in this region is from the south and the southeast, cold and nutrient enriched filaments from the coastal upwelling pass the Walvis Ridge, and divide it in a western low-productivity part (45-50 gC/m^2/year [36,37], 30-70 gC/m^2/year, organic material flux rates <1gC/m^2/year, [34]) and an eastern high-productivity part (150 g/m^2/year [19]). This is strongly reflected by increasing TOC values from west to east, with up to 6 wt% near the African coast and <0.2 wt% in the southwest [34,38]. The same trend is observed in the sediment accumulation rates which are on average <1 cm/1000 on the Walvis Ridge and more than 3 cm/1000 at the African coast [34,23].

Comparative studies of the Walvis Ridge and the coastal upwelling area clearly show the enhanced decay of organic matter in the sediments of transect 2 as reported by lower $\delta^{13}C$ values derived from benthic foraminifera [39]. The investigated Cape Basin transects therefore represent an open-ocean regime with some coastal influence (transect 1) and a high productivity coastal regime (transect 2).

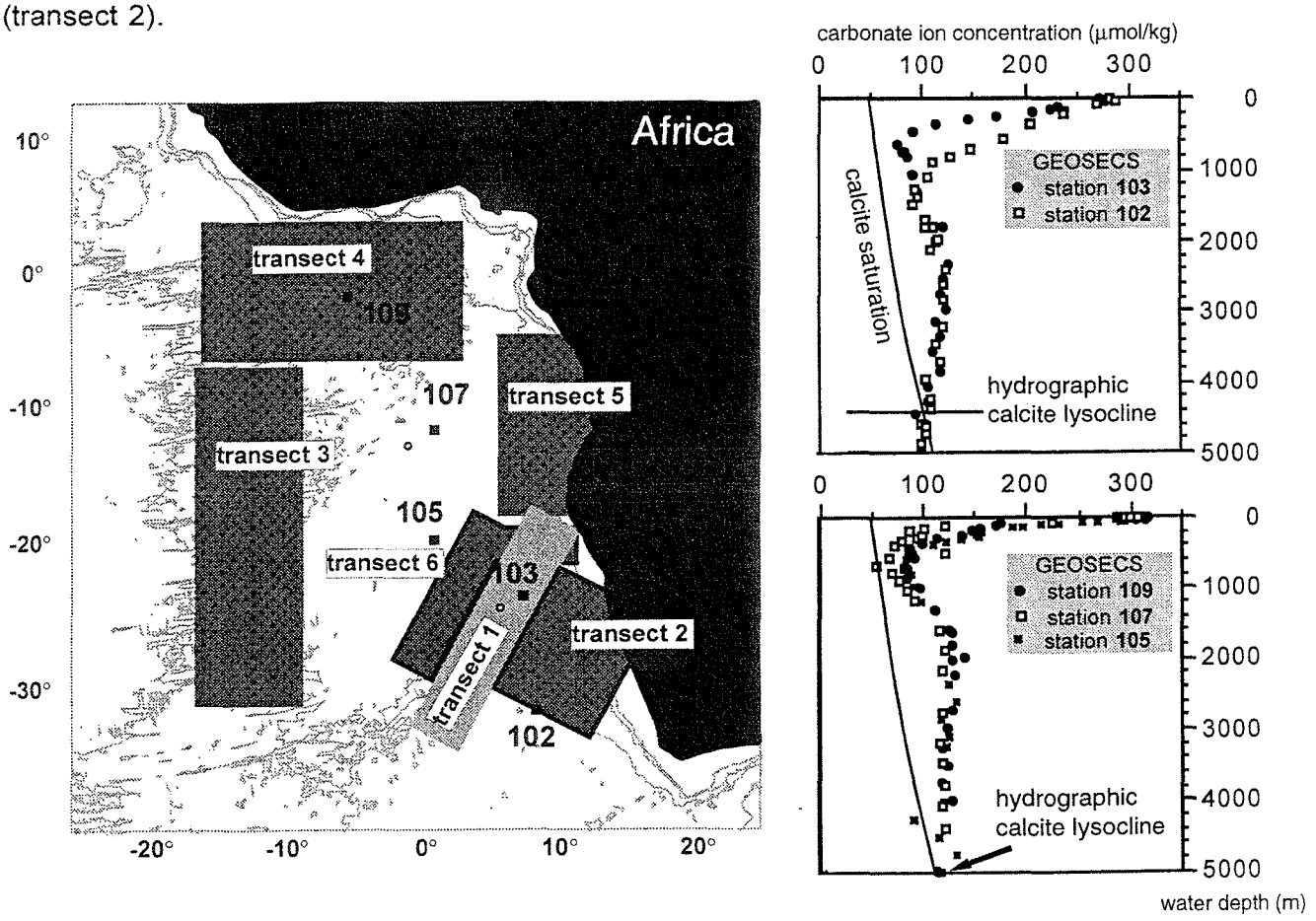

Fig. 4: Location of investigated transects and GEOSECS stations. GEOSECS stations 109, 107, and 105 show rather constant carbonate ion concentrations [CO_3^{2-}] with increasing water depth for the deep Cape Guinea and Angola Basin. The hydrographic lysocline within these basins is encountered at the water depth at which the [CO_3^{2-}] crosses the calcite saturation curve. In contrast GEOSECS stations 103 and 102 display decreasing [CO_3^{2-}] with depth indicating the presence of AABW in the deep Cape Basin. The hydrographic calcite lysocline is therefore encountered at 4400 m water depht, around 600 m shallower than compared to the Guinea and Angola Basin.

3.2 Angola Basin

We studied four different transects within the Angola Basin. Compared to all other transects, the investigated Mid-Atlantic Ridge area (transect 3) is influenced by the southern South Equatorial Current (SEC) (Fig. 1), which is commonly referred to as a low-productivtity (30-45 gC/m^2/year [37], 40 gC/m^2/year [40]) regime. As the Mid-Atlantic Ridge section is characterized by low primary productivity and relatively low carbonate export compared to the equatorial or coastal regions [22] we investigated the equatorial section (transect 4) separately. The eastern tropical Atlantic (Guinea Basin) is strongly influenced by the strong NE trade winds during the northern hemisphere summer months. High primary production (60-100 gC/m^2/year, [37], 157 gC/m^2/year, [41]) and cool SST (22-25°C) occur from about 3°N to 7°S [42] coupled with equatorial upwelling. In addition, terrigenous organic material is supplied to the equatorial region [43] and increases the TOC in the sediment. According to Fig. 5, TOC values from the equatorial region are on average increased by a factor of 2 compared to the Mid-Atlantic Ridge region.

Again, the coastal Angola Basin transect (transect 5) and the Walvis Ridge-Angola Basin transect (transect 6) cover highly different regions with respect to organic matter and calcium carbonate content and accumulation rates. The primary productivity rates between 8° and 18°S range between 125 g and 180 gC/m/year [37]. Although in general, carbonate production along the eastern high productivity areas is increased by a factor of 4 to 5 compared to the open ocean [1], transect 5 is strongly dominated by the terrigenous clay input from the Congo River, resulting in unusually low carbonate percentages (Fig. 5) in the northeastern section of the basin [44]. Although, on average, the sedimentation rates along the Southwest-African continental slope are >4 cm/1000 years or even higher in the vicinity of the Kunene river [44], they reach a maximum of 27 cm/1000 years [45] in the vicinity of the Congo River. The sediments here reflect the high accumulation rates of organic matter from the productive waters above [17] and the additional supply of riverine particulate carbon [23]. There are strong indications for the oxidation of organic matter from the investigation of water mass properties at around 11°S: The oxygen, phosphate, and nitrate anomaly is most pronounced just at the upper continental rise reflecting fluxes of oxygen and nutrients across the sediment-water interface, probably resulting from the decompositon of plankton [11]. Compared with the equatorial and Mid-Atlantic Ridge region, TOC values from transect 5 are increased by a factor of 10.

Transect 6 has the same hydrographic setting as transect 1 and is therefore influenced by the BOC. Although both transects are located very close to one other and are governed by the same surface hydrography (BOC), the deep surface samples of both transects are exposed to different deep water mass bodies. As the $CaCO_3$ and TOC contents and sediment accumulation rates are in the same range as in transect 1, the differences in *G. bulloides* preservation pattern derived from both transects should reflect the different deep water mass properties within either basin. In contrast to the differences in deep water distribution, the hydrography between 500 to 2500 m is

generally characterized by AAIW/UCDW and NADW so that we used samples from between these water depth for both transects.

4. Results and Discussion

4.1 Cape Basin

To determine the position of the calcite lysocline in the northern Cape Basin, we investigated surface sediment samples from 167 m to 5102 m water depth splitt into two transects which differ significantly in accumulation rates and organic matter content.

Walvis Ridge-Cape Basin (transect 1)

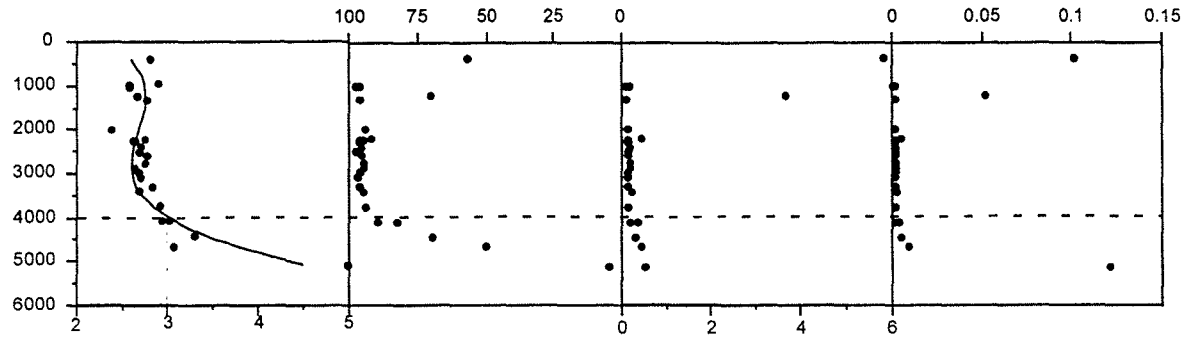

Coastal Cape Basin (transect 2)

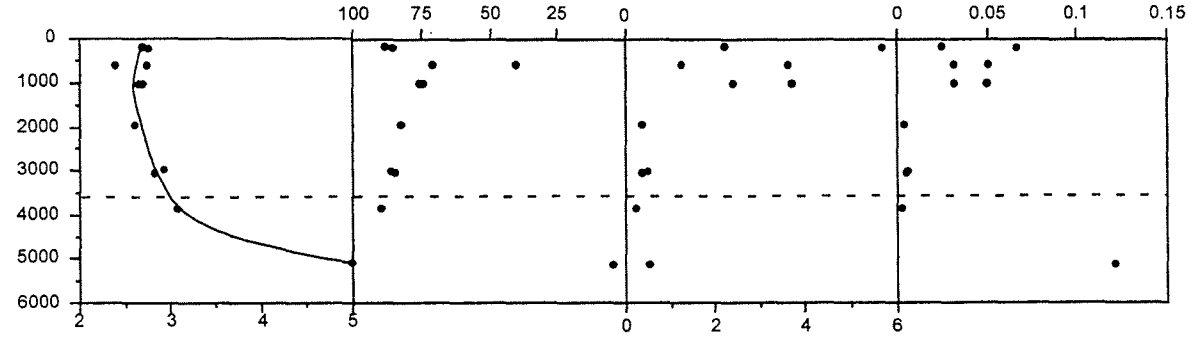

Mid-Atlantic Ridge (transect 3)

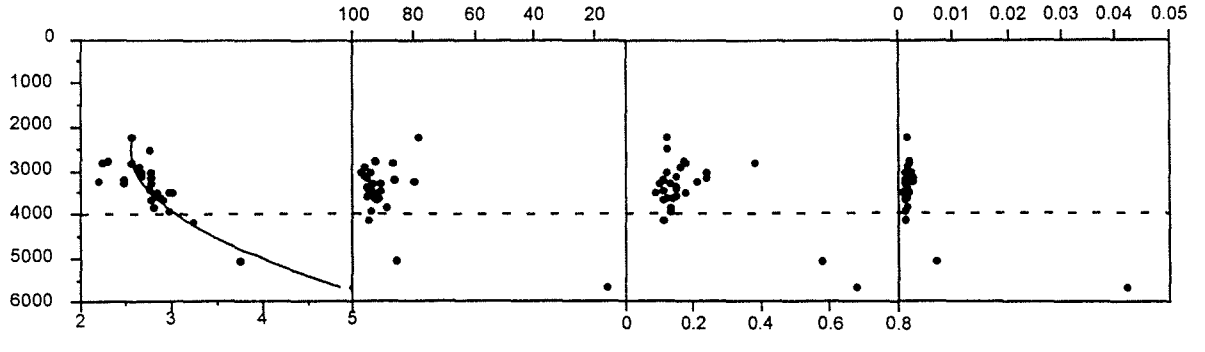

water depth (m) | BDX' | $CaCO_3$ (wt%) | TOC (wt%) | Rain ratio

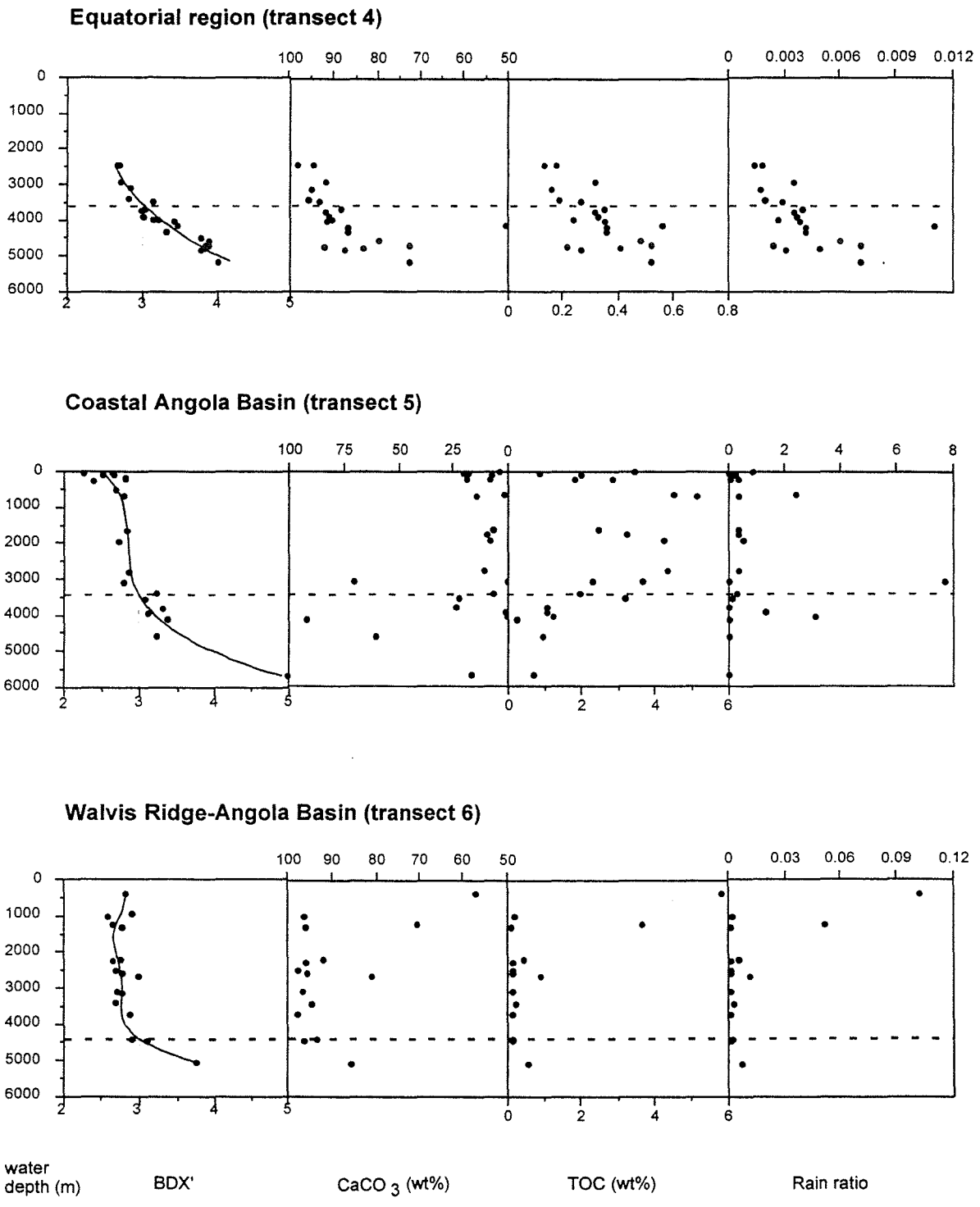

Fig. 5: Determination of the sedimentary calcite lysocline within the eastern South Atlantic basins. The progressive dissolution of *Globigerina bulloides* ultrastructure is expressed as BDX' and compared with $CaCO_3$ data, total organic content (TOC), and rain ratio which are often used as calcium carbonate dissolution proxies. $CaCO_3$ and TOC data were taken from [24], [34], [48], [49], additional unpublished data were kindly supplied by P. Müller and T. Wagner.

BDX' values from the Walvis Ridge-Cape Basin transect range between 2.5 and 5, whereas *G. bulloides* preservation from the upper water column down to 4000 m is good to moderate and decreases strongly over the following 1000 m (Fig. 4). The calcite lysocline is encountered at 4000 m, which is also reflected by a decrease in $CaCO_3$ and an increase in TOC content of the sediment (Appendix 1, Fig. 4). The ratio of organic to inorganic carbon content is expressed as the rain ratio which clearly increases below 4000 m. In former studies, in particular the $CaCO_3$ content was used to determine the calcite lysocline based on the observation that calcareous sediments are less well-preserved with increasing water depth. As seen in Fig. 5, the $CaCO_3$ content and the TOC content of the investigated surface samples are inversely correlated. According to our observation, the rain ratio works well in the open-ocean region for determining the sedimentary calcite lysocline (some coastal influence is clearly indicated from two surface samples from the eastern part of the Walvis Ridge with increased TOC content and lower $CaCO_3$ values). Inferred from our data from transect 1, the calcite lysocline within the northern Cape Basin seems to be predominantly a water mass signal. As documented in Fig. 2, the more corrosive water mass AABW (indicated by a critical $[CO_3^{2-}]$ below 85 µmol/l in Fig. 2) is encountered within the Cape Basin and absent in the Angola Basin. The onset of decreasing *G. bulloides* preservation patterns coincides with the NADW/AABW transition which is around 4000 m in the northern Cape Basin. As shown by the Walvis Ridge-Cape Basin transect, the sedimentary calcite lysocline in the open-ocean Cape Basin seem to reflect the present-day deep water mass distribution.

Compared with transect 1, the sharp decrease in the *G. bulloides* preservation of the coastal Cape Basin surface samples is observed around 400 m shallower. We attribute the rise in the position of the sedimentary calcite lysocline to the increased production of metabolic CO_2 in the coastal regions which contributes to the dissolution of calcite within the sediment [17]. In the coastal regions, increased amounts of organic matter are reflected by high TOC contents in the surface sediments and its extensive degradation is clearly indicated by lower $\delta^{13}C$ values of benthic foraminifera tests compared to the Walvis Ridge data. As shown in earlier studies [e.g. 19], an increase in the carbon to carbonate rain ratio displaces the onset of calcium carbonate dissolution upward with respect to the water column saturation horizon (hydrographic lysocline). The hydrographic lysocline within the northern Cape Basin is encountered at around 4400 m water depth (Fig. 3), that is 800 m deeper than the sedimentary calcite lysocline within transect 2. As within transect 1, the sedimentary calcite lysocline is around 400 m shallower than the hydrographic lysocline, some additional dissolution within the sediments must also take place in the more open-ocean regime of the northern Cape Basin. Supralysoclinal dissolution (dissolution above the hydrographic lysocline) seems therefore not to be limited to the high productivity regions of the northern Cape Basin. Even small amounts of organic matter (preserved as 0.2-0.6 wt% TOC in the sediment) that coincide with low sedimentation rates (0.8-1cm/1000, [46]) may obviously be sufficient for an offset of 400 m between the hydrographic and the sedimentary lysocline in the more open-ocean environment. As the sediment accumulates slowly, particles are exposed to the sea water much longer and oxygen,

which is required for the degradation process of organic matter, is easily replaced by circulation through the sediment.

In the coastal upwelling region, much more organic matter escapes the recycling process in the upper water column and accumulates within the sediment. Oxygen is consumed within the upper 13 mm of the water-sediment interface [24], therefore limiting the time period over which organic matter can be degraded. Although due to the intensified organic matter degradation and the associated higher dissolution rates of calcareous material, the burial rate of *G. bulloides* tests is more than four times higher. The degree of supralysoclinal dissolution in the northern Cape Basin seems to be mainly controlled by the interplay of supply and degradation of organic matter and its burial rate: It is stronger in the Namibian coastal region due to the increased supply of organic matter and its degradation within the surface sediment, and finally stopped by the oxygen deficit that cannot be equalized as sediment accumulates rapidly. In the more open-ocean region, the degradation process could proceed over a much longer time period because sedimentation rates are low, even though the amount of organic matter is considerably smaller in the first place.

This is best seen in *G. bulloides* preservation patterns within the upper 1000 m: The highest sedimentation rates across the continental shelf and slope protect *G. bulloides* tests of the coastal sediments from massive dissolution although TOC values are at a maximum (Fig. 5). BDX' values of the Walvis Ridge-Cape basin transect within the upper 1000 m are as high as those from the coastal transect, although TOC values are six times lower compared to the coastal region (when the two samples from the eastern part are excluded). A decrease in the sedimentation rates by at least a factor of four also causes good to moderate preservation of *G. bulloides* tests in the upper water column on the Walvis Ridge. In addition, between 500 m and 1500 m the AAIW/UCDW water mass is encountered which has a lower [CO_3^{2-}] than the underlying NADW (Fig. 2, 3) but which affects both transects equally. A further lowering of the carbonate ion concentration via organic matter degradation results in a good to moderate preservation of *G. bulloides* tests even at shallow depths.

Our reconstructions of the sedimentary calcite lysocline within the northern Cape Basin between 4000 and 4200 m water depth [47,32,44], is in accordance with earlier findings for the open ocean. For the coastal regions it was estimated to lie within the same range although investigation of planktic foraminiferal ultrastructure point insteadt to a value of 3800 m water depth in this region [32]. The calcite preservation potential of the Cape Basin would be overestimated, as within the more open-ocean regime the calcite lysocline is 400 m shallower and along the continental margin even 800 m shallower than the hydrographic lysocline. Whereas within the more open-ocean transect 1 the decrease in *G. bulloides* preservation correlates well with the decrease in $CaCO_3$ content and the increase in TOC content and rain ratio, these often used proxies do not reflect $CaCO_3$ dissolution but rather increased productivity (maximal TOC content) and accumulation of non-calcareous material in the coastal regions.

4.2 Angola Basin

To cover the different hydrographic regimes of the Guinea and Angola Basins, two open-ocean regions, the Mid-Atlantic Ridge (transect 3) and Walvis Ridge-Angola Basin region (transect 6), and two high-productivity regions, the eastern equatorial Atlantic (transect 4) and the Coastal Angola Basin (transect 5) were investigated.

From all the investigated transects, the Mid-Atlantic ridge is a true open-ocean regime [22] with lowest primary productivity, reflected by lowest TOC values (on average <0.2 wt%), low carbonate export rates and therefore lowest rain ratio (Fig. 5) compared to all other transects. We studied *Globigerina bulloides* from surface samples between 2256 m and 5684 m water depth. BDX' values range from 2.2 to 5 and decline gradually compared to the Cape Basin preservation curve pattern. The calcite lysocline is encountered at 4000 m. As the $[CO_3^{2-}]$ in the water column stays nearly constant with increasing water depth [25], Fig. 3), the $[CO_3^{2-}]$ must have been lowered by more than 30 µmol/kg to cross the calcite saturation curve at 4000 m (Fig. 3). The hydrographic lysocline in the deep Guinea and Angola Basin is encountered around 1000 m lower. The effect of respiratory dissolution seems to be enhanced compared to the northern Cape Basin open-ocean transect. The amount of organic matter preserved in the sediment as TOC is similar in both regions, although within the investigated Walvis Ridge-Cape Basin transect, sedimentation rates range between 0.8 and 1 cm/1000 [46] and are therefore higher than within the Mid-Atlantic ridge transect. The lowest sedimentation rates within the Mid-Atlantic ridge transect may account for enhanced supralysoclinal dissolution within the surface sediment of this region. Surprisingly, this effect would be as big as within the coastal transect 2, where the $[CO_3^{2-}]$ is lowered by also 30 µmol/kg.

The influence of supralysoclinal dissolution seems to be even more severe in the eastern equatorial region (transect 4) where TOC values are twice as high as in the Mid-Atlantic Ridge region. The *G. bulloides* preservation curve shows the same steady decline in preservation with increasing water depth. The more steady decline is also clearly reflected in the $CaCO_3$ content and by the steady increase in TOC contents and in the rain ratio. The sedimentary calcite lysocline is located at 3600 m water depth in the equatorial region. Due to the increased organic carbon content, the shallow sedimentary lysocline in the equatorial Atlantic region is developed around 1500 m shallower than the hydrographic lysocline in this region. The existing discrepancy of the sedimentary lysocline and the calculated hydrographic lysocline in the eastern equatorial Atlantic was also observed within the northern equatorial Atlantic: The onset of $CaCO_3$ dissolution is observed at around 3500 m whereas the depth of the critical $[CO_3^{2-}]$ is found at around 4700 m [25]. Therefore, in particular within the equatorial region, the sedimentary calcite lysocline is encountered 1200 to 1400 m shallower than expected. Although the Mid-Atlantic Ridge area encounters only 1/2 to 1/4 of the primary productivity of the equatorial region (preserved as 1/2 of the TOC content in the sediment), this effect seems to be responsible for an offset of the sedimentary calcite lysocline of 800 m above the hydrographic lysocline within the deep Guinea and Angola Basins.

The effect of dilution on the position of the sedimentary calcite lysocline can be studied in detail at transect 5, because it is strongly influenced by the terrigenous clay input from the Congo and Cuene River. As $CaCO_3$ contents are low in the first place and sediment accumulation rates extraordinary high (>>4 cm/1000 to 27 cm/ka), and additional riverine particulate carbon is supplied to the ocean [23], the $CaCO_3$, TOC content, and the rain ratio cannot be used as dissolution proxies in this region (Fig. 5). Compared with the equatorial and Mid-Atlantic Ridge region, TOC values from transect 5 are increased by a factor of 10 and the rain ratio is increased by more than a factor of 100. To determine the position of the sedimentary lysocline within the Angola coastal area, *G. bulloides* between 30 m and 5684 m were investigated. Preservation decreases rapidly within the upper 200 m towards constant good to moderate preservation until at around 3400 m the sedimentary calcite lysocline is encountered. The *G. bulloides* preservation curve pattern resembles that from the coastal Cape Basin transect, although the $CaCO_3$ content is three to four times lower within the Coastal Angola Basin transect. Although the material is much more rapidly covered by mainly terrigenous sediment compared to all other transects, only a much smaller number of calcareous tests would be attacked by the released CO_2. In addition, coatings of dissolved organic matter or PO_4^{3-} could be attached to calcite surfaces, attacking them chemically with the same efficiency as bacteria colonies [17,18]. Within this transect the most significant decoupling of the sedimentary calcite lysocline and the hydrographic lysocline is observed, on the order of 1600 m, in comparison with all data from other transects.

Concerning the Guinea and Angola Basin, the sedimentary calcite lysocline determined from surface samples between 399 m to 5071 m water depth is closest to the position of the hydrographic lysocline at 4400 m water depth. The Walvis Ridge-Angola Basin transect can best be compared with the Walvis Ridge-Cape Basin transect as $CaCO_3$ and TOC contents (Fig. 5) and sediment accumulation rates are similar. Therefore the impact of the different water mass properties of NADW and AABW can be best read off from comparison of both transects. As expected, within the upper 4000 m of the profiles, *G. bulloides* preservation curve patterns are similar because the sediments were exposed to similar water conditions. The effect of supralysoclinal dissolution seems to accounts for a rise in the sedimentary calcite lysocline of around 600 m in the southern Angola Basin.

The AABW deep water mass in the Cape Basin accounts for a rise of the hydrographic lysocline of around 600 m as compared with the Angola Basin (Fig. 3). Although supralysoclinal dissolution should affect both transects equally, the offset of the sedimentary calcite lysocline is smaller in the northern Cape Basin compared to the southern Angola Basin. Again, this difference of 200 m is due to the presence of AABW as the $[CO_3^{2-}]$ is very close to the calcite saturation curve. An additional lowering of the $[CO_3^{2-}]$ of only 10 µmol/kg is needed to cross the calcite saturation curve at around 4000 m depth. As the $[CO_3^{2-}]$ within the deep Angola Basin varies only very little with increasing water depth (Fig. 3), the $[CO_3^{2-}]$ content must be lowered by at least 20 µmol/kg to produce significant calcium carbonate dissolution.

Compared to earlier findings, which determined the depth of the calcite lysocline in the deep Angola Basin to lie between 4700 and 5000 m [14,47], we can clearly show that significant calcium carbonate dissolution starts 600 to 1600 m shallower. In former studies, the $CaCO_3$ content and the percentage of fragmented to whole planktic foraminifera were used as calcium carbonate dissolution proxies [e.g. 14] but were measured on a limited number of samples in the depth interval where the calcite lysocline is encountered. Although it was mentioned that a low level of dissolution exists above 4700 m, which is clearly reflected as a gradual decrease in $CaCO_3$ content as shown in this study, the calcite lysocline was placed at around 4700 m [47]. This depth level was probably chosen because only a minor decline in preservation was indicated from the percentage of fragmented to whole planktic foraminifera. This proxy is commonly referred to as highly sensitive towards dissolution [e.g. 4,2] but leads to more or less contradicting results within the investigated transect [47] that is situated between the Mid-Atlantic ridge and the equatorial transect presented in this study.

Our data support the estimation of Emerson and Bender [19] and Milliman [18] that a significant amount of $CaCO_3$ is lost up to 1000 m above the hydrographic lysocline. Significant dissolution begins even shallower than this, as shown from coastal transects. In particular, the Guinea and Angola Basin were commonly regarded as reservoirs that contained well-preserved calcareous sediments even at great depth. In fact, although the more corrosive deep water mass AABW is virtually absent in these basins, the effect of supralysoclinal dissolution seems to be strong enough to lower the $[CO_3^{2-}]$ to much an extent (up to 35 µmol/kg in the coastal Angola Basin) that the calcite saturation curve is crossed up to 1600 m above the hydrographic lysocline. The calcium carbonate preservation potential of the eastern South Atlantic basin was therefore overestimated in earlier studies.

6. Conclusions

The *Globigerina bulloides* dissolution index (BDX') provides an independent tool to determine the sedimentary calcite lysocline within deep ocean basin and continental margin transects. An abrupt decrease in *G. bulloides* preservation marks the top of the sedimentary calcite lysocline, a shift that may also be seen in decreasing $CaCO_3$ content, increasing TOC content and rain ratio in the more open-ocean transects. These bulk sediment parameters, which are often used to determine calcium carbonate dissolution, may be completely misleading in coastal regions. Both because calcium carbonate may be low in these regions in the first place and TOC contents are increased in coastal surface sediments. The rapid progression of calcite dissolution with water depth is most sensitively reflected by the BDX' within all the different tested hydrographic regimes.

Within the northern Cape Basin, the sedimentary calcite lysocline is 400 m shallower than the hydrographic lysocline and coincides with the NADW/AABW interface at around 4000 m water depth. The sedimentary calcite lysocline rises towards the continental margin probably due to the

increased supply and degradation of organic material within the surface sediments. In general, increased sediment accumulation rates finally stop this process within the upper centimeters of the sediments in contrast to the open-ocean transects. For the coastal Cape Basin, the sedimentary calcite lysocline is encountered at 3600 m water depth. An increase in the TOC content within the surface sediments by on average a factor of 3 (although balanced by an increase in the accumulation rate by a factor of 4), induces a rise of the calcite lysocline of about 400 m compared to the more open-ocean regime of the northern Cape Basin. Significant calcium carbonate loss therefore starts around 400 to 800 m shallower than predicted from hydrographic data alone.

The gap between the hydrographic lysocline and the sedimentary lysocline is even more pronounced in the Guinea and Angola Basin. The sedimentary lysoclines from four transects are 1600 to 1000 m shallower than the calculated hydrographic lysoclines. This cannot be attributed to the presence of any major deep water mass boundaries in the deep Guinea and Angola Basin as hydrographic data from GEOSECS stations 109, 107, and 105 show rather constant [CO_3^{2-}] with increasing water depth. Instead, supralysoclinal dissolution seems to affect deep-sea sediments of the open-ocean and, even more pronounced, coastal sediments.

The role of the organic matter supply and degradation could be best demonstrated by a comparison of the eastern equatorial South Atlantic transect and the Mid-Atlantic Ridge transect, whereby the latter reflects true open-ocean conditions with minimal TOC values and lowest accumulation rates. Within both regions, calcite preservation decreases gradually compared to the rather steep decrease within all other hydrographic regimes. An increase in productivity by a factor of 2 to 4 (reflected in the sediment by almost twice the TOC contents) seems to be linked with a lysocline rise towards 3600 m, around 400 m shallower than in the Mid-Atlantic Ridge region.

Although coastal regions in particular are subject to intense dilution from the continents, which protects calcareous particles by rapid embedding particularly in the vicinity of the Congo River, the effect of supralysoclinal dissolution seems to be at a maximum compared to all other transects. The massive degradation of organic matter within the sediments (TOC values are increased by more than a factor of 10 compared to the open-ocean values) may lower the [CO_3^{2-}] significantly (>35 µmol/kg) and calcareous particles, which additionally constitute only a fraction of the sediment, show distinct dissolution features at even 3400 m water depth.

In the vicinity of the Walvis Ridge, where organic matter supply is considerably lower, the sedimentary calcite lysocline is closest to the hydrographic lysocline depth. However, the offset between hydrographic lysocline and sedimentary calcite lysocline is still 600 m, showing that the carbonate ion content was additionally lowered by around 20 µmol/kg. Although the Atlantic is regarded as the largest present-day deep-sea carbonate sink [1], for the eastern South Atlantic at least, its calcium carbonate preservation potential is considerably lower than expected.

Acknowledgements

We are grateful to G. Wefer and his working group who provided surface sediment samples to us. B. Donner kindly contributed *G. bulloides* from sediment traps. Unpublished TOC and $CaCO_3$ data were kindly provided by P. Müller and T. Wagner. We thank S. Gerhardt for discussing the manuscript. C. Devey kindly corrected the English.

BDX' values presented in this paper are archived in the PANGAEA database at the Alfred Wegener Institute for Polar and Marine Research (http://www.pangaea.de/home/avolbers). This research was funded by the Deutsche Forschunsgemeinschaft (Sonderforschungbereich 261 at the University of Bremen, Contribution No. xx).

References

[1] J.D. Miliman, Production and accumulation of calcium carbonate in the ocean: budget of a nonsteady state, Global Biogeochemical cycles 7(4), (1993) 927-957.
[2] A.N.A. Volbers, R. Henrich, Late Quaternary variations in calcium carbonate preservation of deep-sea sediments in the northern Cape Basin: results from a multiproxy approach, Marine Geol. (subm. in June 2000).
[3] W.S. Broecker, T.-H. Peng, The cause of the glacial to interglacial atmosheric CO_2 change: a polar alkalinity hypothesis, Global Biogeochemical cycles 3(3), (1989) 215-239.
[4] W.R. Howard, W.L. Prell, Late Quaternary $CaCO_3$ production and preservation in the Southern Ocean: Implications for oceanic and atmosheric carbon cycling, Paleoceanography 9(3), (1994) 453-482.
[5] A.L. Gordon, Inter-ocean exchange of thermocline water, J. Geophys. Res. 91, (1986) 5037-5046.
[6] R.R. Dickson, J. Brown, The production of North Atlantic Deep Waters: Sources, rates and pathways, J. Geophys. Res. 99 (C6), (1994) 12319-12341.
[7] D.B. Ellis, T.C.Jr. Moore, Calcium carbonate, opal, and quartz in Holocene pelagic sediments and the calcite compensation level in the South Atlantic Ocean, Journal of Marine Res. 31(3), (1973) 210-227.
[8] J.R. Reid, On the circulation of the South Atlantic Ocean, in: G. Wefer, W.H. Berger, G. Siedler, D.J. Webb (Eds.), The South Atlantic: Present and past circulation, Springer, Berlin, Heidelberg, 1996, pp. 13-44.
[9] G. Siedler, T.J. Müller, R. Onken, M. Arhan, H. Mercier, B.A. King, P.M. Saunders, The zonal WOCE Sections in the South Atlantic, in: G. Wefer, W.H. Berger, G. Siedler, D.J. Webb (Eds.), The South Atlantic: Present and past circulation, Springer, Berlin, Heidelberg, 1996, pp. 83-104.
[10] L.V. Shannon, P. Chapman, Evidence of Antarctic Botttom Water in the Angola Basin at 32°S, Deep-Sea Res. 38 (1991), 1299-1304.
[11] B. Warren, K.G. Speer, Deep circulation in the eastern South Atlantic ocean, Deep-Sea Res. 38 (1), (1991) 281-322.
[12] A.J. Van Bennekom, G.W. Berger, Hydrography and silica budget of the Angola Basin. Netherlands Journal of Sea Research 17, (1984) 149-200.
[13] H. Mercier, K.G. Speer, J. Honnorez, Flow pathways of bottom water through the Romanche and Chain Fracture Zones, Deep-Sea Res. 41(10), (1994) 1457-1477.
[14] W.H. Berger, Planktonic foraminifera: selective solution and paleoclimatic interpretation, Deep-Sea Res. 15, (1968) 31-43.
[15] W.H. Berger, M.-C. Bonneau, F.-L. Parker, Foraminifera on the deep-sea floor: lysocline and dissolution rate. Oceanol. Acta 5 (2), (1982) 249-258.
[16] D. Archer, S. Emerson, C. Reimer, Dissolution of calcite in deep-sea sediments: pH and O_2 microelectrode results. Geochimica et Cosmochimica Acta 53, (1989) 2831-2845.
[17] R.A. Jahnke, D.B. Craven, J.-F. Gaillard, The influence of oraganic matter diagenesis on $CaCO_3$ dissolution at the deep-sea floor, Geochimica et Cosmochimica Acta 58 (11), (1994) 2799-2809.
[18] J.D. Milliman, P.J. Troy, W.M. Balch, A.K. Adams, Y.-H. Li, F.T. Mackenzie, Biologically mediated dissolution of calcium carbonate above the chemical lysocline? Deep-Sea Res. I 46, (1999) 1653-1669.
[19] S. Emerson, M. Bender, Carbon fluxes at the sediment-water interface of the deep-sea: calcium carbonate preservation, J. Mar. Res. 39, (1981) 139-162.
[20] D. Archer, Modeling the calcite lysocline, J. Geophys. Res. 96 (17), (1991) 17037-17050.

[21] B. Hales, S. Emerson, D. Archer, Respiration and dissolution in the sediments of the western North Atlantic: estimates from models of in situ microelectrode measurements of pore water oxygen and pH, Deep-Sea Res. 41(4), (1994) 695-719.
[22] J.D. Miliman, Production and accumulation of calcium carbonate in the ocean: budget of a nonsteady state, Global Biogeochemical cycles 7(4), (1993) 927-957.
[23] S. Emerson, J.I. Hedges, Processes controlling the organic carbon content of open ocean sediments. Paleoceanography 3(5), (1988) 621-634.
[24] C. Rühlemann, P.J. Müller, R.R. Schneider, Organic carbon and carbonate as paleoproductivity proxies: examples from high and low productivity areas of the tropical Atlantic, in: G. Fischer, G. Wefer (Eds.), Use of proxies in paleoceanography: examples from the South Atlantic, Springer-Verlag, Berlin, Heidelberg, 1999, pp. 315-344.
[25] W.S. Broecker, T. Takahashi, The relationship between lysocline depth and *in situ* carbonate ion concentration, Deep-Sea Res. 25, (1978) 65-95.
[26] G. Siedler, T.J. Müller, R. Onken, M. Arhan, H. Mercier, B.A. King, P.M. Saunders, The zonal WOCE Sections in the South Atlantic, in: G. Wefer, W.H. Berger, G. Siedler, D.J. Webb (Eds.), The South Atlantic: Present and past circulation, Springer, Berlin, Heidelberg, 1996, pp. 83-104.
[27] J.M. Barnola, D. Raynaud, Y.S. Korotkevich, C. Lorius, Vostok ice core provides 160 000-year record of atmospheric CO_2, Nature 329, (1987) 408-414.
[28] S. Kemle-von Mücke, H. Oberhänsli, The distribution of living planktic foraminifera in relation to Southeast Atlantic Oceanography, in: G. Fischer, G. Wefer (Eds.), Use of proxies in paleoceanography: examples from the South Atlantic, Springer-Verlag, Berlin, Heidelberg, 1999, pp. 91-115.
[29] A.N.A. Volbers, H.-S. Niebler, J. Giraudeau, H. Schmidt, R. Henrich, Paleoceanographic changes in the northern Benguela upwelling system over the last 245.000 years as derived from planktic foraminifera assemblages, submitted to Deep-Sea Res.
[30] R.C. Thunell, S. Honjo, Calcite dissolution and the modification of planktonic foraminiferal assemblages. Mar. Micropaleontol. 6, (1981) 169-182.
[31] S. van Kreveld-Alfane, Late Quaternary sediment records of mid-latitude northeast Atlantic calcium carbonate production and dissolution, Ph.D. thesis, University of Amsterdam, FEBO B.V., Enschede, The Netherlands, 1996, 212 pp.
[32] N. Dittert, R. Henrich, Carbonate dissolution in the South Atlantic Ocean: evidence from ultrastructure breakdown in *Globigerina bulloides*, Deep-Sea Res. I 47, (2000) 603-620.
[33] J.R.E. Lutjeharms, P.L. Stockton, Kinematics of the upwelling front off Southern Africa, S. Afr. J. mar. Sci. 5, (1987) 35-49.
[34] G. Schmiedl, Late Quaternary benthic foraminiferal assemblages from the eastern South Atlantic ocean: Reconstruction of deep water circulation and productivity changes, Ph.D. thesis, Berichte zur Polarforschung 160, 1995, 207 pp.
[35] P. Chapman, L.V. Shannon, The Benguela ecosystem part II. Chemistry and related processes, Oceanogr. Mar. Biol. Ann. Rev. 23, (1985) 183-251.
[36] W.H. Berger, K. Fischer, C. Lai, G. Wu, Ocean productivity and organic carbon flux. Part I. Overview and maps of primary productivity and export production, University of California, San Diego, SIO Reference 87-30, 1987, 67 pp.
[37] W.H. Berger, Global maps of ocean productivity, in: W.H. Berger, V.S. Smetacek, G. Wefer (Eds), Productivity in the ocean: Present and past, John Wiley, Chichester, 1989, pp. 429-455.
[38] H. Schmidt, Der Benguela-Strom im Bereich des Walfisch-Rückens im Spätquartär (Ed.), Ph.D. thesis, Berichte aus dem Fachbereich Geowissenschaften der Universität Bremen 28, Bremen, 1992, pp. 172.
[39] T. Bickert, G. Wefer, South Atlantic and benthic foraminifer $\delta^{13}C$-deviations: Implications for reconstructing the Late Quaternary deep-water circulation, Deep-Sea Res. 46, (1999) 437-452.
[40] A.C. Mix, Influence of productivity variations on long-term CO_2, Nature 337, (1989) 541-544.
[41] A.L. Longhurst, S. Sathyendranath, T. Platt, C. Caverhill, An estimate of global primary production from satellite radiometer data, J. Plankton Res. 17, (1995) 1245-1271.
[42] A.L. Longhurst, Seasonal cooling and blooming in tropical oceans, Deep-Sea Res. 40, (1993) 2145-2165.
[43] D.J. Verardo, W.F. Ruddiman, Late Pleistocene charcoal in tropical Atlantic deep-sea sediments: Climatic and geochemical significance, Geololgy 24 (9), (1996) 855-857.
[44] W.L. Balsam, F.W.Jr. McCoy, Atlantic sediments: Glacial/interglacial comparisions. Paleoceanography 2(5), (1987) 531-542.
[45] J.H.F. Jansen, T.C.E. Van Weering, R. Gieles, J. Van Iperen, Late Quaternary oceanography and climatology of the Zaire-Congo fan and the adjacent eastern Angola Basin, Neth. J. Sea Res. 17 (2-4), (1984), 201-249.
[46] R.W. Embley, J.J. Morley, Quaternary sedimentation and paleoenvironmental studes off Namibia (southwest Africa), Mar. Geol. 36, (1980) 183-204.

[47] R.C. Thunell, Carbonate dissolution and abyssal hydrograpy in the Atlantic ocean, Marine Geology 47, (1982) 165-180.
[48] T. Wagner, L.M. Dupont, Terrestrial organic matter in marine sediments: analytical approaches and eolian-marine records in the central equatorial Atlantic, in: G. Fischer, G. Wefer (Eds.), Use of proxies in paleoceanography: examples from the South Atlantic, Springer-Verlag, Berlin, Heidelberg, 1999, pp. 547-574.
[49] R.R. Schneider, B. Price, P.J. Müller, D. Kroon, I. Alexander, Monsoon related variations in Zaire (Congo) sediment load and influence of fluvial silicate supply on marine productivity in the east equatoial Atlantic during the last 200,000 years. Paleoceanography 12, (1997) 463-481.

3. Calcium carbonate corrosiveness in the South Atlantic during the LGM as inferred from changes in the preservation of *Globigerina bulloides*: A proxy to determine deep water circulation pattern?

Volbers, A.N.A. and Henrich, R.

University of Bremen, Faculty of Geosciences, Department of Paleoceanography and Sedimentology, P.O. Box 33 04 40, D-28334 Bremen, Germany,
phone: +49(0)421 218 7135 fax: ++49 (421) 218 7431 email: avolbers@uni-bremen.de

Abstract

NADW weakening during LGM was inferred from fluctuations in benthic foraminiferal distributions, $\delta^{13}C$ of benthic foraminifers and carbonate preservation within the South Atlantic Ocean. As the modern Atlantic Ocean is dominated by the interactions of North Atlantic Deep Water (NADW) and Antarctic Bottom Water (AABW), which differ significantly in their physical and chemical properties, the position of the NADW/AABW transition was regarded as a useful proxy for reconstructing the evolution of the relative importance of the two water masses. According to Berger and Wefer, (1996) this „boundary" is seen on the sea floor as a foraminifera lysocline. However, when using the calcite lysocline for the reconstruction of South Atlantic deep water mass distribution pattern during the LGM, we have to take into account that deep-sea calcium carbonate preservation is predominantly controlled by three factors: the rate of calcareous plankton production, the saturation state of the sourrounding water mass and the production of metabolic CO_2 in the sediment by the degradation of organic matter. So far, this „respiratory dissolution" was regarded as a minor process although its importance on the global calcium carbonate budget was emphasized by Emerson and Bender (1981). In this regard, Volbers and Henrich (subm.) observe significant calcite dissolution in the eastern South Atlantic surface sediments several hundred meters above the calcite saturation horizon in the water column. As we do not know about the impact of respiratory dissolution on LGM sediments, proxy data that deal with the calcium carbonate preservation state of South Atlantic LGM sediments should be treated with some care. Nevertheless, the importance of ocean circulation in modulating the global climate warrants the use of additional proxies to resolve the conflicting signals from paleocirculation proxies in the South Atlantic (e.g. Rutberg et al., 2000). In this study, we use the *Globigerina bulloides* dissolution index (BDX'; Volbers and Henrich, subm.) to determine the preservation state of calcareous South Atlantic deep-sea sediments during the LGM. When compared to the core-top data set, BDX' data are within a smaller range throughout the whole water column during the LGM and do not decrease as rapidly below the calcite lysocline. This points to a rather less stratified ocean than compared to the modern South Atlantic Ocean. In addition, the position of the calcite lysocline was similar in the western and eastern basin, reflecting that the access of Southern Component Water (SCW) to the eastern South Atlantic Basin was not

limited during LGM. In this sense, our data support the theory of reduced dominance of Northern Component Water in the Atlantic Ocean in favor of SCW.

1. Introduction

Climatic shifts are strongly related to deep-water reorganizations and can occur within a few 100 years or less (e.g. Adkins et al., 1997). Allen et al. (1999) provide evidence for a closely coupled ocean-atmosphere system of the northern hemisphere during the Last Glacial Maximum (LGM). During the LGM the North Atlantic region and Europe recieved a strong cooling of more than 10°C (CLIMAP 1981; Guiot et al., 1989). According to Lynch-Stieglitz et al. (1999) the speed of the Gulf Stream decreased by about 35% during this time period. The Gulf Stream is an important part of today's global ocean circulation as it carries warm surface water northwards where it cools and sinks to the seafloor to form North Alantic Deep Water (NADW, Dickson and Brown, 1994). During this process, a huge amount of heat is released to the atmosphere, contributing to Europe's mild climate today. As long as salty water from the south is supplied and vertical mixing continually removes surface water, the system is stable regarding the formation of NADW (Rahmstorf, 1997).

Extensive reorganization in the intermediate and deep water circulation has been hypothesized to have occurred during the LGM. There is evidence that around 21 kyrs ago, ocean circulation was sluggish (e.g. Duplessy, 1999). Annual mean meridional heat transport seems to have been reduced by about 30% at low latitudes according to model data (Lynch-Stieglitz et al.; 1999). Accordingly, NADW production appears to have been decreased (Curry and Lohmann, 1983; Boyle and Keigwin, 1987; Oppo and Fairbanks, 1987; Duplessy et al. 1988; Charles and Fairbanks, 1992; Labeyrie et al., 1996; Rutberg et al., 2000). A reduction of NADW by 50% was suggested by Schäfer-Neth and Paul (2001), being compensated by intermediate water export from via the glacial Atlantic, the Glacial North Antarctic Intermediate Water (GNAIW, Sarnthein et al., 1994; Oppo and Lehmann, 1993). Although there is substantial support for a glacial weakening on the one hand, Cd/Ca, Ba/Ca and $^{231}Pa/^{230}Th$ ratios suggest only little changes from the LGM to the Holocene on the other (Lea and Boyle, 1990; Boyle, 1992; Yu et al., 1996). As emphazised by Rutberg et al. (2000), the importance of ocean circulation in modulating the global climate warrants the use of additional proxies to resolve this conflict. Here we use lysocline shifts to reveal specific oceanic reorganisations during the LGM. We present calcium carbonate preservation data determined by the *Globigerina bulloides* dissolution index (BDX', Volbers and Henrich, subm.1 and 2) to determine the position of the calcite lysoline. Via core-top calibrations we are able to infer changes in its position in the western and eastern South Atlantic basin. Early studies proposed that the position of the modern calcite lyocline, is linked to the transition of NADW and Antarctic Bottom Water (AABW; Berger, 1968). Its position during the LGM might give clues on the distribution pattern of NADW and AABW during this time period (Berger and Wefer, 1996).

2. Modern and past South Atlantic deep water circulation

The world´s oceans circulation was firstly described by Broecker as the „Global Ocean Conveyor Belt" in which the Atlantic Ocean plays a key role (Broecker et al., 1985; Gordon, 1986; Broecker, 1991). Not only South Atlantic surface water masses cross the equator but also intermediate and deep water from the south move northwards. This flow is compensated by the supply of NADW, a warm and well-ventilated water mass which can be distinguished from other deep water masses by its low nutrient concentration and relatively high $\delta^{13}C$ values of dissolved inorganic carbon (Dickson and Brown, 1994). On its way to the southern ocean, it subdivids the Circumpolar Deep Waters (CDW) from the south at middepth. The upper branch of CDW, the Upper Circumpolar Deep Water (UCDW), can be traced through the Atlantic Ocean due to its silica maximum (Talley, 1996). The Lower Circumpolar Deep Water (LCDW) from the Drake Passage overrides the denser waters from the Weddell Sea and fills the deep western basin and the Cape Basin. LCDW and the Weddell Sea Deep Water (WSDW) are commonly referred to as AABW, which is a cold water mass of low salinity (Siedler et al., 1996). Whereas NADW is formed in the Greenland, Iceland, and Labrador Seas, AABW orginates near Antarctica and contains less oxygen and higher nutrients (e.g. Reid, 1996). The inflow of South Atlantic deep waters into the eastern South Atlantic basin is controlled by the submarine barrieres of the Mid-Atlantic Ridge in the west, and by the Walvis Ridge in the south. Since only small quantities of AABW can enter the Guinea and Angola Basin via the Romanche Fracture Zone (sill depth 4350 m) and the Walvis Passage (sill depth around 4200 m), they are predominately filled by NADW (Van Bennekom and Berger, 1984; Shannon and Chapman, 1991; Warren and Speer, 1991; Mercier et al. 1994).

When simulating past climate changes, the formation of deep water at high northern latitudes seems to be a crucial point (e.g. Ganopolski et al., 1998; Ganopolski and Rahmstorf, 2001). According to the computer model of Ganopolski et al. (1998) simulating the atmospheric and oceanic circulations of the LGM, ocean circulation changes might have amplified Northern Hemisphere cooling during the LGM by about 50%. In response to sea-ice advance from around 75°N to 55°N, a southward shift of NADW formation occured (Ganopolski et al., 1998; Stocker, 1998). As the density of the sinking waters was reduced, they might have penetrated less deeply, resulting in the formation of Glacial North Atlantic Intermediate Water (GNAIW; Boyle and Keigwin, 1987; Zahn, 1992; Weaver, 1994, Broecker, 1997). Accordingly, AABW could have penetrated further into the northern North Atlantic as inferred from paleoceanographic data (Ganopolski et al. 1998; Sarnthein et al. 1994; Stocker, 1998; Duplessy et al., 1988). The modern asymmetry between the western and eastern South Atlantic regarding its deep water mass distribution may have not existed during times of decreased NADW production. From $\delta^{13}C$ data it was inferred from Bickert (1992) that AABW was present in the Angola Basin during glacial periods. These late Pleistocene shifts in the NADW/AABW transition as determined by proxies such as $\delta^{13}C$ or Ca/Cd are also reflected by changes in the calcium carbonate preservation pattern as they are linked with a redistribution of the carbonate system,

including a reduction in the atmospheric CO_2 content and a shallowing of the calcite lysocline in the South Atlantic deep basins.

3. The imprint of South Atlantic deep water mass distribution on the BDX' record obtained from surface sediments

Deep sea calcium carbonate burial is mediated by the depth of the calcite lysocline which is marked by the first signs of significant dissolution in deep-sea sediments (Milliman, 1999). One of the major controls on the depth of the lysocline is the calcite saturation depth. At this depth level, the carbonate ion concentration of the bottom water $[CO_3^{2-}]_{bw}$ equals the carbonate ion concentration at calcite saturation $[CO_3^{2-}]_{sat}$. Above this level, sea waters bathing the sediments are supersaturated and calcareous sediments should be well-preserved, whereas they get dissoved in the undersaturated waters below this depth level. As calcite solubility increases with depth (pressure effect), water depth and the $[CO_3^{2-}]$ of the surrounding water mass should be the dominant controls on calcium carbonate preservation.

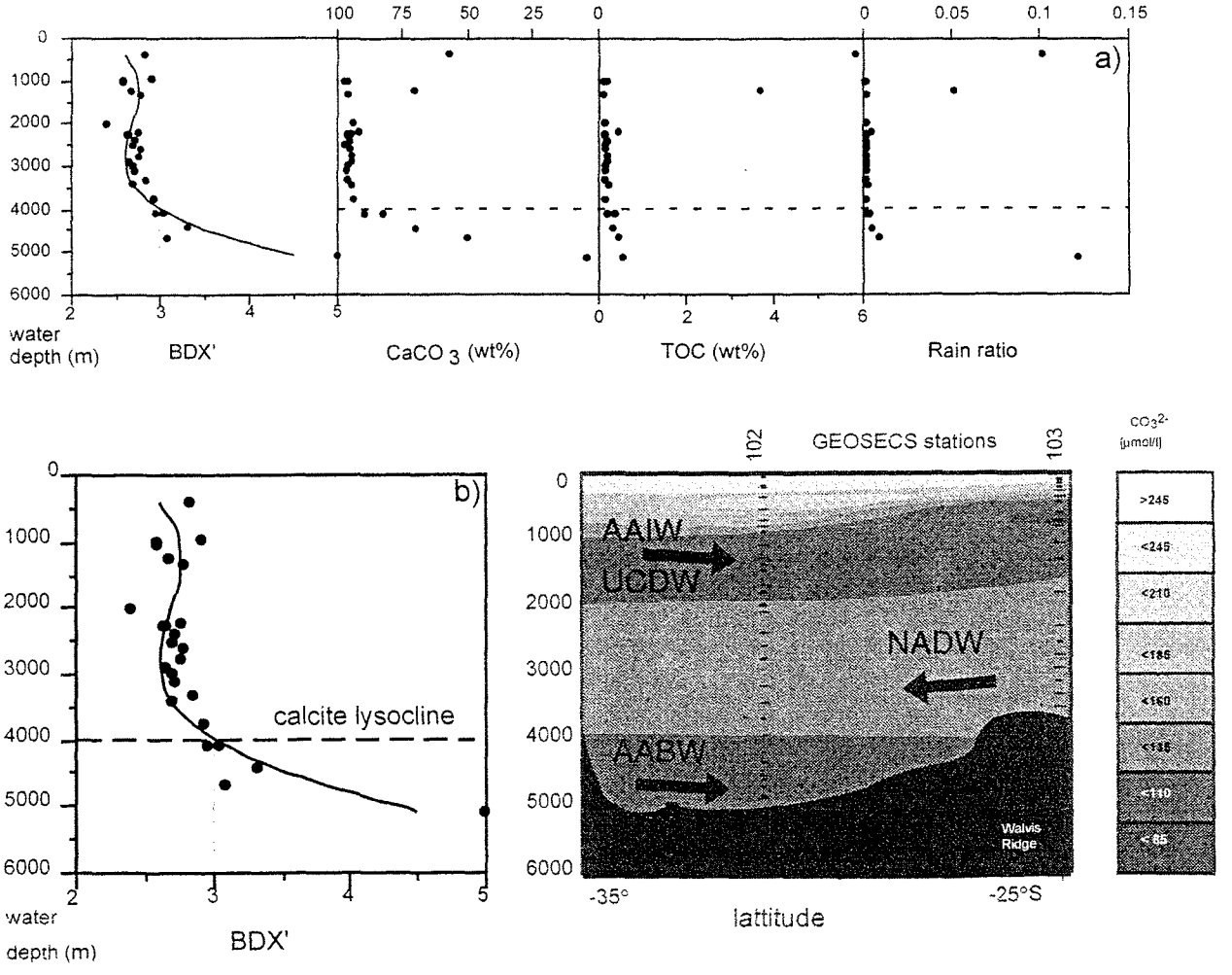

Fig. 1: a) Determination of the sedimentary calcite lysocline within the northern Cape Basin. The progressive dissolution of *Globigerina bulloides* ultrastructure is expressed as BDX' and compared with $CaCO_3$ data, total organic content (TOC), and rain ratio which are often used as calcium carbonate dissolution proxies, b) the calcite lysocline, as determined via the BDX' proxy, coincids with the NADW/AABW transition which reflects changes in the $[CO_3^{2-}]$ (taken from Volbers and Henrich, subm.).

However, as summarized by Sigman and Boyle (2000), continued studies of seafloor dissolution have indicated that pore water undersaturation due to oxidation of organic matter within the sediments is also a significant driver of calcite dissolution. The importance of this effect was already introduced 20 years ago by Emerson and Bender (1981) but so far mainly treated as an effect of minor importance. But nevertheless, when this additional „respiratory dissolution" is taken into account, the depth of the lysocline does not necessarily correspond to the calcite saturation depth.

To determine the modern position of the calcite lysocline, all South Atlantic basin were investigated. Here we present a short summary of the findings of Volbers and Henrich (subm.) from the eastern South Atlantic and present new data from the western South Atlantic. In the Cape Basin the calcite lysocline is encountered at 4000 m as determined via the BDX' (for detailed description of the BDX' see material and methods, 4.2.), and reflected by a decrease in $CaCO_3$ and an increase in TOC content in surface sediment samples. Inferred from these data the calcite lysocline within the northern Cape Basin appears to be predominantly a water mass signal. The more corrosive water mass AABW fills the deep Cape Basin below 4000 m reflected by the onset of decreasing *G. bulloides* preservation (Fig.1). The situation is different for the Guinea and Angola Basin, where AABW is virtually absent. The Walvis Ridge, a submarine barrier, limits AABW progradation into the eastern South Atlantic Basin. Here, the calcite lysocline is encountered at 4000 m water depth in the deep Angola Basin. As due to the absence of AABW the $[CO_3^2]$ content in the water column stays nearly constant with increasing water depth (Broecker and Takahashi, 1978). In order to account for the observed bad preservation pattern, additional dissolution due to microbial degradation of organic matter in the uppermost sediment layer has to be invoked. By this, the additional lovering of the $[CO_3^{2-}]$ is in the order of 30 µmol/kg to cross the calcite saturation curve at 4000 m (Volbers and Henrich, subm.). The very low sedimentation rates within the Mid-Atlantic ridge transect may account for enhanced supralysoclinal dissolution within the surface sediment of this region. Around 20 years ago, supralysoclinal dissolution has been predicted by Emerson and Bender (1981). According to the authors, a significant amount of $CaCO_3$ can be lost up to 1000 m above the predicted calcite lysocline. The shallowing of the calcite lysocline in the equatorial and coastal areas may account for additional dissolution in the sediment due to the degradation of additional organic material, that is supplied to the ocean floor in these regions due to increased productivity.

In order to depict the modern position of the calcite lysocline in the western South Atlantic and to compare it with its position during the LGM, 75 surface sediment samples were investigated. Fig. 2 shows the present water mass configuration inferred from GEOSECS data (modified from Gerhardt and Henrich, 2001) in which results from *G. bulloides* ultrastructural investigation were plotted. We observe moderate preservation of *G. bulloides* test features (2.9 to 3.1) from samples in the intermediate depth level, where AAIW and UCDW are located. Samples that are bathed by NADW reveal better preservation even below 3000 m depth than samples located within AAIW and UCDW. A significant decrease in *G. bulloides* preservation is observed at around 3500 m water depth at

35°S latitude, this level decends down to 3900 m at 25°S and reaches finally 3800 m in the equatorial region. Till 20°S, the calcite lysocline as determined by the BDX', seems to be closely linked with the AABW/NADW transition but seems to be shallower in the equatorial region because of additional dissolution by organic matter degradation.

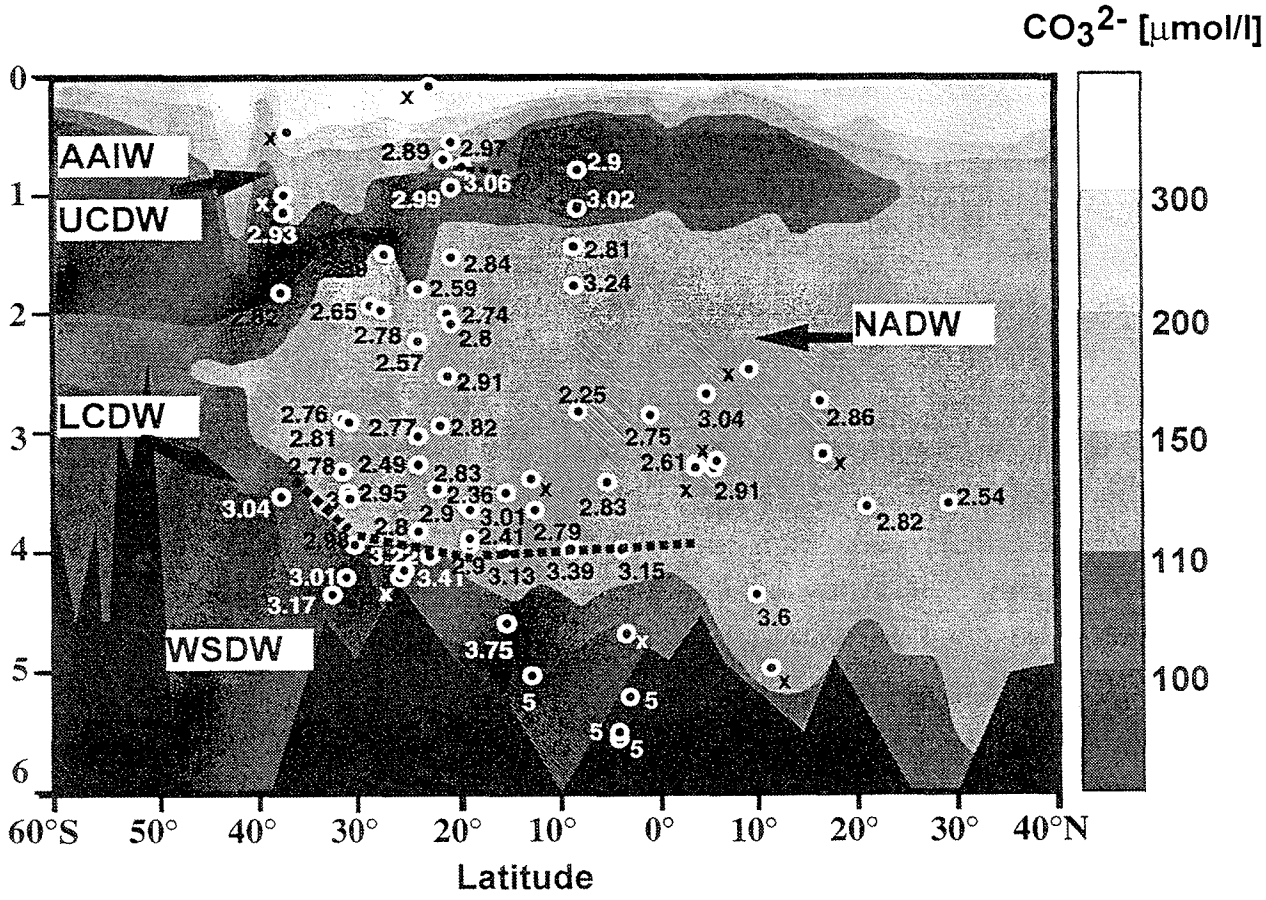

Fig. 2: BDX' results from surface samples introduced in this study in relation with the modern western Atlantic water mass distribution as determined by Gerhardt and Henrich (2001). Samples within upper NADW show best preservation of *G. bulloides* tests, whereas samples within AAIW and UCDW have slightly increased BDX' values, indicating some (local) calcite dissolution at the intermediate depth level today. *Globigerina bulloides* preservation declines in the NADW/AABW transition zone, where the deep calcite lysocline is encountered. In samples indicated by x, the BDX' failed because the minimum number of *G. bulloides* (<10) was not available.

Material and methods

4.1. LGM core material

The LGM was defined as the 23 to 19 ka calendar age period (or 19.5-16.1 ka corrected ^{14}C age) on the first EPILOG workshop in May 1999 in Delmenhorst. In this study, 48 cores from all over the South Atlantic (Fig. 3) were investigated in order to determine their calcium carbonate preservation state. The majority of these cores were recovered on various RV METEOR cruises, whereas the rest was taken from RV Sonne and Victor Hensen cruises. The stratigraphic control in all investigated cores is based on a combination of $\delta^{18}O$ and ^{14}C (AMS). If ^{14}C dates have not been available, oxygen isotope stage 2.22 was identified, which corresponds to a ^{14}C age of about 16 ka and a calendar age of 18.9 ka (Mix and Ruddiman, 1985; Bard, 1998). Further details on stratigraphy

are given in Niebler et al. (subm.). LGM material was wet-sieved to separate the fine from the coarse fraction which was then dried and weighted. Whenever available, 30 *G. bulloides* from the LGM coarse fraction were investigated to determine the position of the sedimentary calcite lysocline in the South Atlantic. Ultrastructural investigations were performed on a ZEISS DSM 940 A (10 mm working distance, 10 kN accelarating voltage) and carried out at a magnification of 4000x. In order to do this, at least 10 specimen per sample were glued to a SEM stub and gold coated.

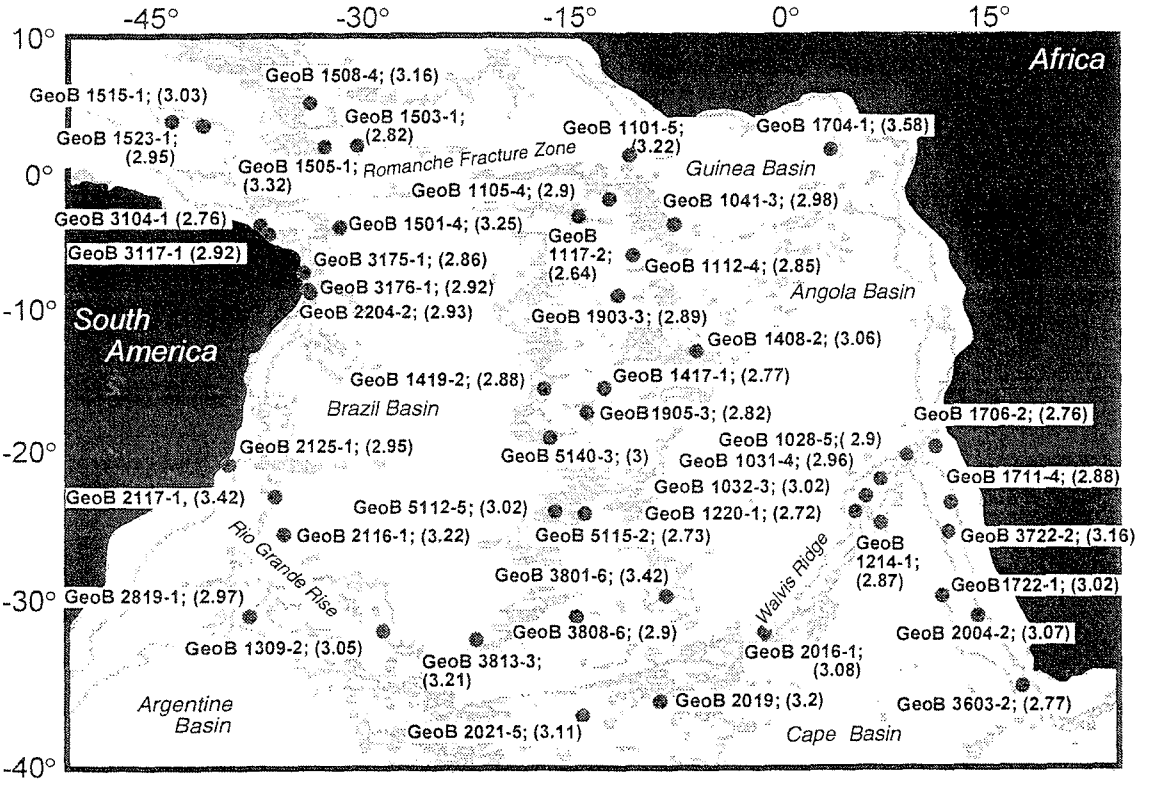

Fig. 3: Map of core locations from which LGM samples were determined. BDX' results are shown in brackets.

4.2. The *Globigerina bulloides* dissolution index (BDX')

Globigerina bulloides is among the most abundant planktic foraminifera in the eastern South Atlantic today (Kemle-von Mücke and Oberhänsli, 1999). It is a reliable indicator of foraminiferal carbonate preservation via the identification of six dissolution stages based on four distinct ultrastructural features (spines, pores, ridges, interpore area). In this study, the (sedimentary) „calcite lysocline" as defined by Milliman (1993) is set to the depth level where the first observation of significant carbonate dissolution in calcareous sediments was observed, which is reflected by the BDX' preservation stage of 3 (Volbers and Henrich, subm.).The following is a brief characterization of the preservation features and preservation stages used in this study:

stage 0-1 (excellent preservation): recognized by round pores, smooth interpore areas, intact ridges, and high spines. It is only observed on *G. bulloides* tests taken from mooring samples (after storage in mercury-saturated seawater which, of course, may have led to some additional dissolution features).

stage 1-2 (very good to good preservation): identified by slightly widened pores, partly etched interpore areas, slightly denuded ridges and spines. Only observed at *G. bulloides* tests taken from mooring samples, hardly observed in surface sediment samples.

stage 2-3 (good to moderate preservation): recognized by funnellike pores, etched and roughened interpore areas, denuded ridges and spines. This preservation stage is normally found in surface sediments under slightly corrosive conditions.

stage 3-4 (bad preservation): revealed by partly interconnected pores, partial removal of the surface layer, strongly reduced ridges and spines. It is an indicator of moderate corrosive conditions much as occur during the respiration of organic matter in the eastern South Atlantic surface sediments.

stage 4-5 (very bad preservation): indicated by interconnected pores, removal of the surface layer, missing ridges and spines. This preservation stage is found in surface sediments under highly corrosive conditions.

stage 5: indicated by the absence of intact tests due to severe dissolution.

The BDX' value was calculated according to the follwing equations:

$$P=(P_{(pores)}+P_{(interpore\ area)}+P_{(spines)}+P_{(ridges)})/4 \qquad (1)$$

The preservation state (P, between 0.5 and 4.5) of each single *G. bulloides* is calculated from the preservation of each criterion investigated (pores, interpore area, spines, and ridges) divided by the number of criteria, which is four. This method assures that every criterion is judged equally when calculating the BDX':

$$BDX'= \sum P/ nT \qquad (2)$$

With $\sum P$ as the sum of all individual preservation states of *G. bulloides* divided by the number of investigated tests (nT).

5. Results and discussion

According to the present west-east asymmetry of South Atlantic deep water mass distribution pattern, we provide two graphs, one covering the western Atlantic basin (Fig. 4a), and the other the east Atlantic basin (Fig. 4b).

5.1 Western South Atlantic

As determined via the BDX', LGM sediment samples reveal good to moderate preservation throughout the water column till the calcite lysocline is encountered. In the western Atlantic Ocean, the calcite lysocline is located at around 3500 m water depth in the northern and southern parts of the study area with decreasing depth level in the southermost part of the investigated area. This is around 500 m shallower than today. In between, from 15° to 0°S, BDX' reveal good to moderate preservation of *G. bulloides* even below 4000 m water depth, indicating that the calcite lysocline seems to have been slightly deeper in this region than today. Below the lysocline a rather gradual increase in dissolution is observed which is in contrast to the steeper gradient observed under modern conditions.

As indicated by Fig. 2, BDX' data obtained from surface sediment samples reflect modern South Atlantic oceanography. In contrast, according to Fig. 4, BDX' values as determined from LGM samples are rather evenly distributed throughout the water column of the LGM (Fig. 4a). As we do not see any significant changes in BDX' preservation, could this account for an ocean that was significantly less stratified in the intermediate and upper deep water layer during the LGM? Similar results were reported by Gerhardt and Henrich (subm.) who investigated the preservation state of *Limacina inflata*, a pteropod which secrets an aragonitic shell. During LGM, they observe a rather regular increase in their *Limacina inflata* index (LDX) with water depth in western South Atlantic sediments. In contrast, LDX data from surface sediments reflect the modern water mass distribution pattern. Good preservation of *L. inflata* tests was found within surface waters and upper NADW whereas rather poor preservation was reported from samples, that are bathed by aragonite-corrosive intermediate water masses of southern origin, such as AAIW and UCDW (Gerhardt and Henrich, 2001).

This modern contrast in both *L. inflata* and *G. bulloides* test preservation pattern is diminished during the LGM. These results seem to point to a water mass that is only slightly corrosive to aragonite and calcite, most probably reflecting the presence of GNAIW in the western South Atlantic. There is evidence from $\delta^{13}C$ and Cd/Ca data of Oppo and Horrowitz (2000) that GNAIW extended at least as far south as 28°S during the LGM. According to Gerhardt and Henrich (subm.) the aragonite saturation state at the sediment-water interface within GNAIW might have been similar to that within modern UNADW conditions. This would also explain rather constant BDX' data in the 0-2000 m level.

5.2 Eastern South Atlantic basins

As in the western South Atlantic, BDX' data point to a significantly less stratified ocean. When compared to the core-top data set of the eastern South Atlantic (Volbers and Henrich, subm.), BDX' values are within a narrower range. BDX' values vary only slightly within the 0-3000 m depth intervall and do not decrease as rapidly below the calcite lysocline as observed in the modern

ocean. The position of the calcite lysocline during the LGM was encountered at around 3200 m water depth in the southernmost part of the investigated area and drops towards the equator. In the northern Guinea Basin, a deep calcite lysocline is observed, which is slightly below 4000 m water depth.

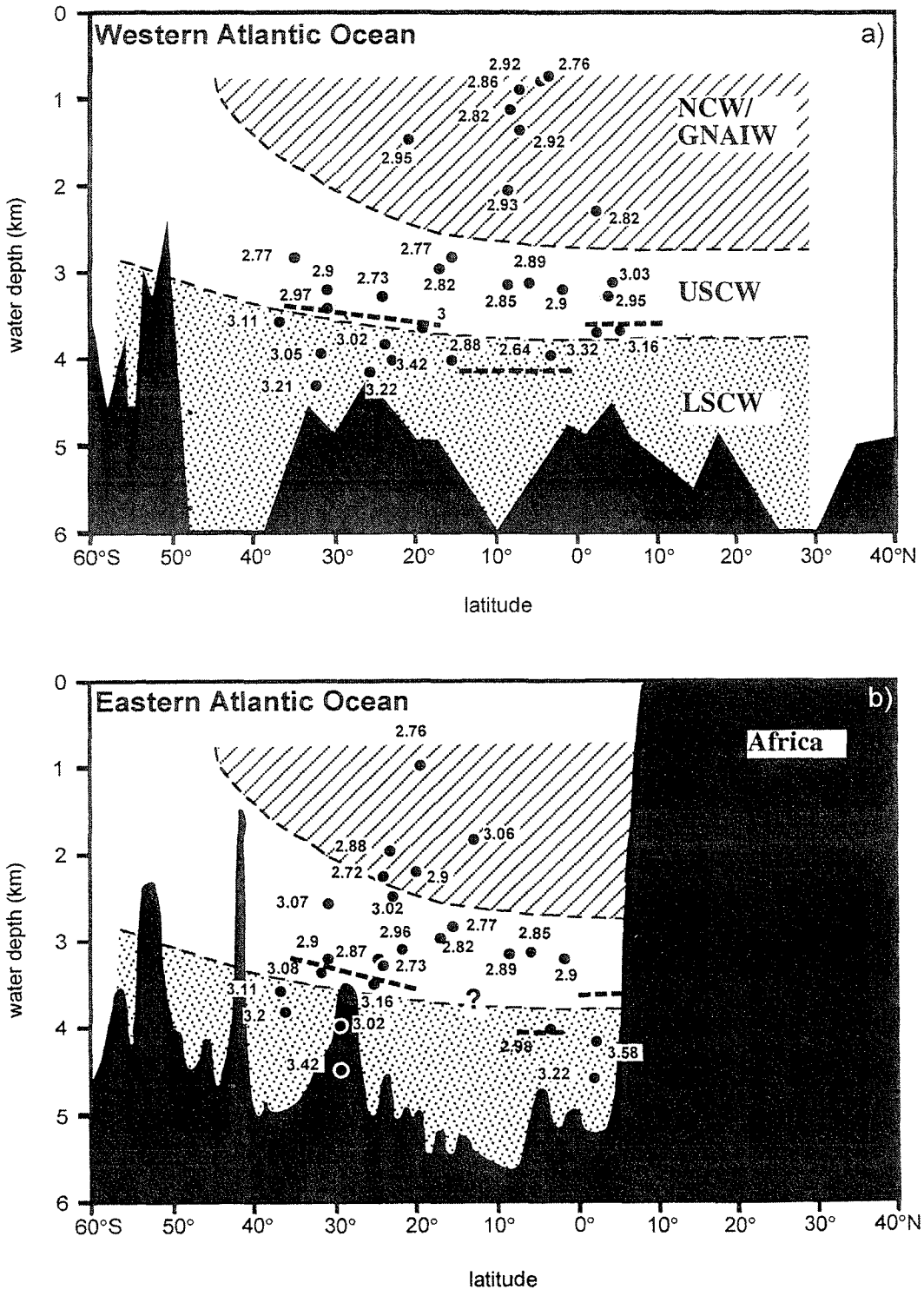

Fig. 4: BDX' data are seperated into western and eastern Atlantic transects. The results are plotted against the LGM water mass distribution model of Bickert (1992). BDX' data reveal good to moderate preservation throughout the water column until the calcite lysocline is enountered.

Our data imply that the position of the calcite lysocline during the LGM differed significantly from the one today. In the modern eastern South Atlantic Ocean, the calcite lysocline is shallowest in the equatorial Atlantic Ocean (Volbers and Henrich, subm.) but at its deepest position of all eastern South Atlantic basin during LGM. According to the authors, enhanced supply and degradation of organic material in the equatorial region seems to account for the observed dissolution in the supersaturated equatorial waters. Attributing to this effect, the position of the calcite lysocline rises several hundred meters in the equatorial region compared its position in the deep Angola and Guinea Basin today.

Whereas there is a contrast in the modern deep water mass distribution between the Guinea and Angola Basin (dominated by NADW) and the Cape Basin (AABW below 4000 m), this north-south asymmetry seems to have been diminished during the LGM. $\delta^{13}C$ data of benthic foraminifera point towards the presence of AABW in the eastern South Atlantic basin. This interpretation is supported by the similar calcium carbonate preservation pattern of the western and eastern South Atlantic deep-sea basin.

5.2 Deep-water mass distribution during the LGM

Whereas slightly better preservation of *L. inflata* shells within the 2000-3000 m level during LGM was attributed to the presence of GNAIW at this depth, the aragonite compensation depth (ADC) was suggested to reflect the GNAIW/SCW boundary (Gerhardt and Henrich, subm.). According to the authors, the ACD was around 500 m shallower compared to today, probably reflecting a highly aragonite-corrosive water mass below 3000 m in the western South Atlantic Ocean. The usage of the ACD or the calcite lysocline for the reconstruction of past water mass distribution pattern has to be carried out with caution, because the mechanism of respiratory dissolution in the modern sediments is poorly understood and its effect on LGM sediments not known. From the modern view, calcium carbonate dissolution in deep-sea sediments is controlled by two important factors, the general undersaturation of the surrounding water mass with respect to aragonite and calcite and the local undersaturation in the sediments due to the production of metabolic CO_2. As we are not able to separate these factors in the past, the usage of the calcite lysocline or the ACD to determine the South Atlantic water mass configuation during the LGM might therefore be biased to some extent.

What we finally see from *Globigerina bulloides* ultrastructural investigation of LGM sediment material is, that 1) BDX' data are within a smaller range throughout the whole water column than in the modern ocean; 2) *G. bulloides* preservation state does not decrease as rapidly below the calcite lysocline as observed in the modern ocean (Volbers and Henrich, subm.); 3) the position of the calcite lysocline seems to have been the same depth level in both the western and eastern South Atlantic Ocean during the LGM; 4) was around 400 m shallower in the north and south of the

investigated area; 5) the course of the calcite lysocline is opposite to its modern mode in the equatorial region with a deep lysocline below 4000 m.

A rather uniform water mass which is supersaturated with respect to calcite is indicated by good to moderate preservation of *G. bulloides* until 3500 m, probably reflecting the glacial counterpart of NADW. According to Duplessy et al. (1988), the GNAIW core was reconstructed by calculated $\delta^{13}C$ values of total dissolved CO_2 as determined from benthic foraminiferal $\delta^{13}C$ values down to almost 3000 m between 15°S and 15°N with an adjecting mixing zone down to 3500 m. Since the presence of the modern west-east asymmetry was not observed by Duplessy et al. (1988), Bickert (1992), Bickert and Wefer (1996) and in this study, a rise of SCW in the water column to depth levels up to 3500 m seems to have occured in the Atlantic Ocean. The position of the calcite lysocline during the LGM as determined by the BDX' could reflect the core of the southern counterpart of AABW, the SCW. According to Bickert (1992), this glacial water mass could be divided into an upper (USCW) and lower part (LSCW) by characteristic $\delta^{13}C$ values. From our data we cannot clearly determine whether USCW is a separate water mass as suggested by Bickert (1992) or reflects the mixing between NCW/GNAIW and SCW. When referred to BDX' values within USCW, which are in a narrow range, and reflect continous worsening below the calcite lysocline, the first assumption is favored from calcium carbonate preservation pattern.

7. Conclusions

From ultrastructural investigations of the planktic foraminifera *Globigerina bulloides* from LGM core material we infer that the position of the calcite lysocline was on average several hundred meters shallower compared to its modern position in South Atlantic basin. BDX' data point to a less stratified ocean during LGM inferred from the following observations: BDX' values are within a smaller range throughout the whole water column and *G. bulloides* preservation state does not decrease as rapidly below the calcite lysocline as observed in the modern ocean. As the position of the calcite lysocline was at the same depth level in both the western and eastern South Atlantic Ocean we conclude that the modern west-east asymmetrie in South Atlantic was not present during the LGM because deep waters from the south rose in the water column and were able to penetrate into the Angola and Guina Basin.

Acknowledgements

We are grateful to M. Frenz who supplied the sand fraction of LGM core material to us and we thank S. Gerhardt for discussing the manuscript. BDX' values presented in this paper are archived in the PANGAEA database at the Alfred Wegener Institute for Polar and Marine Research (http://www.pangaea.de/home/avolbers). This research was funded by the Deutsche Forschunsgemeinschaft (Sonderforschungbereich 261 at the University of Bremen, Contribution No. xx).

References

Adkins, J.F., Boyle, E.A., Keigwin, L, and Cortijo, E., 1997. Variability of the North Atlantic thermohaline circulation during the last interglacial period. Nature 390, 154-156.

Allen, J.R.M., Brandt, U., Brauer, A., Hubberten, H.-W., Huntley, B., Keller, J., Kraml, M., Mackensen, A., Minigram, J., Negendank, J.F.W., Nowaczyk, N.R., Oberhänsli, H:, Watts, W.A., Wulf, S., and Zolitschka, B., 1999. Rapid environmental changes in southern Europe during the last glacial period. Nature 400, 740-743.

Bard, E., 1998. Geochemical and geophysical implications of the radiocarbon calibration. Geochimica et Cosmochimica Acta 62, 2025-2038.

Berger, W.H., 1968. Planktonic foraminifera: selective solution and paleoclimatic interpretation, Deep-Sea Res. 15, 31-43.

Berger, W.H. and Wefer, G., 1996. Central themes of South Atlantic circulation, in The South Atlantic: Present and past circulation, edited by Wefer, G., Berger, W.H., Siedler, G., and Webb, D.J, 1-11, Springer, Berlin, Heidelberg, New York.

Bickert, T., 1992. Rekonstruktion der spätquartären Bodenwasserzirkulation im östlichen Südatlantik über stabile Isotope benthischer Foraminiferen. Berichte aus dem Fachbereich Geowissenschaften der Universität Bremen, vol. 27, 205 pp.

Bickert, T. and Wefer, G., 1996. Late Quaternary deep water circulation in the South Atlantic: Reconstruction from carbonate dissolution and benthic stable isotopes, in The South Atlantic: Present and past circulation, edited by Wefer, G., Berger, W.H., Siedler, G., and Webb, D.J., pp. 599-620, Springer, Berlin, Heidelberg.

Boyle, E.A., 1992. Cadmium and $\delta^{13}C$ paleochemical ocean distributions during the Stage 2 glacial maximum. Annu.Rev. Earth Planet. Sci 20, 245-287.

Boyle, E.A. and Keigwin, L., 1987. North Atlantic thermohaline cirulation during the past 20,000 years linked to high-latitude surface temperature. Nature 350, 35-40.

Broecker, W.S., 1991. The great ocean conveyor. Oceanogr. 4, 79-89.

Broecker, W.S., 1997. Thermohaline circulation, the Achilles heel of our climate system: Will man made CO_2 upset the current balance? Science 278, 1582-1588.

Broecker, W.S., Peteet, D.M., and Rind, D., 1985. Does the ocean-atmosphere system have more than one stable mode of operation? Nature 315, 21-26.

Broecker, W.S. and Takahashi, T., 1978. The relationship between lysocline depth and *in situ* carbonate ion concentration. Deep-Sea Res. 25, 65-95.

Charles, C.D. and Fairbanks, R.G.,1992. Evidence from Southern Ocean sediments for the effect of North Atlantic deep-water flux on climate. Nature 315, 21-26

CLIMAP Project Member, 1981. Seasonal reconstructions of the Earth's surface at the last glacial maximum. Geol. Soc. Am, GSA Map and Chart Ser. MC-36, Boulder, Colorado, 18 pp.

Curry, W.B. and Lohmann, G., 1983. Reduced advection into Atlantic Ocean deep eastern basins during last glaciation maximum. Nature 308, 317-342.

Dickson, R.R. and Brown, J., 1994. The production of North Atlantic Deep Waters: Sources, rates and pathways. J. Geophys. Res. 99 (C6), 12319-12341.

Duplessy, J.C., Shackleton, N.J., Fairbanks, R.G., Labeyrie, L., Oppo, D., and Kallel, N., 1988. Deepwater source variation during the last climateic cycle and their impact on global deepwater circulation. Paleoceanography 3, 343-360, 1988.

Duplessy, J.-C., 1999. Climate and the Gulf Stream. Nature 402, 593-594.

Emerson, S. and Archer, E., 1990. Calcium carbonate preservation in the ocean. Phil Trans R Soc Lond A 331, 29-40.

Fichefet, T., Hovine, S., and Duplessy, J. C.A., 1994. A model study of the Atlantic thermohaline circulation during the last glacial maximum. Nature 372, 252-255.

Ganopolski, A., Rahmstorf, S., Petoukhow, V., and Claussen, M., 1998. Simulation of modern and glacial climates with a coupled global model of intermediate complexity. Nature 391, 351-356.

Ganopolski, A. and Rahmstorf, S., 2001. Rapid changes of glacial climate simulated in a coupled climate model. Nature 409, 153-158.

Gerhardt, S. and Henrich, R. (2001). Shell preservation of *Limacina inflata* (Pteropoda) in surface sediments from the Central and South Atlantic Ocean: a new proxy to determine the aragonite saturation state of water masses. Deep-Sea Res. I 48 (9), 2051-2071.

Gerhardt, S. and Henrich, R. (subm.). Intermediate water circulation during the last glacial maximum in the South Atlantic Ocean inferred from changes in the shell preservation of *Limacina inflata* (Pteropoda). Submitted to Deep-Sea Res. I.

Gordon, A.L., 1986. Interocean exchange of thermocline water. J. Geophys. Res. 91, 5037-5046.

Guiot, J., Pons, A., de Beaulieu, J.L., and Reille, M., 1989. A 140,000-year continental climate reconstruction from two European pollen records. Nature 338, 309-313,

Kemle-von Mücke, S. and Oberhänsli, H., 1999. The distribution of living planktic foraminifera in relation to Southeast Atlantic Oceanography, in Use of proxies in paleoceanography:

examples from the South Atlantic, edited by Fischer, G. and Wefer, G., pp. 91-115. Springer-Verlag, Berlin, Heidelberg.

Labeyrie et al., 1996. Hydrographic change of the Southern Ocean (southeast Indian sector) over the last 230 kyr. Paleoceanography 11, 57-76.

Lea, D.W. and Boyle, E.A., 1990. Foraminiferal reconstruction of barium distributions in water masses of the glacial ocean. Paleoceanography 5, 719-742.

Lynch-Stieglitz, J., Curry, W.B., and Slowey, N., 1999. Weaker Gulf Stream in the Florida Straits during the Last Glacial Maximum. Nature 402, 644-647.

Mercier, H., Speer, K.G., and Honnorez, J., 1994. Flow pathways of bottom water through the Romanche and Chain Fracture Zones. Deep-Sea Res. 41(10), 1457-1477.

Miliman, J.D., 1993. Production and accumulation of calcium carbonate in the ocean: budget of a nonsteady state. Global Biogeochemical cycles 7(4), 927-957.

Milliman, J.D., Troy, P.J., Balch, W.M., Adams, A.K., Li, Y.-H., and Mackenzie, F.T., 1999. Biologically mediated dissolution of calcium carbonate above the chemical lysocline? Deep-Sea Res. I 46, 1653-1669.

Mix, A.C.,and Ruddiman, W.F., 1985. Structure and timing of the last deglaciation: Oxygen isotope evidence. Quat. Sci. Rev. 4, 59-108.

Niebler, H.-S., Mulitza, S., Donner, B., Arz, H., Pätzold, J, and Wefer, G., subm. Sea-surface temperature in the equatorial and South Atlantic Ocean during the Last Glacial Maximum (23-19 ka). Submitted to Paleoceanography.

Oppo, D.W. and Fairbanks, R.G., 1987. Variability in the deep and intermediate water circulation of Atlantic Ocean during the past 25,000 years: Northern hemisphere modulation of the Southern Ocean. Earth Planet. Sci. Lett 86, 1-15.

Oppo, D.W. and Horowitz, M., 2000. Glacial deep water geometry: South Atlantic benthic forminiferal Cd/Ca and $\delta^{13}C$ evidence. Paleoceanography 15 (2), 147-160.

Oppo, D.W. and Lehmann, S.J., 1993. Mid-depth circulation of the subpolar North Atlantic during the last glaical maximum. Science 259, 1148-1152.

Pedersen, T.F., 1983. Increased productivity in the eastern equatorial Pacific during the last glacial maximum (19,000 to 14,000 yr B.P.). Geology 11, 16-19.

Rahmstorf, S., 1997. Risk of sea-change in the Atlantic. Nature 388, 825-826.

Reid, J.R., 1996. On the circulation of the South Atlantic Ocean. In The South Atlantic: Present and past circulation, edited by Wefer, G., Berger, W.H., Siedler, G., and Webb, D.J., pp. 13-44, Springer, Berlin, Heidelberg.

Rutberg, R.L., Hemming, S.R., and Goldstein, S.L., 2000. Reduced North Atlantic Deep Water flux to the glacial Southern Ocean inferred from neodymium isotope ratios. Nature 2000, 935-938.

Sarnthein,M., Winn, K., Jung, S.J.A., Duplessy, J.C., Labeyrie, L.D., Erlenkeuser, H., and Ganssen, G., 1994. Changes in East Atlantic deepwater circulation over the last 30,000 years: eight time slice reconstructions. Paleoceanography 9, 209-267.

Schäfer-Neth, C. and Paul, A.,2001. Circulation of the glacial Atlantic: a synthesis of global and regional modelling, in The northern North Atlantic, edited by Schafer, P, Ritzrau, W., Schlüter, M., and Thiede, J.,.pp. 441-462, Springer,Berlin, Heidelberg, New York.

Shannon, L.V. and Chapman, P., 1991. Evidence of Antarctic Bottom Water in the Angola Basin at 32°S. Deep-Sea Res. 38 (10), 1299-1304.

Siedler, G., Müller, T.J., Onken, R., Arhan, M., Mercier, H., King, B.A., and Saunders, P.M.,, 1996. The Zonal WOCE Sections in the South Atlantic, in The South Atlantic: Present and past circulation, edited by Wefer, G., Berger, W.H., Siedler, and Webb, D.J., pp. 83-104, Springer, Berlin, Heidelberg.

Sigman, D.M, and Boyle, E.A., 2000. Glacial/interglacial variations in atmospheric carbon dioxide. Nature 407, 859-869.

Talley, L.D., 1996. Antarctic Intermediate Water in the South Atlantic, in The South Atlantic: Present and past circulation, edited by Wefer, G., Berger, W.H., Siedler, G., and Webb, D.J., pp. 219-238, Springer, Berlin Heidelberg.

Van Bennekom, A.J. and Berger, G.W., 1984. Hydrography and silica budget of the Angola Basin. Netherlands Journal of Sea Research 17, 149-200.

Volbers, A.N.A. and Henrich, R., subm. Present water mass calcium carbonate corrosiveness in the eastern South Atlantic inferred from ultrastructural breakdown of Globigerina bulloides in surface sediments. Submitted to Earth and Planetary Science Letters.

Warren, B. and Speer, K.G., 1991. Deep circulation in the eastern South Atlantic ocean, Deep-Sea Res. 38 (1), 281-322.

Weaver, A.J., Aura, S.M., and Myers, P.G., 1994. Interdecadal variability in an idealised model of the North Atlantic. J Geophys. Res. 99, 12423-12442.

Yu, E.-J., Francois, R., and Bacon, M.P., 1996. Similar rates of modern and last glacial ocean thermohaline ciculation inferred from radiochemical data. Nature 379, 689-694.

Zahn, R. 1992. Deep ocean circulation puzzle. Nature 356, 744-746.

4. Paleoceanographic changes in the Northern Benguela Upwelling System over the last 245.000 years as derived from planktic foraminifera assemblages

Andrea N. A. Volbers*, Hans-Stefan Niebler, #Jacques Giraudeau, Heike Schmidt, and Rüdiger Henrich

*University of Bremen, Faculty of Geosciences, Department of Paleoceanography and Sedimentology, P.O. Box 33 04 40, D-28334 Germany

#Université Bordeaux I, Avenue des Facultés, 33405 Talence, France

Abstract

Planktic foraminiferal records from sediment cores recovered from the Walvis Ridge and the northern Cape Basin indicate changes in the spacial and temporal variability in the degree of upwelling during the past 245 kyrs. From characteristic planktic foraminiferal assemblages three hydrographic regimes (open-oceanic, intermediate, upwelling) were distinguished downcore by factor analysis. During periods of intensified upwelling, northern Benguela upwelling cells were displaced westward and increased in size, covering areas at least three times as large as at the present day. Distinct upwelling events were recognized during oygen isotopic event (OIE) 7.4, 6.5/6.4, 6.2, 5.53, 5.4, 5.2, 4.2 and during oxygen isotopic stage (OIS) 3 and 2. During OIE 7.4 and 5.4 the maximum upwelling extent was recorded and during OIE 5.1 upwelling was at its minimum. Paleo sea surface temperature (SST) reconstructions, derived from planktic foraminifera using the classical tranfer function approach, document lower SSTs during periods of intensified upwelling whereas SSTs derived from alkenones in contrast show glacial to interglacial temperature shifts. A good correlation between upwelling events in the northern Benguela region and increases in equatorial seasonality implies that both regions respond to the same mechanism, probably changes in the trade wind intensity.

1. Introduction

Equatorial currents, in particular where they interact with the eastern boundary current systems, may significantly contribute to the bulk of the last glacial maximum (LGM) cooling within the tropics (Mix et al., 1999). During the LGM coastal and equatorial upwelling seem to have intensified compared to today (Sarnthein et al., 1988). In glacial periods, trade winds are assumed to

strengthen and to induce intensification of the wind-driven upwelling systems coupled with an increase of global productivity (Sarnthein et al., 1988). This draws down CO_2 from the atmosphere to the ocean resulting in global cooling. Sediments which underlie the major upwelling centers preserve important information on past variations in the strength and areal extent of upwelling, information of great relevance to studies of global carbon budgets and of the role of this process in climate changes (cf Peterson et al., 1995). Biotic parameters indicate extension of upwelling and divergence in the equatoral and eastern boundary current regions during LGM (CLIMAP, 1981; Mix, 1989), a feature also observed in the sediments from beneath the Benguela Upwelling System (BUS), on which this study concentrates. The Benguela Current (BC) plays a crucial role in the thermohaline circulation, as it transports warm and salty surface-water from the southern hemisphere to the as it transports warm and salty surface-water from the southern hemisphere to the northern hemisphere (Fig. 1). Therefore, long and short term changes in this area are of special importance, in particular as they do not follow the classic glacial to interglacial cycles (Schmidt, 1992; Summerhayes, et al., 1995; Jansen, Ufkes & Schneider, 1996; Little et al., 1997a; Little et al., 1997b; Schmiedl et al., 1997). Planktic foraminifera assemblages are widely used for paleoceanographic reconstructions since they well reflect hydrographic surface parameters (e.g. Thiede, 1975; Molfino et al., 1982; Thackeray & Herbert, 1991; Dowsett, 1991; Oberhänsli et al., 1992; Kohfeld et al., 1996; Mix & Morey, 1996; Pflaumann et al., 1996; Niebler & Gersonde, 1998; Mix et al., 1999). In the Benguela region, cold and nutrient-rich waters from 200-500 m depth well up In the Benguela region, cold and nutrient-rich waters

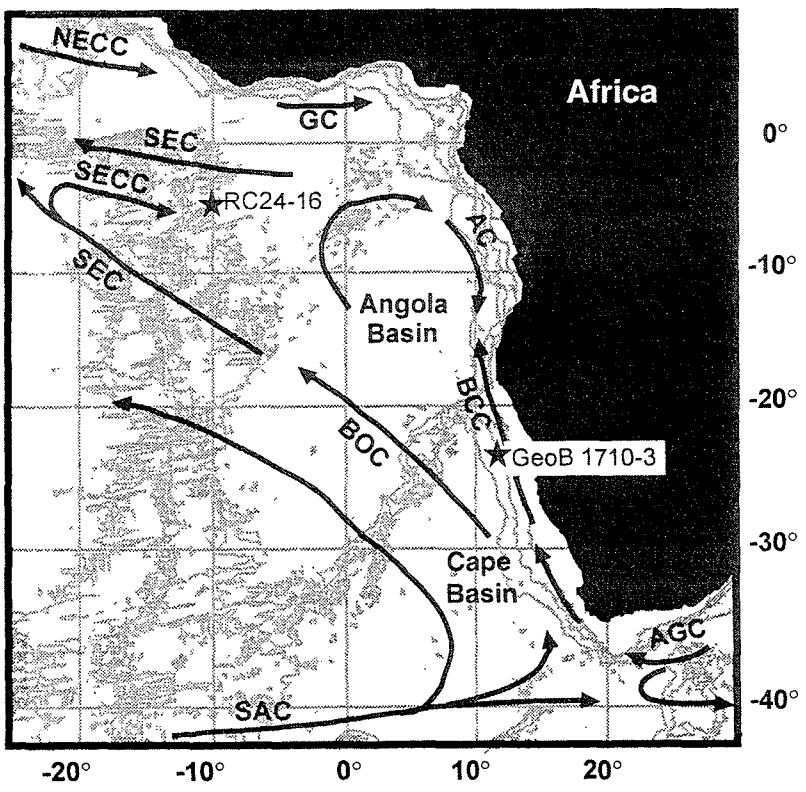

Fig. 1: South Atlantic surface circulation pattern and position of sediment cores GeoB 1710-3 and RC24-16. NECC... North Equatroiral Counter Current, SEC... South Equatorial Current, SECC... South Equatorial Counter Current, GC... Guinea Current, AC... Angola Current, BCC... Benguela Coastal Current, BOC... Benguela Oceanic Current, AGC... Agulhas Current, SAC...South Atlantic Current

from 200-500 m depth well up (Shannon, 1985; Dingle & Nelson, 1993) and provide a high productivity regime that stimulates intense primary production and cold-water planktic foraminifera assemblages. In the Benguela region, the upwelling fauna consists of *Neogloboquadrina pachyderma* sin. (Giraudeau, 1993; Ufkes & Zachariasse, 1993). *Neogloboquadrina pachyderma* sin. was previously regarded as a typical polar species restricted to surface waters below 7°C

(e.g. Bé & Tolderlund, 1971). North of the Arcic Front, this species composes greater than 90% of all surface assemblages (e.g. Pflaumann et al., 1996). Its massive occurrence in the Benguela coastal waters (Ufkes & Zachariasse, 1993) above 14°C is therefore surprising although it is not limited to this region. Minor abundances of this species were also reported from the Oman and Somalia upwelling areas where its growth and reproduction seems to be tied to the upwelling period (Ivanova et al., 1999).

As mentioned by Ivanova et al. (1999) there is no general consensus on factors controlling the distribution of *N. pachyderma* sin. For the Benguela region Giraudeau (1993) and Giraudeau & Rogers (1994) showed that water temperature is the main factor of its distribution. *Neogloboquadrina pachyderma* sin. was used as an environmental indicator and maximum abundances of this species, called PS events (pachyderma sinistral events) by Little et al. (1997a), were linked to intensified upwelling, increased productivity and lower sea surface temperatures (SSTs) in the Benguela region (Oberhänsli, 1991; Schmidt, 1992; Little et al., 1997a,b; Ufkes et al., 2000).

Since common global factor models and temperature transfer functions concentrate mainly on oligotrophic or mesotrophic ecological conditions they exclude upwelling regions as enhanced biological productivity can bias temperature-related transfer function models (Molfino et al., 1982; Chen & Prell, 1998; Watkins & Mix, 1998). Therefore local factor models and local transfer function equations for the Benguela region were calculated (Giraudeau & Rogers, 1994). Relevant for this approach is, that within the Benguela region, the distribution of planktic foraminifera is mainly temperature-controlled as stated by Giraudeau & Rogers (1994). In this paper we use the slightly modified model by Giraudeau & Rogers (1994) to check areal extent of northern Benguela upwelling cells during the late Quaternary. The Benguela factor model was applied on planktic foraminiferal counts from several other cores from the Walvis Ridge. To investigate the areal extent of Walvis Bay and Lüderitz upwelling cell we introduce planktic foraminiferal counts of GeoB 1710-3 from northern Cape Basin. Furthermore, we present paleo SSTs derived from a newly established planktic foraminfer transfer function.

2. Hydrography of the Benguela System and its imprint in the modern planktic foraminiferal assemblages

The BC forms the eastern boundary current of the South Atlantic Subtropical Gyre. It extends from 35°S to 17°S, interacting with the warm Angola Current in the north and the Angulhas Current in the south (Fig. 1). At about 30°S, the BC splits into the Benguela Oceanic Current (BOC) which flows to the west, and the colder Benguela Coastal Current (BCC) moving northward (Stramma & Peterson, 1989). The BCC is grouped into a northern part (17°S to 25°S) and a southern part (25°S to 35°S) which are distinguished by variations in upwelling intensity (Shannon, 1985; Lutjeharms & Meeuwis,

1987) and which bear different planktic foraminiferal assemblages (Giraudeau, 1993). The BCC is separated from the warmer waters of the subtropical Atlantic by a well developed thermal front (Shannon, 1985) around the shelf edge. The prevailing southerly and southeasterly winds induce coastal upwelling of cold and nutrient-rich South Atlantic Central Water (SACW, Shannon, 1985). Additionally, upwelling at the shelf edge was reported by Hart & Currie (1960).

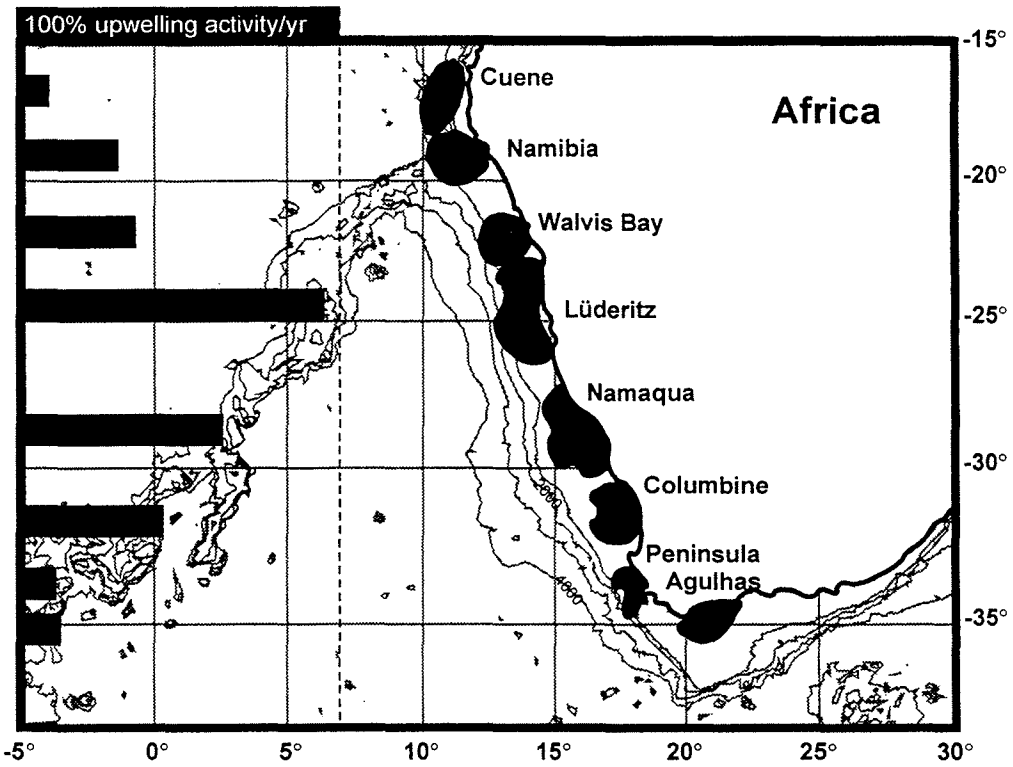

Fig. 2: Geographic location and annual frequency of occurrence of eight identified upwelling cells within the Benguela System (redrawn from Lutjeharms & Meeuwis, 1987).

In the northern Benguela region a decrease in wind stress reduces the intensity of the upwelling in comparison with the coastal areas of 25°S to 31°S which experience the most intense upwelling and lowest SSTs (Shannon, 1985; Lutjeharms & Meeuwis, 1987). Upwelled waters originate from a shallower depth in the north compared to the south where water may locally originate from a depth of more than 300 m (Shannon, 1985). These differences in source areas are portrayed by characteristic planktic foraminiferal assemblages (Giraudeau, 1993): The upwelled waters in the north that seasonally mix with warm equatorial waters from the Angola Basin are preferently colonized by *T. quinqueloba*, which represents the warm-end member of the foraminiferal upwelling association. *Neogloboquadrina pachyderma* sin. dominates the more intense upwelling cells in the south. According to Giraudeau (1993), high relative abundances, e.g. more than 70% of *N. pachyderma* sin., indicate upwelling of SACW, in which a small proportion of cold and nutrient-rich Antarctic Intermediate Water (AAIW) is entrained. AAIW originates by sinking at the Polar Front and occurs in water depths between 450-900 m in the study area (Stramma & Peterson, 1989).

A broad mixing area, which is an important component of the total upwelling regime today, extends more than 600 km seaward (Lutjeharms & Stockton, 1987). Filaments may even increase the area of high productivity. Hence, the total offshore extent of upwelling may cover a distance up to 1000 km from the coastal sites (Lutjeharms et al., 1991). Surface water masses of the mixing zone are relatively nutrient enriched and colder in comparison to the surrounding low productivity regimes of the open ocean (Lutjeharms & Stockton, 1987; Shillington et al., 1990).

With respect to the above cited oceanographic configuration, the investigated core sites are located as follows: Core GeoB 1710-3 is located 280 km away from the Namibian coast, beneath the broad-mixing filamentous domain induced by the Walvis Bay and Lüderitz upwelling cell (Fig. 2).

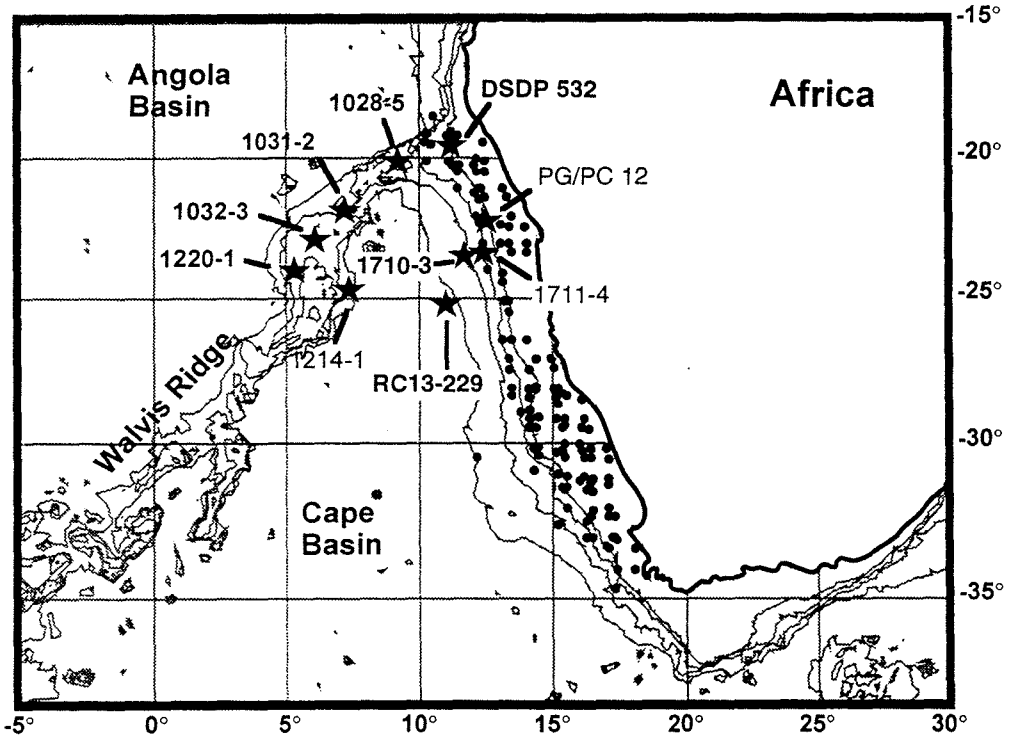

Fig. 3: Stars outline geographic location of investigated (bold) gravity cores. Dots represent surface sediment census counts of planktic foraminifera used in this study (Giraudeau, 1993; Niebler, 1995).

Walvis Bay cell (around 22°S) has an average seaward extension of 240 km and during a three year period of study, upwelling at Walvis Bay was at least two times lower compared to upwelling in the Lüderitz cell (around 25°S), which is regarded as the center of upwelling. Lüderitz cell displays an average seaward extention of 270 km away from the coast (Lutjeharms & Meeuwis, 1987). DSDP 532 sampled part of the Namibia upwelling cell (Fig. 2 and Fig. 3), which is at least three times weaker than the Lüderitz cell today (Lutjeharms & Meeuwis, 1987). All other stations (GeoB 1220-1, GeoB 1032-3, GeoB 1031-2, and GeoB 1028-5) are located on the Walvis Ridge, an area not affected by today's coastal upwelling.

3. Materials and methods

Gravity core GeoB 1710-3 (23.43°S, 11.7°E, 2987 m water depth, 1045 cm core length) was recovered from the continental slope off Namibia during R.V. Meteor cruise M20/2 (Schulz et al., 1992). Oxygen isotope analyses from the benthic foraminifera *Cibicidoides wuellerstorfi* provide the basic stratigrapic framework for the core (Bickert & Wefer, 1999). For micropaleontological investigations, all samples were freeze-dried, weighed, and washed through a 63 µm sieve. The samples were then dry-sieved into the fractions 63-125 µm, 125-250 µm, 250-500 µm, and >500 µm.

Census counts of planktic foraminifera were conducted on the >125 µm fraction in order to include small specimen of *N. pachyderma* and *T. quinqueloba*. All samples were split into subsamples using a mircrosplitter. A minimum of at least 300 non-fragmented planktic foraminiferal specimen were identified using an OLYMPUS SZ 40 microscope. All planktic foraminiferal species were identified using the taxonomic concepts of Hemleben et al. (1989). For the purpose of this paper, right-coiling *N. pachyderma* and *N. pachyderma-N. dutertrei* intergrates (PDI) were grouped as *N. pachyderma* dex. whereas species with a wider opening and at least five chambers were counted as *N. dutertrei*.

Since common transfer function models exclude the coastal upwelling area off SW Africa, we developed a model exclusively for the Benguela region, which is based on 135 surface samples from the southwest African continental margin from 35°S to 17°S and 18°E to 10°E (Fig. 3). The surface samples are evenly distributed on the sea floor and contain altogether a total of twenty four taxa of planktic foraminifera. As on average, 300 individuals from the fraction >125 µm were counted by Giraudeau (1993) and Niebler (1995), these surface samples comprise the ideal reference data set. Species that make up less than 2% in any sample were excluded. We also excluded *Globorotalia hisuta*, *Globorotalia scitula,* and *Globorotalia crassaformis* because they generally prefer deep habitats (Lohmann, 1992; Ravelo & Fairbanks, 1992). The transfer function was calculated with the program package CABFAC of Klovan & Imbrie (1971) and Imbrie & Kipp (1971). The Q-mode principal component analysis (factor analysis) combines a large number of species into a smaller number of assemblages (factors). This step provides two matrices: the varimax factor loading matrix, which explains the importance of the individual factor in each sample, while the varimax factor score matrix explains the species importance in each factor. According to Backhaus et al. (1989), loadings >0.4 and scores >0.2 are significant. In a second step a multiple stepwise regression accoring to the REGRESS program (Imbrie & Kipp, 1971) was used to calculate ecological equations between modern sea-surface temperature and the faunal assemblages derived from CABFAC. SSTs for the austral summer (January to March) and austral winter (July to September) and the annual mean from 10 m water depth were taken from Levitus & Boyer (1994) and interpolated to the nearest tenth degree in latitude and longitude. Q-mode factor analysis was completed in order to define a transfer function for the estimations of past SSTs according to the statistical method developed by Imbrie & Kipp (1971). The Benguela factor model consists of three

planktic foraminiferal assemblages, called „factors", which explain 95,3% of the total variance. The equation „F135-15-3" (135 surface samples, 15 taxa, 3 factors) was developed for paleotemperature reconstruction.

Downcore samples which have no core-top equivalents show up as no-anlaog-situations (appendix 1). For the purpose of this paper, no analog situations with <20% of one species were tolerated as they still may be interpreted with care. As carbonate dissolution can strongly alter planktic foraminiferal assemblages, all GeoB 1710-3 samples were examined with respect to carbonate preservation applying several independent dissolution proxies. Sample 883 cm was strongly altered by carbonate dissolution and was therefore excluded from the data set (Volbers & Henrich, subm.).

Foraminiferal assemblages of GeoB 1710-3, RC13-229, and five cores from Walvis Ridge were then compared with the Benguela factor model. Planktic foraminiferal counts from RC13-229 (25.30°S, 11.18°E) were taken from CLIMAP (1981) and the age model from Oppo & Rosenthal (1994). Planktic foraminiferal assemblages of DSDP 532 (19.44°S, 10.31°E) were counted by Oberhänsli (1991), with at least 300 tests of the fraction >125 µm. PDI were counted as *N. pachyderma* dex. Oxygen isotope stratigraphy is based on oxygen isotope values of *G. bulloides* and the distribution of *Gephyrocapsa lacunosa* (Oberhänsli, 1991). Planktic foraminiferal census counts from GeoB 1220-1 (24.03°S, 5.31°E) GeoB 1032-3 (22.92°S, 6.04°E), GeoB 1031-4 (21.88°S, 7.10°E), and GeoB 1028-5 (20.11°S, 9.19°E) were taken from Schmidt (1992). At least 400 tests >150 µm were examined. *N. pachyderma-N. dutertrei* intergrates, *N. pachyderma* dex., and *N. dutertrei* were counted seperately, PDI were added to *N. pachyderma* dex. for the purpose of this paper. The age model for GeoB 1028-5 was taken from Müller et al. (1997). It is based on $\delta^{18}O$ records of *Globigerinoides ruber* (white) and *G. bulloides* (Schneider et al., 1995; Schneider et al., 1996). The stratigraphic framework of GeoB 1032-3 consists of the $\delta^{18}O$ record from *C. wuellerstorfi* (age model after Bickert (1992) and Bickert & Wefer (1996). The age model for GeoB 1031-4 and GeoB 1220-1 was taken from Schmidt (1992) and is based on $\delta^{18}O$ values from *G. ruber* (white) and *G. inflata*.

4. Results

4.1 Benguela factor model

To interprete the planktic foraminiferal assemblages of GeoB 1710-3, we used a model that slightly differs from the one of Giraudeau & Rogers (1994) as it is based on a different surface sediment data set and a different SST data source (Levitus & Boyer, 1994). The Benguela factor model consists of three factors and the great majority of the samples displays communalities >0.9. Factor 1, which contributes 38.6% of the total variance is defined exclusively by *G. inflata* (table 1). This factor characterizes the outer shelf and the slope of the Benguela region and the Walvis Ridge (open-oceanic assemblage) (Fig. 4). Factor 1 is absent between 25°S to 22°S.

Taxa	Factors		
	Factor 1 (open-oceanic)	**Factor 2** (up-welling)	**Factor 3** (inter-mediate)
G. siphonifera	0.019	-0.008	-0.008
G. anfracta	0	0	-0.001
G. bulloides	0.124	-0.057	**-0.571**
N. dutertrei	0.065	0.015	-0.05
G. falconensis	0.014	0.017	-0.005
G. glutinata	0.014	-0.008	-0.013
G. inflata	**0.985**	0.033	0.066
P. obliquiloculata	0.002	0.001	0.001
N. pachyderma sin.	-0.021	**0.964**	0.138
N. pachyderma dex.	-0.009	**0.218**	**-0.779**
T. quinqueloba	-0.034	0.122	-0.063
G. ruber	0.043	-0.015	-0.01
G. sacculifer	0.026	-0.003	-0.004
G. truncatulinoides	0.067	-0.01	0
O. universa	-0.018	-0.056	-0.193
Variance (%)	38.6	34.37	22.35
Cummulative variance (%)	38.6	72.97	95.32

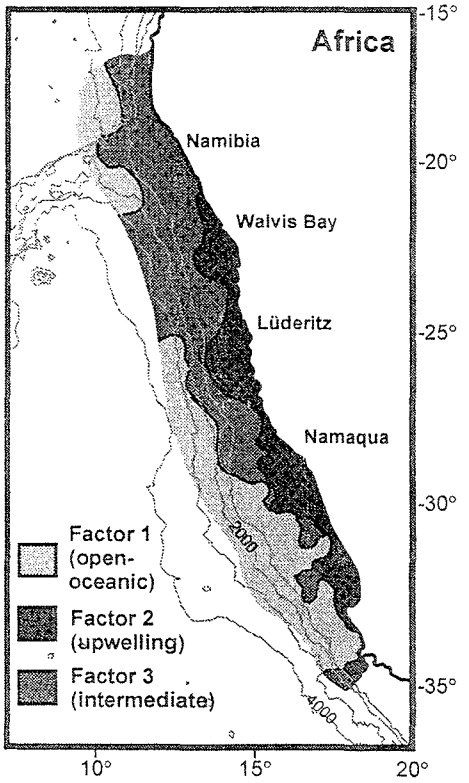

Table 1: Varimax factor score matrix derived from Q-mode factor analysis of the planktic foraminiferal census data (135 sediment samples, 13 taxa). **Fig. 4:** Composite map of the dominant geographic areas of planktic foraminiferal factors produced by Q-mode factor analysis.

The second factor is dominated by *N. pachyderma* sin. with minor contribution of *N. pachyderma* dex. and 34.37% of the total variance. This factor (upwelling assemblage) characterizes the innermost shelf between 34°S and 21°S and underlies the most active upwelling cells (Walvis Bay, Lüderitz, Namaqua, Columbine). Factor 3 consits of *N. pachyderma* dex. and *G. bulloides* and displays 22.35% of the total variance. This assemblage characterizes the middle shelf and upper slope environment between 29°S to 17°S. South of 29°S it is restricted to small patches associated with Factor 1. This factor represents the mixing of warmer oligotrophic waters with colder waters from coastal upwelling (intermediate assemblage). The transfer functions for temperature estimates have adjusted standard errors of 0.4°C (table 2) for austral summer temperatures (Jan-Mar, adjusted mcc: 0.86), 0.3°C for austral winter temperatures (Jul-Sep, adjusted mcc: 0.83), and 0.3°C for annual temperatures (adjusted mcc: 0.82). The scatter plots of residuals (Fig. 5) show that positive and negative residuals (observed temperatures minus estimated values) of either equation are equally distributed.

	Jan-Mar		Jul-Sep		annual	
Variable	Regression coefficient	S.E. of regression coefficent	Regression coefficient	S.E. of regression coefficent	Regression coefficient	S.E. of regression coefficent
F1-SQ	-12.21406	2.01622	-5.80988	1.44243	-7.50249	1.52435
F2-SQ	-5.27948	2.13552	-2.38005	1.52776	-3.51160	1.61457
F3-SQ	-6.72485	1.33440	-3.72878	0.95463	-4.44516	1.00886
F1xF2	-4.00180	3.03455	-2.28679	2.17094	-2.29742	2.29430
F1xF3	1.49942	2.37334	1.20107	1.69791	0.64744	1.79438
F2xF3	0.31945	2.56655	0.89694	1.83613	0.56425	1.94046
F1	7.85300	4.00816	4.67355	2.86748	5.13112	3.03039
F2	-0.74439	4.21466	0.06426	3.01521	0.09399	3.18655
F3	-0.64857	3.12571	-1.46058	2.23615	-0.30256	2.36320
Intercept	23.71124		16.51532		20.54012	
Standard error	0.39		0.28		0.29	
Mul. corr. coeff.	0.86		0.83		0.82	

Table 2: Correlation matrix between the varimay factors and the environmental parameers, and statistics of the transfer functions. Standard errors and multiple correlation coefficents are adjusted for degree of freedom.

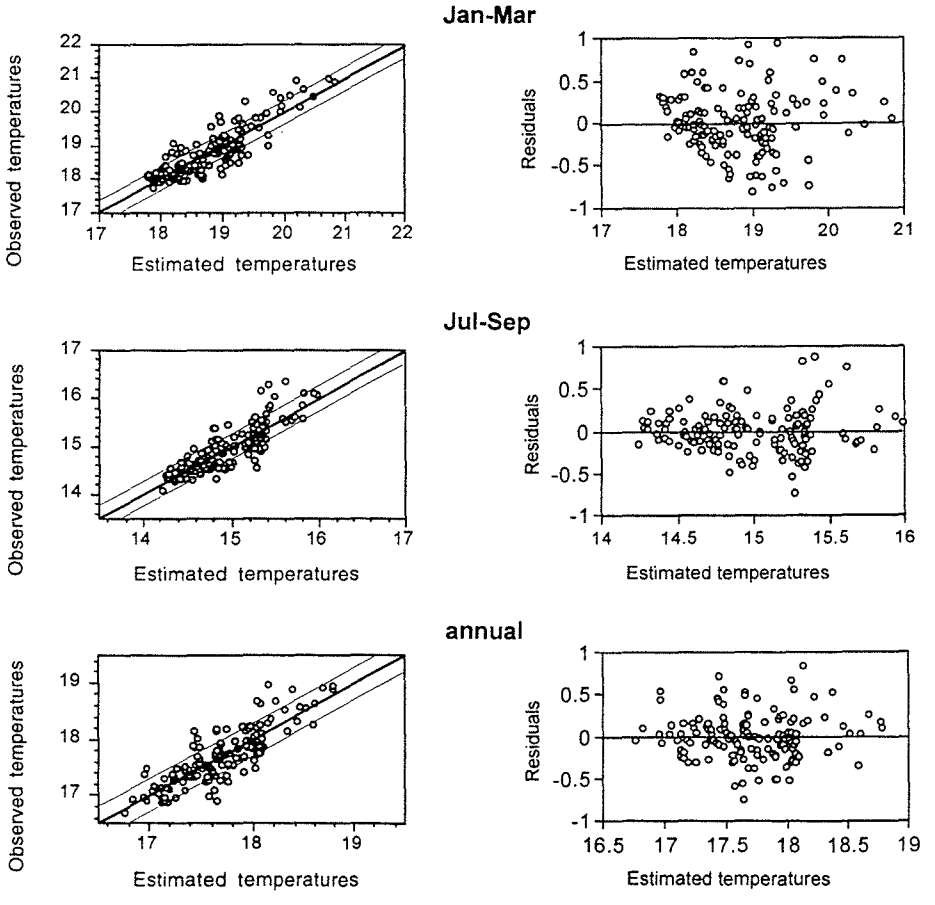

Fig. 5: Scatter diagrams of estimated sea-surface temperatures (°C) versus observed sea-surface temperatures produced by the regression equations, and scatter plots of residuals (observed temperatures minus estimated temperatures) verssus surface temperatures).

4.2 Sediment cores from the Cape Basin

GeoB 1710-3:

GeoB 1710-3 fauna consists of eight species which comprise 95% of all planktic foraminifera species recognized. *Neogloboquadrina pachyderma* dex. is the most abundant of all species with maximum abundances of up to 59%, and is negatively correlated to *N. pachyderma* sin. which dominates the assemblages of oxygen isotope stage (OIS) 3 and 2. In addition *N. pachyderma* sin. shows rapid oscillations in relative abundances from 1-61% of the total assemblages. Thirteen PS events are displayed by GeoB 1710-3 during the last 245 kyrs (Fig. 6). *Globigerina bulloides* records the third highest abundance in the core, and is slightly enhanced during interglacial periods such as oxygen isotopic event (OIE) 5.5 and 5.1. *Turborotalita quinqueloba* is most abundant during OIS 7 and 6, whereas *G. inflata* shows two pronounced abundance maxima up to 24% at OIE 5.5 and 5.1. *Globigerinella calida* has maximal abundances during the Holocene and during OIS 4, and is in general relatively independent of glacial-interglacial conditions. Increased values of *Neogloboquadrina dutertrei* up to 20% are observed during interglacials with maximum abundance at OIE 5.1. Besides peak abundance at the beginning of the Holocene, *Globigerinita glutinata* is evenly distributed during the last 245 kyrs.

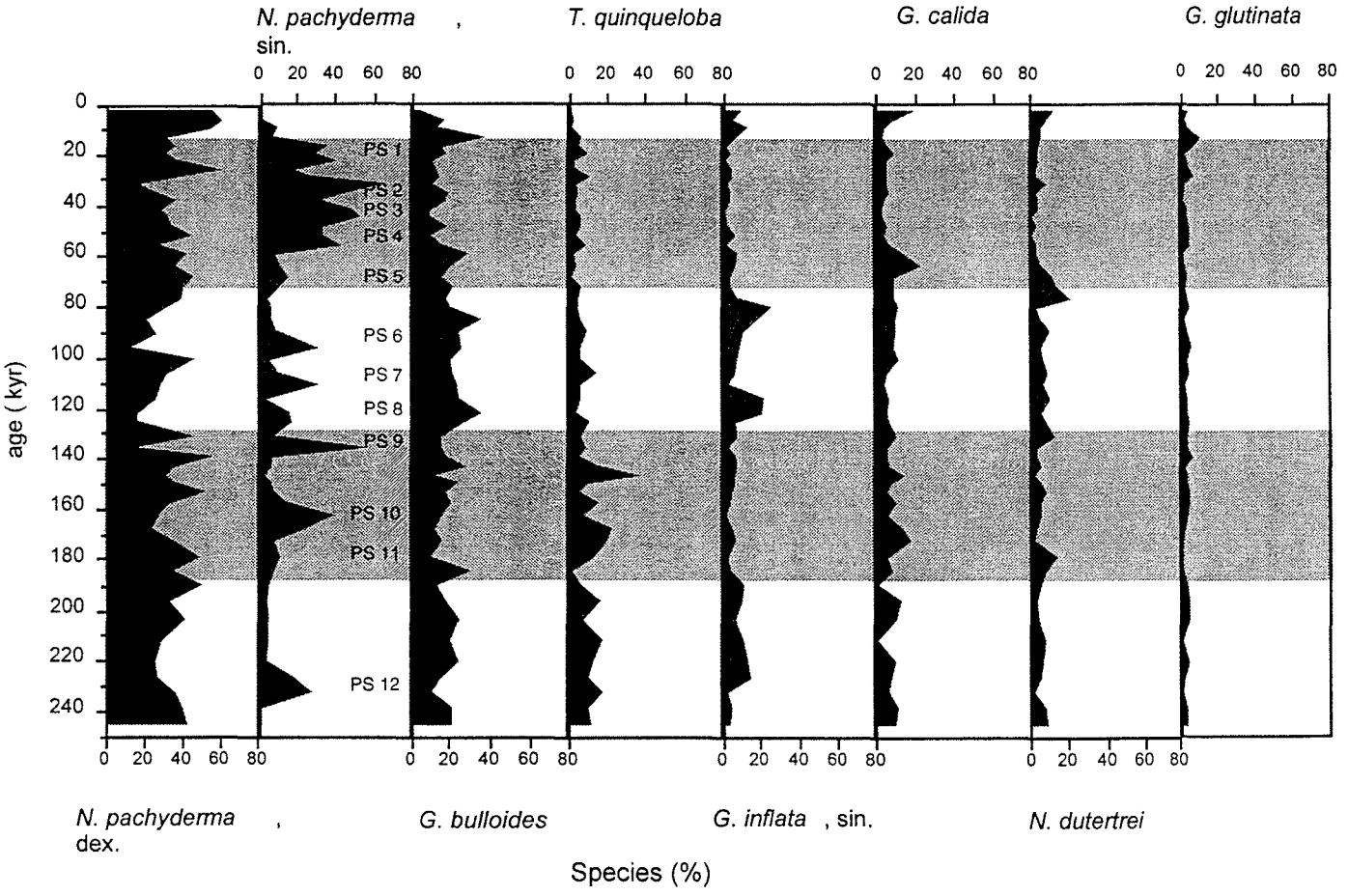

Fig. 6: Relative abundances of the main planktic foraminifera species of GeoB 1710-3 in %. Peak abundances of *Neogloboquadrina pachyderma* sin. („PS events") as introduced by Little et al. (1997a) are labeled PS1 - PS12. Grey bars represent glacial periods.

Factor 3 (intermediate assemblage) explains most of GeoB 1710-3 faunal associations of the last 245 kyrs (Fig. 7) and is only insignificant during OIS 3, and OIE 6.2. Factor 2 (upwelling assemblage) is the second important factor and displays short periods of high significance over the last 245 kyrs (OIE 7.4, 6.5/6.4, 6.2, 5.5, 5.4, 5.2, and 4.2) besides persisting dominance during OIS 3 and 2. During OIS 5, factor F1 (oceanic assemblage) is significant and displays peak values during OIE 5.5 and 5.3.

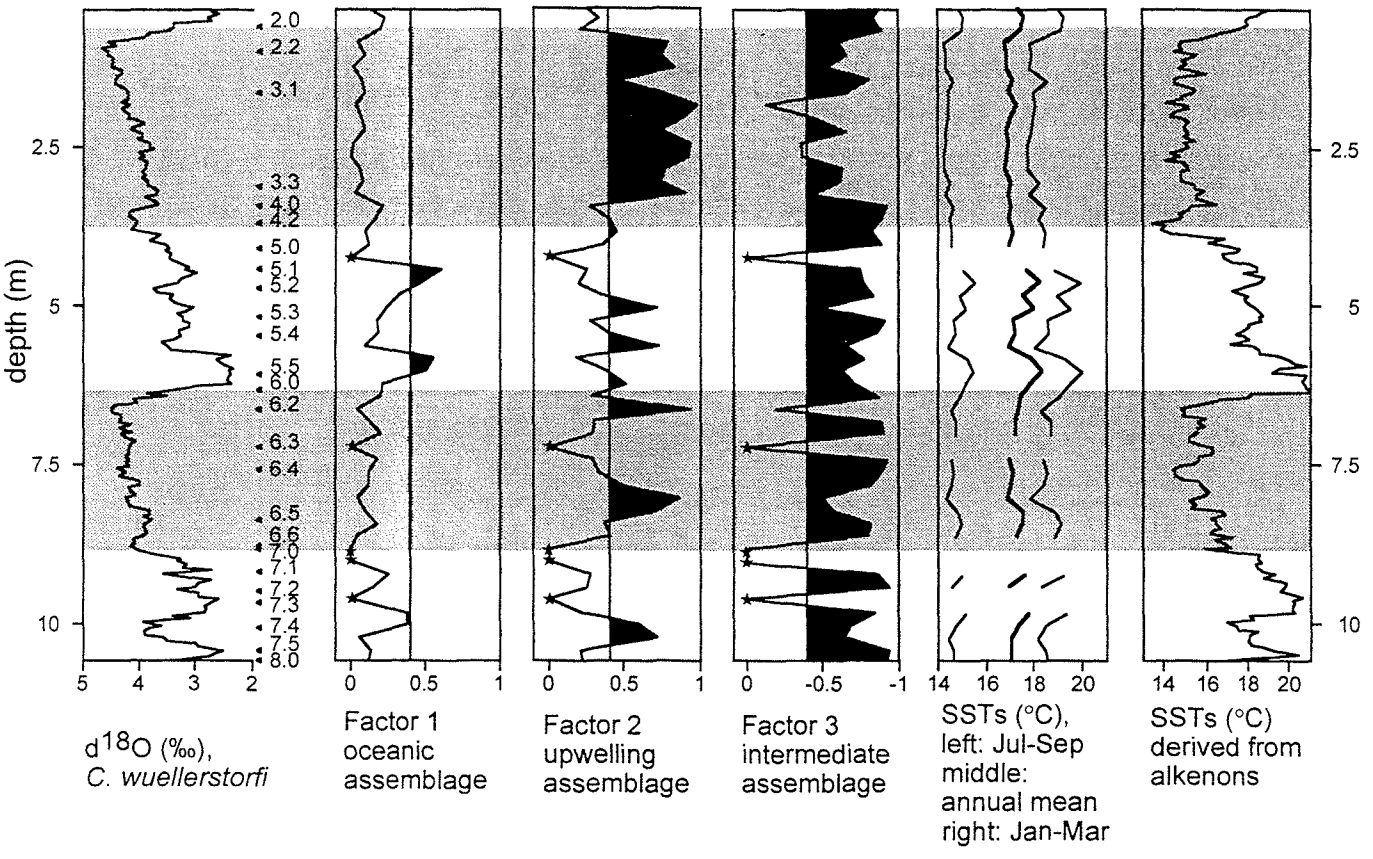

Fig. 7: Graphic representation of GeoB 1710-3 parafactor loading matrix, stars represent no-analog situations. Age model after Bickert & Wefer (1999). Paleo sea surface temperatures derived from alkenons after Kirst et al. (1999). Grey bars represent glacial periods.

From planktic foraminifera of GeoB 1710-3 paleo SSTs were calculated. Glacial to interglacial SST are on the order of a few degrees Celsius. Austral summer SSTs range from 17.7 to 20°C and austral winter SSTs vary from 14.3°C-15.5°C. Annual SST range from 16,8°C to 18,4°C. Highest SSTs are displayed during OIE 5.5, 5.3, 5.1 and holocene. Lowest SST occur during OIE 6.5/6.4, and during OIS 3-2.

RC13-229:

As data from RC 13-229 are limited to intervall 2.5-3.19 m, the individual results are not graphically shown (see Appendix 1). According to CLIMAP (1984) OIE 5.5 is represented at the 2.9 m level and this level was therefore chosen for reconstruction of Walvis Bay cell and Lüderitz cell in this study. For the 2.9 m level (OIE 5.51) Factor 1 is the dominant factor, Factor 3 is also significant, austral

summer and winter SSTs are 19.2°C and 15.2°C, and the reconstructed annual SST is 18.0°C.

Using the age model from Oppo & Rosenthal (1994), OIE 5.4 was set at the 2.76 m level. Factor 3 is the dominant factor and Factor 2 is also significant. Reconstructed SST are the same or slightly cooler than for OIE 5.51: 19.2°C (summer), 15.0°C (winter), and 17.7°C (annual).

Additionally, OIE 5.53 was determined at the 3.08 m level. Factor 2 dominates over Factor 3 and SSTs are 18.5°C for summer, 14.7°C for winter, and 17.6°C for the annual mean.

4.3 Sediment cores from the Walvis Ridge

Five sediment cores comprise a W-E transect across the Walvis Ridge (Fig. 3) with GeoB 1220-1 furthest to the west and DSDP 532 to the east, only 200 km away from the coast of Angola. DSDP 532 contains sediments up to OIS 13 (Fig. 8) and time resolution compared to all other cores is rather low, therefore high fluctuations of characteristic planktic foraminiferal assemblages may not necessarily be reflected.

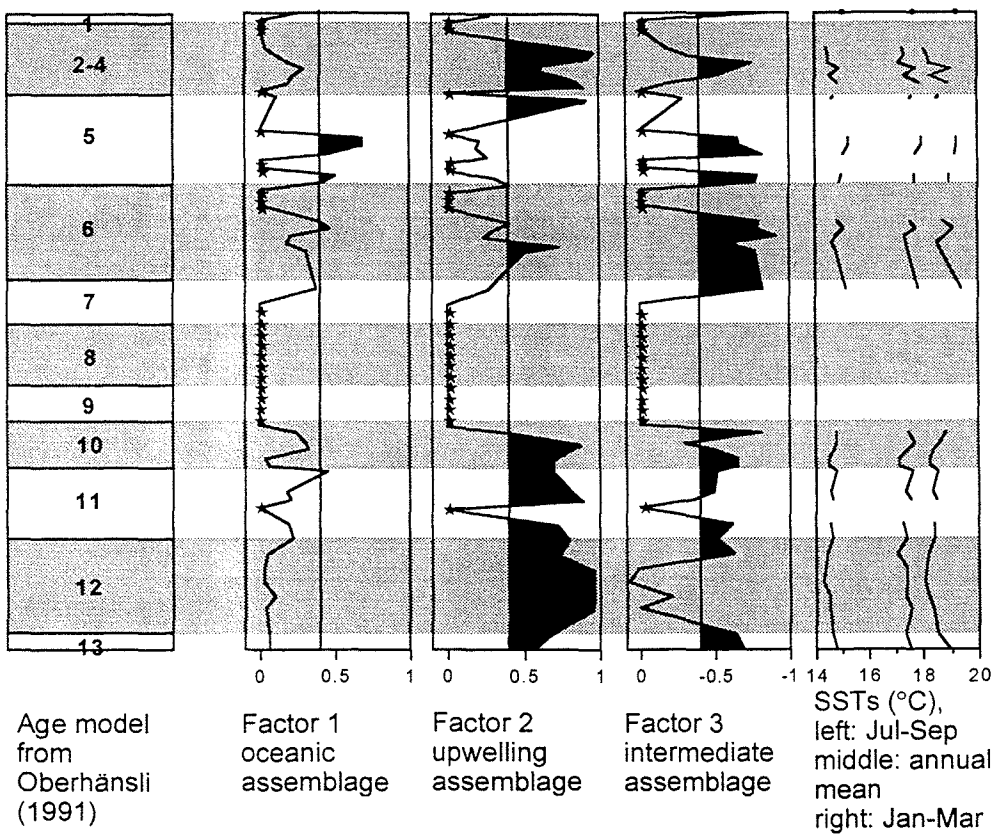

Fig. 8: Graphic representation of DSDP 532 parafactor loading matrix, stars represent no-analog situations. Age model from Oberhänsli (1991). Grey bars represent glacials.

Factor 2 is most important throughout OIS 13 to 10, at the beginning of OIS 6, at the end of OIS 5 and during OIS 4-2. Factor 3 is strongest during OIS 11 and 10 and OIS 6 and 5. Factor 1 is only significant during short time periods of OIS 6 and 5. OIS 9 to 7 are marked by no analogue situations

due to the overwhelming occurrence of *G. falconensis*.

The GeoB 1028-5 fauna is dominated by Factor 3 thoughout the last 280 kyrs (Fig. 9), followed by Factor 1 which is significant mainly during interglacial periods.

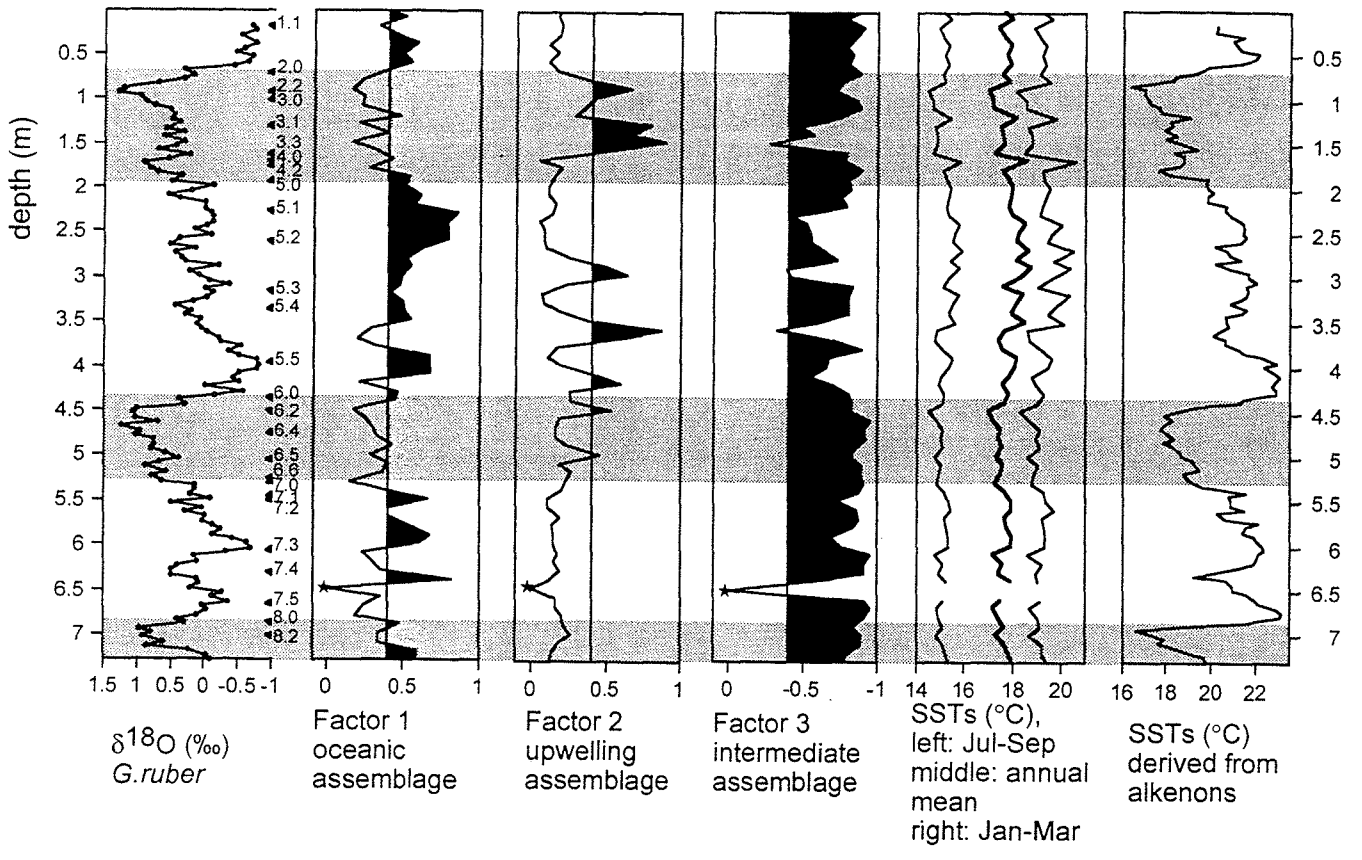

Fig. 9: Graphic representation of GeoB 1028-5 parafactor loading matrix, stars respresent not-analog situations. Age model and paleo sea surface temperatures from Müller et al. (1997). Grey bars represent glacial periods.

Factor 2 is restricted to OIE 6.5, 6.2, 5.53, 5.4, and 5.3/5.2 and OIS 3 to 2. Compared to GeoB 1028-5, GeoB 1031-4 fauna show increasing importance of factor 1 throughout the last 250 kyrs although Factor 3 is still dominant besides OIE 7.5/7.4 (Fig. 10). During this time period, Factor 2 has maximum significance and is also present during OIE 5.4 and 3.3. Further to the west, Factor 2 is not significant during the last 280 kyrs. The foraminiferal assemblages of GeoB 1032-3 are dominated by Factor 3. Factor 1 is strongest during OIE 7.2, 5.4, 5.2/5.1, and 2.2. GeoB 1032-3 fauna cannot be completely explained by our model, as shown by the high numbers of no-analog situations (Fig. 11) due to increasing abundances of *Globigerinoides ruber*, *Globorotalia truncatulinoides*, *Globigerinoides sacculifer*, and *Pulleniatina obliquiloculata* towards the west.

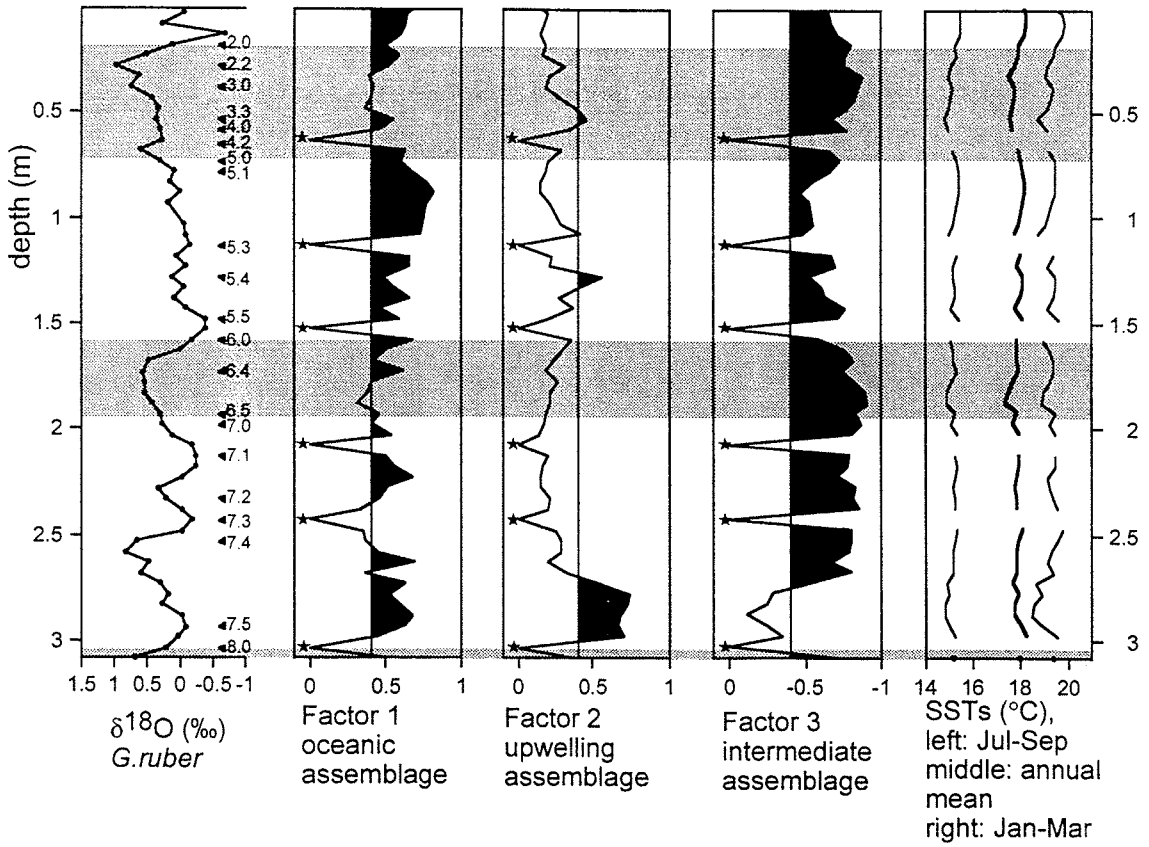

Fig. 10: Graphic representation of GeoB 1031-2 parafactor loading matrix, stars represent no-analog situtations. Age model from Schmidt (1992). Grey bars represent glacial periods.

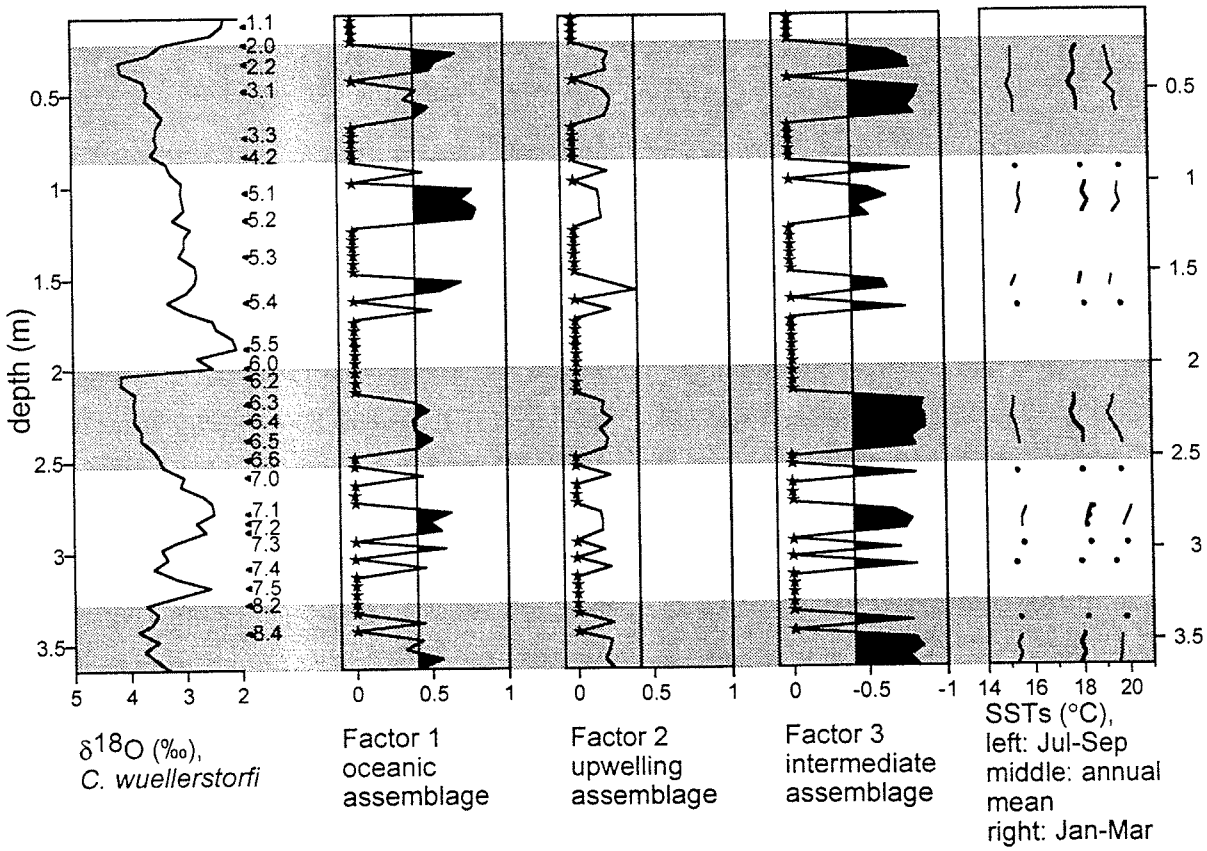

Fig. 11: Graphic representation of GeoB 1032-3 parafactor loading matrix, stars represent no-analog situtations. Age model after Bickert (1992) and Bickert & Wefer (1996). Glacials in grey.

GeoB 1220-1 planktic foraminifera fauna consists of even higher percentages of these subtropical-tropical species and therefore only planktic foraminiferal assemblages of glacial periods can partly be explained with our model (Fig. 12).

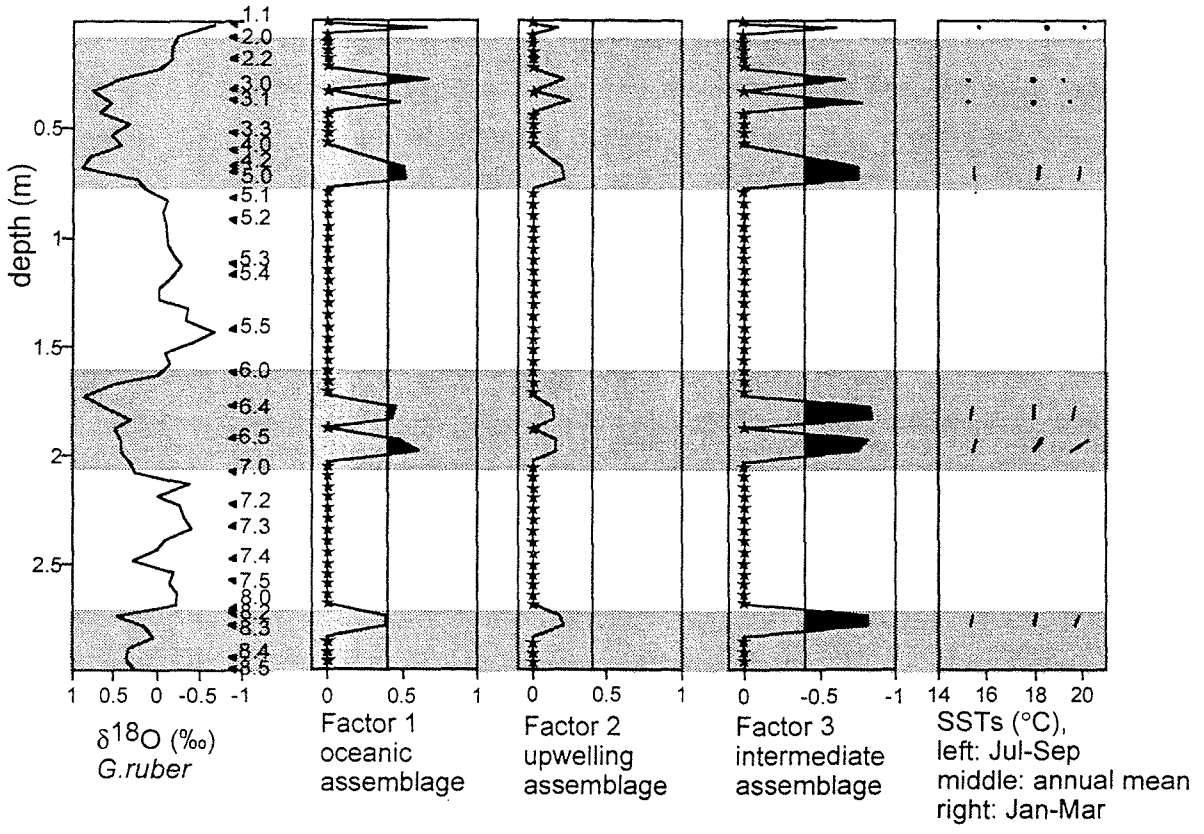

Fig. 12: Graphic representation of GeoB 1220-1 parafactor loading matrix, stars represent no-analog situtations. Age model from Schmidt (1992). Grey bars represent glacial periods.

Temperature reconstructions from planktic foraminifera of five cores from the Walvis Ridge are in the range of 14.3°C to 20.6°C. Summer SSTs range between 18.0°C and 20.6°C, whereas winter SSTs are between 14.3-15.7°C and annual SST are between 17.0°C-18.8°C. Temperature ranges of the two easternmost cores, DSDP 532 and GeoB 1028-5, are higher than those of the cores further to the west. Summer SSTs are between 18.0°C-19.4°C and winter SSTs between 14.3°C-15.3°C. Annual SSTs range between 17.1°C-18.0°C. DSDP 532 displays warmest SST at the end of OIS 7 (Fig. 8). GeoB 1028-5 shows summer SSTs between 18.1°C and 20.6°C and winter temperatures between 14.4°C and 15.9°C. Annual SSTs are between 17.0°C and 18.8°C. OIE 3.3 displays the warmest temperatures, followed by OIE 5.3/5.2 (Fig. 9). Coldest temperatures are obtained during 6.2 and 2.2. Summer SSTs of GeoB 1031-4 range between 18.5°C-19.8°C and winter SSTs between 14.9°C-15.5°C, with an annual range between 17.4°C-18.3°C (Fig. 10). Data from OIE 5.5 are limited, and warmest SSTs are displayed during Holocene. Coldest SSTs were reconstructed for OIE 3.3 and OIE 7.4/7.5. From GeoB 1032-3 and GeoB 1220-1, data are limited due to numerous no analog situations (Fig. 11, Fig. 12).

5. Discussion

The planktonic foraminiferal assemblages of six cores are described by the three factors of the Benguela model. The upwelling assemblage (Factor 2), the intermediate assemblage (Factor 3) and the open-ocean assemblage (Factor 1), show rapid changes in significance throughout the late Quaternary and from this we can reconstruct changes in the BUS. Over the last 245 kyrs, the surface waters over the core locations were dominantly derived from variable mixing of the warm oligothropic offshore waters with the cool, upwelled waters from the coast. This is reflected by the overwhelming dominance of Factor 3 (Fig. 7-Fig. 12). Over long periods of the past 245 kyrs, the areal extent of northern Benguela upwelling cells was mainly restricted to the proximity of the African coast as seen today. However, distinct short intervals of considerably larger extension not linked to glacial-interglacial cycles are recognized. When reconstructing periods of intensified upwelling, we expect to see fluctuations in the significance of Factor 2. Increased upwelling intensity would displace the boundary between the eutrophic and mesotrophic water masses to the west as the upwelling cells widened. In addition, these upwelled waters may have originated from greater depth (Oberhänsli, 1991; Ufkes et al., 2000). Therefore Factor 2 should also show up in the more westward cores and Factor 3 should also be displaced to the west. The opposite is expected during times when the upwelling is reduced to the present day situation. Due to lowered upwelling intensity, the areal extent of Northern Benguela upwelling cells is expected to be smaller than today. Therefore, Factor 2 would not even be present in the innermost cores, whereas planktic foraminiferal fauna would be dominated by Factor 3 respectively.

5.1 Walvis Bay/Lüderitz cell

We assume that intensified upwelling results in a westward extension of the Walvis Bay and Lüderitz cells, which might have been connected during periods of maximal upwelling (Fig. 13). From GeoB 1710-3 we can determine maximal westward extension of the Walvis Bay/Lüderitz upwelling cell during OIE 3.1 and 6.2 (Fig. 8). We can clearly show westward widening of the upwelling cells to far more than 280 km away from the coast, reflected by the exclusive significance of Factor 2 (upwelling assemblage). During OIE 7.4, 6.5/6.4, 5.4, 5.2 and OIS 2, the areal extent of Walvis Bay/Lüderitz cell must have been smaller than during OIS 3 and OIE 6.2 reflected by the co-existence of the intermediate assemblage (Factor 3). We can therefore conclude that the upwelling cells periodically extended to the GeoB 1710-3 location. RC13-229 data show that this core was at the outer edge of the Lüderitz upwelling cell during OIE 5.4 because the intermediate assemblage dominates RC13-229 fauna (Fig. 13). During OIE 5.53 and OIE 4.2 Factor 2 is of minor importance compared to Factor 3, showing that the GeoB 1710-3 location was at the outer edge of the Walvis Bay/Lüderitz cell. Further to the south, the Lüderitz cell extended to the RC 13-229 position during OIE 5.53. Summing up, short periods of intensified upwelling during OIE 7.4, 6.5/6.4, 5.53, 5.4, 5.2, 4.2 and OIS 3 and 2 are reflected by the upwelling assemblage (Factor 2) of planktic foraminifera. This is in agreement with the work from Schmiedl et al. (1997) on benthic foraminifera which suggests increased primary productivity during distinct time periods such as e.g. OIE 5.4 and 5.2 and during OIS 4 to 2.

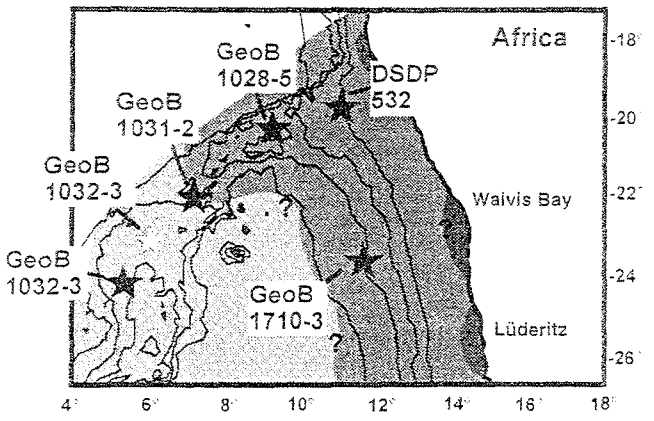

a) Holocene

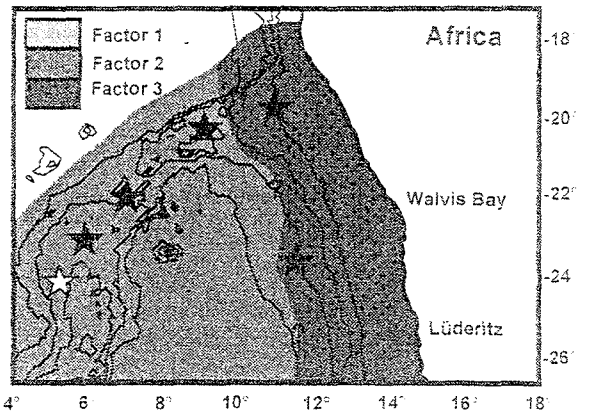

b) OIE 2.2

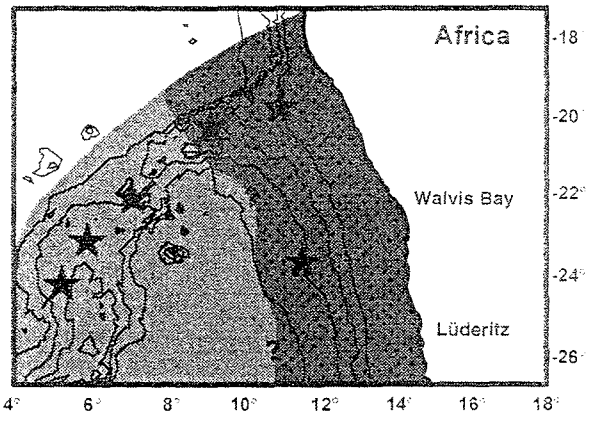

c) OIE 3.1

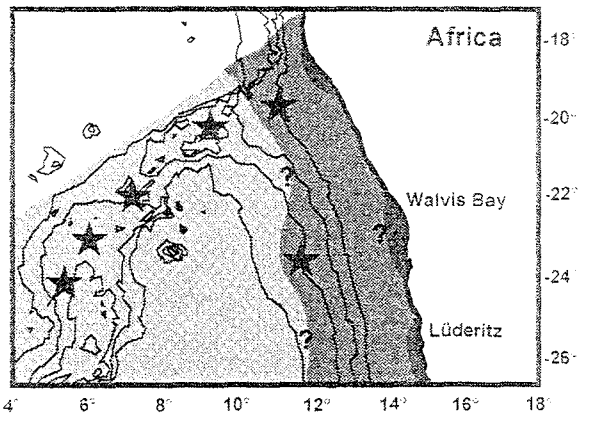

d) Upwelling minimum, OIE 5.1

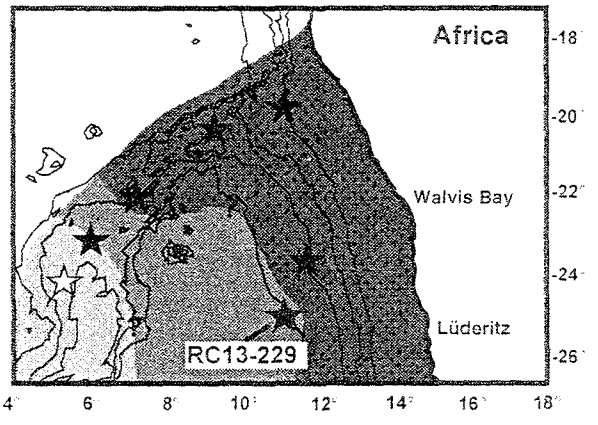

e) Upwelling maximum, OIE 5.4

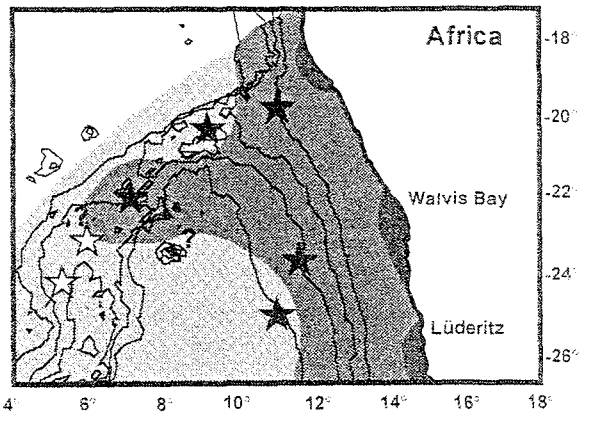

f) OIE 5.51

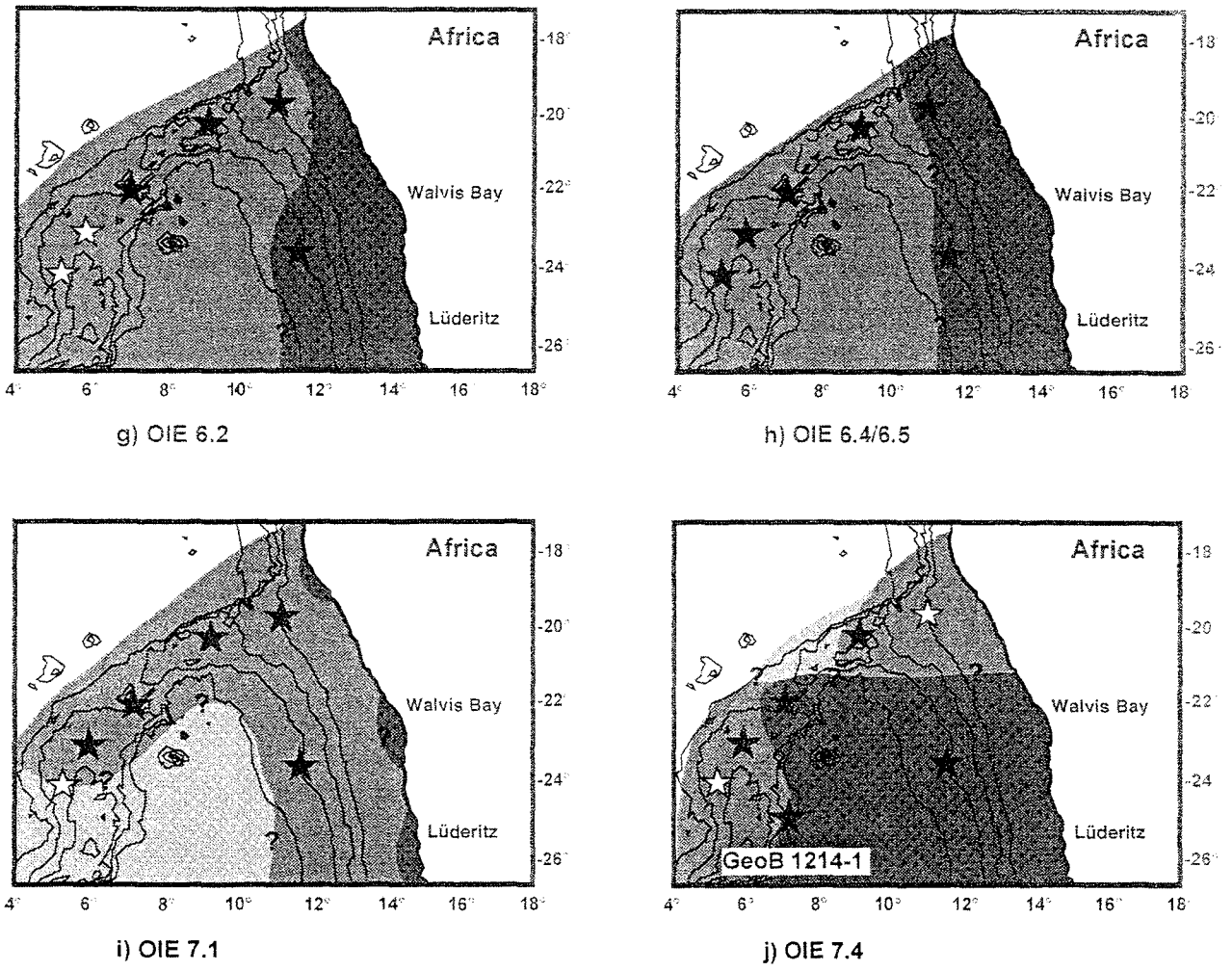

g) OIE 6.2

h) OIE 6.4/6.5

i) OIE 7.1

j) OIE 7.4

Fig. 13: Graphic interpretation of parafactor loading matrix of all investigated cores during distinct time periods (a-j) to reconstruct areal extent of northern Benguela upwelling cells (no analog situations are not illustrated). Figure 13j also shows location of GeoB 1214-1 because investigation of benthic foraminifera indicate a high productivity fauna during OIE 7.4 (Schmiedl et al., 1997).

In addition, a high productivity benthic foraminiferal fauna is common during OIE 7.4, 6.5-6.1 and OIS 3 to 2.

The areal extent of the Walvis Bay upwelling cell was smallest during OIE 5.1 and during OIE 5.51. The open-ocean assemblage yields highest values. At GeoB 1710-3 the intermediate assemblages is still the dominant factor whereas RC13-229 further to the west is dominated by the intermediate assemblage (Fig. 13). We can therefore conclude that open-ocean waters invaded the BUS when upwelling intensity was small. The areal extent of the Northern Benguela upwelling cells during these time periods is unknown.

5.2 Namibia/Walvis Bay Upwelling cell

The areal extent of the Namibia upwelling cell can be reconstructed in greater detail. During periods of increased upwelling intensity, the Namibia and Walvis Bay upwelling cells might have been connected to one another (Fig. 13). DSDP 532, closest to the coast of Angola, shows continous upwelling from OIS 13 to 10 and the end of OIS 5 to 2 (Fig. 8). High abundances of *N. pachyderma* sin. during OIS 12 and 13 could be explained as enrichment of this resistant species because of severe carbonate dissolution (Diester-Haas, 1985). However, there is also evidence for high productivity during OIS 12 and 10 from GeoB 1214-1 (Fig. 3) benthic foraminiferal fauna (Schmiedl et al., 1997). For the purpose of this paper, we focus on the last 245 kyrs. Factor 2 dominates in the middle of OIS 6, and from the end of OIS 5 to OIS 2. DSDP 532 was therefore part of the Namibia upwelling cell during these time periods. During OIS 6 and 5 the intermediate assemblage is dominant and upwelling was limited to the coastal area east of DSDP 532. During OIS 5 the open-ocean assemblages yield significant values together with the intermediate assemblages and upwelling in the Namibia cell was therefore lowest. This is in accordance with the data from GeoB 1028-5 where planktic foraminiferal fauna show a high significance of Factor 1 during Holocene, OIE 5.1-5.4 and parts of 5.5 (Fig. 9). The siginificance of the upwelling assemblage is restricted to a few short-term events such as 6.5, 6.2, 5.5, 5.4 5.2, and during OIS 3 and 2. During OIE 5.4 and 3.3 and the beginning of OIS 3, the upwelling assemblage is the dominant factor and the Namibia upwelling cell extended to the GeoB 1028-5 position. Neither of these events is reflected by GeoB 1031-4 fauna except during OIE 5.4 (Fig. 10). GeoB 1031-4 was outside the Namibian upwelling cell during the last 200 kyrs, as shown by the continous significance of the intermediate assemblage and the open-ocean assemblage. During OIE 5.1 and parts of OIE 5.3, the open-ocean assemblage was the dominant factor, showing the most intense open-ocean character. Surprisingly during OIE 7.5/7.4 the upwelling assemblage dominated the open-ocean assemblages. As this event is not reflected by GeoB 1028-5 fauna, it is likely that the Walvis Bay/Lüderitz upwelling cell from the south extended toward GeoB 1031-4 during this time period. There is some support from a high productivity benthic foraminifera fauna of GeoB 1214-1 (Schmiedl et al., 1997). GeoB 1032-3 fauna show a significance of the upwelling assemblage only during OIE 5.4 (Fig. 11). The upwelling influence is only small, as either the intermediate assemblage and the open-ocean assemblage dominate. From GeoB 1032-3 we can infer that neither upwelling cell covered this position during the last 280 kyrs. However, increased numbers of no-analog situations limit our interpretation of GeoB 1032-3 data. Maximum significance of the open-oceanic assemblages is reported at OIE 5.3, 5.2/5.1 and 2.2. Besides OIE 5.2/5.1, the intermediate assemblage is still the most important factor during the last 280 kyrs. GeoB 1220-1 and also GeoB 1032-3 show higher relative abundances of subtropical-tropical planktic foraminiferal fauna than in the easternmost cores and clearly reflect limitations of our model near the outer edge of the Benguela system (Fig. 11, Fig.12).

5.3 Paleo-temperature reconstructions

Foraminiferal assemblage temperature estimates provide a warm and a cool season and an annual temperature estimate. Paleotemperature ranges throughout the last 245 kyrs are rather small. GeoB

1710-3 reflects the highest variablity in temperature range of all investigated cores, with warmest SSTs during interglacial periods and coldest during glacial periods. However, low temperatures are not necessarily restricted to glacial periods, e.g. during OIE 5.4 typical glacial values are displayed. Temperature differences between Holocene and LGM are -2.2°C for summer SST, -1,1°C for winter SST and -1.3°C for annual SST. Identical temperature differences are calculated between OIE 5.5 and OIE 6.2. Seasonal differences during LGM were smaller than during Holocene, as seasonality is around 4.6°C during Holocene and 3.5°C during LGM. The same seasonality differences are displayed for OIE 5.5 and OIE 6.2. Temperatures during OIE 5.5 were slightly warmer than today, in addition, SSTs during OIE 5.3 and OIE 5.1 reached or slightly exceed Holocene values.

For the same core, paleo SSTs derived from alkenones display typical glacial to interglacial fluctuations with generally low temperatures during glacials and higher temperatures during interglacials. The alkenone technique employs unsaturation ratios of long-chain ketones that are linearly related to water temperature (Sikes & Keigwin, 1994), independent of relative species abundances, and supposed to represent an average warm season signal (January-June) of the mixed surface layer in the Benguela region (Kirst et al., 1999). Uk'37 temperature estimates of GeoB 1710-3 show a broad SST range from 13.5°C to 21.2°C (Kirst et al., 1999). Generally, upwelling events fall together with low paleo SSTs besides OIE 4.2 (PS 5), where upwelling intensity is rather low (Fig. 7) but minimum temperature (13.5°C) is displayed. Additionally, at the beginning of OIE 5.5, temperature estimates are at a maximum (21.2°C, 128 kyrs), although planktic foraminifera assemblages reflect an upwelling event (PS 9) and foraminiferal temperature estimates reach maximum 8 kyrs later (Fig.6, Fig. 7). As for the overall trend, temperature estimates derived from planktic foraminfera and alkenones of GeoB 1710-3 show the same pattern, temperature records from GeoB 1028-5 are rather different (Fig. 9). No characteristic pattern is observed from planktic foraminiferal SSTs, probably due to differences in counting, as compared to the reference data set, planktic foraminfera >150µm were counted. Information from smaller species like *N. pachyderma* and *T. quinqueloba* could be lost or somewhat limited and therefore contribute to the small amplitude of paleoSST pattern of GeoB 1028-5.

In figures 7 and 9, differences in temperature range and timing are displayed. In general, paleo SSTs from planktic foraminifera fluctuate in a smaller range than generally expected e.g. from LGM to Holocene (CLIMAP, 1981). SSTs derived from the alkenone method clearly display glacial/interglacial temperature cycles, whereas the planktic foraminifer SSTs reflect a higher frequency variability not related to glacial/interglacial cyclicity. The differences in temperature ranges are probably due to different controls on both organism groups and methods (e.g. Sikes & Keigwin, 1994; Weaver et al., 1999): Coccolithophores are expected to live in the mixed layer within the photic zone, with maximum abundance in the upper water column above the thermocline (Sikes & Keigwin, 1994) in contrast to the planktic foraminiferal populations which live between 0 and 100 m (Ravelo & Fairbanks, 1992; Oberhänsli et al., 1992). Hence, as surface waters receive strong cooling or warming, planktic foraminifera, as a group, may generally display a somewhat smoothed signal in

comparision with the signal from *Emiliania huxleyi*, which is the predominant coccolithophorid species producing alkenons (Conte et al., 1995) and overwhelmingly dominant in the surface layers of this region (Giraudeau et al., 1993).

As, on the other hand, north of 25°S the main upwelling period is between March and November, and peaks around August (Shannon, 1985), the average warm season signal (Jan-Jun) derived from alkenones (Kirst et al., 1999) would not reflect the cooler SSTs that go along with enhanced upwelling. Coccolithophores bloom in mature stratified upwelled waters which are depleted in nutrients (Michell-Innes & Winter, 1987), therefore only a low diversity coccolithophore population is able to colonize the surface waters in the short time of upwelling relaxation (Giraudeau et al., 1993). According to Giraudeau et al. (1993), the Benguela region favors two main species whose habitats are mainly controlled by nutrients: *Emiliania huxleyi* dominates the surface and thermocline layer whereas *Gephyrocapsa oceanica* preferently inhabites the subsurface waters below the thermocline. Only the third species, *Coccolithus pelagicus,* which inhabits subsurface waters is rather temperature-controlled (Giraudeau et al., 1993). 100% of the *G. oceanica* and *C. pelagicus* population from samples of the outer shelf were malformed whereas none of the specimen in surface sediments of the Namibian coninental margin were (Giraudeau, 1993)]. As stated by Giraudeau et al. (1993) malformation in the Benguela region is not linked to nutrient deficiency but to transportation of subsurface water from the north, extending from 17° to 23°S. If this hypothesis is true, then the alkenone temperature signal from the Benguela region is 1) an average signal of a rather upwelling-free season and 2) probably a mixing from local and transported alkenone material.

Although planktic foraminiferal distribution in the Benguela system seems to be primarely controlled by sea-surface temperature (Giraudeau & Rogers, 1994), other ecological factors like enhanced biological production, changes in salinity or interspecies competions may contribute to some incoherency. As outlined by Mix et al. (1999), it is possible that transfer functions may still work in such situations as long as the statistical relationships between the various controls remain constant through time. Therefore paleotemperature reconstructions in this extraordinary oceanic setting must be carried out using various methods in order to determine their limitations and ranges of application as it was done for the equatorial Atlantic by Sikes & Keigwin (1994).

5.4 Paleoceanographic implications

Our data show periods of severe intensification of upwelling in the northern Benguela region during the past 245 kyrs (Fig. 13) and as documented from DSDP 532 data even further back into time. As documented by Little et al. (1997) PS events of the last 120 kyrs determined from GeoB 1711-4 (Fig. 3) and PG/PC12 fauna, coincide with high equatorial seasonality records (McIntyre et al., 1989). For the last 245 kyrs, PS events and equatorial seasonality records of RC24-16 (Fig. 1) are plotted in Fig. 14. It seems clear, that for this time period enhanced equatorial seasonality and increased upwelling activity of northern Benguela System are linked. There is an ongoing debate concerning the processes that control both regions (McIntyre et al., 1989; Oberhänsli, 1991; Diester-Haass et

al., 1992; Schmidt, 1992; Schneider et al., 1995; Jansen et al., 1996; Mix & Morey, 1996; Little et al., 1997; Hostetler & Mix, 1999).

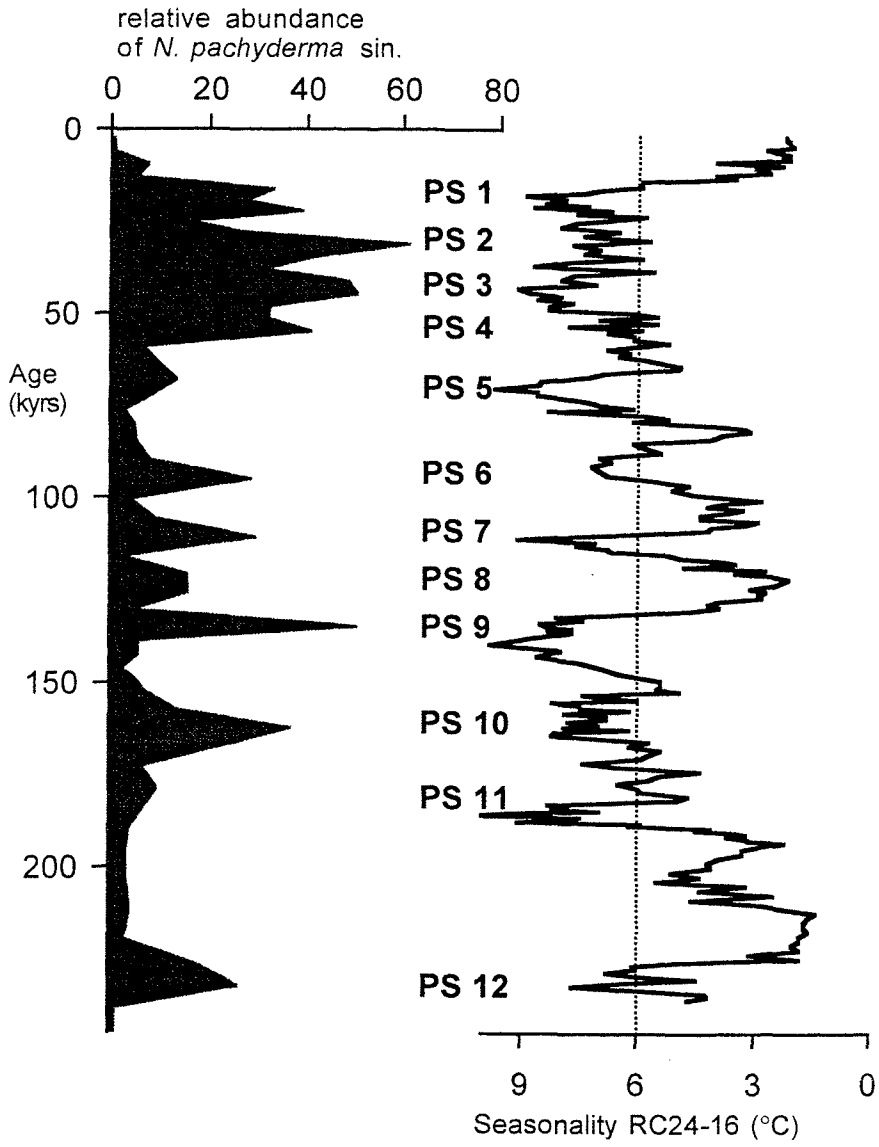

Fig. 14: Comparision of northern Benguela upwelling events indicated by *N. pachyderma* sin. maximal abundances (PS events) from GeoB 1710-3 (Cape Basin) with equatorial seasonality (°C) (data from McIntyre et al., 1989).

An intensification of the equatorward flow of the eastern boundary currents is documented by well-developed subpolar and transitional assemblages during LGM (CLIMAP, 1981) and further back into time (McIntyre et al., 1989). In contrast to the western equatorial Atlantic, the eastern part shows marked temporal variations in SSTs and foraminiferal assemblages with dominant periodicities centered on 23 kyr produced by orbitally forced variations in trade wind and monsoon-controlled divergence, and advection of heat from high southern latitudes (McIntyre et al., 1989).

Several possibilities exist to explain coupling of the Benguela upwelling region and the equatorial Atlantic in the past. The Benguela Current might have expanded further into the equatorial region (Pokras, 1987; Schneider, 1991), cooling the eastern equatorial waters during glacials. However,

reconstructions of northward shifts of the Angola-Benguela Front (ABF) show that its northernmost position was either 12°S during the late Quaternary according to Shi et al. (1997) or north of 9°S during OIS 4-3 after Jansen et al. (1996). Although for most of the past 220 kyr the ABF was north (Jansen et al., 1996) or at its present position (Schneider et al., 1995), the BC did not penetrate into the Gulf of Guinea (Jansen et al., 1996). Therefore waters from the BC do not seem to have been entrained into the equatorial region along the African coast. This is consistent with the results of Mix & Morey (1996).

Shannon et al. (1989) reported episodic input of Subantarctic water into the Benguela region and suggest that these cold intrusions may be important for the transfer of heat and water between the hemispheres. Therefore another possible way to cool eastern equatorial waters is through transport of colder waters from higher latitudes towards the equator, lowering SSTs in this region. If this occurs, higher abundances of cold water planktic foraminifera, like *N. pachyderma* sin., would be expected in the south compared to the north. The low relative abundances of *N. pachyderma* sin. in the southern Cape Basin and high relative abundances of this species in the northern part found by Little et al. (1997a,b) provide strong evidence against cold-water advection of sub-Antarctic waters from the Subtropical convergence.

It is therefore more likely that cool waters from enhanced coastal upwelling were transported equatorward. During austral winter (Jun-Sep) today, southeast trade winds are at their strongest, the current strength of the SEC is enhanced and SSTs in the Benguela region reach a minimum (see excellent summary on equatorial surface oceanography in McIntyre et al. (1989). According to Mix & Morey (1996), the BC is not strong enough at present to cause extreme cooling in the central equatorial Atlantic, but in glacial times, the cool waters from the Benguela System may have turned westward between 10° and 20°S (around 17°S, Diester-Haass et al., 1992) and finally entered the equatorial zone. Therefore equatorial seasonality could be enhanced through cold water input from the BUS via the BOC (Schneider et al., 1995). As we can show northern Benguela upwelling events taking place on a sub-Milankovitch scale, and lowering equatorial seasonality varies on a sub-Milankovitch scale, this scenario was not limited to a glacial-interglacial cycle as previously thought. We therefore favor the theory that at times of northern Benguela PS events equatorial upwelling also increased due to stronger zonal trade winds, which lowered equatorial SSTs, additionally amplified by the cool waters of the BS.

We believe that the BS contributes to the equatorial cooling not only during LGM (PS 1) as proposed by Mix et al. (1999) but also during twelve other time intervals during the past 245 kyrs. The BS should therefore be regarded as a crucial system influencing not only the equatorial region but also cross-equatorial teleconnections (Little et al., 1997b) between the South and North Atlantic.

6. Conclusions

(1) Changes in the areal extent of northern Benguela upwelling cells and the associated variations in upwelling intensity can be reconstructed from planktic foraminiferal assemblages. Characteristic downcore assemblages from the Cape Basin and Walvis Ridge can be best explained by a three factor model, with *N. pachyderma* sin. and to a minor extent *N. pachyderma* dex. representing the upwelling factor whereas the open-oceanic factor is monitored exclusively by *G. inflata*. The intermediate factor which documents the mixing of open-oceanic waters and newly upwelled waters, consists of *N. pachyderma* dex. and *G. bulloides*. From changes in significance of the factors downcore, we can reconstruct the extent of northern Benguela upwelling cells over the last 245 kyrs in great detail. We can clearly show that upwelling intensity is not linked to a glacial-interglacial cycle but rather fluctuates on a sub-Milankovitch scale.

(2) All investigated cores reflect intermediate or open-oceanic conditions for most of the past 245 kyrs but periodically document increased upwelling activity. GeoB 1710-3 reflects thirteen upwelling events (PS 1 to PS 13) during OIE 7.4, 6.5/6.4, 6.2, 5.53, OIE 5.4, 5.2, 4.2 and OIS 3 and 2. Most of them are also displayed in Walvis Ridge cores and therefore show intensification of the following cells: Namibia, Walvis Bay, and Lüderitz which probably merged together during the periods of most intense upwelling. During OIE 5.51 and 5.1 upwelling was lowest and open-oceanic waters invaded the Benguela System.

(3) This work demonstrates the necessity for a multiparameter approach for SST reconstructions in this region, as paleo SSTs from the alkenone method and transfer function of planktic foraminifera either vary significantly on the Walvis Ridge (GeoB 1028-5) or show a similar trend but different amplitude in the northern Cape Basin (GeoB 1710-3). This work provides some support for the hypothesis that temperature is upon the major control parameter that governs planktic foraminiferal distribution in the Benguela upwelling system, although care must be taken as not all factors and their impact on regional distribution patterns are known in detail.

7. Acknowledgments

We thank H. Oberhänsli who kindly provided planktic foraminifera counts and the stratigraphy of DSDP 532. We would like to acknowledge R. R. Schneider and S. Gerhardt for discussion, and R. Sieger for providing his software package PaleoToolBox/WinTransfer and his help with the database PANGAEA (www.pangaea.de). C. Devey kindly corrected the English. This research was funded by the Deutsche Forschungsgemeinschaft (Sonderforschungsbereich 261 at Bremen University, Contribution No. xxx).

Results from factor analysis (Appendix 1) presented in this paper are archived in the PANGAEA database at the Alfred Wegener Institute for Polar and Marine Research (http://www.pangaea.de/home/avolbers/).

References:

Backhaus, K., Erichson, B., Plinke, W., Schuchard-Ficher, C., and R. Weiber (Ed.), *Multivariate Analysemethoden*, vol. 5., 418 pp., Springer, Berlin, Heidelberg, New York, London, Paris, Tokyo, 1989.

Bé, A. W. H., and D. S. Tolderlund, Distribution and ecology of living planktonic foraminifera in surface waters of the Atlantic and Indian Oceans, in *The micropaleontology of oceans*, edited by D. M. Funnell, and W. R. Riedel, pp. 105-149, Cambridge University Press, Cambridge, 1971.

Bickert, T., *Rekonstruktion der spätquartären Bodenwasserzirkulation im östlichen Südatlantik über stabile Isotope benthischer Foraminiferen.* Berichte aus dem Fachbereich Geowissenschaften der Universität Bremen, vol. 27, 205 pp., Bremen, 1992.

Bickert, T., and G. Wefer, Late Quaternary deep water circulation in the South Atlantic: Reconstruction from carbonate dissolution and benthic stable isotopes, in *The South Atlantic: Present and past circulation*, edited by G. Wefer et al., pp. 599-620, Springer, Berlin, Heidelberg, 1996.

Bickert, T., and G. Wefer, South Atlantic and benthic foraminifer $\delta^{13}C$-deviations: Implications for reconstructing the Late Quaternary deep-water circulation, *Deep-Sea Res., 46,* 437-452, 1999.

Chen, M.-T., and W. L. Prell, Faunal distribution patterns of planktonic foraminifers in surface sediments of the low-latitude Pacific, *Palaeogeogr., Palaeoclimatol., Palaeoecol., 137,* 55-77, 1998.

CLIMAP Project Members, *Seasonal reconstructions of the Earth's surface at the last glacial maximum. Geol. Soc. Am. Map and Chart Ser.,* MC-36, 18 pp., Boulder, Colorado, 1981.

CLIMAP Project Members, The last interglacial ocean, *Quat. Res., 21*, 123-224, 1984.

Conte, M. H., Thompson, A., Eglinton, G., Green, J. C, Lipid biomarker diversity in the coccolithophorid *Emiliania huxleyi* (Prymnesiophyceae) and the related species *Geophyrocapsya oceanica. J. Phycol., 31*, 272-281, 1995.

Dingle, R. V., and G. Nelson, Sea-bottom temperature, salinity and dissolved oxygen on the continental margin off South-Western Africa. *S. Afr. J. Mar. Sci., 13*, 33-49, 1993.

Dieser-Haass, L., Late Quaternary sedimentation on the eastern Walvis Ridge, SE Atlantic (HPC 532 and 4 piston cores), *Mar. Geol., 65*, 145-189, 1985.

Dieser-Haass, L., Meyers, P. A., and P. Rothe, the Benguela Current and associated upwelling on the southwest African margin: a synthesis of the Neogene-Quaternary sedimentary record at DSDP sites 362 and 532 in *Upwelling Systems: Evolution since the early Miocene,* edited by C. P. Summerhayes et al., pp. 331-342, Geol. Soc. Spec. Publ., vol. 64, Geological Society London,1992.

Dowsett, H. J., The development of a long-range foraminifer transfer function and application to Late Pleistocene north Atlantic climatic extremes, *Paleoceanography 6(2),* 259-273, 1991.

Giraudeau, J., Planktonic foraminiferal assemblages in surface sediments from the southwest African continental margin, *Mar. Geol., 110*, 47-62, 1993.

Griaudeau, J., Monteiro, M. S., and K. Nikodemus, Distribution and malformation of living coccolithophores in the northern Benguela upwelling system off Namibia, *Mar. Micropal.,* 22: 93-110, 1993.

Giraudeau, J., and J. Rogers, Phytoplankton biomass and sea-surface temperature estimates from sea-bed distribution of nannofossils and planktonic foraminifera in the Benguela upwelling system. *Micropaleont., 40(3),* 275-285, 1994.

Hart, T. J., and R. I. Currie, The Benguela Current, *Discovery Rep., 31*, pp. 123-298, 1960.

Hemleben, C., Spindler, M., and O. R. Anderson (Ed.), *Modern planktionic foraminifera.* Springer, New York, pp. 363, 1989.

Hostetler, S. W., and A. C. Mix, Reassessment of ice-age cooling of the tropical ocean and atmosphere, *Nature, 399*, 673-676, 1999.

Imbrie, J., and N. G. Kipp, A new micropaleontological method for quantitative paleoclimatology: Application to a late Pleistocene Caribbean core, in *The late Cenozoic glacial ages*, edited by K. K. Turekian, pp. 71-181, Yale Univ. Press, New Haven, 1971.

Ivanova, E.M., Conan, S.M.-H., Peeters, F.J.C. & Troelstra, S.R. (1999). Living *Neogloboquadrina pachyderma* sin and its distribution in the sediments from Oman and Somalia upwelling areas. *Marine Micropaleontolgy,* 36, 91-107.

Jansen, J. H. F., Ufkes, E., and R. R. Schneider, Late Quaternary movements of the Angola-Benguela-Front, SE Atlantic, and implications for advection in the equatorial ocean, in *The South Atlantic: present and past circulation,* edited by G. Wefer et al., pp. 553-575, Springer, Berlin, 1996.

Kirst, G. J., Schneider, R. R., Müller, P. J., von Storch, I., and G. Wefer, Late Quaternary temperature variability in the Benguela Current system derived from alkenones. *Quaternary Res., 52,* 92-103, 1999.

Kohfeld, K. E., Fairbanks, R. G., Smith, S. L., and I. D. Walsh, *Neogloboquadrina pachyderma* (sinistral coiling) as paleoceanographic tracers in polar oceans. Evidence from Northeast Water

Polynya plankton tows, sediment traps, and surface sediments, *Paleoceanography, 11(6),* 679-699, 1996.

Klovan, J. E., and Imbrie, J., An algorithm and FORTRAN IV Program for large scale Q-mode factor analysis and calculation of factor scores. *Math. Geol., 3*: 61-77, 1971.

Levitus, S., and Boyer, T. (Ed.), *World Ocean Atlans*, vol. 4, Temperature. NOAA Atlas NESDIS 4, U.S. Govt. Printing Office, 1994.

Little, M. G., Schneider, R. R., Kroon, D., Price, B., Summerhayes, C. P., and M. Segl, Trade Wind forcing of upwelling, seasonality, and Heinrich events as a response to sub-Milankovitch climate variability. *Paleoceanography, 12(4),* 568-576, 1997a.

Little, M. G., Schneider, R. R., Kroon, D., Price, B., Bickert, T., and G. Wefer, Rapid palaeoceanographic changes in the Benguela Upwelling System for the last 160,000 years as indicated by abundances of planktonic foraminifera. *Palaeogeogr., Palaeoclimat., Palaeoecol., 130,* 135-161, 1997b.

Lohmann, G. P., Increasing seasonal upwelling in the subtropical South Atlantic over the past 700,000 yr: Evidence from deep-living planktonic foraminifera, *Mar. Micropal., 19,* 1-12, 1992.

Lutjeharms, J. R. E., and J. M. Meeuwis, The extent and variability of South-East Atlantic upwelling, *S. Afr. J. mar. Sci., 5,* 51-62, 1987.

Lutjeharms, J. R. E., and P. L. Stockton, Kinematics of the upwelling front off Southern Africa, *S. Afr. J. mar. Sci., 5,* 35-49, 1987.

Lutjeharms, J. R. E., Shillington, F. A., and R. Duncombe, Observations of extreme upwelling filaments in the Southeast Atlantic Ocean, *Science, 253,* 774-776, 1991.

McIntyre, A., Ruddiman, W. F., Karlin, K., and A. C. Mix, Surface water response of the equatorial Atlantic Ocean to orbital forcing, *Paleoceanography, 4,* 19-55, 1989.

Michell-Innes, B. A., and A. Winter, Coccolithophores: a major phytoplanktion component in mature upwelled waters off the Cape Peninsula, South Africa in March, 1983, *Mar. Biol., 95,* 25-30, 1987.

Mix, A. C., Pleistocene Paleoproductivity: Evidence from organic carbon and foraminiferal species, in *Productivity of the ocean: present and past,* edited by W. H. Berger et al., pp. 313-336, John Wiley & Sons, Chichester, New York, Brisbane, Toronto, Singapore, 1989.

Mix, A. C., and A. E. Morey, Climate feedback and Pleistocene variations in the Atlantic South Equatorial Current, in *The South Atlantic: Present and past circulation,* edited by G. Wefer et al., pp. 503-525, Springer, Berlin Heidelberg, 1996.

Mix, A. C., Morey, A. E., Pisias, N. G., and S. W. Hostetler, Foraminiferal faunal estimates of paleotemperature: Circumventing the no-analog problem yields cool ice age tropics, *Paleoceanography, 14(3),* 350-359, 1999.

Molfino, B., Kipp, N. G., and J. J. Morley, Comparison of foraminiferal, coccolithophorid, and radiolarian paleotemperature equations: assemblage coherency and estimate concordancy, *Quaternary Res., 17,* 279-313, 1982.

Müller, P. J., Cepek, M., Ruhland, G., and R. R. Schneider, Alkenone and coccolithophorid species changes in late Quaternary sediments from the Walvis Ridge: Implications for the alkenone paleotemperature method, *Palaeogeogr., Palaeoclimat., Palaeoecol., 135,* 71-96, 1997.

Niebler, H.-S. (Ed.), *Rekonstruktion von Paläo-Umweltparametern anhand von stabilen Isotopen und Faunen-Vergesellschaftungen planktischer Foraminiferen im Südatlantik. Berichte zur Polarforschung,* vol. 167, 198 pp., 1995.

Niebler, H.-S., and R. Gersonde, A planktic foraminiferal transfer function for the southern South Atlantic Ocean, *Marine Micropaleontology, 34,* 213-234,1998.

Oberhänsli, H., Upwelling signals at the Northeastern Walvis Ridge during the past 500,000 years, *Paleoceanography, 6(1),* 53-71, 1991.

Oberhänsli, H., Bénier, C., Meinecke, G., Schmidt, H., Schneider, R., and G. Wefer, Planktonic foraminifers as tracers of ocean currents in the eastern South Atlantic, *Paleoceanography, 7(5),* 607-632, 1992.

Oppo, D. W., and Y. Rosenthal, Cd/Ca changes in a deep Cape Basin core over the past 730,000 years: Response of circumpolar deepwater variability to northern hemisphere ice sheet melting?, *Paleoceanography, 9(5),* 661-675, 1994.

Peterson, L.C. (Rapporteuer), Abbott, M. R., Anderson, D. M., Caulet, J.-P., Conté, M. H., Emeis, K.-C., Kemp, A. E. S., and C. P. Summerhayes, Group Report: How do Upwelling Systems vary through time? in *Upwelling in the ocean. Modern processes and ancient records*, edited by C. P. Summerhayes et al., pp 285-311, Wiley, Chichester, New York, Brisbane, Toronto, Singapore, 1995.

Pflaumann, U., Dupra, J., Pujol, C., and L. Labeyrie, SIMMAX: A modern analog technique to deduce Atlantic sea surface temperatures from planktonic foraminifera in deep-sea sediments, *Paleoceanography, 11,* 15-35, 1996.

Pokras, E. M., Diatom record of late Quaternary climatic change in the eastern equatorial atlantic and tropical africa, *Paleoceanography, 2(3),* 273-286, 1987.

Ravelo, A. C., and R. G. Fairbanks, Oxygen isotopic composition of multiple species of planktonic

foraminifera: recorders of the modern photic zone temperature gradient, *Paleoceanography, 7(6)*, 815-831, 1992.

Sarnthein, M., Winn, K., Duplessy, J.-C., and M. R. Fontugne, Global variations of surface ocean productivity in low and mid latitudes: Influence on CO_2 reservoirs of the deep ocean and atmosphere during the last 21,000 years, *Paleoceanography, 3(3)*, 361-399, 1988.

Schmidt, H. (Ed.), *Der Benguela-Strom im Bereich des Walfisch-Rückens im Spätquartär, Berichte aus dem Fachbereich Geowissenschaften der Universität Bremen*, vol. 28, 172 pp, Bremen, 1992.

Schmiedl, G., Mackensen, A., and P. J. Müller, Recent benthic foraminifera from from the eastern South Atlantic Ocean: Dependence on food supply and water masses, *Marine Micropalenotology, 32*, 249-287, 1997.

Schneider, R. R. (Ed.), *Spätquartäre Produktivitätsänderungen im östlichen Angola-Becken: Reaktion auf Variationen im Passat-Monsun-Windsystem und in der Advektion des Benguela-Küstenstrom. Berichte aus dem Fachbereich Geowissenschaften der Universität Bremen*, vol. 21, 198 pp., Bremen, 1991.

Schneider, R. R., Müller, P. J, and G. Ruhland, Late Quaternary surface circulation in the east equatorial South Atlantic: Evidence from alkenone sea surface temperatures. *Paleoceanography, 10*, 197-219, 1995.

Schneider, R. R., Müller P. J., Ruhland, G., Meinecke, G., Schmidt, H., and G. Wefer, Late Quaternary surface temperatures and productivity in the east-equatorial South Atlantic: Response to changes in trade monsoon wind forcing and surface water advection, in *The South Atlantic: Present and Past Circulation,* edited by G. Wefer et al., pp. 527-551, Springer, Berlin, 1996.

Schulz, H. D., Beese, D., Breitzke, L., Brück, B., Brügger, B., Dahmke, A., Dehning, D., Diekampf, V., Donner, B., Ehrhardt, I., Gerlach, H., Giese, M., Glud, R., Gumprecht, R., Gundersen, J., Henning, R., Hinrichs, S., Petermann, H., Richter, M., Sagemann, J., Schmidt, W., Schneider, R., Scholz, M., Segl, M., Werner, U., and M. Zabel (Ed.), *Bericht und erste Ergebnisse über die Meteor-Fahrt M20/2. Abidjan - Dakar, 27.12.1991-3.2.1992. Berichte aus dem Fachbereich Geowissenschaften der Universität Bremen,* vol. 25, 173 pp., Bremen, 1992.

Shannon, L. V., The Benguela ecosystem part I. Evolution of the Benguela. Physical features and processes, *Oceanogr. Mar. Biol. Ann. Rev., 23*, 105-182,1985.

Shannon, L. V., Lutjeharms, J. R. E., and J. J. Agenbag, Episodic input of Subantarctic water into the Benguela region, *S. Afr. J. of Sci., 85*, 317-322, 1989.

Shi, N., Dupont, L. M., Beug, H.-J., and R. Schneider, Vegetation and climate history of SW Africa: a marine palynological record of the last 300,000 years, *Vegetation History and Archaeobotany, 6,* 117-131, 1997.

Shillington, F. A., Peterson, W. T., Hutchings, L., Probyn, T. A., Waldron, H. N., and J. J. Agenrag, A cool upwelling filament off Namibia, southwest Africa: preliminary measurements of physical and biological features, *Deep-Sea Res., 37*, 1753-1772, 1990.

Sikes, E. L., and L. D. Keigwin, Equatorial Atlantic sea surface temperature for the last 30 kyr: A comparison of Uk'37, $\delta^{18}O$ and foraminiferal assemblage temperature estimates, *Paleoceanography, 9(1)*, 31-45, 1994.

Summerhayes, C. P., Kroon, D., Rosell-Melé, A., Jordan, R. W., Schrader, H.-J., Hearn, R., Villanueva, J., Grimalt, J. O., and G. Eolington, Variability in the Benguela Current upwelling system over the past 70,000 years, *Prog. Oceanog., 35*, 207-251, 1995.

Stramma, L., and R. G. Peterson, Geostrophic transport in the Benguela Current Region, *J. of Phys. Oceanogr., 19*, 1440-1448, 1989.

Thackeray, J. F., and Herbert, R. S., Environmental indices from planktonic foraminifera in Late Holocene sediments off Walvis Bay, *S. Afr. J. of Sci., 87*, 611-613, 1991.

Thiede, J., Distribution of foraminifera in surface waters of a coastal upwelling area, *Nature, 253*, 712-714, 1975.

Ufkes, E., and W.-J. Zachariasse, Origion of coiling differences in living neogloboquadrinids in the Walvis Bay region, off Namibia, southwest Africa, *Micropaleont., 39 (3)*, 283-287, 1993.

Ufkes, E., Jansen, J.H.F. & Schneider, R.R. (2000). Anomalous occurrences of Neogloboquadrina pachyderma (left) in a 420-ky upwelling record from Walvis Ridge (SE Atlantic). *Marine Micropaleontology,* 40, 23-42.

Volbers, A.N.A. & R. Henrich (submitted). Late Quaternary variations in calcium carbonate preservation of deep-sea sediments in the northern Cape Basin: results from a multiproxy approach. *Marine Geology*, Special edition on Neogene and Quaternary evolution of the Benguela system.

Watkins, J. M., and A. C. Mix, Testing the effects of tropical temperature, productivity, and mixed-layer depth on foraminiferal transfer functions, *Paleoceanography, 13(1),* 96-105, 1998.

Weaver, P. P. E., Chapman, M. R., Eglinton, G., Zhao, M., Rutledge, D., and G. Read, Combined coccolith, foraminiferal, and biomarker reconstruction of paleoceanographic conditions over the past 120 kyr in the northern North Atlantic (59°N, 23°W), *Paleoceanography, 14(3)*, 336-349.

Part III *Summary and conclusions*

1. Summary

As calcareous deep-sea carbonates act as a large and reactive reservoir for CO_2, changes in temporal and spatial distribution in calcium carbonate accumulation and preservation pattern are important input parameters for models which try to explain past changes in atmospheric pCO_2 and to predict future climate changes. This PhD thesis concentrates on the usage of planktic foraminifera as paleoceanographic indicators. Planktic foraminifera are among the most important producers of calcium carbonate in the world`s ocean. As determined from South Atlantic surface sediments in this study, on average 40% of the total $CaCO_3$ on the sea-floor consists of planktic foraminiferal carbonate. This is a minimum contribution as the fraction <63 µm, (juvenile planktic foraminifera) was excluded. Planktic foraminiferal carbonate is the main constituent of the calcareous fraction in the equatorial Atlantic Ocean and on parts of deep ocean ridges, such as the Mid-Atlantic Ridge or the Walvis Ridge (>50%). In contrast, its contribution to the calcareous fraction of the sediments from the South African continental margin is less than 25%, and coccolithophores dominate the sediments of the coastal upwelling regions (Baumann et al., in prep). This observation is in accordance with the findings from manuscript 4 which show that the accumulation of planktic foraminifera in the Benguela region (determined via the planktic foraminiferal number per g sediment) responds to changes in upwelling intensity and is generally lower during periods of increased coastal upwelling.

The degree of upwelling in the Benguela System was assumed to be monitored by the abundance of *Neogloboquadrina pachyderma* sin. (Oberhänsli, 1991; Schmidt, 1992; Little et al., 1997; Ufkes et al., 2000). Investigations of surface sediments suggested, that characteristic planktic foraminiferal assemblages reflect the hydrographic conditions in this regions, e.g. *N. pachyderma* sin. was found almost exclusively in surface sediments beneath the modern Benguela coastal upwelling cells, whereas the more open-oceanic species *Globorotalia inflata* seems to reflect the outer limits of the Benguela upwelling system (Giraudeau and Rogers, 1994). To finally reconstruct the areal extent of northern Benguela upwelling cells during the past 245 kyrs, the Benguela factor model was applied to seven sediment cores from the northern Cape Basin and Walvis Ridge. As demonstrated in manuscript 4, upwelling intensity was increased during OIE 7.4, 6.5/6.4, 6.2, 5.53, 5.4, 5.2, 4.2 and during OIS 3 and 2 compared to today.

Besides variations in the strength of the biologic pump, changes in the $CaCO_3$ cycle are expected to influence the CO_2 content of our atmosphere. This thesis evaluates the effects of calcium carbonate dissolution on deep-sea sediments from various oceanographic regions of the South Atlantic Ocean. But what is the ideal proxy to reliably determine deep-sea calcium carbonate dissolution in all the different hydrographic regimes of the South Atlantic? As emphazised by Diester-Haass (1976, 1977, 1978, 1985) the most commonly used calcium carbonate dissolution

proxies do also reflect changes in productivity. The purpose of manuscript 1, which focusses on a sediment core from the Benguela region, was to compare the results of all these conventionel dissolution proxies with one another and to verify them by a new dissolution proxy, the BDX'. The BDX' describes the ultrastructural preservation state of *Globigerina bulloides* and was established as the ideal proxy to determine the position of the calcite lysoclines in all the different South Atlantic deep ocean basin and continental environments.

As postulated by Berger (1968) and Berger and Wefer (1996), the calcite lysocline in western South Atlantic basins and the Cape Basin coincides roughly with the NADW/AABW transition where a rapid decrease in the $[CO_3^{2-}]_{bottom\ water}$ was observed. However, the results of manuscript 2 show that significant calcium carbonate dissolution occurs in deep-sea sediments from above the calcite saturation depth (the depth, at which $[CO_3^{2-}]_{bottom\ water} = [CO_3^{2-}]_{calcite\ saturation}$; „hydrographic lysocline") and have important implications on the use of the calcite lysocline as a water mass proxy. Until recently, the importance of respiratory dissolution in the sediments due to organic matter oxidation has been underestimated when calculating the global calcium carbonate budget. Calcium carbonate accumulation in the South Atlantic is therefore not solely driven by the production of calcium carbonate, and the $[CO_3^{2-}]_{bottom\ water}$, but also by respiratory dissolution. So far, attempts to quantify these local effects are in the range of 20% to 90% redissolution of the calcium carbonate flux to the sea floor (Emerson and Archer, 1990; Jahnke et al. (1994); Pfeifer et al., in prep.).

As pointed out by Emerson and Bender (1981) models used to explain the relationship between calcite saturation in the oceans and the preservation of calcareous sediments have not considered the effect of metabolic CO_2 generated at the sediment water interface. The position of the modern sedimentary calcite lysocline therefore monitors the level of equal preservation, regardless the different impact of the processes driving dissolution in the particular region. The exact determination of the modern lysocline depth (manuscript 2) in relation to its position during the LGM (manuscript 3) is urgently needed because changes in the position of the lysocline are important input parameters for models which seek to explain the 1/3 lowering of the atmospheric CO_2 during the LGM. The position of the sedimentary calcite lysocline during LGM was on average several hundred meters shallower compared to its modern depth level. In addition, as the position of the calcite lysocline was similar in the western and eastern South Atlantic basin, the access of Southern Component Water (SCW) to the eastern South Atlantic Basin does not seem to have been limited by the Walvis Ridge. The goal of this effort is to outline the basic spreading pattern of deep ocean water masses and to help to understand the role of ocean chemical redistributions in glacial/interglacial atmospheric CO_2 cycles. In this sense, our data support the theory of reduced dominance of NADW in the Atlantic Ocean during the LGM.

2. Conclusions and outlook

As shown by this thesis, planktic foraminifera are among the most important constituents of South Atlantic deep-sea sediments and have proven to be useful organisms for paleoceanographic studies.

As planktic foraminifera reflect surface water conditions well, they yield important proxy parameters to reconstruct ocean history. Characteristic species assemblages could used to determine the degree of paleo-upwelling in coastal upwelling regions. Results from the Benguela region demonstrate, that upwelling intensity does not vary on a glacial/interglacial scale as previously anticipated but seem to respond to the strength of the trade winds during the late Quaternary. In this sense, micropaleontological investigations of planktic foraminifera as carried out in this study, can significantly increase our understanding of ocean circulation in relation to atmospheric circulation pattern.

According to the high proportion of planktic foraminiferal carbonate on the total $CaCO_3$ of deep-sea sediments, planktic foraminiferal dissolution proxies are expected to reflect the position of the calcite lysocline well. As demonstrated in this study, the BDX' appears to reflect the $[CO_3^{2-}]$ in the pore waters of deep-sea sediments and could be used throughout the South Atlantic Ocean because of the high relative abundance of *Globigerina bulloides*. As *Globigerina bulloides* is an abundant species in the global ocean, the BDX' might also be applied on sediments from the Pacific or Indian Ocean. In addition, a similar index could be devoloped for other species, such as *Globigerinoides sacculifer*.

The importance of respiratory or supralysocline dissolution in deep-sea sediments seems to have been underestimated for a long time. As pointed out by Lohmann (pers. communication), the decoupling of the hydrographic and sedimentary calcite lysocline is predicted locally but results from sediments are still scarce. In this regard, this study provides sedimentological evidence of calcium carbonate dissolution above the hydrographic lysocline.

The purpose of further studies is to combine geochemical approaches and sedimentological investigations in order to determine the impact of respiratory dissolution on deep-sea sediments. Since the development and the improvement of in-situ (microsensor) techniques during the past 20 years, high resolution concentration profiles can be obtained without sampling artifacts. Results from model approaches which calculate organic matter decay and redissolution of the calcite flux to the sediment (e.g. Peiffer et al, in prep.) could therefore be directly compared to results from calcium carbonate dissolution proxies, such as the BDX'. Attributing to this idea, these studies should be carried out along the continental margins, where high amounts of organic material are supplied to the deep-sea sediments, to get information of the conditions in the sediment and its effect on calcareous tests.

3. Epilogue

Although the impact of all natural factors and processes on atmospheric CO_2 are not yet fully understood, the atmosphere and the oceans are considered to be in approximately steady state with respect to CO_2 exchange, when the effect of anthropogenic addition of CO_2 to the atmosphere are excluded (Sigman and Boyle, 2000). However, from 1860 till now a temperature increase of 0.6°C (+/-0.2°C) and a sea-level increase between 0.1 to 0.2 m occured and the effects of additional anthropogenic CO_2 will be highly relevant for our climate of the next decades. To stabilize the atmospheric CO_2 content, and to keep climate changes and their effects to a minimum, there is the idea to fix more CO_2 in the organic life cycle, suggesting that the natural balance of CO_2 uptake in some regions of the oceans balanced by CO_2 release in others, could be moved towards increased uptake of CO_2 by the oceans. In fact, there seems to be evidence that modest sequestration of atmospheric CO_2 is in principle possible by artificial addition of iron to the Southern Ocean where photosynthesis by marine phytoplankton and the associated uptake of carbon is thought to be currently limited by the availability of iron (Watson et al., 2000). Unfortunately, as emphazised by the authors, there is little known about the period and geographical extent over which sequestration would be effective. If political negotiations, such as the Kyoto protocol (1997), fail to limit further emissions of anthropogenic greenhous gases, study of this problem might be the most important task of the 21st century.

Auch das größte Problem dieser Welt hätte gelöst werden können, solange es noch klein war
Laotse

4. References

Baumann, K-H., B. Böckel, B. Donner, S. Gerhardt, R. Henrich, A. Vink, A. Volbers, H. Willems, K. Zonneveld: Contribution of calcareous plankton groups to the carbonate budget of South Atlantic surface sediments (in prep.).

Berger, W.H., 1968. Planktonic foraminifera: selective solution and paleoclimatic interpretation, Deep-Sea Res. 15, 31-43.

Berger, W.H. and Wefer, G., 1996. Central themes of South Atlantic circulation, in The South Atlantic: Present and past circulation, edited by Wefer, G., Berger, W.H., Siedler, G., and Webb, D.J, 1-11, Springer, Berlin, Heidelberg, New York.

Diester-Haasss, L., 1976. Quaternary accumulation rates of biogenous and terrigenous components on the East Atlantic continental slope off NW Africa, Mar. Geol. 21, 1-14.

Diester-Haass, L., 1977. Radiolarian/planktonic foraminiferal ratios in a coastal upwelling region. J. of Foraminiferal Res. 7 (1), 26-33.

Diester-Haass, L., 1978. Sediments as an indicator of upwelling. In: Boje, R., Tomczak, M. (Eds.), Upwelling ecosystems. Springer, Berlin, 261-281.

Diester-Haass, L., 1985. Late Quaternary sedimentation on the eastern Walvis Ridge, SE Atlantic (HPC 532 and 4 pisten cores). Mar. Geol. 65, 145-189.

Emerson, S. and Archer, E., 1990. Calcium carbonate preservation in the ocean. Phil Trans R Soc Lond A 331, 29-40.

Emerson, S. and Bender, M., 1981. Carbon fluxes at the sediment-water interface of the deep-sea: calcium carbonate preservation, J. Mar. Res. 39, 139-162.

Giraudeau, J. and Rogers, J., 1994. Phytoplankton biomass and sea-surface temperature estimates from sea-bed distribution of nannofossils and planktonic foraminifera in the Benguela upwelling system. Micropaleontology 40(3), 275-285.

Jahnke, R.A., Craven, D.B., and Gaillard, J.-F., 1994. The influence of oraganic matter diagenesis on $CaCO_3$ dissolution at the deep-sea floor, Geochimica et Cosmochimica Acta 58 (11), 2799-2809.

Kyoto Protocol to the United Nations framework convention on climate change (10.12.1997), available from: www.isi.fhg.de/e/publikation/pdf/kyoto.pdf

Little, M.G., Schneider, R.R., Kroon, D., Price, B., Bickert, T., and Wefer, G., 1997. Rapid palaeoceanographic changes in the Benguela Upwelling System for the last 160,000 years as indicated by abundances of planktonic foraminifera. Palaeogeogr., Palaeoclimat., Palaeoecol.130, 135-161.

Oberhänsli, H., 1991. Upwelling signals at the Northeastern Walvis Ridge during the past 500,000 years. Paleoceanography, 6(1), 53-71.

Pfeifer, K., Hensen, C., Adler, M., Wenzhöfer, F., Weber, B., and Schulz, H.D., in prep. Modeling of subsurface calcite dissolution regarding respiration and reoxidation processes of marine sediments in the equatorial upwelling off Gabon.

Schmidt, H., 1992. Der Benguela-Strom im Bereich des Walfisch-Rückens im Spätquartär, Berichte aus dem Fachbereich Geowissenschaften der Universität Bremen, vol. 28, pp. 172.

Sigman, D.M, Boyle, E.A., 2000. Glacial/interglacial variations in atmospheric carbon dioxide. Nature 407, 859-869.

Ufkes, E., Jansen, J.H.F., and Schneider, R.R., 2000. Anomalous occurrences of *Neogloboquadrina pachyderma* (left) in a 420-ky upwelling record from Walvis Ridge (SE Atlantic). Marine Micropaleontology 40, 23-42.

Watson, A.J., Bakker, D.C.E., Ridgwell, A.J., Boyd, P.W., and Law, C.S., 2000. Effect of iron supply on Southern Ocean CO_2 uptake and implications for glacial atmospheric CO_2. Nature 407, 730-733.

Part IV *Appendix*

1. Presentation at national and international conferences

A. Volbers & Henrich, R (1999): Quantitative Erfassung spätquartärer planktischer Foraminiferen-Gemeinschaften unter besonderer Berücksichtigung ihres Erhaltungszustandes in den östlichen südatlantischen Tiefseebecken. 2. Geologica, Stuttgart.

A. Volbers, R. Henrich & H.-S. Niebler (1999): Quantitative Erfassung spätquartärer planktischer Foraminiferen-Gemeinschaften und Untersuchungen zur Karbonatlösung an einem Schwerelotkern (GeoB 1710-3) aus dem östlichen Südatlantik. 14. Sedimentologentreffen, Terra Nostra 4/999, S. 276, Bremen.

A. Volbers, R. Henrich & H.-S. Niebler (1999): Examination of late Quaternary planktic foraminiferal assemblages and investigations of carbonate preservation in the sediment core GeoB 1710-3 from the eastern South Atlantic. Workshop on Paleoceanography, Bern, Schweiz.

A. Volbers, S. Gerhardt & R. Henrich (2000): Shell preservation of *Globigerina bulloides* (planktic foraminifera) and *Limacina inflata* (Pteropoda): new proxies for carbonate corrosiveness of water masses. EGS Millenium Conference on Earth, Planetary & Solar Systems Sciences, Nizza, Frankreich. News letter European Geophysical Society, Nr. 74.

A. Volbers, H.-S. Niebler, J. Giraudeau, H. Schmidt & R. Henrich (2000): Paleoceanographic changes in the northern Benguela upwelling system over the last 245 kyrs as derived from planktic foraminifera assemblages. EGS Millenium Conference on Earth, Planetary & Solar Systems Sciences, Nizza, Frankreich. News letter European Geophysical Society, Nr. 74.

A. Volbers, H.-S. Niebler, J. Giraudeau, H. Schmidt & R. Henrich (2000): Paleoceanographic changes in the northern Benguela upwelling system over the last 245 kyrs as derived from planktic foraminifera assemblages. Workshop on „Quaternary evolution of the Benguela coastal upwelling systems-responses to local and global climate changes", Carcans, Frankreich.

A. Volbers, S. Gerhardt & R. Henrich (2000): Shell preservation of *Globigerina bulloides* (planktic foraminifera) and *Limacina inflata* (Pteropoda): new proxies for carbonate corrosiveness of water masses. 15. Sedimentologentreffen, Leoben, Schweiz.

A. Volbers, S. Gerhardt & R. Henrich (2000): Shell preservation of *Globigerina bulloides* (planktic foraminifera) and *Limacina inflata* (Pteropoda): new proxies for carbonate corrosiveness of water masses. 20. Regional Meeting of Sedimentology (IAS), Dublin, Irland.

R. Henrich, Baumann, K-H., Böckel, B.,S. Gerhardt, Kinkel, H. & A. Volbers (2001): Pelagische Karbonatproduktion und Erhaltung im Südatlantik. 16. Sedimentologentreffen, Jena.

2. Danksagung

Ich danke Herrn Prof. Dr. Henrich für die Vergabe dieser Arbeit und deren Betreuung über die letzten drei Jahre. Herrn Prof. Dr. Fütterer danke ich für die freundliche Übernahme des Zweitgutachtens.

Besonders möchte ich meiner Arbeitsgruppe „Sedimentologie/Paläontologie" der Uni Bremen und dem SFB 261 für das gute Betriebsklima danken. Ich danke Herrn Dr. Karl-Heinz Baumann für die freundliche Unterweisung am REM und Herrn Michael Frenz für die Bereitstellung von aufbereitetem LGM-Probenmaterial und die Benutzung unpublizierter Grunddaten für die Berechung von planktischen Foraminiferen-Karbonat. Frau Helga Heilmann und Frau Renate Henning danke ich für die stets hervorragende Organisation in der Materialbeschaffung und für die Hilfestellung bei den kleinen alltäglichen Problemen. Ines Reenen danke ich für das zuverlässige Picken von planktischen Foraminiferen. Weiterhin danke ich Oliver Esper, Sabine Gerhardt, Matthias Gröger, René Höppner, Dieter Kaiser und Michael Streng sowohl für die ausgiebigen fachlichen Diskussionen als auch für gute Freundschaft.

Insbesondere möchte ich mich bei Herrn Prof. Dr. Gerold Wefer und seiner Arbeitsgruppe für die Bereitstellung von Oberflächenmaterial aus dem Südatlantik bedanken. Frau Dr. Barbara Donner danke ich für die Abgleichung der Foraminiferen-Nomenklatur und für Foraminiferen-Material aus Fallenproben. Bei Herrn Dr. Torsten Bickert, Herrn Dr. Peter Müller und Herrn Dr. Tom Wagner bedanke ich mich für die Freigabe unpublizierter Daten. Herrn Dr. Hans-Stefan Niebler danke ich für die gute Zusammenarbeit bei unserem gemeinsamen Paper. Herr Dr. Rainer Sieger war stets mein Retter in der Not, wenn es um Pangea oder Mac-Rechner ging. Das gleiche gilt für Herrn Prof. Dr. Collin Devey bezüglich der Englischkorrektur von drei Manuskripten, vielen Dank dafür! Mein ganz besonderer Dank geht auch an Herrn Dr. Pat Lohmann für sein äußerst reges Interesse an meinen Manuskripten.

Sehr herzlich möchte ich mich auch bei meiner Familie bedanken, die mich während meines gesamten Studiums immer unterstützt und mir zur Seite gestanden hat.